Methods in Molecular Biology 1582

Springer Protocols

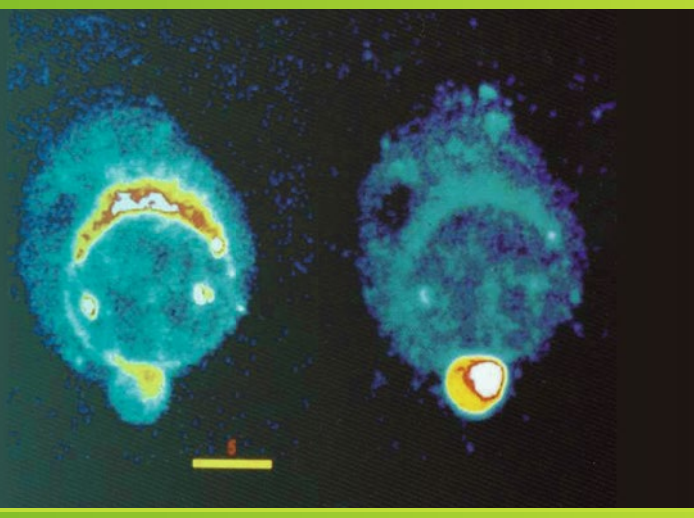

Claudio Casoli *Editor*

Human T-Lymphotropic Viruses

Methods and Protocols

Humana Press

METHODS IN MOLECULAR BIOLOGY

Series Editor
John M. Walker
School of Life and Medical Sciences
University of Hertfordshire
Hatfield, Hertfordshire, AL10 9AB, UK

For further volumes:
http://www.springer.com/series/7651

Human T-Lymphotropic Viruses

Methods and Protocols

Edited by

Claudio Casoli

University of Milano, Milano, Italy

Humana Press

Editor
Claudio Casoli
University of Milano
Milano, Italy

ISSN 1064-3745 ISSN 1940-6029 (electronic)
Methods in Molecular Biology
ISBN 978-1-4939-6870-1 ISBN 978-1-4939-6872-5 (eBook)
DOI 10.1007/978-1-4939-6872-5

Library of Congress Control Number: 2017933704

Cover illustration: Two in vitro HTLV-2-infected T lymphocytes stained with anti-Tax-2 polyclonal antibody (yellow). Scale bar= 5 μm. Provided by Dr. Claudio Casoli.

Printed on acid-free paper

This Humana Press imprint is published by Springer Nature
The registered company is Springer Science+Business Media LLC
The registered company address is: 233 Spring Street, New York, NY 10013, U.S.A.

Dedication

With sadness and sorrow, I mourn for Dr. Giovanna Tosi who passed away in July 20, 2016, at the age of 52, after a long illness. Dr. Tosi was assistant professor of immunology at the University of Insubria, Varese. She leaves her old mother Graziella and three sisters, Flavia, Elena, and Adriana.

I met Giovanna in 1988 when I came back to Italy after a long stay abroad. She had just obtained the master's degree in biology at the University of Padova and, as young Ph.D. student, was initiating her research career in Immunology at the University of Verona. It was not difficult to realize soon how sharp was that girl in thinking, planning, and performing science. She rapidly joined my group and she remained with me ever since, becoming over the years my most important collaborator.

Giovanna was a brilliant immunogeneticist. She dedicated her first years of research to studying the genetic association of type 1 diabetes to HLA class II polymorphism, contributing to clarify the importance of the combination of both DQA and DQB specific alleles in generating the strongest susceptibility to the disease [1].

She then became interested in the regulation of the expression of HLA class II genes in diseases and particularly in infections by human retroviruses. She was the first to show, in a series of papers between 2000 and 2002, that the HIV Tat transactivator could be modulated in its function by the major regulator of HLA class II expression, the CIITA transactivator encoded by the AIR-1 locus discovered in the laboratory [2, 3]. This paved the way for the identification of CIITA as a restriction factor for human retrovirus.

Indeed those first evidences were soon followed by the Giovanna's seminal discovery that CIITA acts as a restriction factor also for human oncogenic retroviruses HTLV-2 and HTLV-

1, utilizing a similar, although not identical, mechanism of inhibition of the function of the HTLV-2 and HTLV-1 transactivators Tax-2 and Tax-1, respectively [4–6].

Most recently, she discovered that CIITA could block also the Tax-1-dependent NF-kB constitutive activation in HTLV-1 infected cells, a major mechanism of neoplastic transformation by HTLV-1 leading to Adult T cell Leukemia, thus opening the way for future new strategies to counteract virus-mediated oncogenesis [7].

Giovanna was among the first to envisage that the genetic manipulation of tumor cells with CIITA may not only render tumor cells MHC class II-positive but also modify their immunogenic characteristics and induce them to act as surrogate antigen-presenting cells of their own tumor antigens in vivo. This hypothesis was verified in a series of seminal experiments in the mouse model and has served to propose a novel approach for anti-tumor vaccines [8] that is now part of a collaborative project granted by the European Community [9].

Despite the rapid progression of the disease in the last few months, Giovanna continued to work in the lab and to teach immunology to her beloved students at the medical school, with unbeatable enthusiasm. She leaves us with a scientific, moral, and ethical legacy that will last forever.

Roberto Accolla

References

1. Tosi G, Facchin A, Pinelli L, Accolla RS (1994) Diabetes Care 17:1045–1049
2. Tosi G, De Lerma Barbaro A, D'Agostino A, Valle MT, Megiovanni AM, Manca F, Caputo A, Barbanti-Brodano G, Accolla RS (2000) Eur J Immunol 30:19–28
3. Accolla RS, Mazza S, De Lerma Barbaro A, De Maria A, Tosi G (2002) Eur J Immunol 32:2783–2791
4. Casoli C, De Lerma Barbaro A, Pilotti E, Bertazzoni U, Tosi G, Accolla RS (2004) Blood 103: 995–1001
5. Tosi G, Pilotti E, Mortara L, De Lerma Barbaro A, Casoli C, Accolla RS (2006) Proc Natl Acad Sci USA 103:12861–12866
6. Tosi G, Forlani G, Andresen V, Turci M, Bertazzoni U, Franchini G, Poli G, Accolla RS (2011) J Virol 85:10719–10729
7. Forlani G, Abdallah R, Accolla RS, Tosi G (2016) J Virol 90:3708–3721
8. Accolla RS, Lombardo L, Abdallah R, Raval G, Forlani G, Tosi G (2014) Front Oncol 4:32. doi:10.3389/fonc.2014.00032
9. http://www.hepavac.eu/

Preface

In the last two decades, the major health international organizations have correctly addressed their efforts to fight the spread of the AIDS pandemic, and many reports and specialist books have documented the wealth of HIV-1 research that has been carried out. This book aims to attract the readers' attention to other members of the Retrovirus family, namely the human T-lymphotropic viruses (HTLVs), which, despite the frequency of the infection and the severity of the diseases associated with them, remain not so well known to people working in the medical fields. It is intended to promote and improve the interest in the study of HTLV pathogenicity and the related health problems. To this end, the most updated technical information about HTLV determination and the methods to investigate their interaction with the host immune system and interfering pathogens are reported.

The book is organized into five main parts. Part I covers essential aspects of epidemiology and virus transmission. Part II includes novel and robust methodologies for studying the effects of trans-activating regulatory HTLV proteins, while Part III provides the latest techniques for genotyping and gene expression analysis. Part IV addresses cellular phenotype and dynamics. Finally, Part V contains an overview of progress on new therapeutic strategies against HTLV infection. Although the main topic of this book is HTLV-1 (human T-cell leukemia virus type 1), it also deals with other HTLV infections, as in the case of bovine leukemia virus (BLV), covering the major highlighted issues with the hope that this work could give new impulse for opening a wider debate among researchers.

I would like to thank all participants who submitted their chapters, for their great efforts in bringing this book to fruition.

Milano, Italy *Claudio Casoli*

Contents

Contributors

Yao Akpamagbo • *Laboratory of Molecular Virology, George Mason University, Manassas, VA, USA*

Sandrine Alais • *Equipe Oncogenèse Rétrovirale, Lyon, Cedex, France; Equipe labellisée "Ligue Nationale Contre le Cancer", Lyon, France; International Center for Research in Infectiology, INSERM U1111 - CNRS UMR5308, Lyon, Cedex, France; Ecole Normale Supérieure de Lyon, Lyon, Cedex, France; Université Lyon 1, Lyon, France*

Luiz Carlos Junior Alcantara • *Fundação Oswaldo Cruz (FIOCRUZ), Salvador, Bahia, Brazil*

Jacob Al-Saleem • *Center for Retrovirus Research, The Ohio State University, Columbus, OH, USA; Department of Veterinary Biosciences, The Ohio State University, Columbus, OH, USA*

Thessika Hialla Almeida Araújo • *Fundação Oswaldo Cruz (FIOCRUZ), Salvador, Bahia, Brazil*

Charles R.M. Bangham • *Section of Virology, Wright-Fleming Institute, Imperial College School of Medicine, London, UK*

Robert A. Barclay • *Laboratory of Molecular Virology, George Mason University, Manassas, VA, USA*

Pierre-Yves Barez • *Molecular Biology (GxABT) and Molecular and Cellular Epigenetics (GIGA), University of Liege, Gembloux and Liege, Belgium*

Ali Bazarbachi • *Faculty of Medicine, Department of Anatomy, Cell Biology and Physiology, American University of Beirut, Beirut, Lebanon; Faculty of Medicine, Department of Internal Medicine, American University of Beirut, Beirut, Lebanon*

Elisa Bergamo • *Section of Biology and Genetics, Department of Neurosciences, Biomedical and Movement Sciences, University of Verona, Verona, Italy*

Umberto Bertazzoni • *Section of Biology and Genetics, Department of Neurosciences, Biomedicine and Movement Sciences, University of Verona, Verona, Italy*

Fabio Bignami • *Center for Medical Research and Molecular Diagnostic, GEMIB Laboratory, Parma, PR, Italy; Department of Clinical Sciences, University of Milan, Milan, Italy*

Federica Bozzano • *Molecular Immunology, University of Genova, Genova, Italy*

Alix de Brogniez • *Molecular Biology (GxABT) and Molecular and Cellular Epigenetics (GIGA), University of Liege, Gembloux and Liege, Belgium*

Alexandre Carpentier • *Molecular Biology (GxABT) and Molecular and Cellular Epigenetics (GIGA), University of Liege, Gembloux and Liege, Belgium*

Olivier Cassar • *Unité d'Epidémiologie et Physiopathologie des Virus Oncogènes, Département de Virologie, Institut Pasteur, Paris, France; CNRS, UMR 3569, Paris, France*

Ilaria Cavallari • *Istituto Oncologico Veneto, IRCCS, Padova, Italy*

Vincenzo Ciminale • *Department of Surgery, Oncology and Gastroenterology, University of Padova, Padova, Italy; Istituto Oncologico Veneto, IRCCS, Padova, Italy*

Donna M. D'Agostino • *Department of Biomedical Sciences, University of Padova, Padova, Italy*

Erica Diani • *Section of Biology and Genetics, Department of Neurosciences, Biomedicine and Movement Sciences, University of Verona, Verona, Italy*
Hélène Dutartre • *Equipe Oncogenèse Rétrovirale, Lyon, Cedex, France; Equipe labellisée "Ligue Nationale Contre le Cancer", Lyon, France; International Center for Research in Infectiology, INSERM U1111 - CNRS UMR5308, Lyon, Cedex, France; Ecole Normale Supérieure de Lyon, Lyon, Cedex, France; Université Lyon 1, Lyon, France*
Antoine Gessain • *Unité d'Epidémiologie et Physiopathologie des Virus Oncogènes, Département de Virologie, Institut Pasteur, Paris, France; CNRS, UMR 3569, Paris, France*
Nicolas A. Gillet • *Molecular and Cellular Epigenetics, Interdisciplinary Cluster for Applied Genoproteomics (GIGA) of University of Liège (ULg), Liège, Belgium; Molecular and Cellular Biology, Gembloux Agro-Bio Tech, University of Liège (ULg), Gembloux, Belgium*
Patrick L. Green • *Center for Retrovirus Research, The Ohio State University, Columbus, OH, USA; Department of Veterinary Biosciences, The Ohio State University, Columbus, OH, USA; Compreshensive Cancer Center and Solove Research Institute, The Ohio State University, Columbus, OH, USA; Department of Molecular Virology, Immunology, and Medical Genetics, The Ohio State University, Columbus, OH, USA*
Christine Gross • *Institute of Clinical and Molecular Virology, Friedrich-Alexander-Universität Erlangen-Nürnberg, Erlangen, Germany*
Geronimo Gutierrez • *Instituto de Virología, Centro de Investigaciones en Ciencias Veterinarias y Agronómicas, INTA, Castelar, Argentina*
Olivier Hermine • *Department of Hematology, Necker Hospital, University of Paris Descartes, Paris, France*
Fatah Kashanchi • *Laboratory of Molecular Virology, George Mason University, Manassas, VA, USA*
Mamuka Kvaratskhelia • *Center for Retrovirus Research, The Ohio State University, Columbus, OH, USA; College of Pharmacy, The Ohio State University, Columbus, OH, USA*
Renaud Mahieux • *Equipe Oncogenèse Rétrovirale, Lyon, Cedex, France; Equipe labellisée "Ligue Nationale Contre le Cancer", Lyon, France; International Center for Research in Infectiology, INSERM U1111 - CNRS UMR5308, Lyon, Cedex, France; Ecole Normale Supérieure de Lyon, Lyon, Cedex, France; Université Lyon 1, Lyon, France*
Mariangela Manicone • *Department of Surgery, Oncology and Gastroenterology, University of Padova, Padova, Italy*
Ambroise Marçais • *Department of Hematology, Necker Hospital, University of Paris Descartes, Paris, France*
Andrea De Maria • *Molecular Immunology, University of Genova, Genova, Italy*
Francesco Marras • *Molecular Immunology, University of Genova, Genova, Italy*
Allison Mathiesen • *Laboratory of Molecular Virology, George Mason University, Manassas, VA, USA*
Anat Melamed • *Section of Virology, Wright-Fleming Institute, Imperial College School of Medicine, London, UK*
Sonia Minuzzo • *Department of Surgery, Oncology and Gastroenterology, University of Padova, Padova, Italy*
Colin Murphy • *UCD School of Medicine and Medical Science, University College Dublin, Dublin, Ireland*

Rihab Nasr • *Faculty of Medicine, Department of Anatomy, Cell Biology and Physiology, American University of Beirut, Beirut, Lebanon*
Kinza Noor • *Laboratory of Molecular Virology, George Mason University, Manassas, VA, USA*
Elisabetta Pilotti • *Center for Medical Research and Molecular Diagnostic, GEMIB Laboratory, Parma, PR, Italy*
Michelle L. Pleet • *Laboratory of Molecular Virology, George Mason University, Manassas, VA, USA*
Vittoria Raimondi • *Department of Molecular Medicine, University of Padova, Padova, Italy*
Filipe Ferreira de Almeida Rego • *Fundação Oswaldo Cruz (FIOCRUZ) and Universidade Católica do Salvador, Salvador, Bahia, Brazil*
Michal Reichert • *Department of Pathology, National Veterinary Research Institute, Pulawy, Poland*
Francesca Rende • *Department of Surgery, Oncology and Gastroenterology, University of Padova, Padova, Italy*
Maria Grazia Romanelli • *Section of Biology and Genetics, Department of Neurosciences, Biomedicine and Movement Sciences, University of Verona, Verona, Italy*
Noreen Sheehy • *Centre for Research in Infectious Diseases, School of Medicine and Medical Science, University College Dublin, Dublin, Ireland*
Riccardo Alessio Sozzi • *Department of Environmental Sciences, University of Parma, Parma, Italy*
Andrea K. Thoma-Kress • *Institute of Clinical and Molecular Virology, Friedrich-Alexander-Universität Erlangen-Nürnberg, Erlangen, Germany*
Karina Trono • *Instituto de Virología, Centro de Investigaciones en Ciencias Veterinarias y Agronómicas, INTA, Castelar, Argentina*
Luc Willems • *Molecular Biology (GxABT) and Molecular and Cellular Epigenetics (GIGA), University of Liege, Gembloux and Liege, Belgium*

Part I

Epidemiology and Transmission

Chapter 1

Serological and Molecular Methods to Study Epidemiological Aspects of Human T-Cell Lymphotropic Virus Type 1 Infection

Olivier Cassar and Antoine Gessain

Abstract

We estimated that at least 5–10 million individuals are infected with HTLV-1. Importantly, this number is based on the study of nearly 1.5 billion people living in known human T-cell lymphotropic virus type 1 (HTLV-1) endemic areas, for which reliable epidemiological data are available. However, for some highly populated regions including India, the Maghreb, East Africa, and some regions of China, no consistent data are yet available which prevents a more accurate estimation. Thus, the number of HTLV-1 infected people in the world is probably much higher. The prevalence of HTLV-1 prevalence varies depending on age, sex, and economic level in most HTLV-1 endemic areas. HTLV-1 seroprevalence gradually increases with age, especially in women. HTLV-1 has a simian origin and was originally acquired by humans through interspecies transmission from STLV-1 infected monkeys in the Old World. Three main modes of HTLV-1 transmission have been described; (1) from mother-to-child after prolonged breast-feeding lasting more than six months, (2) through sexual intercourse, which mainly, but not exclusively, occurs from male to female and lastly, (3) from contaminated blood products, which contain HTLV-1 infected lymphocytes. In specific areas, such as Central Africa, zoonotic transmission from STLV-1 infected monkeys to humans is still ongoing.

The diagnostic methods used to study the epidemiological aspects of HTLV-1 infection mainly consist of serological assays for the detection of antibodies specifically directed against different HTLV-1 antigens. Screening tests are usually based on enzyme-linked immunoabsorbent assay (ELISA), chemiluminescence enzyme-linked immunoassay (CLEIA) or particle agglutination (PA). Confirmatory tests include mostly Western blots (WB)s or innogenetics line immunoassay (INNO-LIA™) and to a lesser extent immunofluorescence assay (IFA). The search for integrated provirus in the DNA from peripheral blood cells can be performed by qualitative and/or quantitative polymerase chain reaction (qPCR). qPCR is widely used in most diagnostic laboratories and quantification of proviral DNA is useful for the diagnosis and follow-up of HTLV-1 associated diseases such as adult T-cell leukemia (ATL) and tropical spastic paraparesis/HTLV-1 associated myelopathy (TSP/HAM). PCR also provides amplicons for further sequence analysis to determine the HTLV-1 genotype present in the infected person. The use of new generation sequencing methodologies to molecularly characterize full and/or partial HTLV-1 genomic regions is increasing. HTLV-1 genotyping generates valuable molecular epidemiological data to better understand the evolutionary history of this virus.

Key words HTLV-1 seroprevalence, HTLV-1 epidemiology, HTLV-1 transmission, Diagnostic methods, Genotyping

Claudio Casoli (ed.), *Human T-Lymphotropic Viruses: Methods and Protocols*, Methods in Molecular Biology, vol. 1582,
DOI 10.1007/978-1-4939-6872-5_1, © Springer Science+Business Media LLC 2017

1 Introduction

In 1980, the laboratory of RC. Gallo (National Institutes of Health, USA) reported the isolation of the Human T-cell leukemia virus type 1 (HTLV-1), currently called Human T-cell lymphotropic virus type 1. This was the first oncoretrovirus to be discovered in humans. HTLV-1 was present in the peripheral blood cells of an African-American patient suffering from a T lymphoproliferative disease, originally considered to be a cutaneous T-cell lymphoma, with a leukemic phase [1, 2]. The virus was thus named Human T-Cell Leukemia/Lymphoma Virus (HTLV). It was later recognized that this cutaneous lymphoma was in fact an adult T-cell leukemia/lymphoma (ATL), a severe T-cell lymphoproliferation, originally described in Japan in 1977 by Takatsuki et al. [3]. The epidemiological characteristics of ATL in Japan strongly suggested an environmental factor, which prompted researchers to search for an oncogenic virus in the tumor cells. In 1981, a virus was isolated in Japan and called Adult T-Cell Leukemia/Lymphoma Virus (ATLV). Japanese and American scientists rapidly demonstrated that both isolates corresponded to the same virus, and agreed to name it HTLV-1. In parallel, the causal association between ATL and HTLV-1 was established [4]. In 1985, HTLV-1 infection was also associated with a chronic neuromyelopathy, named Tropical Spastic Paraparesis/HTLV-1 associated myelopathy (TSP/HAM) [5] and later with other clinical conditions including uveitis, infective dermatitis, and myositis [6].

1.1 Epidemiological Aspects of HTLV-1 Infection

HTLV-1 is unevenly distributed worldwide, with clusters of high endemicity often located near areas where the virus is nearly absent. Adult HTLV-1 seroprevalence is estimated to be at least 1–2% in high endemic regions, but can reach 20–40% in people older than 50 years in some foci. The areas of highest endemicity are the Southwestern region of the Japanese archipelago, parts of the Caribbean and its surrounding regions, foci in South America including parts of Colombia, French Guyana, and Brazil, some areas of intertropical Africa (such as South Gabon), the middle East (such as the Mashhad region in Iran), and isolated clusters in Australo-Melanesia. The only HTLV-1 endemic region in Europe is Romania [6–9]. The origin of this puzzling geographical/ethnic repartition is not well understood. It is likely linked to a founder effect in some groups, followed by the persistence of a high viral transmission rate due to favorable local environmental and cultural situations [10–13]. HTLV-1 seroprevalence increases gradually with age, especially among women in all highly endemic areas, independently of the socio-economic and cultural environments. This may be due to the accumulation of sexual exposures with age, or to a cohort effect [6–9].

There are three main modes of HTLV-1transmission: (1) mother-to-child transmission, which is mainly linked to prolonged

breast-feeding lasting more than 6 months. 10–25% of the breast-fed children born from HTLV-1 infected mothers become infected. A high HTLV-1 proviral load in milk or in blood cells, as well as high HTLV-1 antibody titers in the serum and long duration of breast-feeding (>6 months) represent major risk factors for HTLV-1 transmission from mother-to-child [14, 15]; (2) sexual transmission, which mainly, but not exclusively, occurs from male-to-female, and is thought to be responsible for the increased seroprevalence with age in women [16]; (3) transmission through contaminated blood products (containing HTLV-1 infected lymphocytes), which is responsible for acquired HTLV-1 infection in approximately 40–60% of blood recipients [17, 18]. Additionally, zoonotic transmission from non-human primates (NHP)s can occurs, at least in specific West and Central African rural populations.

It is difficult to precisely estimate the number of HTLV-1 infected people worldwide. The number of healthy carriers is probably more than one million in Japan. Africa is considered to be the largest endemic area in the world with a few million infected people. The best recent worldwide estimates are at least from 5 to 10 million HTLV-1 infected individuals [7]. However, these results are based on only the approximately 1.5 billion people living in known HTLV-1 endemic areas. It is very difficult to make correct estimates in other highly populated regions such as China, India, the Maghreb, or east Africa. The actual number of HTLV-1 carriers is likely to be much higher [6–9].

1.2 Epidemiological Aspects of the Main HTLV-1 Associated Diseases (ATL and TSP/HAM)

Large series of ATL patients have been reported in several HTLV-1 endemic areas including Japan [19], some Caribbean islands (especially Jamaica, Trinidad, Martinique) [20], numerous countries of South and Central America (Brazil, Peru, Colombia, French Guyana) [12, 21, 22], and Iran. They have also been reported in immigrants originating from high HTLV-1 endemic areas living in Europe (mainly France and UK) [23, 24] and the USA [25]. Sporadic cases of ATL have also been described in Australo-Melanesia [26, 27], North, West and South African countries [28], and Romania [29]. Studies performed primarily in Brazil, some African countries, and French Guyana concluded that ATL prevalence is usually underestimated until it is specifically investigated. This is due to several factors including the difficulty to diagnose chronic and smoldering ATL cases, and the very rapid evolution of some cases of acute leukemia and lymphoma [12, 19]. In addition, laboratory tests for HTLV-1 are not easily available in some tropical areas, especially in African countries. ATL occurs mostly in adults at least 20–30 years after the HTLV-1 infection. The age at onset differs depending on the geographic origin of the infected individuals. The average age of onset in Central and South America and the Caribbean area is approximately 40 years while it is around 60 years in Japan [19, 30]. The reason for this difference is

unknown but may be related to various genetic, epigenetic, or environmental cofactors. ATL occurs mostly in people infected during childhood by prolonged breast-feeding. HTLV-1 infected male carriers have a three to fivefold higher risk of developing ATL than female carriers. The epidemiology of ATL has been best studied in Japan where nearly 1000 new cases of ATL are diagnosed annually and nearly 1000 patients die of ATL each year [19]. The annual incidence of ATL among HTLV-1 carriers is approximately 60/100,000, with an estimated lifetime risk of 6–7% for men and 2–3% for women. The prevalence and incidence of ATL are less known in other high HTLV-1 endemic areas [19].

The lifetime risk among HTLV-1 carriers for TSP/HAM is estimated to be approximately 0.25–3%, (i.e., lower than ATL). TSP/HAM mainly occurs in adults, with a mean age at onset of 40–50 years [31, 32]. In contrast to ATL (male/female ratio = 1.4), TSP/HAM is more common in women than in men, with a sex ratio of 0.4. Blood transfusion is a major risk factor for TSP/HAM. The co-incidence of ATL and TSP/HAM has been rarely reported. In general, 2–10% of infected individuals will develop an HTLV-1 associated disease (ATL, TSP/HAM, uveitis, infective dermatitis) during their life-time (Table 1).

Table 1
HTLV-1 associated diseases during infected individuals' life-time The strength of association is based on epidemiological studies as well as molecular data, animal models, and intervention trials. ++++: proven association, +++: probable association, ++: likely association. *SIBM*: sporadic inclusion body myositis

Diseases	Association
Adulthood	
Adult T-cell leukemia/lymphoma (ATL)	++++
Tropical spastic paraparesis/HTLV-1 associated myelopathy (TSP/HAM)	++++
Intermediate uveitis (Japan/Caribbean)	+++
Myositis (polymyositis and SIBM)	+++
Infective dermatitis (very rare)	+++
HTLV-1 associated arthritis (Japan)	++
Bronchiectasis — (Central Australia)	++
Childhood	
Infective dermatitis (Jamaica/Brazil/Africa)	++++
TSP/HAM (very rare)	++++
ATL (very rare)	++++

1.3 Molecular Epidemiology of HTLV-1: Existence of Geographical Subtypes

HTLV-1 is genetically stable, an unusual feature for a retrovirus. This is probably because viral amplification occurs mostly via clonal expansion of infected cells, rather than by reverse transcription. The low sequence variation of HTLV-1 can be used as a molecular tool to follow the migrations of infected populations, in the recent or distant past, to gain new insights into the origin, evolution, and modes of dissemination of these retroviruses and their hosts [33]. The few nucleotide substitutions observed among HTLV-1 strains are indeed specific to the geographic origin of the patients rather than the associated pathology. There are four major geographic subtypes (genotypes). They include the cosmopolitan a-subtype, the Central African b-subtype, the Central African d-subtype, and the Australo-Melanesian c-subtype. A limited number of strains found in Central Africa belong to other rare subtypes (e, f, g) [7–9]. The Cosmopolitan a-subtype, which comprises several geographical subgroups (Japanese, West African, North African, etc.), is the most widespread. It is endemic in Japan, the Caribbean area, Central and South America, and North and West Africa as well as part of the Middle East. The sequence variability within the a-subtype is very low but differs depending on geographic origin. It reaches 2.5% in the gp21-env gene and 2% in the LTR region [34]. This very likely reflects the recent dissemination (some centuries) of this genotype from a common ancestor. The Australo-Melanesian c-subtype is the most divergent relative to the reference strain (ATK-1). This reflects an ancient speciation, with a long period of isolation of the populations living in different islands of the Pacific area [35]. The appearance of these HTLV-1 subtypes in humans is linked to interspecies transmission between STLV-1 infected monkeys and humans, followed by variable periods of evolution in the human host. Indeed, STLV-1, the simian counterpart of HTLV-1, infects several species of nonhuman primates (NHPs) of the Old Word, ranging from chimpanzees and gorillas to mandrills, as well as several African small monkey species and a wide range of macaques. Such interspecies transmission is still ongoing for central African hunters [36, 37]. STLV-1 infection is also associated with the development of ATL in some NHPs [2]. There is no strong evidence that a specific mutation or a genotype is associated with the development of TSP/HAM or ATL in an asymptomatic carrier.

1.4 Laboratory Diagnosis of HTLV-1

Concerning epidemiological aspects of HTLV-1, most of the studies are still performed on series of blood donors, pregnant women, or hospitalized patients. However, such surveys are obviously not representative of the general population of the studied countries. In very few cases, population-based studies are done in some villages, towns, or even regions of a given country [7].

HTLV-1/2 is usually diagnosed by the detection of specific antibodies in plasma or serum [38–40] directed against immunodominant regions of both HTLV-1 and HTLV-2 structural proteins

[41]. In cases where it is difficult to obtain serum or plasma samples, a dried blood spot collected on filter paper may also be used for HTLV detection [42] especially for large-scale epidemiological studies [43] or for pregnant women in the prenatal period [44]. Other biological fluids suitable for anti-HTLV-1 antibody screening include breast milk [45], which is a direct source of infection and can be sampled noninvasively, urine [46], and saliva [47].

The diagnosis of HTLV-1 infection is also frequently performed after amplification of proviral DNA by polymerase chain reaction (PCR). Direct detection of the virus can also be performed by viral culture, but this technique requires specialized and properly equipped laboratories.

1.4.1 Serologic diagnosis of HTLV-1

HTLV-1/2 serology comprises an antibody-screening step followed by confirmation (Fig. 1). Diagnosis can then be completed by serological differentiation of antibodies directed against the two different viral types. Several serological diagnostic tests have been developed to detect or confirm the presence of antibodies directed against HTLV-1 and HTLV-2 infection. They are routinely used in the form of commercialized diagnostic kits, which are approved by governmental/European agencies before commercialization.

Serological Screening Techniques

Enzyme-linked Immunosorbent Assay (ELISA)

This colorimetric test is widely used because of its level of standardization and the large number of available commercial kits. The "first generation" kits, using antigens derived from viral lysates, were very sensitive but generated many false-positive reactions [48]. Manufacturers have added recombinant proteins derived from the transmembrane protein (GD21) of HTLV-1 and HTLV-2 as well as specific synthetic peptides originating from HTLV-1 (including MTA-I or rgp46-I) and HTLV-2 (including K55 or rgp46-II) external glycoproteins [38, 39, 49]. These "mixed" kits recognize both HTLV-1 and HTLV-2 infection with good sensitivity and specificity. The anti-HTLV serum or plasma antibodies, fixed on the antigen from the solid phase, are revealed by a conjugate consisting of a labeled anti-immunoglobulin antibody, the "indirect method," or by HTLV specific labeled antigens, the "sandwich method" (MP Diagnostics™ HTLV-I/II ELISA 4.0). The optical density observed in each well is directly proportional to the amount of anti-immunoglobulin antibody conjugated with an enzyme, such as horseradish peroxidase. More recently, kits using a chemiluminescent microparticle technique for the revelation step, the rHTLV-I/II assay (Abbott Laboratories, Abbott Park, IL), have been developed and adapted for large-scale screening of samples for HTLV-1/2 antibodies [50, 51].

This method does not differentiate between infection with either one or both viruses due to the high homology between some HTLV-1 and HTLV-2 structural proteins. These kits are thus commercialized under the label "HTLV-1/2" [38, 39, 49, 52].

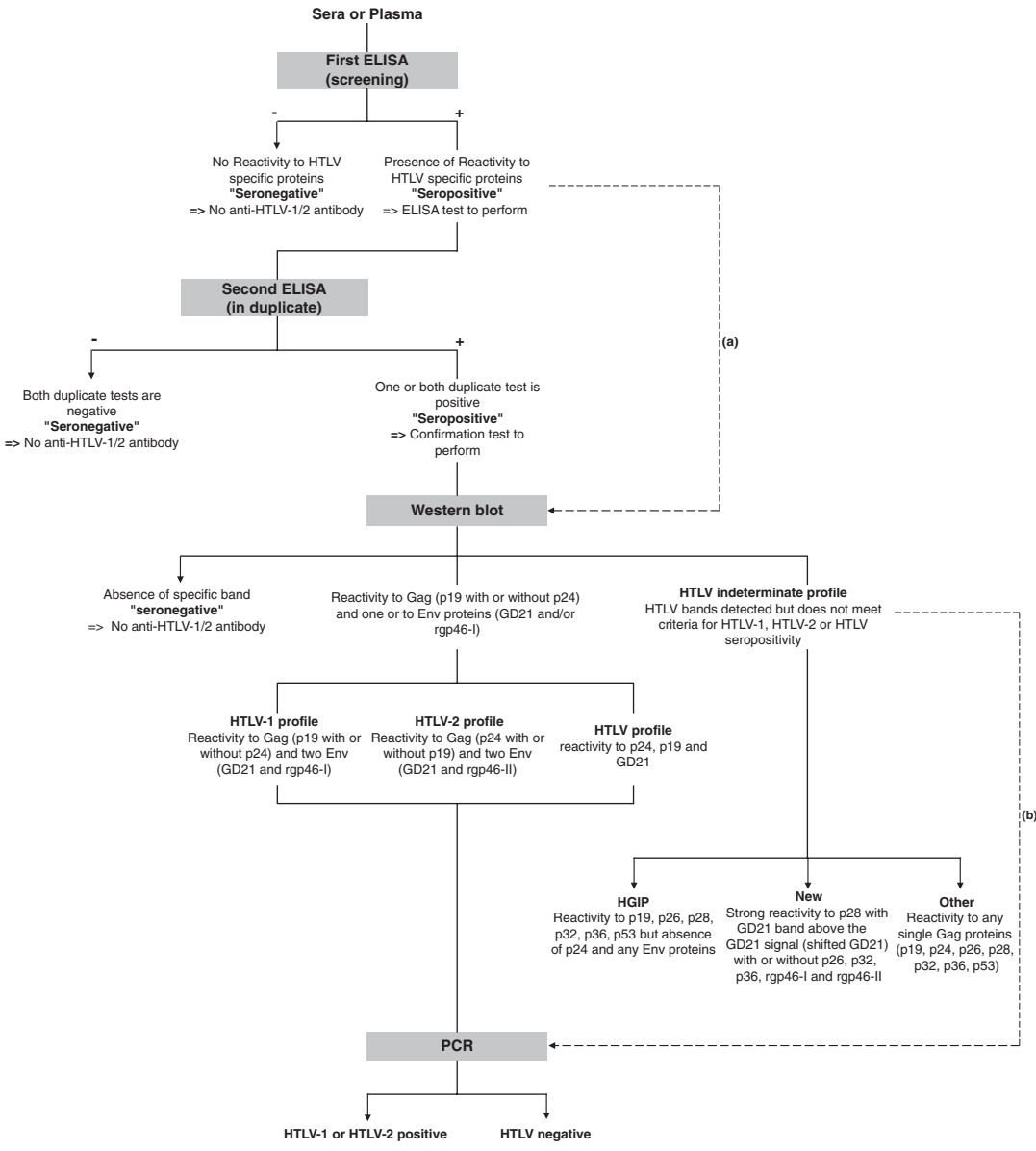

Fig. 1 Serologic and molecular testing algorithm for the determination and confirmation of HTLV-1/2 infection. If the initial screening using an enzyme immunoassay (ELISA) is positive, a second screening assay is carried out in duplicate using the same sample. If one of the reactions (or both) is positive, the sample is considered reactive and a confirmation test by Western blot is performed. Positivity criteria are then those determined by the kit manufacturer. Here, diagnostic criteria used are those of the most frequently employed Western blot kit, in the Americas and Europe, according to the manufacturer's instructions. In some cases, proviral DNA amplification by PCR may be implemented to confirm the presence of the virus. In some laboratories, the enzyme immunoassay "INNO-LIA" is implemented instead of Western blot to confirm the presence of HTLV-1/2 antibodies. (**a**) Performed in some laboratory. (**b**) Performed in some research laboratory

Gelatin Particle Agglutination (PA)

The agglutination of gelatin particles technique (PA) is based on the specific immuno-agglutination of inactive gelatin particles sensitized or not (negative control) with HTLV-1 antigens. Antigens are obtained by concentration of the supernatant of cell cultures producing the virus. A positive reaction is characterized by agglutination of the coated particles. The evaluation of the result is either qualitative or quantitative. This technique is easy to implement and requires no equipment other than that provided by the manufacturer. PA shows good sensitivity and specificity [53–56]. Formerly largely implemented by the Japanese Red Cross, the PA technique is now replaced by an automated chemiluminescence enzyme-linked immunoassay (CLEIA) test (CL4800 testing system, Fujirebio, Tokyo, Japan) followed by a commercial Western blotting test (ProBlot HTLV-1, Fujirebio, Tokyo, Japan) as confirmatory method for blood donor testing [57].

Indirect Immunofluorescence Assay (IFA)

The Indirect IFA allows the detection, confirmation, and titration of antibodies directed against HTLV-1 and HTLV-2 viruses [58, 59]. This technique uses cells from the MT2 and C19 cell lines, which are productively infected with HTLV-1 and HTLV-2, respectively. Glass slides are coated with approximately 75% of uninfected CEM cells and 25% of either MT2 or C19 cells [59, 60]. The cells are then fixed and permeabilized using acetone. Positive and negative control samples are required on each slide to interpret the assay. Comparison between the two cell lines generally allows the discrimination between HTLV-1 and HTLV-2 infection. Serial dilution of the sera can be used to determine antibody titers. Interpretation of the result is usually easy, although samples originating from individuals living in tropical countries (especially sub-Saharan Africa and Melanesia) often show significant background. This technique requires the maintenance of continuous cell lines with a high level of antigen expression, which is only possible in specialized and appropriately equipped laboratories [58–60].

Special attention must be given to the existence of a silent serological phase prior to HTLV seroconversion, especially after transfusion of contaminated blood. PCR amplification may be useful for detecting HTLV-1 infection prior to seroconversion [18, 61, 62].

Serological Confirmatory Techniques

Radioimmunoprecipitation Assay (RIPA)

The radioimmunoprecipitation assay is used as a confirmatory assay and allows the detection of HTLV antibodies using radioisotopes as the detector molecule [63, 64]. In this technique, the antigen is derived from HTLV-1/2 transformed cell lines that have been metabolically labeled with ^{35}S methionine or ^{35}S cysteine for a few hours in methionine-cysteine-free medium. RIPA is more costly than Western blot and requires specific authorization for the use of radioactive isotopes. However, RIPA has the

advantage of higher sensitivity due to more intense signals and higher specificity due to the lack of endogenous background enzymes as in ELISA [64].

Immunoblot Test or Western Blot (WB)

All samples exhibiting a signal repeatedly greater than or equal to the threshold value by a screening assay must be tested using a confirmation test, usually an immunoblot test or WB. The WB tests have steadily improved over the years. The first commercialized tests did not properly allow the detection of antibodies directed against the Env proteins, which were partly degraded during the process of viral lysate purification. In the early 1990s, manufacturers added a recombinant transmembrane glycoprotein rgp21 (GD21) to the HTLV-1 viral lysate. The rgp21 is composed of HTLV-1 and HTLV-2 common epitopes to increase the sensitivity of detection [65, 66].

More recent versions of the WB kits not only confirm the presence of HTLV viruses, but also differentiate between the two viral types by the inclusion of an external recombinant glycoprotein specific for HTLV-1 or HTLV-2 viruses (MTA-1 and K-55 respectively) [66–68]. These kits enable the confirmation of both HTLV-1 and HTLV-2 infections by combining specific (1) native inactivated disrupted viral proteins, (2) recombinant proteins, and (3) synthetic peptides. The modification of the GD21 recombinant peptide sequence, present in the most recent version of the WB kit (MP Diagnostics ™ HTLV Blot 2.4), makes it more specific and sensitive [69]. The use of this kit has been recently approved by the U.S. Food and Drug Administration [70].

The positivity criteria for interpreting the WB test have steadily evolved. In the late 1980s, the Centre for Disease Control (CDC) in the United States recommended that a sample be declared positive if it reveals the presence of anti-Gag (p24) and anti-Env (gp46 or precursor gp61/68) antibodies [71]. In 1992, the CDC stated that the criteria should also include reactivity to the p24gag protein and the native gp46env protein and/or the recombinant GD21 protein [72]. The World Health Organization (WHO) defines the positivity criteria as the presence of anti-envelope and anti-Gag (p19 or p24) proteins. The CDC criteria are more restrictive than those of the WHO and some samples considered to be positive according to the WHO criteria are indeterminate based on those of the CDC [73]. In Europe, more restrictive criteria are applied in most countries and require reactivity against at least one anti-Gag (p19 or p24) and two anti-Env (gp21 and gp46) proteins, whether native or recombinant [74, 75]. According to the instructions of the MP Diagnostics™ HTLV Blot 2.4 kit, which is widely used worldwide, the seropositivity criteria for HTLV-1 includes reactivity to p19gag, with or without p24gag, and to GD21 with the presence of the rgp46-I peptide called MTA-1. Reactivity to p24gag, with or without p19gag, and

to GD21 with a rgp46-II signal against the K-55 peptide, reveals seropositivity toward HTLV-2. In general, samples showing anti-gag reactivity with a p24 signal stronger than that of p19 favor an HTLV-2 infection [68].

All samples with only partial reactivity toward some of these viral proteins are considered to be indeterminate and are considered to be negative when they show no reactivity. Despite these improvements in the specificity of WB assays, indeterminate serological patterns remain quite frequent and represent a concern for routine screening in blood banks especially in the Americas, Africa, South-East Asia, and Middle East [76–79]. The significance of these frequent indeterminate WB results remains mostly unknown and a matter of debate [76–84]. In rare cases these patterns have been associated with:

1. HTLV-1, but mostly HTLV-2 infection exhibiting atypical HTLV serology [85, 86],
2. HTLV-1 seroconversion [18, 62, 87],
3. Infection by a different HTLV, such as HTLV-3 or HTLV-4 [88–91],
4. Cross-reactivity against other microbial agents, especially Plasmodium falciparum in South-East Asia, Indonesia, and Central Africa [60, 92–94].

The indeterminate HTLV-1 serology results comprise a large variety of band profiles including either unique (but faint), multiple, or clear bands [77, 79, 87, 95, 96]. A frequent pattern, named "HGIP" for HTLV Gag indeterminate pattern, has been described by our group [97]. We showed that such reactivity was associated with neither HTLV-1 nor HTLV-2 infection [60]. The HGIP pattern is now described in the most widely used WB kit (MP Diagnostics™ HTLV Blot 2.4). Recently, our group defined a new WB pattern, called "N," exhibiting strong reactivity against p28 and GD21 but, for this latter viral protein, at a position slightly above the normal position (shifted GD21) [98]. This novel profile is sometimes associated with faint reactivity against other Gag-encoded proteins (p26, p32, p36, and p53) and possibly reactivity against MTA-1 and/or K55 peptides (Fig. 2 and Table 2).

Line Immuno Assay (LIA®)

The enzyme immunoassay "INNO-LIA™ HTLV1/2 Score" is intended to confirm the presence of antibodies against HTLV-1 and/or HTLV-2 in serum or plasma, and to differentiate between HTLV-1 and HTLV-2 infections (Innogenetics NV, Ghent, Belgium). This assay uses highly purified recombinant HTLV proteins (rp19, rp24: I/II and rgp21: I/II) and synthetic peptides (gp46: I/II and p19: I) fixed on a nylon membrane [99, 100].

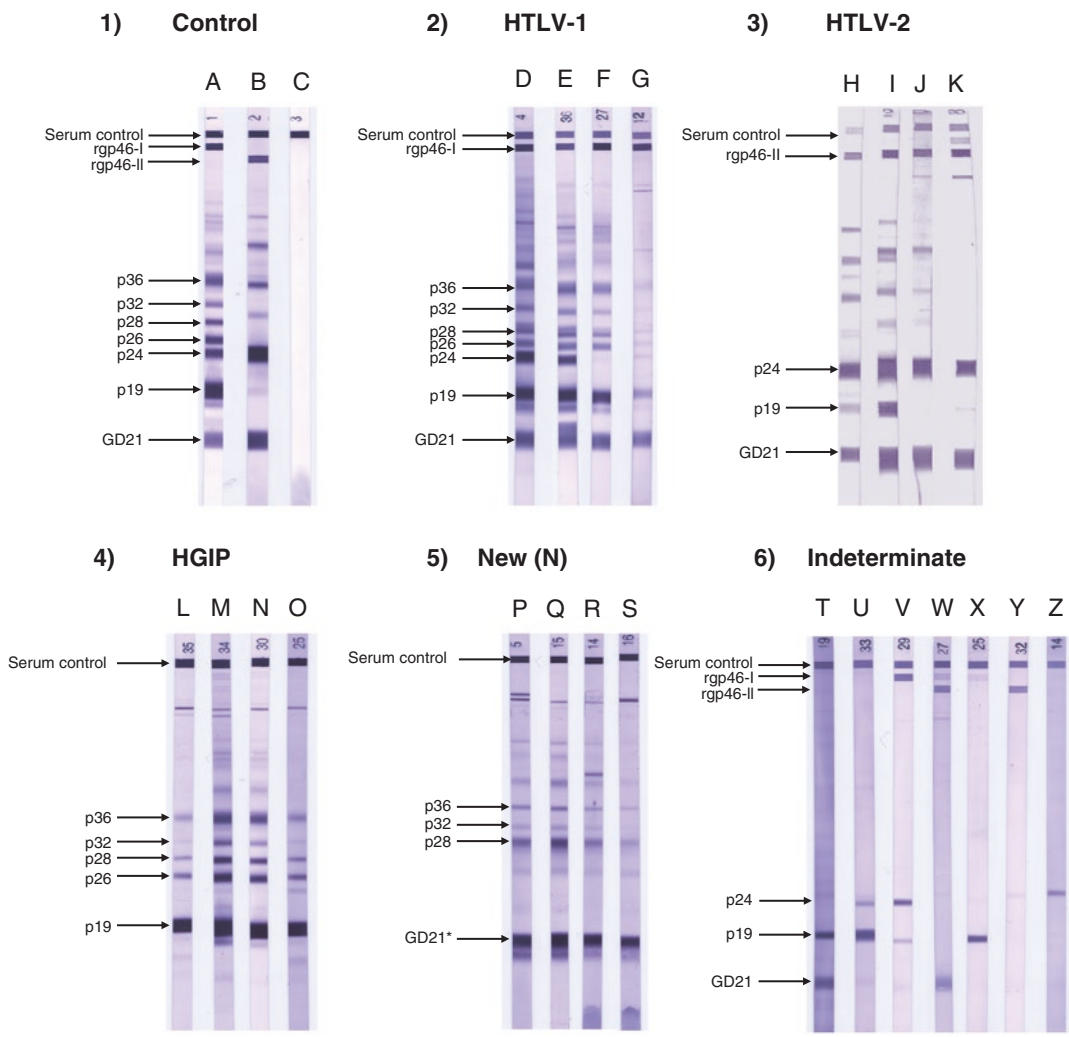

Fig. 2 Representative sero-reactivity pattern obtained with the MP DiagnosticsTM HTLV Blot 2.4 detection kit. The MPD HTLV Blot 2.4 kit contains a recombinant GD21 common for HTLV-1 and HTLV-2 plus two synthetic peptides: rgp46-I and rgp46-II specific for HTLV-1 and HTLV-2 respectively. (1) Control HTLV-1 (*A*), control HTLV-2 (*B*) and negative control (C); (2) HTLV-1 pattern (*D–G*); (3) HTLV-2 pattern (*H–K*); (4) "HGIP" pattern (*L–O*); (5) New HTLV indeterminate pattern provisionally called "New HTLV indeterminate" pattern with *asterisk* (*) GD21 signal slightly above the GD21 specific signal (*P–S*) [98]; (6) Different HTLV indeterminate pattern (*T–Z*)

The antigenicity of these proteins and peptides is either common to HTLV-1 and HTLV-2 antibodies or specific for each virus type to allow confirmation and differentiation in a single reaction. Two non-type specific "Gag" (p19 and p24) and "Env" bands (gp46 and gp21) are used to confirm the presence of anti-HTLV antibodies. The presence of specific antibodies for HTLV-1 (p19gag and gp46-I-env) and HTLV-2 (gp46-II-env) proteins can

Table 2
HTLV Western blot interpretation based on the most widely used WB kit (MP Diagnostics™ HTLV Blot 2.4)

Profile of viral bands	Interpretation
GD21, p19gag, (p24gag), rgp46-I	HTLV-1
GD21, (p19gag), p24gag, rgp46-II	HTLV-2
GD21, p19gag, p24gag	HTLV
p19gag, p26gag, p28gag, p32gag, p36gag	Indeterminate "HGIP" pattern
GD21 but above GD21 classical signal, p28gag	Indeterminate "N" pattern
One unique band or pattern different from HGIP and "N"	Indeterminate
No band	Negative

(−) The presence of bands in brackets is optional

discriminate between HTLV-1 and HTLV-2 infections. Each strip also contains four control lines: a negative control (streptavidin) and three positive control lines (low, medium, and strong anti-human immunoglobulin), providing qualitative quantification of the response (low/medium/high) [99–102].

Luciferase Immunoprecipitation System (LIPS)

The luciferase immunoprecipitation system is a highly sensitive antibody detection method that uses recombinant antigens fused to the luciferase protein. The amount of luciferase-fused antigen captured by antibodies in a test sample is measured as the luciferase activity without using secondary antibodies for detection. Originally developed to analyze whole proteome antibody response profiles [103], this assay was then used for the detection of anti-HTLV antibodies in symptomatic and asymptomatic carriers [104]. It has been recently used to identify asymptomatic HTLV-1 carriers among blood donors in Japan [57].

The pooling of samples can be a useful surveillance strategy to improve the knowledge of the spread of viral infections among various population groups. This approach has already been applied to HIV [105]. This pooling strategy has also been implemented for serologic HTLV surveillance among population groups with a low estimated prevalence (<2%) [106]. Meanwhile, the pooling of samples may compromise the sensitivity of the detection method used for blood donor screening and clinical diagnostics. Thus, this technique should only be reserved for serologic surveillance studies [107].

1.4.2 Molecular Diagnosis of HTLV-1

Molecular techniques are generally employed for the confirmation of HTLV-1 infection and genotyping of HTLV-1 proviral strains. The molecular detection of HTLV has greatly evolved since the development of PCR in the 1980s due to the ability of this method to amplify specific genomic sequences in a few hours from a relatively small amount of proviral DNA sample. PCR is currently the most widely used technique to confirm and/or support serological assays [108–111].

PCR Assays

This technique, which utilizes primers and probes corresponding to specific regions of the genome to be amplified, makes it possible to:

1. Demonstrate HTLV infection and validate serological results,
2. Determine the HTLV type(s) responsible for the infection (HTLV-1, 2, 3, or 4),
3. Provide amplified proviral DNA for sequence analyses.

HTLV-1 is a cell-associated virus. It is thus not easy to routinely determine the RNA viral load [112]. Determination of the proviral load (PVL) is based on the amplification of proviral DNA which is usually obtained from (1) peripheral blood mononuclear cells, (2) peripheral blood leukocyte concentrates, (3) lymph nodes, or (4) skin biopsy. It can also be detected from breast-milk, semen, urine, and saliva [113, 114]. PCR methods are fast, specific, sensitive, and reproducible. They have become the gold standard for the detection of HTLV infection, especially in hospital laboratories, and are the most currently used methods.

Qualitative PCR methods were initially developed using HTLV-1 and HTLV-2 specific primers. Type-specific amplification, using HTLV-1 or HTLV-2 specific primers, following a first amplification using HTLV consensus primers has also been used. The PCR products can also be detected using labeled internal probes by the Southern blot (SB) hybridization technique [110].

Assays specifically intended to investigate for HTLV-1 proviral load have included various semiquantitative PCR techniques [115–117]. However, these techniques were not fully quantitative since they depend on the co-amplification of a heterologous internal standard housekeeping gene (i.e., beta-globin), or template dilution series with subsequent qualitative and spot blot hybridization [118]. Therefore, mainly due to variations in amplification efficiency between the internal standard and target sequences, the semiquantitative PCR methods cannot accurately measure the proviral copy numbers in infected cells and are no longer implemented.

Then, quantitative polymerase chain reaction (qPCR) methods, also called real-time PCR, have been implemented to determine HTLV-1 and HTLV-2 proviral DNA load. Real-time PCR is a highly sensitive technique with a wide detection scale, ranging from 10 to 10^6 copies per reaction [119–123]. Two distinct chemistries

have been developed for real-time PCR; (1) SYBR® Green-based detection using SYBR® Green dye, a double strand DNA binding dye, to detect the PCR product as it accumulates during PCR amplification [119] and (2) TaqMan®-based detection, which uses a fluorogenic probe specific to the target gene to detect target as it accumulates during PCR amplification [120–122].

The PCR methods, via primer and probe design, usually detect only one genotype per amplification reaction (singleplex), especially the most prevalent genetic variant; the HTLV-1a Cosmopolitan genotype. This method was later improved and a triplex qPCR assay has been developed for simultaneous detection, genotyping, and quantification of PVL of HTLV-1, -2 and -3 infections in a single amplification reaction [108, 123, 124].

A new approach to nucleic acid detection, called digital droplet PCR (ddPCR), has been recently developed. This is especially useful for HTLV-1 detection in samples with low cell numbers such as cerebrospinal fluid [125, 126]. This novel technique allows the direct absolute quantification of a target gene in a given sample. The DNA is initially fragmented using a restriction enzyme and partitioned into thousands of nanoliter-sized droplets before amplification on a thermocycler. The droplets are then queried for fluorescent signal [127]. Each droplet is designated as either positive or negative for the target probe by the amplitude of its recorded fluorescence signal. This method, which allows a direct approach to target gene quantification, may provide a more precise and reliable method for PVL quantification.

The reliable quantification of HTLV-1 PVL is critical for understanding clinical outcomes and to evaluate therapeutic intervention of HTLV-1 infected patients. For example, several studies demonstrated that the HTLV-1 PVL is higher in TSP/HAM patients than in asymptomatic individuals [128–130], suggesting that the PVL could be a good prognostic marker of disease development [129, 131]. HTLV-1 transmission studies showed that sexual and mother-to-child transmission are associated with a higher PVL [16, 114, 132].

PCR has also been useful for the characterization of full and partial HTLV-1 genomes in molecular epidemiological studies [33, 133, 134]. Most of our current understanding of HTLV-1 genome variability comes from the sequencing of viral coding genes (*Gag*, *Env*, *Pol*) and noncoding (LTR) regions. Sequencing capacity has substantially increased due to the use of new high-throughput technologies. A large set of complete HTLV-1 genome sequences from Brazil has recently been sequenced using this next-generation sequencing (NGS) technology [135].

Clonality of HTLV-1 Infection

The first demonstration of clonal integration of the HTLV-1 provirus in tumor cells of an ATL patient by SB analysis was crucial in establishing the causal link between HTLV-1 and cancer [136, 137].

The demonstration of integration of the HTLV-1 provirus in the cancer cells (leukemic, lymph-node, skin infiltrate, pleural, or ascites fluid) has been the gold standard for the diagnosis of ATL for nearly two decades [138–140]. Monoclonal integration of the HTLV-1 provirus is never detected by Southern blot in the malignant cells from patients with other T-cell malignancies, even in patients who are also HTLV-1 infected. Integrated proviruses in ATL are often defective with a conserved PX region. Only one copy is usually integrated in tumor cells, while two to three copies are detected in 5–20% of ATL cases [141]. This method is no longer used because it is time-consuming, costly, needs a radiolabeled probe, and requires a relatively large amount of DNA, especially when several digestions are needed. This method is also not very sensitive (1–5%). Other methods to detect and study HTLV-1 clonality have been developed using various PCR-based methods such as inverse PCR, ligation-mediated PCR, and inverse long PCR [142–146]. These PCR-based methods are more rapid and more sensitive than the classical SB assay. Studies using these techniques have shown that clonal expansion of infected cells is "a way of life" for HTLV-1 infection [147]. Indeed, clonal expansion of HTLV-1 infected cells occurs in asymptomatic carriers and in TSP/HAM patients [146]. These assays clearly show that ATL appears on a previously established background of clonally expanding HTLV-1 infected cells [143]. It has also been possible to demonstrate that lymphocytes cross the blood-brain barrier in TSP/HAM patients, based on the identification of common integration sites in lymphocytes from cerebrospinal fluid blood [148]. The use of PCR-based methods has also shown that persistent clonal expansion of HTLV-1 infected circulating cells occurs over the course of several years in asymptomatic infected carriers, as well as in ATL and TSP/HAM patients [146, 149]. These methods have also been successfully applied to the study of HTLV-2 and STLV-1 infection [150, 151]. HTLV-1 clonality and integration sites have more recently been analyzed using a novel high-throughput method [152, 153]. This has led to the development of the oligoclonality index, which is used to estimate the size and distribution of HTLV-1 clones [152, 153]. These methods and their application are described, in detail, in the chapter (Chapter 10) by C. Bangham in this book. This assay has also been applied to the study of HTLV-2 [154]. A novel high-throughput method to investigate the clonality of HTLV-1 infected cells, based on proviral integration, has also been recently developed and validated [155].

In conclusion, diagnosis of epidemiological aspects of HTLV-1 infection remains mainly based on serological screening and confirmatory tests as well as quantitative PCR. Meanwhile, recent technological innovations for both serological and molecular aspects (e.g., digital droplet PCR and NGS technologies) are increasingly implemented.

References

1. Poiesz BJ, Ruscetti FW, Gazdar AF, Bunn PA, Minna JD, Gallo RC (1980) Detection and isolation of type C retrovirus particles from fresh and cultured lymphocytes of a patient with cutaneous T-cell lymphoma. Proc Natl Acad Sci U S A 77(12):7415–7419
2. (1996) Human T-cell lymphotropic viruses. IARC Monogr Eval Carcinog Risks Hum 67: 261–390
3. Takatsuki K, Uchiyama T, Sagawa K, Yodoi J (1977) Adult T cell leukemia in Japan. In: Seno S, Takaku F, Irino S (eds) Topics in hematology. Excerpta Medica, Amsterdam, pp 73–77
4. Yoshida M, Miyoshi I, Hinuma Y (1982) Isolation and characterization of retrovirus from cell lines of human adult T-cell leukemia and its implication in the disease. Proc Natl Acad Sci U S A 79(6):2031–2035
5. Gessain A, Barin F, Vernant JC et al (1985) Antibodies to human T-lymphotropic virus type-I in patients with tropical spastic paraparesis. Lancet 2(8452):407–410
6. Goncalves DU, Proietti FA, Ribas JG et al (2010) Epidemiology, treatment, and prevention of human T-cell leukemia virus type 1-associated diseases. Clin Microbiol Rev 23(3):577–589
7. Gessain A, Cassar O (2012) Epidemiological aspects and world distribution of HTLV-1 infection. Front Microbiol 3:388
8. Proietti FA, Carneiro-Proietti AB, Catalan-Soares BC, Murphy EL (2005) Global epidemiology of HTLV-I infection and associated diseases. Oncogene 24(39):6058–6068
9. Verdonck K, Gonzalez E, Van Dooren S, Vandamme AM, Vanham G, Gotuzzo E (2007) Human T-lymphotropic virus 1: recent knowledge about an ancient infection. Lancet Infect Dis 7(4):266–281
10. Mueller N (1991) The epidemiology of HTLV-I infection. Cancer Causes Control 2(1):37–52
11. Plancoulaine S, Buigues RP, Murphy EL et al (1998) Demographic and familial characteristics of HTLV-1 infection among an isolated, highly endemic population of African origin in French Guiana. Int J Cancer 76(3):331–336
12. Gerard Y, Lepere JF, Pradinaud R et al (1995) Clustering and clinical diversity of adult T-cell leukemia/lymphoma associated with HTLV-I in a remote black population of French Guiana. Int J Cancer 60(6):773–776
13. Azarpazhooh MR, Hasanpour K, Ghanbari M et al (2012) Human T-lymphotropic virus type 1 prevalence in Northeastern Iran, Sabzevar: an epidemiologic-based study and phylogenetic analysis. AIDS Res Hum Retroviruses 28(9)
14. Hino S (2011) Establishment of the milk-borne transmission as a key factor for the peculiar endemicity of human T-lymphotropic virus type 1 (HTLV-1): the ATL Prevention Program Nagasaki. Proc Jpn Acad Ser B Phys Biol Sci 87(4):152–166
15. Ureta-Vidal A, Angelin-Duclos C, Tortevoye P et al (1999) Mother-to-child transmission of human T-cell-leukemia/lymphoma virus type I: implication of high antiviral antibody titer and high proviral load in carrier mothers. Int J Cancer 82(6):832–836
16. Roucoux DF, Wang B, Smith D et al (2005) A prospective study of sexual transmission of human T lymphotropic virus (HTLV)-I and HTLV-II. J Infect Dis 191(9):1490–1497
17. Okochi K, Sato H, Hinuma Y (1984) A retrospective study on transmission of adult T cell leukemia virus by blood transfusion: seroconversion in recipients. Vox Sang 46(5):245–253
18. Manns A, Murphy EL, Wilks R et al (1991) Detection of early human T-cell lymphotropic virus type I antibody patterns during seroconversion among transfusion recipients. Blood 77(4):896–905
19. Iwanaga M, Watanabe T, Yamaguchi K (2012) Adult T-cell leukemia: a review of epidemiological evidence. Front Microbiol 3:322
20. Plumelle Y, Pascaline N, Nguyen D et al (1993) Adult T-cell leukemia-lymphoma: a clinico-pathologic study of twenty-six patients from Martinique. Hematol Pathol 7(4):251–262
21. Blank A, Yamaguchi K, Blank M, Zaninovic V, Sonoda S, Takatsuki K (1993) Six Colombian patients with adult T-cell leukemia/lymphoma. Leuk Lymphoma 9(4–5):407–412
22. Pombo-de-Oliveira MS, Carvalho SM, Borducchi D et al (2001) Adult T-cell leukemia/lymphoma and cluster of HTLV-I associated diseases in Brazilian settings. Leuk Lymphoma 42(1–2):135–144
23. Matutes E, Taylor GP, Cavenagh J et al (2001) Interferon alpha and zidovudine therapy in adult T-cell leukaemia lymphoma: response and outcome in 15 patients. Br J Haematol 113(3):779–784
24. Gessain A, Gout O, Saal F et al (1990) Epidemiology and immunovirology of human

T-cell leukemia/lymphoma virus type I-associated adult T-cell leukemia and chronic myelopathies as seen in France. Cancer Res 50(17 Suppl):5692S–5696S

25. Harrington WJ Jr, Ucar A, Gill P et al (1995) Clinical spectrum of HTLV-I in south Florida. J Acquir Immune Defic Syndr Hum Retrovirol 8(5):466–473
26. Kirkland MA, Frasca J, Bastian I (1991) Adult T-cell leukaemia lymphoma in an aborigine. Aust N Z J Med 21(5):739–741
27. Einsiedel L, Cassar O, Bardy P, Kearney D, Gessain A (2013) Variant human T-cell lymphotropic virus type 1c and adult T-cell leukemia, Australia. Emerg Infect Dis 19(10):1639–1641
28. Jogessar VB, de Bruyn CC, Bhigjee AI, Naicker VL, Bill PL, Tait D (1992) Adult T-cell leukaemia/lymphoma associated with HTLV-I in *Natal*. S Afr Med J 81(10):528–529
29. Veelken H, Kohler G, Schneider J et al (1996) HTLV-I-associated adult T cell leukemia/lymphoma in two patients from Bucharest, Romania. Leukemia 10(8):1366–1369
30. Yamaguchi K, Watanabe T (2002) Human T lymphotropic virus type-I and adult T-cell leukemia in Japan. Int J Hematol 76(Suppl 2):240–245
31. Gessain A, Gout O (1992) Chronic myelopathy associated with human T-lymphotropic virus type I (HTLV-I). Ann Intern Med 117(11):933–946
32. Gotuzzo E, Cabrera J, Deza L et al (2004) Clinical characteristics of patients in Peru with human T cell lymphotropic virus type 1-associated tropical spastic paraparesis. Clin Infect Dis 39(7):939–944
33. Gessain A, Gallo RC, Franchini G (1992) Low degree of human T-cell leukemia/lymphoma virus type I genetic drift in vivo as a means of monitoring viral transmission and movement of ancient human populations. J Virol 66(4):2288–2295
34. Mahieux R, Ibrahim F, Mauclere P et al (1997) Molecular epidemiology of 58 new African human T-cell leukemia virus type 1 (HTLV-1) strains: identification of a new and distinct HTLV-1 molecular subtype in Central Africa and in Pygmies. J Virol 71(2):1317–1333
35. Cassar O, Capuano C, Bassot S et al (2007) Human T lymphotropic virus type 1 subtype C melanesian genetic variants of the Vanuatu Archipelago and Solomon Islands share a common ancestor. J Infect Dis 196(4):510–521
36. Kazanji M, Mouinga-Ondeme A, Lekana-Douki-Etenna S et al (2015) Origin of HTLV-1 in hunters of nonhuman primates in Central Africa. J Infect Dis 211(3):361–365
37. Filippone C, Betsem E, Tortevoye P et al (2015) A severe bite from a nonhuman primate is a major risk factor for HTLV-1 infection in hunters from Central Africa. Clin Infect Dis 60(11):1667–1676
38. Courouce AM, Pillonel J, Saura C (1999) Screening of blood donations for HTLV-I/II. Transfus Med Rev 13(4):267–274
39. Thorstensson R, Albert J, Andersson S (2002) Strategies for diagnosis of HTLV-I and -II. Transfusion 42(6):780–791
40. Gessain A, Dezzuti CS, Cowan EP, Lal RB (2007) Huamn T-cell lymphotropic viruses types 1 and 2. In: Murray PR, Baron EJ, Jorgensen JH, Landry ML, Pfailler MA (eds) Manual of clinical microbiology, vol 2, 9th edn. ASM Press, Washington, DC, pp 1330–1339
41. Lal RB (1996) Delineation of immunodominant epitopes of human T-lymphotropic virus types I and II and their usefulness in developing serologic assays for detection of antibodies to HTLV-I and HTLV-II. J Acquir Immune Defic Syndr Hum Retrovirol 13(Suppl 1):S170–S178
42. Parker SP, Taylor MB, Ades AE, Cubitt WD, Peckham C (1995) Use of dried blood spots for the detection and confirmation of HTLV-I specific antibodies for epidemiological purposes. J Clin Pathol 48(10):904–907
43. Hogan C, Iles J, Frost EH et al (2016) Epidemic history and iatrogenic transmission of blood-borne viruses in mid-20th century Kinshasa. J Infect Dis 214(3)
44. Boa-Sorte N, Purificacao A, Amorim T, Assuncao L, Reis A, Galvao-Castro B (2014) Dried blood spot testing for the antenatal screening of HTLV, HIV, syphilis, toxoplasmosis and hepatitis B and C: prevalence, accuracy and operational aspects. Braz J Infect Dis 18(6):618–624
45. Matsubara F, Haraguchi K, Harada K, Koizumi A (2012) Screening for antibodies to human T-cell leukemia virus type I in Japanese breast milk. Biol Pharm Bull 35(5):773–776
46. Oelemann WM, Lowndes CM, Verissimo Da Costa GC et al (2002) Diagnostic detection of human immunodeficiency virus type 1 antibodies in urine: a brazilian study. J Clin Microbiol 40(3):881–885
47. Miyoshi I, Sawada T, Iwahara Y, Ishii K, Kubonishi I, Taguchi H (1992) Excretion of HTLV-I in saliva. JAMA 267(2):236
48. Biggar RJ, Saxinger C, Gardiner C et al (1984) Type-I HTLV antibody in urban and rural Ghana, West Africa. Int J Cancer 34(2):215–219

49. Andersson S, Thorstensson R, Ramirez KG et al (1999) Comparative evaluation of 14 immunoassays for detection of antibodies to the human T-lymphotropic virus types I and II using panels of sera from Sweden and West Africa. Transfusion 39(8):845–851
50. Malm K, Kjerstadius T, Andersson S (2010) Evaluation of a new screening assay for HTLV-1 and -2 antibodies for large-scale use. J Med Virol 82(9):1606–1611
51. Qiu X, Hodges S, Lukaszewska T et al (2008) Evaluation of a new, fully automated immunoassay for detection of HTLV-I and HTLV-II antibodies. J Med Virol 80(3): 484–493
52. Berini CA, Susana Pascuccio M, Bautista CT et al (2008) Comparison of four commercial screening assays for the diagnosis of human T-cell lymphotropic virus types 1 and 2. J Virol Methods 147(2):322–327
53. Fujino R, Kawato K, Ikeda M, Miyakoshi H, Mizukoshi M, Imai J (1991) Improvement of gelatin particle agglutination test for detection of anti-HTLV-I antibody. Jpn J Cancer Res 82(4):367–370
54. Ikeda M, Fujino R, Matsui T, Yoshida T, Komoda H, Imai J (1984) A new agglutination test for serum antibodies to adult T-cell leukemia virus. Gann 75(10):845–848
55. Maeda Y, Imai J, Kiyokawa H, Kanamura M, Hino S (1989) Performance certification of gelatin particle agglutination assay for anti-HTLV-1 antibody: inconclusive positive results. Jpn J Cancer Res 80(10):915–919
56. Satake M, Yamaguchi K, Tadokoro K (2012) Current prevalence of HTLV-1 in Japan as determined by screening of blood donors. J Med Virol 84(2):327–335
57. Furuta RA, Ma G, Matsuoka M, Otani S, Matsukura H, Hirayama F (2015) Reevaluation of confirmatory tests for human T-cell leukemia virus Type 1 using a luciferase immunoprecipitation system in blood donors. Transfusion:880–889
58. Gallego S, Recalde A, Gastaldello R, Isa M, Nates S, Medeot S (1997) Kinetics study of human retrovirus antigens expression in T lymphocytic cell lines by indirect immunofluorescence assay. Viral Immunol 10(3): 149–157
59. Gallo D, Penning LM, Hanson CV (1991) Detection and differentiation of antibodies to human T-cell lymphotropic virus types I and II by the immunofluorescence method. J Clin Microbiol 29(10):2345–2347
60. Mahieux R, Horal P, Mauclere P et al (2000) Human T-cell lymphotropic virus type 1 gag indeterminate western blot patterns in Central Africa: relationship to Plasmodium falciparum infection. J Clin Microbiol 38(11):4049–4057
61. Agbalika F, Honderlick P, Ferchal F, Perol Y (1991) Use of PCR amplification for diagnosis of HTLV-I infection after blood transfusion. Mol Cell Probes 5(5):345–349
62. Cesaire R, Bera O, Maier H et al (1999) Seroindeterminate patterns and seroconversions to human T-lymphotropic virus type I positivity in blood donors from Martinique, French West Indies. Transfusion 39(10): 1145–1149
63. Gessain A, Caudie C, Gout O et al (1988) Intrathecal synthesis of antibodies to human T lymphotropic virus type I and the presence of IgG oligoclonal bands in the cerebrospinal fluid of patients with endemic tropical spastic paraparesis. J Infect Dis 157(6):1226–1234
64. Gallo D, Penning LM, Diggs JL, Hanson CV (1994) Sensitivities of radioimmunoprecipitation assay and PCR for detection of human T-lymphotropic type II infection. J Clin Microbiol 32(10):2464–2467
65. Lillehoj EP, Alexander SS, Dubrule CJ et al (1990) Development and evaluation of a human T-cell leukemia virus type I serologic confirmatory assay incorporating a recombinant envelope polypeptide. J Clin Microbiol 28(12):2653–2658
66. Roberts BD, Foung SK, Lipka JJ et al (1993) Evaluation of an immunoblot assay for serological confirmation and differentiation of human T-cell lymphotropic virus types I and II. J Clin Microbiol 31(2):260–264
67. Brodine SK, Kaime EM, Roberts C, Turnicky RP, Lal RB (1993) Simultaneous confirmation and differentiation of human T-lymphotropic virus types I and II infection by modified western blot containing recombinant envelope glycoproteins. Transfusion 33(11):925–929
68. Wiktor SZ, Alexander SS, Shaw GM et al (1990) Distinguishing between HTLV-I and HTLV-II by western blot. Lancet 335(8704):1533
69. Varma M, Rudolph DL, Knuchel M et al (1995) Enhanced specificity of truncated transmembrane protein for serologic confirmation of human T-cell lymphotropic virus type 1 (HTLV-1) and HTLV-2 infections by western blot (immunoblot) assay containing recombinant envelope glycoproteins. J Clin Microbiol 33(12):3239–3244
70. FDA US. 2014. http://www.fda.gov/BiologicsBloodVaccines/BloodBloodProducts/ApprovedProducts/LicensedProductsBLAs/BloodDonorScreening/InfectiousDisease/ucm080466.htm#anti_HTLV_Assays

71. CDC (1988) Licensure of screening tests for antibody to human T-lymphotropic virus type I. Morb Mortal Wkly Rep 37(736–40):45–47
72. CDC (1993) Recommendations for counseling persons infected with human T-lymphotrophic virus, types I and II. Centers for Disease Control and Prevention and U.S. Public Health Service Working Group. MMWR Recomm Rep 42:1–13
73. WHO (1990) Acquired immunodeficiency syndrome. proposed WH criteria for interpreting results from western blot assays for HIV-1, HIV-2 and HTLV-I/HTLV-II. Wkly Epidemiol Rec 65:281–283
74. HERN (1996) Seroepidemiology of the human T-cell leukaemia/lymphoma viruses in Europe. The HTLV European Research Network. J Acquir Immune Defic Syndr Hum Retrovirol 13(1):68–77
75. Zaaijer HL, Cuypers HT, Dudok de Wit C, Lelie PN (1994) Results of 1-year screening of donors in The Netherlands for human T-lymphotropic virus (HTLV) type I: significance of Western blot patterns for confirmation of HTLV infection. Transfusion 34(10):877–880
76. Khabbaz RF, Heneine W, Grindon A, Hartley TM, Shulman G, Kaplan J (1992) Indeterminate HTLV serologic results in U.S. blood donors: are they due to HTLV-I or HTLV-II? J Acquir Immune Defic Syndr 5(4):400–404
77. Zanjani DS, Shahabi M, Talaei N, Afzalaghaee M, Tehranian F, Bazargani R (2011) Molecular analysis of human T cell lymphotropic virus type 1 and 2 (HTLV-1/2) seroindeterminate blood donors from Northeast Iran: evidence of proviral tax, env, and gag sequences. AIDS Res Hum Retroviruses 27(2):131–135
78. Lu SC, Chen BH (2003) Seroindeterminate HTLV-1 prevalence and characteristics in blood donors in Taiwan. Int J Hematol 77(4):412–413
79. Costa JM, Segurado AC (2009) Molecular evidence of human T-cell lymphotropic virus types 1 and 2 (HTLV-1 and HTLV-2) infections in HTLV seroindeterminate individuals from Sao Paulo, Brazil. J Clin Virol 44(3):185–189
80. Garin B, Gosselin S, de The G, Gessain A (1994) HTLV-I/II infection in a high viral endemic area of Zaire, Central Africa: comparative evaluation of serology, PCR, and significance of indeterminate western blot pattern. J Med Virol 44(1):104–109
81. Gessain A, Mathieux R (1995) HTLV-I "indeterminate" western blot patterns observed in sera from tropical regions: the situation revisited. J Acquir Immune Defic Syndr Hum Retrovirol 9(3):316–319
82. Rouet F, Meertens L, Courouble G et al (2001) Serological, epidemiological, and molecular differences between human T-cell lymphotropic virus Type 1 (HTLV-1)-seropositive healthy carriers and persons with HTLV-I Gag indeterminate Western blot patterns from the Caribbean. J Clin Microbiol 39(4):1247–1253
83. Busch MP, Switzer WM, Murphy EL, Thomson R, Heneine W (2000) Absence of evidence of infection with divergent primate T-lymphotropic viruses in United States blood donors who have seroindeterminate HTLV test results. Transfusion 40(4):443–449
84. Abrams A, Akahata Y, Jacobson S (2011) The prevalence and significance of HTLV-I/II seroindeterminate Western blot patterns. Viruses 3(8):1320–1331
85. Berini CA, Eirin ME, Pando MA, Biglione MM (2007) Human Tcell lymphotropic virus types I and II (HTLV-I and -II) infection among seroindeterminate cases in Argentina. J Med Virol 79(1):69–73
86. Olah I, Fukumori LM, Smid J, de Oliveira AC, Duarte AJ, Casseb J (2010) Neither molecular diversity of the envelope, immunosuppression status, nor proviral load causes indeterminate HTLV western blot profiles in samples from human T-cell lymphotropic virus type 2 (HTLV-2)-infected individuals. J Med Virol 82(5):837–842
87. Martins ML, Santos AC, Namen-Lopes MS, Barbosa-Stancioli EF, Utsch DG, Carneiro-Proietti AB (2010) Long-term serological follow-up of blood donors with an HTLV-indeterminate western blot: antibody profile of seroconverters and individuals with false reactions. J Med Virol 82(10):1746–1753
88. Calattini S, Betsem E, Bassot S et al (2009) New strain of human T lymphotropic virus (HTLV) type 3 in a Pygmy from Cameroon with peculiar HTLV serologic results. J Infect Dis 199(4):561–564
89. Mahieux R, Gessain A (2011) HTLV-3/STLV-3 and HTLV-4 viruses: discovery, epidemiology, serology and molecular aspects. Viruses 3(7):1074–1090
90. Wolfe ND, Heneine W, Carr JK et al (2005) Emergence of unique primate T-lymphotropic viruses among central African bushmeat hunters. Proc Natl Acad Sci U S A 102(22):7994–7999
91. Calattini S, Chevalier SA, Duprez R et al (2005) Discovery of a new human T-cell lymphotropic virus (HTLV-3) in Central Africa. Retrovirology 2(1):30

92. Hayes CG, Burans JP, Oberst RB (1991) Antibodies to human T lymphotropic virus type I in a population from the Philippines: evidence for cross-reactivity with Plasmodium falciparum. J Infect Dis 163(2):257–262
93. Porter KR, Liang L, Long GW et al (1994) Evidence for anti-Plasmodium falciparum antibodies that cross-react with human T-lymphotropic virus type I proteins in a population in Irian Jaya, Indonesia. Clin Diagn Lab Immunol 1(1):11–15
94. Lal RB, Rudolph D, Alpers MP, Sulzer AJ, Shi YP, Lal AA (1994) Immunologic cross-reactivity between structural proteins of human T-cell lymphotropic virus type I and the blood stage of Plasmodium falciparum. Clin Diagn Lab Immunol 1(1):5–10
95. Jacob F, Santos-Fortuna E, Azevedo RS, Caterino-de-Araujo A (2008) Serological patterns and temporal trends of HTLV-1/2 infection in high-risk populations attending Public Health Units in Sao Paulo, Brazil. J Clin Virol 42(2):149–155
96. Mangano AM, Remesar M, del Pozo A, Sen L (2004) Human T lymphotropic virus types I and II proviral sequences in Argentinian blood donors with indeterminate Western blot patterns. J Med Virol 74(2):323–327
97. Mauclere P, Le Hesran JY, Mahieux R et al (1997) Demographic, ethnic, and geographic differences between human T cell lymphotropic virus (HTLV) type I-seropositive carriers and persons with HTLV-I Gag-indeterminate Western blots in Central Africa. J Infect Dis 176(2):505–509
98. Filippone C, Bassot S, Betsem E et al (2012) A new and frequent human T-cell leukemia virus indeterminate Western blot pattern: epidemiological determinants and PCR results in central African inhabitants. J Clin Microbiol 50(5):1663–1672
99. Sabino EC, Zrein M, Taborda CP, Otani MM, Ribeiro-Dos-Santos G, Saez-Alquezar A (1999) Evaluation of the INNO-LIA HTLV I/II assay for confirmation of human T-cell leukemia virus-reactive sera in blood bank donations. J Clin Microbiol 37(5):1324–1328
100. Zrein M, Louwagie J, Boeykens H et al (1998) Assessment of a new immunoassay for serological confirmation and discrimination of human T-cell lymphotropic virus infections. Clin Diagn Lab Immunol 5(1):45–49
101. Caterino-de-Araujo A, Sacchi CT, Goncalves MG et al (2015) Short communication: current prevalence and risk factors associated with human T lymphotropic virus type 1 and human T lymphotropic virus type 2 infections among HIV/AIDS patients in Sao Paulo, Brazil. AIDS Res Hum Retroviruses 31(5):543–549
102. Verdonck K, Gonzalez E, Maldonado F et al (2009) Comparison of three ELISAs for the routine diagnosis of human T-lymphotropic virus infection in a high-prevalence setting in Peru. Trans R Soc Trop Med Hyg 103(4):420–422
103. Burbelo PD, Ching KH, Mattson TL, Light JS, Bishop LR, Kovacs JA (2007) Rapid antibody quantification and generation of whole proteome antibody response profiles using LIPS (luciferase immunoprecipitation systems). Biochem Biophys Res Commun 352(4):889–895
104. Burbelo PD, Meoli E, Leahy HP et al (2008) Anti-HTLV antibody profiling reveals an antibody signature for HTLV-I-associated myelopathy/tropical spastic paraparesis (HAM/TSP). Retrovirology 5:96
105. McMahon EJ, Fang C, Layug L, Sandler SG (1995) Pooling blood donor samples to reduce the cost of HIV-1 antibody testing. Vox Sang 68(4):215–219
106. Chang CS, Wu YW, Pan YC, Chen ZY, Wang CS (2002) Feasibility of human T-lymphotropic virus type I screening using pooled sera. J Formos Med Assoc 101(11):775–778
107. Andersson S, Gessain A, Taylor GP (2001) Pooling of samples for seroepidemiological surveillance of human T-cell lymphotropic virus types I and II. Virus Res 78(1–2):101–106
108. Vandamme AM, Van Laethem K, Liu HF et al (1997) Use of a generic polymerase chain reaction assay detecting human T-lymphotropic virus (HTLV) types I, II and divergent simian strains in the evaluation of individuals with indeterminate HTLV serology. J Med Virol 52(1):1–7
109. Vet JA, Majithia AR, Marras SA et al (1999) Multiplex detection of four pathogenic retroviruses using molecular beacons. Proc Natl Acad Sci U S A 96(11):6394–6399
110. Heneine W, Khabbaz RF, Lal RB, Kaplan JE (1992) Sensitive and specific polymerase chain reaction assays for diagnosis of human T-cell lymphotropic virus type I (HTLV-I) and HTLV-II infections in HTLV-I/II-seropositive individuals. J Clin Microbiol 30(6):1605–1607
111. Liu H, Shah M, Stramer SL, Chen W, Weiblen BJ, Murphy EL (1999) Sensitivity and specificity of human T-lymphotropic virus (HTLV) types I and II polymerase chain reaction and several serologic assays in screening a population with a high prevalence of HTLV-II. Transfusion 39(11–12):1185–1193

112. Derse D, Heidecker G, Mitchell M, Hill S, Lloyd P, Princler G (2004) Infectious transmission and replication of human T-cell leukemia virus type 1. Front Biosci 9:2495–2499
113. Lins L, de Carvalho VJ, de Almeida Rego FF et al (2012) Oral health profile in patients infected with HTLV-1: clinical findings, proviral load, and molecular analysis from HTLV-1 in saliva. J Med Virol 84(9):1428–1436
114. Li HC, Biggar RJ, Miley WJ et al (2004) Provirus load in breast milk and risk of mother-to-child transmission of human T lymphotropic virus type I. J Infect Dis 190(7):1275–1278
115. Wattel E, Mariotti M, Agis F et al (1992) Quantification of HTLV-1 proviral copy number in peripheral blood of symptomless carriers from the French West Indies. J Acquir Immune Defic Syndr 5(9):943–946
116. Ono A, Mochizuki M, Yamaguchi K, Miyata N, Watanabe T (1995) Increased number of circulating HTLV-1 infected cells in peripheral blood mononuclear cells of HTLV-1 uveitis patients: a quantitative polymerase chain reaction study. Br J Ophthalmol 79(3):270–276
117. Feuer G, Fraser JK, Zack JA, Lee F, Feuer R, Chen IS (1996) Human T-cell leukemia virus infection of human hematopoietic progenitor cells: maintenance of virus infection during differentiation in vitro and in vivo. J Virol 70(6):4038–4044
118. Abbott MA, Poiesz BJ, Byrne BC, Kwok S, Sninsky JJ, Ehrlich GD (1988) Enzymatic gene amplification: qualitative and quantitative methods for detecting proviral DNA amplified in vitro. J Infect Dis 158(6):1158–1169
119. Lee TH, Chafets DM, Busch MP, Murphy EL (2004) Quantitation of HTLV-I and II proviral load using real-time quantitative PCR with SYBR Green chemistry. J Clin Virol 31(4):275–282
120. Dehee A, Cesaire R, Desire N et al (2002) Quantitation of HTLV-I proviral load by a TaqMan real-time PCR assay. J Virol Methods 102(1–2):37–51
121. Estes MC, Sevall JS (2003) Multiplex PCR using real time DNA amplification for the rapid detection and quantitation of HTLV I or II. Mol Cell Probes 17(2–3):59–68
122. Naderi M, Paryan M, Azadmanesh K, Rafatpanah H, Rezvan H, Mirab Samiee S (2012) Design and development of a quantitative real time PCR assay for monitoring of HTLV-1 provirus in whole blood. J Clin Virol 53(4):302–307
123. Besson G, Kazanji M (2009) One-step, multiplex, real-time PCR assay with molecular beacon probes for simultaneous detection, differentiation, and quantification of human T-cell leukemia virus types 1, 2, and 3. J Clin Microbiol 47(4):1129–1135
124. Moens B, Lopez G, Adaui V et al (2009) Development and validation of a multiplex real-time PCR assay for simultaneous genotyping and human T-lymphotropic virus type 1, 2, and 3 proviral load determination. J Clin Microbiol 47(11):3682–3691
125. Brunetto GS, Massoud R, Leibovitch EC et al (2014) Digital droplet PCR (ddPCR) for the precise quantification of human T-lymphotropic virus 1 proviral loads in peripheral blood and cerebrospinal fluid of HAM/TSP patients and identification of viral mutations. J Neurovirol 20(4):341–351
126. Rosadas C, Puccioni-Sohler M (2015) Relevance of retrovirus quantification in cerebrospinal fluid for neurologic diagnosis. J Biomed Sci 22:66
127. Pinheiro LB, Coleman VA, Hindson CM et al (2012) Evaluation of a droplet digital polymerase chain reaction format for DNA copy number quantification. Anal Chem 84(2): 1003–1011
128. Desdouits M, Cassar O, Maisonobe T et al (2013) HTLV-1-associated inflammatory myopathies: low proviral load and moderate inflammation in 13 patients from West Indies and West Africa. J Clin Virol 57(1):70–76
129. Nagai M, Usuku K, Matsumoto W et al (1998) Analysis of HTLV-I proviral load in 202 HAM/TSP patients and 243 asymptomatic HTLV-I carriers: high proviral load strongly predisposes to HAM/TSP. J Neurovirol 4(6):586–593
130. Lezin A, Olindo S, Oliere S et al (2005) Human T lymphotropic virus type I (HTLV-I) proviral load in cerebrospinal fluid: a new criterion for the diagnosis of HTLV-I-associated myelopathy/tropical spastic paraparesis? J Infect Dis 191(11):1830–1834
131. Takenouchi N, Yao K, Jacobson S (2004) Immunopathogensis of HTLV-I associated neurologic disease: molecular, histopathologic, and immunologic approaches. Front Biosci 9:2527–2539
132. Murphy EL, Lee TH, Chafets D et al (2004) Higher human T lymphotropic virus (HTLV) provirus load is associated with HTLV-I versus HTLV-II, with HTLV-II subtype A versus B, and with male sex and a history of blood transfusion. J Infect Dis 190(3):504–510
133. Cassar O, Einsiedel L, Afonso PV, Gessain A (2013) Human T-cell lymphotropic virus type 1 subtype C molecular variants among Indigenous Australians: new insights into the

molecular epidemiology of HTLV-1 in Australo-Melanesia. PLoS Negl Trop Dis 7(9)

134. Komurian F, Pelloquin F, de The G (1991) In vivo genomic variability of human T-cell leukemia virus type I depends more upon geography than upon pathologies. J Virol 65(7):3770–3778
135. Pessoa R, Watanabe JT, Nukui Y et al (2014) Molecular characterization of human T-cell lymphotropic virus type 1 full and partial genomes by Illumina massively parallel sequencing technology. PLoS One 9(3):e93374
136. Yoshida M, Seiki M, Yamaguchi K, Takatsuki K (1984) Monoclonal integration of human T-cell leukemia provirus in all primary tumors of adult T-cell leukemia suggests causative role of human T-cell leukemia virus in the disease. Proc Natl Acad Sci U S A 81(8):2534–2537
137. Wong-Staal F, Hahn B, Manzari V et al (1983) A survey of human leukaemias for sequences of a human retrovirus. Nature 302(5909):626–628
138. Ikeda S, Momita S, Kinoshita K et al (1993) Clinical course of human T-lymphotropic virus type I carriers with molecularly detectable monoclonal proliferation of T lymphocytes: defining a low- and high-risk population. Blood 82(7):2017–2024
139. Yamaguchi K, Seiki M, Yoshida M, Nishimura H, Kawano F, Takatsuki K (1984) The detection of human T cell leukemia virus proviral DNA and its application for classification and diagnosis of T cell malignancy. Blood 63(5):1235–1240
140. Gessain A, Moulonguet I, Flageul B et al (1990) Cutaneous type of adult T cell leukemia/lymphoma in a French West Indian woman. Clonal rearrangement of T-cell receptor beta and gamma genes and monoclonal integration of HTLV-I proviral DNA in the skin infiltrate. J Am Acad Dermatol 23(5 Pt 2):994–1000
141. Tamiya S, Matsuoka M, Etoh K et al (1996) Two types of defective human T-lymphotropic virus type I provirus in adult T-cell leukemia. Blood 88(8):3065–3073
142. Wattel E, Vartanian JP, Pannetier C, Wain-Hobson S (1995) Clonal expansion of human T-cell leukemia virus type I-infected cells in asymptomatic and symptomatic carriers without malignancy. J Virol 69(5):2863–2868
143. Cavrois M, Wain-Hobson S, Gessain A, Plumelle Y, Wattel E (1996) Adult T-cell leukemia/lymphoma on a background of clonally expanding human T-cell leukemia virus type-1-positive cells. Blood 88(12):4646–4650
144. Cavrois M, Wain-Hobson S, Wattel E (1995) Stochastic events in the amplification of HTLV-I integration sites by linker-mediated PCR. Res Virol 146(3):179–184
145. Takemoto S, Matsuoka M, Yamaguchi K, Takatsuki K (1994) A novel diagnostic method of adult T-cell leukemia: monoclonal integration of human T-cell lymphotropic virus type I provirus DNA detected by inverse polymerase chain reaction. Blood 84(9):3080–3085
146. Cavrois M, Gessain A, Wain-Hobson S, Wattel E (1996) Proliferation of HTLV-1 infected circulating cells in vivo in all asymptomatic carriers and patients with TSP/HAM. Oncogene 12(11):2419–2423
147. Wattel E, Cavrois M, Gessain A, Wain-Hobson S (1996) Clonal expansion of infected cells: a way of life for HTLV-I. J Acquir Immune Defic Syndr Hum Retrovirol 13(Suppl 1):S92–S99
148. Cavrois M, Gessain A, Gout O, Wain-Hobson S, Wattel E (2000) Common human T cell leukemia virus type 1 (HTLV-1) integration sites in cerebrospinal fluid and blood lymphocytes of patients with HTLV-1-associated myelopathy/tropical spastic paraparesis indicate that HTLV-1 crosses the blood-brain barrier via clonal HTLV-1-infected cells. J Infect Dis 182(4):1044–1050
149. Okayama A, Stuver S, Matsuoka M et al (2004) Role of HTLV-1 proviral DNA load and clonality in the development of adult T-cell leukemia/lymphoma in asymptomatic carriers. Int J Cancer 110(4):621–625
150. Gabet AS, Moules V, Sibon D et al (2006) Endemic versus epidemic viral spreads display distinct patterns of HTLV-2b replication. Virology 345(1):13–21
151. Gabet AS, Gessain A, Wattel E (2003) High simian T-cell leukemia virus type 1 proviral loads combined with genetic stability as a result of cell-associated provirus replication in naturally infected, asymptomatic monkeys. Int J Cancer 107(1):74–83
152. Gillet NA, Malani N, Melamed A et al (2011) The host genomic environment of the provirus determines the abundance of HTLV-1-infected T-cell clones. Blood 117(11):3113–3122
153. Berry CC, Gillet NA, Melamed A, Gormley N, Bangham CR, Bushman FD (2012) Estimating abundances of retroviral insertion sites from DNA fragment length data. Bioinformatics 28(6):755–762
154. Melamed A, Witkover AD, Laydon DJ et al (2014) Clonality of HTLV-2 in natural infection. PLoS Pathog 10(3):e1004006
155. Firouzi S, Lopez Y, Suzuki Y et al (2014) Development and validation of a new high-throughput method to investigate the clonality of HTLV-1-infected cells based on provirus integration sites. Genome Med 6(6):46

Chapter 2

Molecular Epidemiology Database for Sequence Management and Data Mining

Thessika Hialla Almeida Araújo, Filipe Ferreira de Almeida Rego, and Luiz Carlos Junior Alcantara

Abstract

A central database to aggregate sequence information from a range of epidemiological aspects including HTLV-1 pathogenesis, origin, and evolutionary dynamic would be useful to scientists and physicians worldwide. This Chapter describes two online tools for studies related to HTLV-1, the HTLV-1 Molecular Epidemiology Database and the HTLV-1 Subtyping Tool. The HTLV-1 Molecular Epidemiology Database is a tool for sequence management and data mining which allows researchers to download sequences with clinical and demographic information. The HTLV-1 Subtyping Tool is an online software used for HTLV-1 genotyping, the algorithm consists in the alignment of a query sequence with a carefully selected set of predefined reference strains, followed by phylogenetic analysis.

Key words HTLV-1 genotyping tool, HTLV molecular epidemiology, HTLV-1 database, LTR region, LASP HTLV-1

1 Introduction

The sequence analysis of HTLV is being a very useful tool with different approaches depending on the analyzed genomic region. The analysis of the LTR and envelope sequences of this virus is being used, in addition to mtDNA and Y chromosome analysis, to study the human migration and virus genotyping [1]. The HTLV pX gene analysis are useful to understand the functions of its generated proteins and their location into the cell [2], while the analysis of env, pol, and gag sequences has improved the knowledge of possible epitopes for vaccine design and helping to improve diagnostic methods [3, 4].

The HTLV nucleotide sequences, as well as from other viruses, are usually stored in the GenBank (http://www.ncbi.nlm.nih.gov). However, the GenBank lacks the task of giving appropriated sequences with clinical and demographic data for analysis and does not genotype viruses. Because of this was developed the HTLV-1 Molecular

Claudio Casoli (ed.), *Human T-Lymphotropic Viruses: Methods and Protocols*, Methods in Molecular Biology, vol. 1582,
DOI 10.1007/978-1-4939-6872-5_2,

Epidemiology Database, an online data mining tool that retrieves and stores annotated HTLV-1 proviral sequences from clinical, epidemiological, and geographical studies and the HTLV-1 Subtyping Tool [5–7].

2 Materials

In this case, all is needed is a computer with Internet connection and a spreadsheet reader. For analysis beyond the scope of this section, most of the software available can be viewed at http://www.bioinformaticssoftwareandtools.co.in/index.php.

3 Methods

3.1 HTLV-1 Molecular Epidemiology Database

The website interfaces were developed in HTML and server-side scripting written in PHP. The website interface contains specific search fields to allow various data combinations. User queries create a form (form tag) containing the values (variables) selected. This form generates a script that retrieves the data stored in the MySQL database. A second script organizes the data for display on the website, allowing for visualization of the information with the option to download the organized data. The developed database provides information regarding the indexed sequences in GenBank (*see* **Note 1**). In addition, all the sequences were genotyped using the LASP HTLV-1 Automated Subtyping Tool [7]. The user is able to choose search criteria and perform a query to generate an output of relevant sequences and information. The sequence output may be downloaded in FASTA format and the information table in Microsoft Excel spreadsheets .xls format. The HTLV-1 Molecular Epidemiology database is hosted on the Gonçalo Moniz Research Center/Oswaldo Cruz Foundation Research Center server with access at http://htlv1db.bahia.fiocruz.br/.

1. The HTLV-1 Molecular Epidemiology Database homepage displays interface (Fig. 1) that contains numerous fields for refining database queries.
2. One or more fields may be selected.
3. The remaining unused fields will be ignored when searching the database, but their values will be presented in the final result.
4. In the fields identified by the asterisk "*," the user may select multiple choices to make the search more efficient.
5. After choosing the search criteria (Fig. 2), click Run.
6. Next, the browser will be directed to a new page containing the results in table format (Fig. 3).

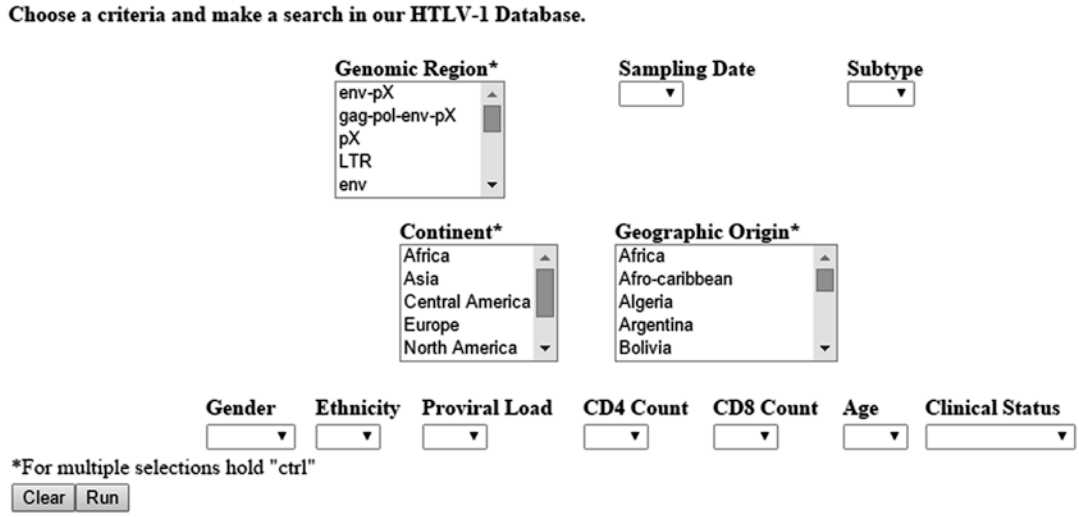

Fig. 1 HTLV-1 Molecular Epidemiology Database homepage displays interface

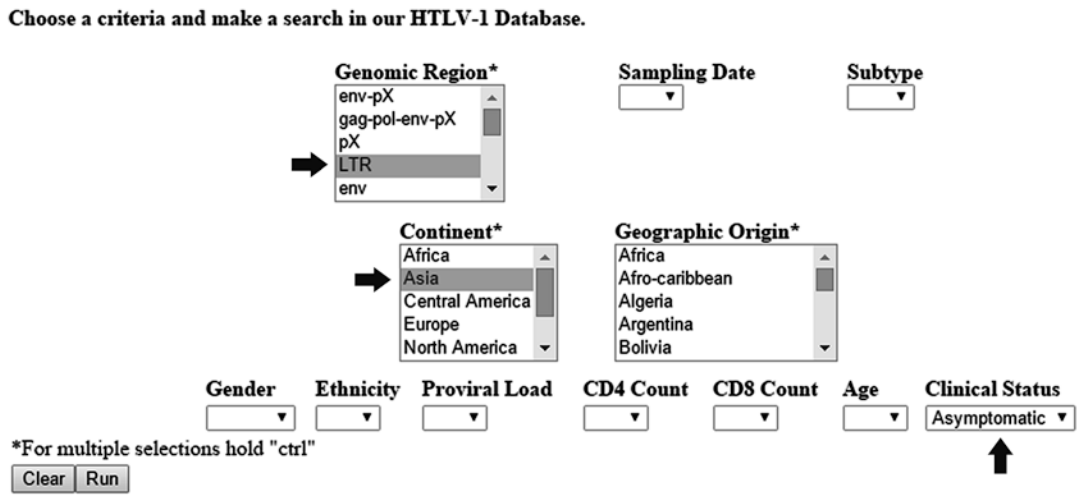

Fig. 2 Selection criteria to search in HTLV-1 Molecular Epidemiology Database homepage (example)

7. Next, select the sequences of interest (Fig. 4). If the user wants to select all sequences, the user should click in the first checkbox.
8. Next, the browser will be directed to the download page (Fig. 5), where the sequence can be downloaded as FASTA or CSV file (*see* **Notes 2** and **3**).
9. The downloaded sequences in FASTA format can be opened in almost all bioinformatics programs.
10. The CSV file can be imported into softwares (STATA, R) for statistical analysis of clinical and demographic information.

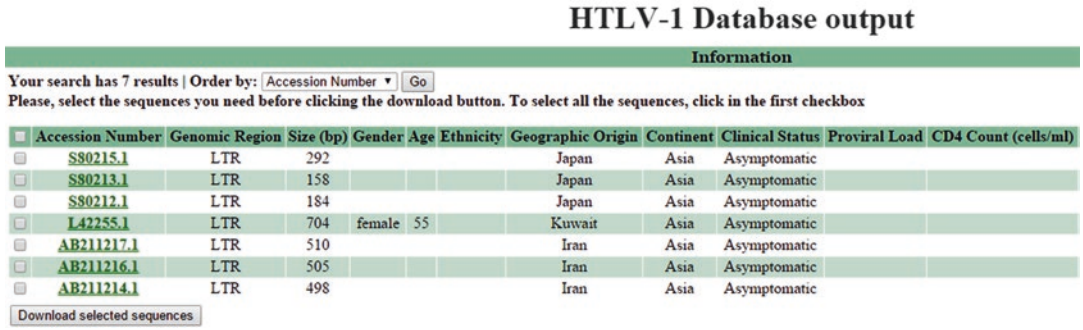
HTLV-1 Database output

Information

Your search has 7 results | Order by: Accession Number Go

Please, select the sequences you need before clicking the download button. To select all the sequences, click in the first checkbox

Accession Number	Genomic Region	Size (bp)	Gender	Age	Ethnicity	Geographic Origin	Continent	Clinical Status	Proviral Load	CD4 Count (cells/ml)
S80215.1	LTR	292				Japan	Asia	Asymptomatic		
S80213.1	LTR	158				Japan	Asia	Asymptomatic		
S80212.1	LTR	184				Japan	Asia	Asymptomatic		
L42255.1	LTR	704	female	55		Kuwait	Asia	Asymptomatic		
AB211217.1	LTR	510				Iran	Asia	Asymptomatic		
AB211216.1	LTR	505				Iran	Asia	Asymptomatic		
AB211214.1	LTR	498				Iran	Asia	Asymptomatic		

Download selected sequences

Fig. 3 Data presentation containing the search results

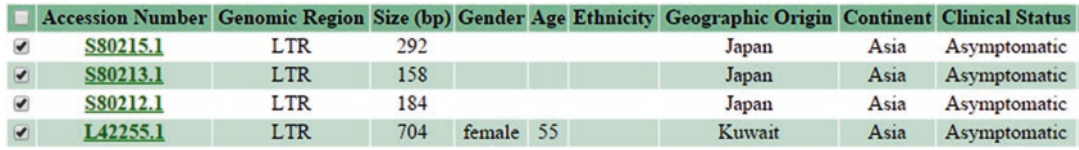

Accession Number	Genomic Region	Size (bp)	Gender	Age	Ethnicity	Geographic Origin	Continent	Clinical Status
S80215.1	LTR	292				Japan	Asia	Asymptomatic
S80213.1	LTR	158				Japan	Asia	Asymptomatic
S80212.1	LTR	184				Japan	Asia	Asymptomatic
L42255.1	LTR	704	female	55		Kuwait	Asia	Asymptomatic

Fig. 4 Selection of sequences of interest (*Checkbox marking*)

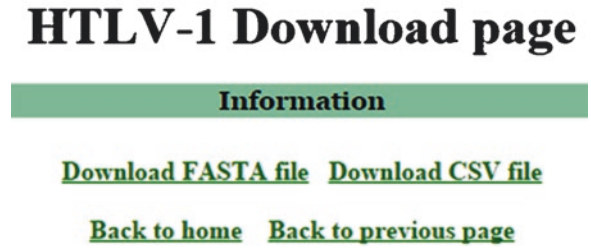
HTLV-1 Download page

Information

Download FASTA file Download CSV file

Back to home Back to previous page

Fig. 5 Page to download the sequences in Fasta format and CSV file containing clinical, phylogenetics and epidemiological data

3.2 HTLV-1 Subtyping Tool

The HTLV-1 Subtyping Tool was developed using Java programming and PHP scripts. This tool accepts up to 1000 sequences at a time (*see* **Notes 4** and **5**). In the first step of the analysis, the genomic region of reference sequence (ATK1 for HTLV-1) is identified using BLAST software. The second step involves the alignment of the query sequence with a complete reference dataset composed of all subtypes. The final step involves the construction of a phylogenetic tree using Tamura-Nei or HKY distance methods with a gamma distribution among site rate heterogeneity, as implemented in PAUP software [8].

A series of PHP scripts are used to read the XML output format produced by the JAVA program and create HTML report pages. The batch report contains information on the sequence name, length, assigned subtype and subgroup, and an illustration of the virus' genome. The HTLV-1 subtyping tool is hosted on the Africa Centre for Health and Population Studies bioinformatics

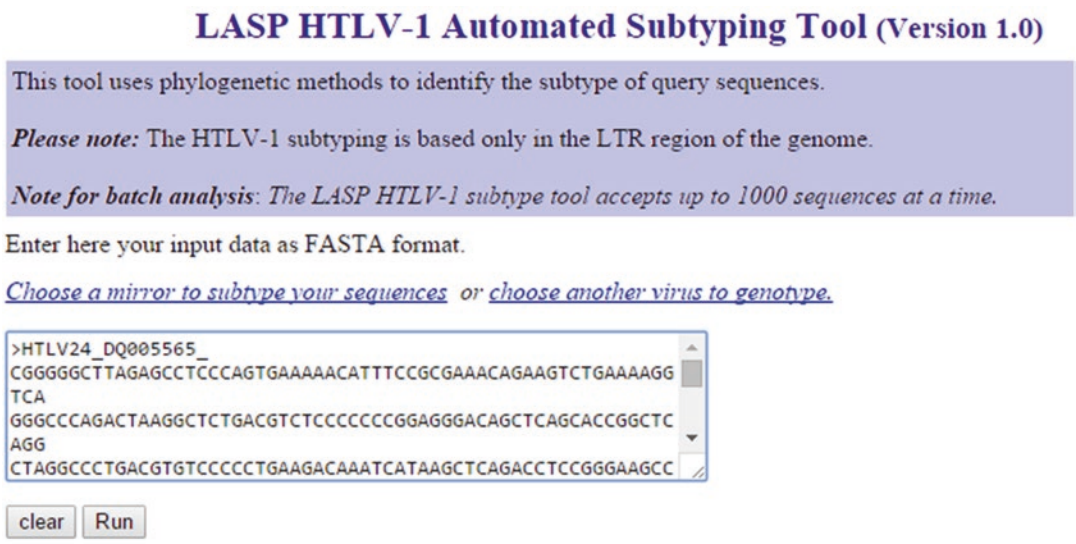

Fig. 6 HTLV-1 Subtyping Tool homepage interface: adding the sequence in FASTA format to run

group, UKZN, South Africa server with access at http://www.bioafrica.net/rega-genotype/html/indexhtlv.html/ (*see* **Note 1**).

1. This tool uses phylogenetic methods to identify the subtype of query sequences.
2. Enter here your input data as FASTA format, after, click Run (Fig. 6).
3. The batch report (Fig. 7) will be the batch report and contain information on the sequence name, length, assigned subtype, and a figure of the HTLV-1 genome. Accessing the report link will take the user to a report to each submitted sequence.
4. The sequence report (Fig. 8) will be composed of three areas named: sequence assignment, analysis details, and phylogenetic analyses.
5. The Sequence assignment contains information on (Fig. 8):
   (a) The sequence submitted (name and length).
   (b) The classification assignment (subtype, subgroup, and bootstrap support).
   (c) A graphical representation of the HTLV-1 genome showing the genomic region of the query sequence with the start and end positions related to the ATK1 genome.
   (d) The motivation of the classification (this is based on the decision tree).
6. The Phylogenetic analysis section contains (Fig. 8):
   (a) The phylogenetic tree in PDF and Nexus format,
   (b) The log file generated by PAUP (contains info on the model of evolution and its parameters).
   (c) The alignment used.

HTLV Genotyping Tool Results

Name	Length	Report	Assignment	Support	Genome
HTLV24_DQ005565_	719bp	Report	subtype_a(subgroup_A)	99.0	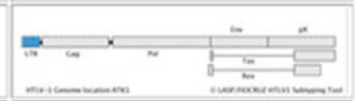
Ni3_Y16497_	719bp	Report	subtype_a(subgroup_B)	99.0	
IDUSSA_DQ005555_	757bp	Report	subtype_a(subgroup_A)	100.0	
BCI1-2_U32552_	693bp	Report	subtype_a(subgroup_A)	100.0	
test2	1190bp	Report	subtype_a(subgroup_B)	100.0	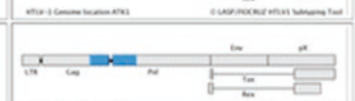
test	1318bp	Report	HTLV1	*NA*	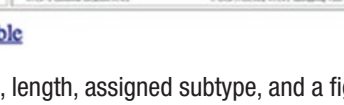

Download results: XML format, CSV table

Fig. 7 The batch report that contains information on the sequence name, length, assigned subtype, and a figure of the HTLV-1 genome. Accessing the report link will take the user to a report to each submitted sequence

Sequence Assignment

Sequence name : HTLV24_DQ005565_, length: 719 bps

Assignment: subtype_a(subgroup_A), Bootstrap: 99.0%

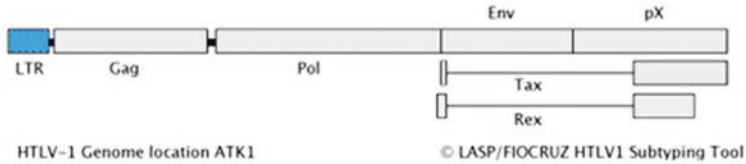

Your sequence start at position 53 and finish at position 769 in the ATK1 genome.
Motivation: *Subtype assigned based on sequence located in the LTR clustering with a HTLV1 subtype and/or subgroup with bootstrap > 60%*

Developed in cooperation with the Evolutionary Biology Group at University of Oxford, UK, the REGA Institute at the Katholieke Universiteit Leuven, Belgium and the Laboratorio Avancado de Saude Publica (LASP) CPqGM/FIOCRUZ, Brazil.

Analysis details

- Phylogenetic analyses
  This section contains the alignments, inferred phylogenetic trees, and detailed results of the evolutionary analysis.

Phylogenetic analyses

Phylogenetic analysis with pure subtypes:

- Export or View the Phylogenetic Tree: PDF, NEXUS format.
- View the PAUP* Log file (Contains bootstrap values for all HIV subtypes)
- Download the alignment (Nexus format).

Fig. 8 The sequence report will be composed of three areas named: sequence assignment, analysis details, and phylogenetic analyses

4 Notes

1. The access numbers in the output page are actual links to the respective sequence in the GenBank page.
2. The FASTA file features a header with the following structure: >accession number, serial number, genomic region, isolate, base pair, subtype and subgroup (if available).
3. The CSV file is a table containing all information presented in the search screen, along with a column called Sequence. That column matches the CSV file serial number, making it possible to relate the information in the CSV file with that in the FASTA file.
4. The HTLV-1 subtyping is based only in the LTR region of the genome.
5. The LASP HTLV-1 subtype tool accepts up to 1000 sequences at a time.

References

1. Brucato N, Cassar O, Tonasso L, Tortevoye P, Migot-Nabias F, Plancoulaine S, Guitard E, Larrouy G, Gessain A, Dugoujon J-M (2010) The imprint of the Slave Trade in an African American population: mitochondrial DNA, Y chromosome and HTLV-1 analysis in the Noir Marron of French Guiana. BMC Evol Biol 10:314
2. Van Prooyen N, Gold H, Andresen V, Schwartz O, Jones K, Ruscetti F, Lockett S, Gudla P, Venzon D, Franchini G (2010) Human T-cell leukemia virus type 1 p8 protein increases cellular conduits and virus transmission. Proc Natl Acad Sci U S A 107:20738–20743
3. Filippone C, Bassot S, Betsem E, Tortevoye P, Guillotte M, Mercereau-Puijalon O, Plancoulaine S, Calattini S, Gessain A (2012) A new and frequent human T-cell leukemia virus indeterminate Western blot pattern: epidemiological determinants and PCR results in central African inhabitants. J Clin Microbiol 50:1663–1672
4. Mota-Miranda ACA, Barreto FK, Amarante MFC, Batista E, Monteiro-Cunha JP, Farre L, Galvão-Castro B, Alcantara LCJ (2013) Molecular characterization of HTLV-1 gp46 glycoprotein from health carriers and HAM/TSP infected individuals. Virol J 10:75
5. Araujo THA, Barreto FK, Luiz Carlos Júnior A, Miranda ACAM (2014) Inferences about the global scenario of human T-cell lymphotropic virus type 1 infection using data mining of viral sequences. Mem Inst Oswaldo Cruz 109:448–451
6. Araujo THA, Souza-Brito LI, Libin P, Deforche K, Edwards D, de Albuquerque-Junior AE, Vandamme A-M, Galvao-Castro B, Alcantara LCJ (2012) A public HTLV-1 molecular epidemiology database for sequence management and data mining. PLoS One 7:e42123
7. Alcantara LCJ, Cassol S, Libin P, Deforche K, Pybus OG, Van Ranst M, Galvão-Castro B, Vandamme AM, de Oliveira T (2009) A standardized framework for accurate, high-throughput genotyping of recombinant and non-recombinant viral sequences. Nucleic Acids Res 37:634–642
8. Wilgenbusch JC and Swofford D (2003) Inferring evolutionary trees with PAUP. Curr Protoc Bioinformatics, Chapter 6, unit 6.4

Chapter 3

Reporter Systems to Study HTLV-1 Transmission

Christine Gross and Andrea K. Thoma-Kress

Abstract

The retrovirus Human T-lymphotropic virus type 1 (HTLV-1) preferentially infects $CD4^+$ T-cells via cell-to-cell transmission, while cell-free infection of T-cells is inefficient. Substantial insights into the different routes of transmission have largely been obtained by imaging techniques or by flow cytometry. Recently, strategies to quantify infection events with HTLV-1 improved. In this chapter, we present two different methods to quantitate virus transmission. Both methods are based on measuring gene activity of *luciferase* with a cost-saving *in-house* luciferase assay. First, we established a reporter Jurkat T-cell line carrying a *luciferase* gene under the control of the HTLV-1 core promoter U3R. Upon co-culture with chronically HTLV-1-infected T-cell lines, reporter cells are infected, and upon expression of the viral transactivator Tax, the viral promoter is activated resulting in enhanced luciferase activity. However, this assay as presented here does not exclude cell fusion as the mechanism allowing intracellular Tax-dependent activation of *luciferase* gene expression. Therefore, we describe a second method, the single-cycle replication-dependent reporter system developed by Mazurov et al. (PLoS Pathog 6:e1000788, 2010) that allows quantitation of HTLV-1 infection in co-cultured cells. Taken together, both methods facilitate quantitation of HTLV-1 transmission and will help to unravel pathways required for cell-to-cell transmission on a quantitative basis.

Key words HTLV-1, Tax, Transmission, U3R, Single-cycle replication-dependent reporter vector, Co-culture, Cell-to-cell transmission

1 Introduction

Substantial insights into transmission of the retrovirus Human T-lymphotropic virus type 1 (HTLV-1) have been obtained by imaging analysis and flow cytometry, which unraveled not only different routes of virus transmission, but also the localization of viral and cellular proteins during this process [1–4]. To quantitate HTLV-1 infection or HTLV-1-mediated cell-to-cell fusion events, co-culture assays between HTLV-1-infected T-cell lines and uninfected, transiently or stably transfected reporter cell lines were developed [3, 5, 6]. The latter carry a reporter gene (GFP, lacZ, luciferase) under control of the HTLV-1 long terminal repeat (LTR) containing the viral promoter, or amplifications of the

Claudio Casoli (ed.), *Human T-Lymphotropic Viruses: Methods and Protocols*, Methods in Molecular Biology, vol. 1582,
DOI 10.1007/978-1-4939-6872-5_3,

Tax-inducible HTLV-1 21 bp repeat [7]. After co-culture, cell-to-cell fusion and infection events occur, and upon expression of the viral transactivator Tax, the viral promoter is activated resulting in enhanced reporter gene activity in the reporter cells. To exclude passive Tax protein transfer eventually resulting in activation of reporter gene expression, improvements were required including irradiation of HTLV-1-infected donor cells before co-culture with reporter Jurkat T-cells [8]. However, one of the first assays allowing quantitative evaluation of HTLV-1 infection was an infectivity assay, which relied on a selectable indicator proviral clone to measure HTLV-1 cell-to-cell transmission in a single round of infection, but which took several weeks to yield experimental results [9]. In this chapter, we present two different methods to quantitate HTLV-1 transmission based on measuring reporter gene activity of *luciferase* with a cost-saving *in-house* luciferase assay. The first method relies on co-culture of chronically HTLV-1-infected T-cell lines with a newly established reporter Jurkat T-cell line Jurkat-U3R-Luc, while the second is based on transient transfection of a single-cycle replication-dependent reporter system [10].

1.1 Reporter T-Cell Line Jurkat-U3R-Luc

First, we cloned the core promoter U3R of HTLV-1, which is located in the 5′ long terminal repeat of the proviral DNA, from the construct pGL3-U3R [11] into the selectable luciferase reporter vector pGL4.20 (pGL4.20 [luc2/Puro]) (Promega, Madison, WI, USA) via *Xho*I/*Hind*III sites. Next, we tested the functionality of the newly generated vector pGL4.20-U3R upon transient transfection of Jurkat T-cells. Compared to the empty vector (pGL4.20), the reporter vector pGL4.20-U3R was strongly transactivated by Tax, but not by the CREB-deficient Tax-mutant M47 (Fig. 1a), confirming earlier observations obtained with different reporter vectors [12]. Thereafter, we established a reporter Jurkat T-cell line Jurkat-U3R-Luc and Jurkat-ctrl by culturing Jurkat T-cells transfected with pGL4.20-U3R or pGL4.20, respectively, in media supplemented with puromycin for 4 weeks. After confirming an increased luciferase activity upon transient transfection of Tax in Jurkat-U3R-Luc, but not in Jurkat-ctrl, cell stocks were prepared (data not shown). We set up a co-culture protocol of these Jurkat cell lines with HTLV-1-infected T-cell lines (MT-2, C91-PL, Fig. 1b), which is described in Subheading 3.1. Upon co-culture, the reporter Jurkat T-cells are infected, the viral transactivator Tax is expressed and is able to activate the U3R, thus, resulting in enhanced luciferase activity (Fig. 1c). This system allows for quantitation of fusion and transmission rates of differentially manipulated HTLV-1-infected T-cell lines (e.g., by small molecules or siRNAs) with co-cultured Jurkat-U3R-Luc cells. However, since transactivation of reporter gene activity could not only arise from new infections, but also from cell fusion (syncytia formation), we describe another, fusion-independent strategy [10], which could be performed in parallel.

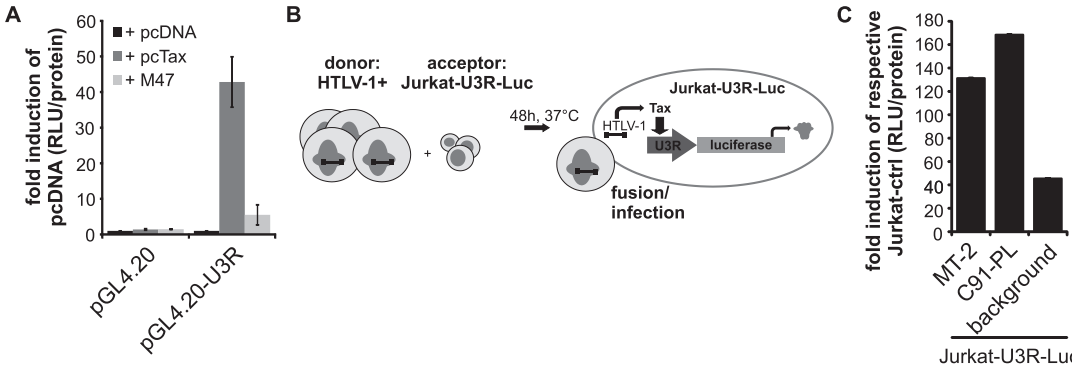

Fig. 1 Co-culture of HTLV-1-infected cells (MT-2 or C91-PL) with reporter Jurkat T-cells. (**a**) Functional testing of the reporter construct pGL4.20-U3R. Jurkat T-cells were transfected with pGL4.20-U3R or the control vector pGL4.20 and co-transfected with pcDNA3.1 (mock), pcTax (wild-type), or the Tax mutant pcTax-M47 (M47) that is deficient in CREB signaling. Luciferase activity was measured in relative light units (RLU) and normalized on protein content. Results are shown as mean RLU/protein ± standard error (SE) of two independent experiments performed in triplicates. (**b**) Model. The reporter T-cell line Jurkat-U3R-Luc carries a *luciferase* gene under control of the HTLV-1 core promoter U3R (3′ UTR and R-region of 5′ long terminal repeat). After co-culture with HTLV-1-infected donor cells (48 h, 37 °C) and fusion/infection events, the viral transactivator Tax activates the U3R, thus, enhancing luciferase. As a control, HTLV-1-infected donor cells are also co-cultured with Jurkat-ctrl cells, carrying a promoterless *luciferase* gene. (**c**) Validation of the reporter T-cell line Jurkat-U3R-Luc upon co-culture with the HTLV-1-infected cell lines MT-2, or C91-PL (ratio 1:1). Luciferase activity was measured in relative light units (RLU) and normalized on protein content (RLU/protein). In parallel, RLU/protein values were determined in co-cultures of HTLV-1-infected donor cells with Jurkat-ctrl cells carrying a promoterless *luciferase* gene. To determine the background activity, luciferase activity was also determined in reporter Jurkat T-cells without co-culture. Results are shown as mean fold induction of RLU/protein ± standard error (SE) over the Jurkat-ctrl cells of one representative experiment performed in triplicates

1.2 Single-Cycle Replication-Dependent Reporter System

The second method, a "one-step transfection/infection co-culture system" [10], was developed by Mazurov et al. and relies on a single-cycle replication-dependent reporter system to measure HTLV-1 transmission (Fig. 2a). This system requires transient transfection of a set of plasmids into donor cells and allows reporter gene expression in newly infected, co-cultured target cells upon reverse transcription only, but not in the transfected cells [10]. Virus packaging plasmids encoding full-length HTLV-1 (pCMVHT1-M; here: wild-type; wt), or carrying a deletion of the *Xho*I fragment in the *env* gene (pCMVHT1M-ΔXho; here: ΔEnv) are used [14]. The latter is pseudotyped with VSV-G (glycoprotein G of the vesicular stomatitis virus). In both packaging plasmids, the minus-strand primer binding site and virion RNA-packaging elements are absent. A CMV-driven *luciferase* (*luc*) gene (pCRU5HT1-inLuc) in antisense orientation that is interrupted by a *gamma-globin* intron in sense is employed as reporter gene. After transcription of the DNA, the intron is spliced via the splice donor (SD) and splice acceptor (SA) sites. The antisense orientation of the reporter gene does not allow translation of the reporter

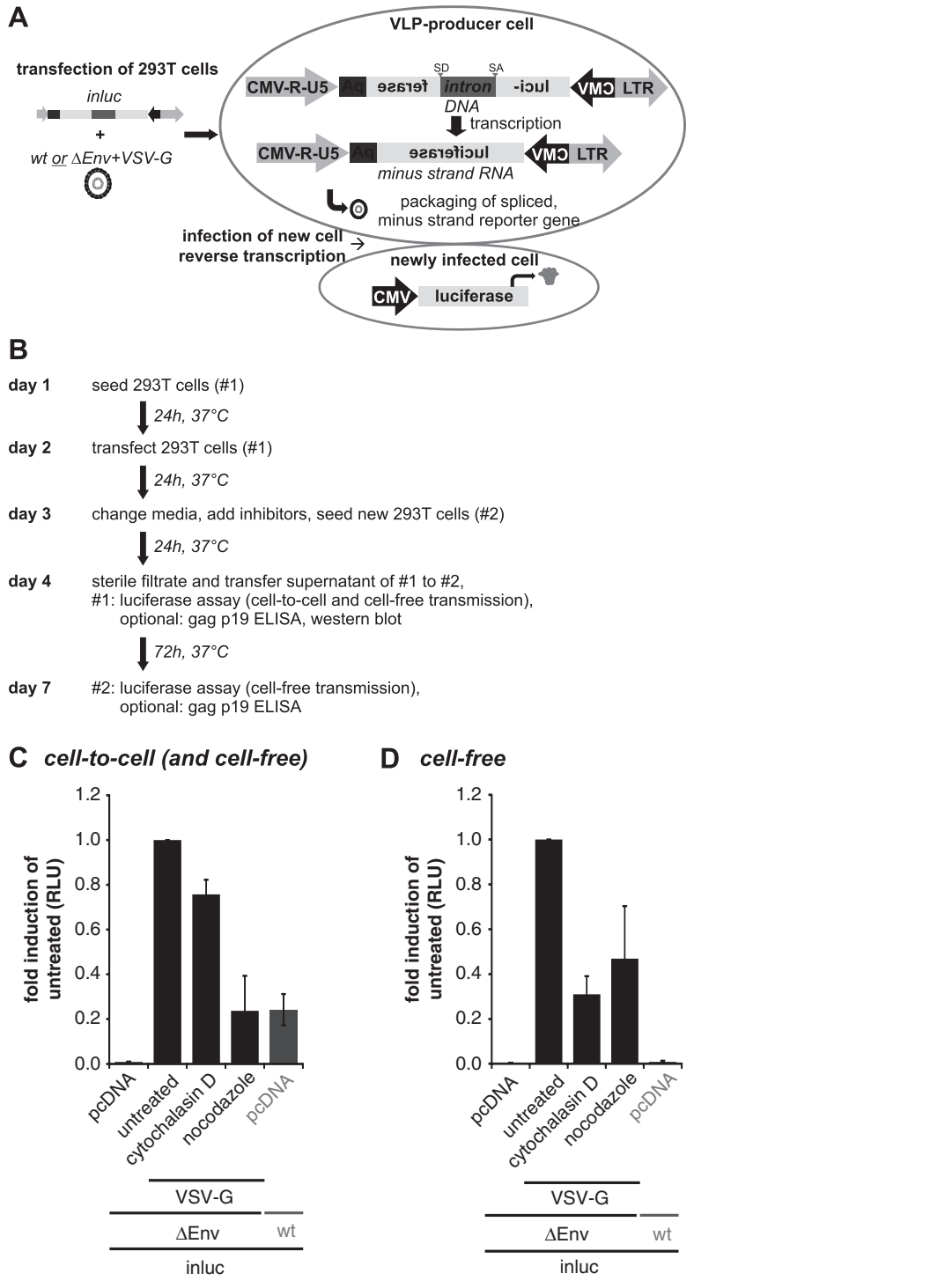

Fig. 2 Single-cycle replication-dependent reporter system to study HTLV-1 transmission. (**a**) Model. 293T cells are co-transfected with an HTLV-1-based reporter plasmid encoding a CMV-driven *luciferase* gene (reporter) in antisense that is interrupted by a sense-oriented intron and with an HTLV-1 packaging vector. The latter either encodes full-length HTLV-1 and the wild-type envelope (env) protein, or it carries a deletion of *env* and is pseudotyped by co-expression of VSV-G (glycoprotein G of the vesicular stomatitis virus). After transfection,

mRNA in transfected cells. This mRNA (minus strand RNA) is packaged into the aforementioned packaging plasmids. After infection of new cells, mRNA is reversely transcribed and the reporter gene (*luc*) is expressed in the target cell (Fig. 2a) [10]. In this chapter, we describe the experimental setup to use the reporter system in transiently transfected 293T cells (Fig. 2b), which allows monitoring of cell-to-cell (Fig. 2c) and cell-free transmission (Fig. 2d) of HTLV-1. Taken together, both methods facilitate quantitation of HTLV-1 transmission and will help to dissect pathways required for cell-to-cell transmission on a quantitative basis.

2 Materials

2.1 Reporter T-Cell Line Jurkat-U3R-Luc

1. Jurkat T-cells.
2. RPMI 1640 medium.
3. Panserin (Pan-Biotech, Aidenbach, Germany).
4. Fetal calf serum (FCS).
5. L-glutamine.
6. 100 U/ml Penicillin.
7. 100 μg/ml Streptomycin
8. Jurkat-U3R-Luc cells (carrying pGL4.20-U3R).
9. Jurkat-ctrl cells (carrying pGL4.20).
10. Puromycin.
11. HTLV-1-infected T-cell lines MT-2 [15].
12. HTLV-1-infected T-cell lines C91-PL [16].
13. Plasmids:
    (a) pGL4.20 (pGL4.20[luc2/Puro]; Promega).
    (b) pGL4.20-U3R (pGL4.20; *luc* gene under control of the U3R promoter of HTLV-1).

Fig. 2 (continued) DNA of the reporter is transcribed and the *gamma-globin* intron is spliced via the splice donor (SD) and splice acceptor (SA) sites. However, the *luciferase* gene cannot be expressed in the transfected cells due to its antisense orientation. After packaging of the minus strand RNA, new cells are infected. Upon reverse transcription, luciferase is expressed and can be measured. VLP, virus-like particle; CMV, cytomegalovirus; R, R region; pA, polyA signal; LTR, long terminal repeat. Modified after [10, 13]. (**b**) Experimental workflow. (**c**, **d**) Luciferase activities of 293T cells reflecting (**c**) cell-to-cell (and cell-free), or (**d**) only cell-free transmission of HTLV-1. (**c**) 293T cells were co-transfected with the reporter vector inluc, HTLV-1 wt packaging plasmids (*gray bar*), or ΔEnv packaging plasmids pseudotyped with VSV-G or nothing (pcDNA3.1; negative control). If required, total amounts of DNA were replenished to 2 μg with pcDNA3.1 (mock). Transfected cells were treated with cytochalasin D (5 μM) or nocodazole (5 μM) as indicated. 48 h after transfection, cell lysates for luciferase assays were obtained and supernatants were filtrated and transferred to new 293T cells. (**d**) After another 72 h, new 293T cells were lysed and luciferase activities were measured in relative light units (RLU). Results are shown as mean RLU ± standard error (SE) of three independent experiments performed in triplicates

(c) pcDNA3.1 (control vector; Invitrogen, Thermo Fisher Scientific, Waltham, MA, USA).

(d) pcTax (expression plasmid for wild-type Tax [12]).

(e) M47 (expression plasmid for CREB-deficient Tax mutant [12]).

14. Phosphate-buffered saline (without Ca^{2+} and Mg^{2+}) (PBSo): 137 mM NaCl, 2.68 mM KCl, 7.3 mM $Na_2HPO_4 \times 2H_2O$, 1.47 mM KH_2PO_4.
15. 2× lysis buffer:50 mM Tris–HCl (pH 7.8), 4 mM dithiothreitol (DTT), 3.8 mM *trans*-1,2-diaminocyclohexane-*N,N,N′,N′*-tetraacetic acid monohydrate (DCTA), 20% (v/v) glycerol, 2% (v/v) Triton X-100. Stored as 2× buffer at −20 °C, freshly diluted to 1× in H_2O when starting the experiment.
16. Assay buffer:100 mM KPO_4 (pH 7.8), 15 mM $MgSO_4$, 5 mM rATP. To avoid precipitates in the assay buffer, first provide water, then add KPO_4 followed by $MgSO_4$ and rATP. Stock solutions (1 M KPO_4 and 1 M $MgSO_4$) are stored at room temperature, 100 mM rATP (Roche Diagnostics, Indianapolis, USA) is stored at −20 °C.
17. Luciferase buffer: 1 mM D(−)-luciferin (Roche) in assay buffer. Protected from light. D(−)-Luciferin is stored at −20 °C.
18. Protein measurement according to Bradford [17] (e.g., Roti®-Quant; Carl Roth, Karlsruhe, Germany).
19. Cell culture flasks.
20. 48-well plates.
21. Thermomixer.
22. White plates.
23. Luminometer.
24. BioPhotometer.
25. Classical lab instrumentation: incubator, laminar flow workbench, centrifuge, reaction tubes.

2.2 Single-Cycle Replication-Dependent Reporter System

1. 293T cells.
2. Dulbecco's Modified Eagle's Medium (DMEM).
3. Plasmids.

(a) pCMVHT1-M; here: wild-type (wt): HTLV-1 packaging plasmid with wild-type envelope (env) [10, 14].

(b) pCMVHT1M-ΔXho; here: ΔEnv: HTLV-1 packaging plasmid with a deletion of the *Xho*I fragment in the *env* gene [14].

(c) pCRU5HT1-inLuc; here: inluc: CMV-driven firefly *luciferase* (*luc*) gene in antisense orientation that is interrupted by a *gamma-globin* intron [10], Addgene Plasmid #58954 (Addgene, Cambridge, MA, USA).

(d) pMD2.G (VSV-G; TronoLab, Geneva, Switzerland): expression plasmid for glycoprotein G of the vesicular stomatitis virus (for pseudotyping), Addgene Plasmid #12259.

(e) pcDNA3.1 (control vector; Invitrogen).

4. PBSo: *see* Subheading 2.1.
5. GeneJuice® (Novagen, Darmstadt, Germany), transfection reagent.
6. 5 μM cytochalasin D, inhibits actin polymerization.
7. 5 μM nocodazole, inhibits microtubule polymerization.
8. Dimethyl sulfoxide (DMSO), solvent of cytochalasin D and nocodazole.
9. Lysis buffer: *see* Subheading 2.1.
10. Assay buffer: *see* Subheading 2.1.
11. Luciferase buffer: *see* Subheading 2.1.
12. Protein measurement according to Bradford [17] (e.g., Roti®-Quant).
13. Cell culture flasks.
14. 12-well plates.
15. Sterile filters (0.45 μM pore size).
16. Sterile syringes (2 ml).
17. Thermomixer comfort.
18. White plates.
19. Luminometer.
20. BioPhotometer.
21. Classical lab instrumentation: incubator, laminar flow workbench, centrifuge, reaction tubes.
22. BSL3 and BSL2 laboratories.

3 Methods

3.1 Cell Cultures

1. Grow Jurkat T-cells in RPMI 1640 and Panserin (1:1) in RPMI 1640 supplemented with 10% fetal calf serum (FCS), L-glutamine and Penicillin (Pen; 100 U/ml)/Streptomycin (Strep; 100 μg/ml). Adjust on 5×10^5 cells/ml every 2–3 days, and keep cell culture flasks in a tilted position.
2. Grow Jurkat-U3R-Luc and Jurkat-ctrl cells, like Jurkat T-cells, in media supplemented with 0.25 μg/ml puromycin. Adjust on 5×10^5 cells/ml every 2–3 days, and keep cell culture flasks in a tilted position.
3. Grow HTLV-1-infected T-cell lines MT-2 and C91-PL in RPMI 1640 supplemented with 10% FCS, L-glutamine, and Pen/Strep, adjust on 2.5×10^5 cells/ml every 2–3 days. Keep cell cul-

ture flasks in a tilted position. If cells are growing well, split cells 1:4 every 2–3 days. Keep cells in a biosafety level (BSL) 3 laboratory, or according to the regulations of your country.

3.2 Reporter Cell Line Jurkat-U3R-Luc

1. Validate the functionality of the reporter construct pGL4.20-U3R: Transfect Jurkat T-cells with 25 μg pGL4.20 or pGL4.20-U3R and co-transfect the cells with 25 μg pcDNA3.1 (mock), pcTax (wild-type) [18] or the Tax-mutant pcTax-M47 (M47) [12] that is deficient in CREB signaling. Briefly, 10^7 Jurkat T-cells per preparation are transferred into an electroporation cuvette (PeqLab, Erlangen, Germany), pulsed (GenePulser Xcell TM Electroporation System; BioRad Laboratories, Munich, Germany; 290 V, 1500 μF, ~30 ms) and afterward transferred to 10 ml pre-warmed transfection medium without antibiotics [19]. After 48 h, cells are lysed and processed for luciferase assays as described in **steps 11–19**. A representative experiment is shown in Fig. 1a.
2. Grow stable cell line Jurkat-U3R-Luc and Jurkat-ctrl for several days.
3. Grow HTLV-1-infected T-cell lines MT-2 and C91-PL for several days (BSL3).
4. Count reporter cells (e.g., by using trypan blue and "Neubauer Improved" chamber), centrifuge 5×10^5 reporter Jurkat T-cells per sample (Jurkat-U3R-Luc, Jurkat-ctrl) (145 × *g* for 5 min at 20 °C), and remove supernatants. It is recommended to perform the experiment in triplicates.
5. Wash cell pellets once with PBSo (centrifuge 145 × *g*, 5 min, 20 °C) and add new media without puromycin (*see* **Note 1**).
6. Seed 500 μl of the reporter Jurkat T-cells (10^6 cells/ml) in a 48-well plate (*see* **Note 2**).
7. Count HTLV-1-infected cells (MT-2, C91-PL). Cells grow in large aggregates, therefore, transfer 1 ml of the cell suspension into a reaction tube and gently pipet cells up and down before counting. Count several independent samples.
8. Spin down HTLV-1-infected cells (0.125×10^6 cells per sample; ratio ($HTLV^+$/Jurkat) = (1:4)), and add 500 μl fresh medium. Add cells to seeded Jurkat-U3R-Luc and Jurkat-ctrl cells to obtain co-cultures (total volume 1 ml; *see* **Notes 3–7**).
9. Incubate the co-cultures at 37 °C for 48 h.
10. Transfer the co-cultured cells into a 1.5 ml reaction tube and centrifuge (145 × *g*, 5 min, 20 °C).
11. Prepare 1× luciferase lysis buffer by diluting 2× lysis buffer stored at −20 °C with H_2O.
12. Wash cell pellets once with PBSo (centrifuge 145 × *g*, 5 min, 20 °C), resuspend the cell pellets in 100 μl 1× luciferase lysis buffer, and transfer to a new reaction tube.

13. Incubate the samples for 30 min at 30 °C on a shaker (Thermomixer) to lyse cells. After efficient lysis, work could be continued under BSL2 conditions.
14. Centrifuge the samples (19,700 × *g*, 5 min, 4 °C), transfer the supernatants containing lysed proteins to a new tube and remove cell debris. Supernatants are kept on ice and used for the detection of luciferase signals and for measuring protein content. Supernatants can be stored at −80 °C.
15. Prepare the assay and luciferase buffer (*see* **Notes 8** and **9**).
16. Pipet 40 µl of each sample into a white 96-well plate.
17. Detect the luciferase signals using a luminometer. This differs depending on the device and programme you use in your laboratory. When using Orion II, connect the assay and luciferase buffer with the respective injectors. Before measuring each well, 50 µl assay buffer and 50 µl luciferase buffer are pumped into the well, and the plate is shaken for 2 s. Relative light units (RLU) are measured.
18. Determine the protein concentration in the supernatants obtained in **step 14**, e.g., by using Roti®-Quant. Dilute Roti®-Quant 1:5 in H_2O and pipet 1 µl protein per sample in 1 ml diluted Roti®-Quant. Measure protein content with a biophotometer using appropriate cuvettes and standard curves.
19. Normalize RLU (*see* **step 17**) on the respective protein content (*see* **step 18**), and calculate the mean of triplicate samples.
20. A representative experiment is shown in Fig. 1c.

3.3 Single-Cycle Replication-Dependent Reporter System

1. Seed 2.5 × 10^5 293T cells (#1) per sample in triplicates in a total volume of 1 ml in 12-well plates and incubate at 37 °C for 24 h. Grow the cells in DMEM supplemented with 10% FCS, L-glutamine, and Pen/Strep.
2. Continue working in the BSL3 or according to the regulations of your country.
3. For transfection with GeneJuice®, mix 50 µl DMEM with 3 µl GeneJuice® per sample and incubate for 5 min at 20 °C. Alternatively, you may use any transfection technique and reagent that is suitable for efficient transfection of 293T cells.
4. Transfer the GeneJuice®-DMEM mixture to the prepared DNA (*see* below) and incubate for 15 min at 20 °C. Transfection samples: mix 0.6 µg pCRU5HT1-inLuc (inluc; reporter), 0.4 µg pCRU5HT1M-ΔEnv (ΔEnv) and either 0.1 µg pcDNA3.1 (negative control) or 0.1 µg VSV-G (pseudotyped viruses). Prepare samples with inluc, ΔEnv and VSV-G four times (*see* **step 7**). Prepare a sample with 0.6 µg inluc, 0.4 µg pCRU5HT1M

(wild-type), and 0.1 μg pcDNA3.1 as a positive control (*see* **Notes 10** and **11**). Prepare all samples in technical triplicates.

5. Transfer the GeneJuice®-DMEM-DNA mixture to the seeded 293T cells and incubate for 24 h at 37 °C.
6. Remove and discard supernatants and change media of all samples to ensure even amounts of viruses in the supernatants of transfected 293T cells.
7. Leave cells transfected with inluc, ΔEnv and VSV-G untreated, or treat samples either with 5 μM cytochalasin D (inhibits actin polymerization), with 5 μM nocodazole (inhibits microtubule formation), or with DMSO (solvent control) (*see* **Note 12**).
8. Seed 1.8×10^5 293T cells (#2) per sample in triplicates in a total volume of 1 ml in 12-well plates and incubate for 24 h at 37 °C. Add one triplicate as negative control.
9. Sterile filtrate the supernatants of transfected 293T cells (#1) using filters and syringes. Take 100 μl of the supernatants and, if desired, measure gag p19 amounts using a gag p19 ELISA (*see* **Note 13**). Transfer the rest of the supernatants to newly seeded 293T cells (#2) and incubate for 72 h at 37 °C.
10. Prepare 1× lysis buffer.
11. Wash the cell pellets of transfected 293T cells (#1) in PBSo (centrifuge 145 × *g*, 5 min, 20 °C), discard the supernatants, resuspend the cell pellets in 100 μl of 1× luciferase lysis buffer, and transfer lysate to a new tube (*see* **Note 14**).
12. Discard the supernatants of the 293T cells (#2) after 72 h of incubation, wash the cell pellets in PBSo (centrifuge 145 × *g*, 5 min, 20 °C), discard the supernatants, resuspend the cell pellets in 100 μl of 1× luciferase lysis buffer, and transfer lysates to new tube (*see* **Note 15**).
13. Incubate samples (*see* **steps 11** and **12**) for 30 min at 30 °C on a shaker (Thermomixer comfort) to lyse cells. After efficient lysis, work could be continued under BSL 2 conditions.
14. Centrifuge the samples (centrifuge 19,700 × *g*, 5 min, 4 °C), transfer the supernatants containing lysed proteins to a new tube, and remove cell debris. Supernatants are kept on ice and used for the detection of luciferase signals and for measuring protein content. Supernatants can be stored at −80 °C.
15. Prepare the assay and luciferase buffer (*see* **Note 9**).
16. Pipet 40 μl of each sample (*see* **steps 11** and **12**) into a white 96-well plate.
17. Detect the luciferase signals using a luminometer. This differs depending on the device you use in your laboratory. When using Orion II, connect the assay and luciferase buffer with the respective injectors. Before measuring each well, 50 μl assay

buffer and 50 μl luciferase buffer are pumped into the well, and the plate is shaken for 2 s. Relative light units (RLU) are measured.

18. The means of three independent experiments each performed in triplicates are shown in Fig. 2c, d.
19. Design experiment according to your requirements (*see* **Notes 16–18**).

4 Notes

1. It is necessary to remove puromycin from the cell culture media of reporter Jurkat T-cells before setting up the co-culture experiment to avoid cell death of MT-2 or C91-PL cells.
2. If you plan to analyze numerous samples, it is possible to use 96-well plates (round bottom). In this case, only seed 10^5 Jurkat T-cells and add cells to the co-culture in a total volume of 200 μl.
3. It is recommended to pretest your HTLV-1-infected donor cells to obtain the most efficient donor cell line. Best results should be obtained with HTLV-1-infected C91-PL cells [5, 20]; however, a high degree of variation between experiments may occur compared to MT-2 cells [5]. Moreover, feel free to try different ratios of donor to acceptor cells, and different incubation periods.
4. If you irradiate HTLV-1-infected donor cells before co-culture with reporter Jurkat T-cells (ratio 1:1), passive Tax protein transfer from donor to acceptor cells should not occur [8]. In parallel, use C8166 cells as donor cells (control) since these cells are HTLV-1-infected, but do not produce infectious virus, and thus, do not enhance reporter gene activity [5, 8].
5. To block viral transmission and as a control for your experiments, pretreat reporter cells with 50 μM azidothymidine (AZT) and/or with sera (1:1000) from HTLV-1-infected donors 3 h before co-culture [8].
6. To block fusion, pretreat reporter cells with monoclonal antibodies against HTLV-1 envelope gp46 (LAT-27), which exhibit neutralizing activity not only in vitro [21] and in co-cultures between MT-2 cells and transiently transfected reporter Jurkat T-cells [5], but also in mice in vivo [22].
7. HTLV-1-infected T-cells secrete exosomes containing Tax and the exosomes are capable of inducing LTR-transactivation when added in excess (0.1, 1.0, or 10 μg) to uninfected CEM cells [23]. However, it is unlikely that in the settings described here, exosomes are responsible for the enhanced luciferase activity since non-concentrated supernatants of MT-2 cells do not enhance LTR-driven luciferase activity [5].

8. If you prefer to use commercially available lysis buffers and luciferase detection reagents, feel free to do so.
9. It is necessary to prepare the buffers freshly as luciferin is not stable and has to be protected from light. It is possible to keep samples at −80 °C until you perform the luciferase assay.
10. To prepare DNA of the HTLV-1 packaging and reporter plasmids from transformed bacteria, use recombination-deficient bacteria like STBL2 (Invitrogen) and incubate for at least 20 h at 30 °C. After isolation of DNA, check integrity of the plasmids by diagnostic digestion. All other plasmids can be amplified according to standard protocols.
11. The reporter system can also be used in transfected Jurkat T-cells as donor cells and Raji/CD4$^+$ B-cells as acceptor cells as described [10]. We also evaluated this co-culture system, but we transfected 10^7 Jurkat T-cells by electroporation using a GenePulser Xcell TM Electroporation System (BioRad Laboratories, Munich, Germany; 290 V, 1500 μF, ~30 ms) and 27.5 μg reporter construct, 17.5 μg packaging plasmid and 5 μg VSV-G or pcDNA3.1. Jurkat T-cells in co-culture with Raji/CD4$^+$ B-cells may be more suitable to study Tax-effects on virus transmission since Tax seems to enhance infection in a cell-type specific manner from Jurkat to Raji/CD4$^+$, but not in 293T cells [10].
12. Make sure that you only add small volumes of cytochalasin D or nocodazole to your cell culture as these reagents are dissolved in DMSO, which could affect cell viability.
13. If desired, gag p19 may be detected using ELISA in the culture supernatants (e.g., from Zeptometrix). Use an appropriate pre-dilution of your samples for the ELISA. In our experiments, we used 1:50 for 293T cells. Performing gag p19 ELISA allows for normalization of luciferase activity to the amount of the viral gag protein in the supernatants.
14. The luciferase signals of these samples reflect cell-to-cell and cell-free transmission of HTLV-1.
15. The luciferase signals of these samples reflect cell-free transmission of HTLV-1 as only cell-free supernatants are transferred to new 293T cells.
16. By using eYFP-based reporter vectors, cell fusion was ruled out as a mechanism of virus transmission since infected cells were not multinucleated [10].
17. To further evaluate the relevance of Tax in viral transmission, an HTLV-1 packaging vector pCMVHT1M-Tax9Q with mutated Tax carrying a nucleotide change creating a stop codon instead of glutamine at position 9 in the Tax coding region [10] may be used in cell lines sensitive to Tax's enhancing effect on virus transmission.

18. The experimental approach described here was recently modified by improving splicing and packaging of the reporter [13].

Acknowledgment

This work was supported by the DFG (SFB 796, C6).

The authors are grateful to Gisela Heidecker-Fanning from the laboratory of the late David Derse (HIV Drug Resistance Program, National Cancer Institute-Frederick, Frederick, Maryland, United States of America) for providing the single-cycle replication-dependent reporter system.

The authors disclaim all liability for direct or consequential damages resulting from the use of the methods described in this chapter.

References

1. Igakura T, Stinchcombe JC, Goon PK et al (2003) Spread of HTLV-I between lymphocytes by virus-induced polarization of the cytoskeleton. Science 299:1713–1716
2. Jones KS, Petrow-Sadowski C, Huang YK et al (2008) Cell-free HTLV-1 infects dendritic cells leading to transmission and transformation of CD4(+) T cells. Nat Med 14:429–436
3. Pais-Correia AM, Sachse M, Guadagnini S et al (2010) Biofilm-like extracellular viral assemblies mediate HTLV-1 cell-to-cell transmission at virological synapses. Nat Med 16:83–89
4. Van Prooyen N, Andresen V, Gold H et al (2010) Hijacking the T-cell communication network by the human T-cell leukemia/lymphoma virus type 1 (HTLV-1) p12 and p8 proteins. Mol Aspects Med 31:333–343
5. Pare ME, Gauthier S, Landry S et al (2005) A new sensitive and quantitative HTLV-I-mediated cell fusion assay in T cells. Virology 338:309–322
6. Astier-Gin T, Portail JP, Lafond F et al (1995) Identification of HTLV-I- or HTLV-II-producing cells by cocultivation with BHK-21 cells stably transfected with a LTR-lacZ gene construct. J Virol Methods 51:19–29
7. Liu M, Yang L, Zhang L et al (2008) Human T-cell leukemia virus type 1 infection leads to arrest in the G1 phase of the cell cycle. J Virol 82:8442–8455
8. Cachat A, Chevalier SA, Alais S et al (2013) Alpha interferon restricts human T-lymphotropic virus type 1 and 2 de novo infection through PKR activation. J Virol 87:13386–13396
9. Delamarre L, Rosenberg AR, Pique C et al (1997) A novel human T-leukemia virus type 1 cell-to-cell transmission assay permits definition of SU glycoprotein amino acids important for infectivity. J Virol 71:259–266
10. Mazurov D, Ilinskaya A, Heidecker G et al (2010) Quantitative comparison of HTLV-1 and HIV-1 cell-to-cell infection with new replication dependent vectors. PLoS Pathog 6:e1000788
11. Mann MC, Strobel S, Fleckenstein B et al (2014) The transcription elongation factor ELL2 is specifically upregulated in HTLV-1-infected T-cells and is dependent on the viral oncoprotein tax. *Virology* 464-465C: 98–110
12. Smith MR, Greene WC (1990) Identification of HTLV-I tax trans-activator mutants exhibiting novel transcriptional phenotypes. Genes Dev 4:1875–1885
13. Shunaeva A, Potashnikova D, Pichugin A et al (2015) Improvement of HIV-1 and human T Cell lymphotropic virus Type 1 replication-dependent vectors via optimization of reporter gene reconstitution and modification with intronic short hairpin RNA. J Virol 89:10591–10601
14. Derse D, Hill SA, Lloyd PA et al (2001) Examining human T-lymphotropic virus type 1 infection and replication by cell-free infection with recombinant virus vectors. J Virol 75:8461–8468
15. Yoshida M, Miyoshi I, Hinuma Y (1982) Isolation and characterization of retrovirus from cell lines of human adult T-cell leukemia and its implication in the disease. Proc Natl Acad Sci U S A 79:2031–2035
16. Ho DD, Rota TR, Hirsch MS (1984) Infection of human endothelial cells by human T-lymphotropic virus type I. Proc Natl Acad Sci U S A 81:7588–7590

17. Bradford MM (1976) A rapid and sensitive method for the quantitation of microgram quantities of protein utilizing the principle of protein-dye binding. Anal Biochem 72:248–254
18. Rimsky L, Hauber J, Dukovich M et al (1988) Functional replacement of the HIV-1 rev protein by the HTLV-1 rex protein. Nature 335: 738–740
19. Mohr CF, Gross C, Bros M et al (2015) Regulation of the tumor marker Fascin by the viral oncoprotein Tax of human T-cell leukemia virus type 1 (HTLV-1) depends on promoter activation and on a promoter-independent mechanism. Virology 485:481–491
20. Alais S, Mahieux R, Dutartre H (2015) Viral source-independent high susceptibility of dendritic cells to human T-cell leukemia virus Type 1 infection compared to that of T lymphocytes. J Virol 89:10580–10590
21. Tanaka Y, Zeng L, Shiraki H et al (1991) Identification of a neutralization epitope on the envelope gp46 antigen of human T cell leukemia virus type I and induction of neutralizing antibody by peptide immunization. J Immunol 147:354–360
22. Saito M, Tanaka R, Fujii H et al (2014) The neutralizing function of the anti-HTLV-1 antibody is essential in preventing in vivo transmission of HTLV-1 to human T cells in NOD-SCID/gammacnull (NOG) mice. Retrovirology 11:74
23. Jaworski E, Narayanan A, Van DR et al (2014) Human T-lymphotropic virus type 1-infected cells secrete exosomes that contain Tax protein. J Biol Chem 289:22284–22305

Chapter 4

Quantitative Analysis of Human T-Lymphotropic Virus Type 1 (HTLV-1) Infection Using Co-Culture with Jurkat LTR-Luciferase or Jurkat LTR-GFP Reporter Cells

Sandrine Alais, Hélène Dutartre*, and Renaud Mahieux*

Abstract

Unlike HIV-1, HTLV-1 viral transmission requires cell-to-cell contacts, while cell-free virions are poorly infectious and almost absent from body fluids. Though the virus uses three nonexclusive mechanisms to infect new target cells: (1) MTOC polarization followed by formation of a virological synapse and viral transfer into a synaptic cleft, (2) genesis of a viral biofilm and its transfer of embedded viruses, or (3) HTLV-1 transmission using conduits. The Tax transactivator and the p8 viral proteins are involved in virological synapse and nanotube formation respectively.

HTLV-1 transcription from the viral promoter (i.e., LTR) requires the Tax protein that is absent from the viral particle and is expressed after productive infection. The present chapter focuses on a series of protocols used to quantify HTLV-1 de novo infection of target cells. These techniques do not discriminate between the different modes of transmission, but allow an accurate measure of productive infection. We used cell lines that are stably transfected with LTR-GFP or LTR-luciferase plasmids and quantified Green Fluorescent Protein expression or luciferase activity, since both of them reflect Tax expression.

Key words HTLV-1, Cell-to-cell infection, Virological synapse, Biofilm, Tax, Luciferase assay, GFP, Flow cytometry

1 Introduction

Human T-cell Leukemia Virus Type-1 (HTLV-1) oncoretrovirus infects 5–10 million people worldwide [1] and causes an aggressive hematological disease named Adult T-cell Leukemia [2], as well as a chronic neurological pathology named HTLV-1 Associated Myelopathy/Tropical Spastic Paraparesis [3]. In vivo, HTLV-1 virions are transmitted through contact between infected cells (mostly $CD4^+$ T-lymphocytes) present in milk, semen or blood, and target cells. Of importance, HTLV-1 can also efficiently infect dendritic cells [4, 5] and therefore likely alters their function [6] and/or their

*These authors contributed equally to this work.

Claudio Casoli (ed.), *Human T-Lymphotropic Viruses: Methods and Protocols*, Methods in Molecular Biology, vol. 1582,
DOI 10.1007/978-1-4939-6872-5_4, © Springer Science+Business Media LLC 2017

ability to migrate. In vitro, cell-free virus can be used, but is poorly infectious [4]. HTLV-1 binding and entry in susceptible cells involves at least three molecules, i.e., Heparan Sulfate Proteoglycans, Glut-1, and Neuropilin-1/BDCA-4 [7, 8]. The current models of HTLV-1 transmission foresee three options: (1) formation of a viral biofilm at the surface of the infected cell followed by its passive transfer; (2) polarization of the MTOC in the infected cell, formation of a virological synapse and viral transfer in the synaptic cleft [9, 10], and (3) thanks to HTLV-1 p8 viral protein, formation of cell conduits that will be used to transfer HTLV-1 [11]. Given that cell-free viruses are absent in body fluids, quantitative methods such as measure of viral RNA load by quantitative RT-PCR, of reverse-transcriptase activity, or ELISA-based assays aimed at detecting the presence of HTLV-1 capsid cannot be implemented. Mazurov et al. have reported a method based on virus-like particles containing reporter genes that allow a quantitative measurement of cell-cell infection [12]. However, because this method uses virus-like particles (VLPs) produced 24 h after co-transfection of different plasmids, it may be different from HTLV-1 viral transmission that occurs through virological synapse and/or biofilm transfer. Moreover in this system, reporter genes expression directly occurs after viral integration and does not require a viral protein expression, thus restricting the analysis of the viral cycle to its early steps.

In this chapter, we describe a system that allows the quantification of HTLV-1 infection after cell-to-cell transmission, using two types of reporter T-cells. Both contain an LTR promoter upstream of either a luciferase gene or the GFP sequence. Tax is absent from the viral particle and is not passively transferred from the infected cells to the target cell [13]. The expression of reporter protein is possible only after infection of target cell followed by reverse-transcription, integration, viral transcription, and Tax translation. Thus, the quantification of luciferase activity or of GFP expression is an accurate readout of viral replication.

2 Materials

2.1 Reagents and Equipments for In Vitro Infection and Cell Irradiation

1. Jurkat LTR-luciferase cell line [14].
2. Jurkat LTR-GFP cell line [4].
3. Jurkat cell line (Clone E6-1, ATCC® TIB-152™).
4. C91PL [15] or MT-2 HTLV-1 [16] infected cell lines (*see* **Note 1**).
5. 1× Phosphate buffered saline (PBS) without $MgCl_2$ and $CaCl_2$.
6. RPMI 1640 medium supplemented with 10% foetal calf serum, 1% glutamine, and penicillin–streptomycin (100 µg/ml) referred throughout the text as RPMI (Life Technologies, Carlsbad, CA, USA).
7. Centrifuge and microcentrifuge.

8. 15 and 50 ml centrifuge tubes, 1.5 ml microfuge tubes, pipet, and tips.
9. Humidified, CO_2-controlled cell incubator.
10. Irradiator (^{137}Cs source; CIS BIO international, Codolet, France).
11. Malassez hematimeter.

2.2 Reagents and Equipments for Luciferase Quantification and GFP Signal Analysis

1. 2–4% paraformaldehyde solution (prepared before being used, from 20% paraformaldehyde solution, electron microscopy science).
2. Luciferase Assay System (Promega, Madison, WI, USA).
3. Bradford-based protein quantification (BioRad, Hercules, CA, USA).
4. Bovine serum albumin solution (BSA) at 10 mg/ml (molecular grade for protein quantification).
5. Bovine serum albumin powder for cytometry analysis.
6. Ultrapure water.
7. 15 and 50 ml centrifuge tubes, 1.5 ml microfuge tubes, pipet, and tips.
8. Centrifuge and microcentrifuge.
9. 96-well round-bottom micro-plates for cell culture.
10. White, flat-bottom micro-plates for luminescence analysis.
11. Luminometer (GloMax® 96 microplate luminometer, Promega).
12. Flow cytometer (FACSCalibur™, Becton Dickinson, Franklin Lakes, NJ, USA).
13. Spectrophotometer with 595 nm filter.
14. Spectrophotometer cowls or flat-bottom translucent micro-plates for spectrophotometer.

3 Methods

The method was used to analyze HTLV-1 productive infection using MT-2 or C91PL (donor cells) co-cultured with Jurkat LTR-luciferase or Jurkat LTR-GFP (reporter T-cells). Infection was then measured by quantification of either luciferase activity or of GFP expression (Fig. 1).

3.1 Irradiation of HTLV-1 Infected Cells or of Control Jurkat Cells

Cell proliferation arrest is performed by sub-lethal irradiation as described below or after mytomycin C treatment (*see* **Note 2**).

1. Wash HTLV-1 infected cells or Jurkat cells with RPMI by centrifugation at 450 × *g* for 5 min.
2. Count HTLV-1 infected cells and control cells.
3. Distribute one million of each cell line into microfuge tube.

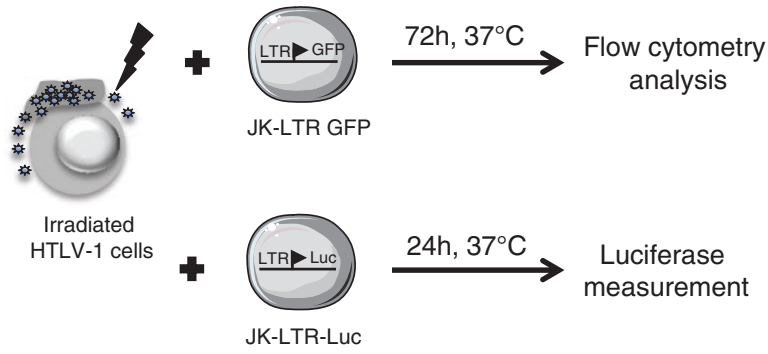

Fig. 1 Schematic representation of the co-culture protocol. The HTLV-1 infected cells/reporter T-cells ratio is set at 1/5

4. Pellet cells at 450 × *g* for 5 min at room temperature.
5. Resuspend cells at 10^6 cells/ml in RPMI.
6. Transfer microfuge tubes into 50 ml tube, which is used as a secondary protection.
7. Irradiate cells at 1.28 Gy/min for 1 h (77 Gy in total).
8. After irradiation, use cells immediately for reporter T-cells infection.

3.2 Cell-to-Cell Infections

1. Centrifuge reporter T-cells at 450 × *g* for 5 min.
2. Resuspend them at 10^6 cells/ml in RPMI.
3. Distribute 100,000-reporter cells/well in 96 round-bottom well plate.
4. Add 20,000-irradiated HTLV-1 infected cells or Jurkat cells (uninfected control).
5. Incubate either 24 h (Jurkat LTR-luciferase) or 72 h (Jurkat LTR-GFP) at 37 °C in cell incubator.

3.3 Analysis of Cell Infection by Luciferase Quantification

3.3.1 Measure of Luciferase Activity (See Note 3)

1. Prepare luciferase solution (LAR) and lysis buffer following manufacturer's instructions. Keep LAR solution in the dark.
2. Transfer cells to microfuge tube containing 1 ml of 1× PBS.
3. Centrifuge cells at 450 × *g* for 5 min.
4. Wash pellet once with 1 ml of 1× PBS.
5. Resuspend cell pellet in 50 µl of 1× passive lysis buffer (diluted in ultrapure water).
6. Incubate 5 min at room temperature and mix gently.
7. Centrifuge 6 min at 6000 × *g*.
8. Transfer supernatant into new 1.5 ml microfuge tube.
9. Transfer 40 µl of supernatant into white flat-bottom 96-well plate.
10. Analyze luciferase activity using luminometer (*see* Table 1).

Table 1
Luminometer settings for luciferase analysis

Delay between injection and measurement, (seconds)	1
LAR injection volume, (µl)	80
Integration time, (seconds)	5

Table 2
Preparation of BSA standard solution

Tube No.	1	2	3	4	5	6	7	8	9
Final concentration (mg/ml)	0	0,5	1	1,5	2	3	4	6	10
Volume (µl) of BSA solution (10 mg/ml)	0	5	10	15	20	30	40	60	100
Volume (µl) of ultrapure water	100	95	90	85	80	70	60	40	0

3.3.2 Determination of Protein Concentration

This step is required for luciferase activity normalization.

1. Prepare and label nine microfuge tubes (1.5 ml) for the standard BSA and one microfuge tube for each sample to be quantified.
2. Distribute 800 µl of ultrapure water in each microfuge tube.
3. Prepare serial dilutions of a BSA solution (*see* Table 2).

NB: BSA dilution can be stored at −20 °C.

4. Transfer 1 µl of each dilution of BSA solution into the labeled microfuge tube.
5. Transfer 5 µl of each sample to be analyzed into the labeled microfuge tube.
6. Add 200 µl of Bradford reagent in all microfuge tubes.
7. Vortex for 5 s.
8. Incubate for 5 min at room temperature.
9. Read absorbance at 595 nm with spectrophotometer.
10. Determine the protein concentration using the standard curve.

3.3.3 Luciferase Data Analyses

1. Subtract background RLU values obtained with uninfected control samples.
2. Divide each RLU values by the amount of protein measured for each sample.
3. Express results as a graph (Fig. 2).

Figure 2 shows a three-fold difference in luciferase signal observed after co-culture with two infected cell lines.

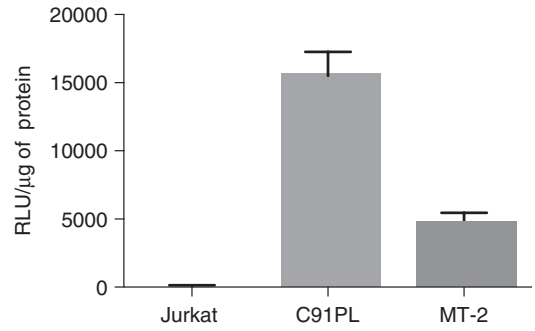

Fig. 2 Jurkat LTR-luciferase cells were co-cultured with irradiated C91PL or MT-2 HTLV-1 infected cells. Luciferase activity was measured 24 h later. Results were normalized according to the amount of protein present in each sample. The graph provides the values of three different experiments

3.4 Quantification of HTLV-1 Infection After GFP Signal Analysis

Using GFP reporter cells allows the evaluation of the number of infected cells after quantification of the percentage of GFP expressing cells, i.e., the level of HTLV-1 infection in each cell, by measuring the mean fluorescence intensity (MFI).

3.4.1 Analysis of GFP Expression by Flow Cytometry (See **Note 4***)*

1. After 72 h, transfer cells from micro-plate to a microfuge tube containing 1 ml of 1× PBS.
2. Pellet cells at 450 × *g* for 5 min.
3. Wash pellet once with 1 ml of 1× PBS.
4. Add 100 µl of 2–4% paraformaldehyde solution for 15 min, at room temperature.
5. Wash cells twice with 1 ml of 1× PBS and centrifuge for 5 min at 450 × *g*.
6. Resuspend cell pellet with 100 µl of 1× PBS/1% BSA.
7. Store at 4 °C (12 h maximum) before performing flow cytometry analyses.

The method was used to quantify GFP signal in cells after co-culture with HTLV-1. Figure 3 shows that 12.1% of Jurkat LTR-GFP cells express detectable level of GFP 72 h after they were mixed with C91PL HTLV-1 infected cells. This result suggests that HTLV-1 does not efficiently infect T-cells, even under conditions where cell-cell contacts are favored. In addition, this method shows that GFP expression is variable, as exemplified by a shift of GFP-positive signal (Fig. 3). This result highlights the variable degree of infection of target cells, ranging from high GFP expressing cells (maximum intensity of 10^3, and the average of intensity peaks around 10^2), to very low level of GFP signal (Fig. 3).

3.4.2 Observation of GFP Expression by Microscopy

In addition to allowing a quantification of the percentage of infected cells, Jurkat LTR-GFP infected cells (i.e., fluorescent) can be visualized under microscope. In that case, cells should be observed 72 h after the beginning of the co-culture (Fig. 4).

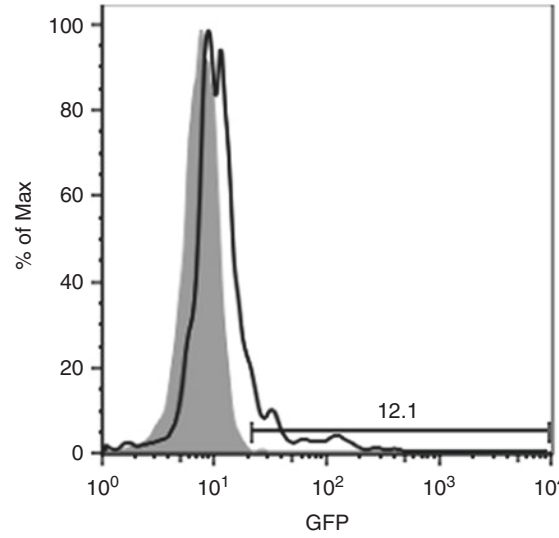

Fig. 3 Detection of GFP positive Jurkat cells after 3 days of co-culture with irradiated C91PL HTLV-1 infected cells (C91PL; *black line*). Jurkat cells (*gray filled graphs*) were used as a negative control. GFP positive cells are indicated

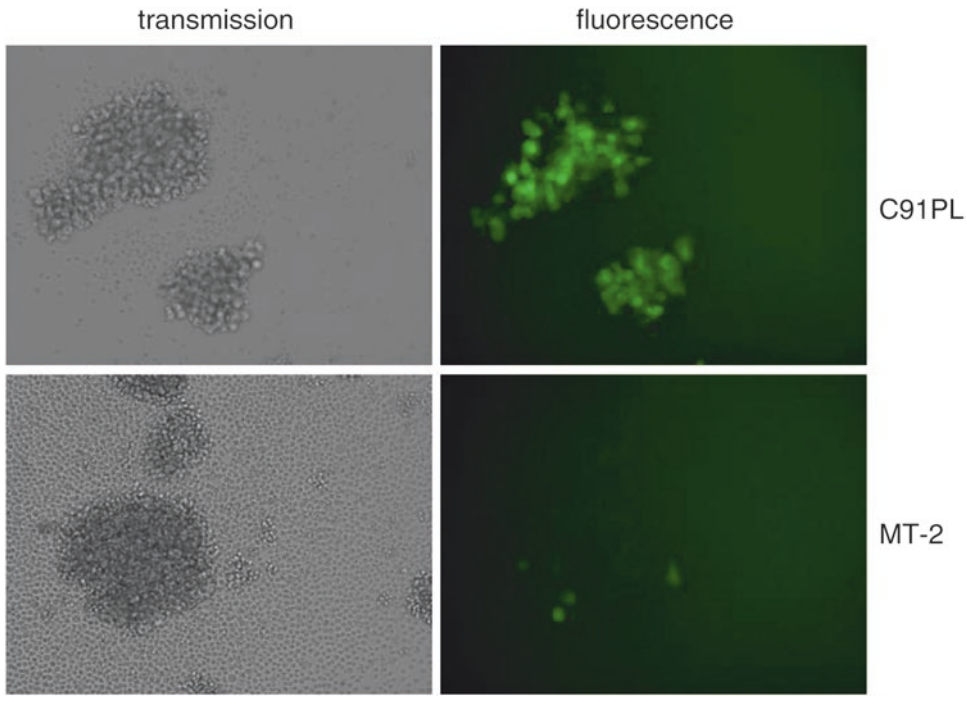

Fig. 4 Jurkat LTR-GFP cells were co-cultured for 3 days either with irradiated C91PL or MT-2 cells. Fluorescence was observed using Evos F1 imaging microscope (AMG). GFP-expressing cells appear in white in the right side of the figure. The *left panels* show the cells in white light (transmission). Pictures were taken with the 10× objective

4 Notes

1. All cells are thawed 1 week before the beginning of the experiment. They are maintained in culture up to 1 month. Cells are grown at 0.5×10^6 cells/ml in either 25 cm^2 flasks containing 10 ml of medium, or in 75 cm^2 flasks containing 20 ml of medium. The cells are diluted every 2–3 days.
2. While performing co-culture experiment, inhibition of HTLV-1 infected cell proliferation is required. If cell irradiation is not possible, an alternative protocol with mytomycin C (50 μg/ml for treatment of 50×10^6 cells, 20 min at 37 °C) can be used as described in current protocols in immunology. Measures of luciferase activity are performed by adapting timing and volumes for a micro-plate analysis.
3. Cell pellets can be stored at −80 °C before performing passive cell lysis. This might be necessary if a time-course experiment is performed. Indeed, to minimize experimental variations it is recommended to lyze and analyze all samples on the same day. Protein concentration calculation may be performed later if lysate is stored at −80 °C.
4. Laser configurations and specifications of each cytometer do not allow providing definite laser values. However, when using FACSCalibur (Becton Dickinson) FSC parameter should be set around 300, while SSC parameters are set around 380. For GFP detection, 405 nm laser is used for excitation and a PMT voltage set around 300. Fluorescence emission peaks at 509 nm. The analysis of uninfected cells is required to determine GFP-negative signal (Fig. 3).

Avoid long-term storage of fixed GFP reporter cells, since GFP fluorescence is sensitive to paraformaldehyde and fluorescence intensity decreases over time.

Acknowledgments

R.M. is supported by ENS Lyon. S.A. and H.D. are supported by INSERM. We thank Dr. Maria-Isabel Thoulouze (Institut Pasteur, Paris) for the gift of Jurkat LTR-luciferase cells. We acknowledge the support of La Ligue Contre le Cancer (programme équipe labellisée).

References

1. Gessain A, Cassar O (2012) Epidemiological aspects and world distribution of HTLV-1 infection. Front Microbiol 3:388
2. Iwanaga M, Watanabe T, Yamaguchi K (2012) Adult T-cell leukemia: a review of epidemiological evidence. Front Microbiol 3:322
3. Yamano Y, Sato T (2012) Clinical pathophysiology of human T-lymphotropic virus-type 1-associated myelopathy/tropical spastic paraparesis. Front Microbiol 3:389
4. Alais S, Mahieux R, Dutartre H (2015) Viral source-independent high susceptibility of dendritic cells to human T-cell leukemia virus Type 1 infection compared to that of T lymphocytes. J Virol 89:10580–10590
5. Jones KS, Petrow-Sadowski C, Huang YK, Bertolette DC, Ruscetti FW (2008) Cell-free HTLV-1 infects dendritic cells leading to transmission and transformation of CD4(+) T cells. Nat Med 14:429–436
6. Journo C, Mahieux R (2011) HTLV-1 and innate immunity. Viruses 3:1374–1394
7. Ghez D, Lepelletier Y, Jones KS, Pique C, Hermine O (2010) Current concepts regarding the HTLV-1 receptor complex. Retrovirology 7:99
8. Pique C, Jones KS (2012) Pathways of cell-cell transmission of HTLV-1. Front Microbiol 3:378
9. Igakura T, Stinchcombe JC, Goon PK, Taylor GP, Weber JN, Griffiths GM, Tanaka Y, Osame M, Bangham CR (2003) Spread of HTLV-I between lymphocytes by virus-induced polarization of the cytoskeleton. Science 299:1713–1716
10. Nejmeddine M, Barnard AL, Tanaka Y, Taylor GP, Bangham CR (2005) Human T-lymphotropic virus, type 1, tax protein triggers microtubule reorientation in the virological synapse. J Biol Chem 280:29653–29660
11. Van Prooyen N, Gold H, Andresen V, Schwartz O, Jones K, Ruscetti F, Lockett S, Gudla P, Venzon D, Franchini G (2010) Human T-cell leukemia virus type 1 p8 protein increases cellular conduits and virus transmission. Proc Natl Acad Sci U S A 107:20738–20743
12. Mazurov D, Ilinskaya A, Heidecker G, Lloyd P, Derse D (2010) Quantitative comparison of HTLV-1 and HIV-1 cell-to-cell infection with new replication dependent vectors. PLoS Pathog 6:e1000788
13. Cachat A, Chevalier SA, Alais S, Ko NL, Ratner L, Journo C, Dutartre H, Mahieux R (2013) Alpha interferon restricts human T-lymphotropic virus type 1 and 2 de novo infection through PKR activation. J Virol 87:13386–13396
14. Pais-Correia AM, Sachse M, Guadagnini S, Robbiati V, Lasserre R, Gessain A, Gout O, Alcover A, Thoulouze MI (2010) Biofilm-like extracellular viral assemblies mediate HTLV-1 cell-to-cell transmission at virological synapses. Nat Med 16:83–89
15. Popovic M, Lange-Wantzin G, Sarin PS, Mann D, Gallo RC (1983) Transformation of human umbilical cord blood T cells by human T-cell leukemia/lymphoma virus. Proc Natl Acad Sci U S A 80:5402–5406
16. Yoshida M, Miyoshi I, Hinuma Y (1982) A retrovirus from human leukemia cell lines: its isolation, characterization, and implication in human adult T-cell leukemia (ATL). Princess Takamatsu Symp 12:285–294

Chapter 5

Isolation of Exosomes from HTLV-Infected Cells

Robert A. Barclay, Michelle L. Pleet, Yao Akpamagbo, Kinza Noor, Allison Mathiesen, and Fatah Kashanchi

Abstract

Exosomes are small vesicles, approximately 30–100 nm in diameter, that transport various cargos, such as proteins and nucleic acids, between cells. It has been previously shown that exosomes can also transport viral proteins, such as the HTLV protein Tax, and viral RNAs, potentially contributing to disease pathogenesis. Therefore, it is important to understand their impact on recipient cells. Here, we describe methods of isolating and purifying exosomes from cell culture or tissue through ultracentrifugation, characterizing exosomes by surface biomarkers, and assays that evaluate the effect of exosomes on cells.

Key words Exosome, HTLV, Ultracentrifugation, Sucrose gradient, Functional assay

1 Introduction

Exosomes are small extracellular vesicles (EVs) that arise from the late endosomal pathway and are released when multivesicular bodies (MVBs) fuse with the plasma membrane, releasing their intraluminal vesicles (ILVs) into the extracellular environment [1–3]. The study of these extracellular vesicles is an important and novel area of research, and is especially relevant in the fields of molecular cell biology, immunology, microbiology, virology, and therapeutic development. In recent years, it has been discovered that exosomes can be taken up by recipient cells and can result in phenotypic changes, which can be either beneficial or detrimental to the cell depending on the donor cell's condition at the time of exosome release, the exosomal content, and the recipient cell's external and internal environment [1–7]. In the case of many viral infections and cancers, exosomes have been implicated in cellular inflammation, antigen presentation, and the transfer of nucleic acids and functional proteins between cells [8–17].

Furthermore, exosomes have also been reported to participate in the delivery of functional miRNAs and proteins which result in modulation of recipient cell gene expression [18–21]. Sometimes,

Claudio Casoli (ed.), *Human T-Lymphotropic Viruses: Methods and Protocols*, Methods in Molecular Biology, vol. 1582,
DOI 10.1007/978-1-4939-6872-5_5,

this can contribute to disease pathogenesis, especially when exosomes originate from infected cells. For instance, EBV-infected cells have been found to produce exosomes with oncoproteins while exosomes from KSHV-infected cells can disrupt natural metabolic signaling [58]. Exosomes derived from HCV-infected cells have been implicated in viral receptor-independent transmission of the virus and HIV-1-infected cells can cause increased cytokine production, which leads to enhanced infectivity [58]. In the case of HTLV-1, exosomes have been observed to contain viral Tax protein, proinflammatory mediators, and viral mRNA transcripts, delivering the aforementioned molecules to recipient cells, aiding in cell survival under stress conditions, and potentially contributing to HTLV-1 pathogenesis [16]. For a more comprehensive set of reviews on exosomes from virally infected cells, readers are referred to a few excellent publications [5, 74, 75].

Exosomes have well-defined shape (under EM) and are approximately 30–100 nm in size [1–3]. They contain classical tetraspanin markers including CD63, CD81, and CD9, ESCRT-pathway proteins such as Alix and TSG101 [4–6], as well as additional cell-specific markers. Detection of these markers by Western blot is often utilized to confirm exosome presence, as these proteins are not found on other extracellular vesicles such as exosome-like vesicles, microvesicles, and apoptotic bodies [4–7, 22, 23]. Isolation of exosomes is most frequently and reliably accomplished by a step-wise centrifugation followed by a sucrose or iodixanol gradient ultracentrifugation protocol, although other procedures such as ultrafiltration are sometimes utilized [4, 5, 60].

It is often desirable to obtain measurements of exosomes within samples, both of shape and size as well as abundance. Visual appraisal via electron microscopy (EM) can provide insights into the physical size and appearance of the exosome. Transmission electron microscopy (TEM) is most commonly used and has been utilized in many recent publications [22–25]. With TEM it is possible to obtain high resolution of ~1 nm of exosomes by fixing the isolated vesicles in gluteraldehyde on a grid, negatively staining them, and visualizing them with a transmission electron microscope [22–27]. This can provide 2D measurements of exosome size and morphology, although sample preparation may result in some shrinkage of vesicles [28].

In addition to measuring the size of extracellular vesicles (EVs), determining the number of exosomes in a sample is also important. Methods and kits to determine exosome abundance include nanoparticle tracking analysis (NTA), densitometry, acetylcholinesterase (AChE) assay, flow cytometry, qNano, and ExoELISA. Nanoparticle tracking analysis (NTA) works by measuring the Brownian motion of particles in a solution to both size and count the number of particles [29–31]. A dark-field microscope equipped with an angled laser and a high-sensitivity camera

measures the scattered light passing through a vesicle suspension. NTA is less precise than TEM, but it can be accomplished with little exosome preparation (although variability does decrease when ultracentrifugation and fluorescent antibody tagging is utilized). NTA also has a shortcoming in determining accurate counts of smaller particles when in the presence of larger vesicles that over-saturate the camera [29, 31]. Densitometry protocols following Western blot involve the use of computer software to calculate the quantitative or semiquantitative data comparing one band to another, and normalizing these values against the background [32]. The use of this method is cautioned, however, as it is highly dependent on good sample preparation, blotting technique, antibody quality, detection method, software, and analysis, most of which are greatly influenced by human error and are difficult to standardize. It is recommended that use of densitometry be used only in a semiquantitative manner compared with multiple controls for better quantification [32–34]. Acetylcholinesterase assay measures the activity of the enzyme AChE, which is present as part of the exosome membrane [35]. Various material including the start material, as well as centrifuged pellets, and OptiPrep™ fractions are processed and suspended in acetylthiocholine and 2-nitrobenzoic acid, incubated, and the optical density (OD) is analyzed at 450 nm with a plate reader spectrophotometer. Higher levels of AChE activity are associated with greater numbers of exosomes [35–37]. Interestingly, anti-AChE beads have also been successfully employed as a method of selectively pulling down exosomes from cell supernatants, which may be a novel way of isolating exosomes from virions that often have the same external markers [37]. Flow cytometry can be of use for quantitating exosomes as well but is likely only valid when coupled with the use of magnetic beads labeled for common exosome surface markers such as CD63, CD81, or CD9, as the commercial flow cytometer cannot accurately detect vesicles with a diameter smaller than ~500 nm [38–40]. The portable qNano™ system by IZON is a method of resistive pulse sensing (RPS), which detects label-free charged particles passing through a size-adjustable nanopore by electrophoresis [41]. It is able to measure the approximate size distribution and numbers of nanoparticles with less time and preparation than TEM; however, it has difficulty distinguishing individual particles when vesicles clump together and instead considers the clump as a single large particle [42]. The qNano™ may also be inaccurate in determining vesicles under 100 nm in diameter, but in general it is a very simple and useful method of measuring exosomes [42–44]. Finally, the ExoELISA™ kit from System Biosciences binds exosome particles to a microtiter plate and a specific marker antibody (i.e., CD63) is used to detect the presence and abundance of exosomes [45]. This protocol allows for the measurement of the specific exosome protein marker (CD63, CD9, CD81) and gives

quantitative results [25, 45], although it has been reported that technical troubles with low signal intensity have sometimes been encountered [46].

Characterization of exosomes by immunoblot or miRNA profile is also important for many experimental procedures to determine exosome origin and cargo. This is of particular interest in many studies of disease pathogenesis, as miRNAs originating from pathogen-infected cells have been shown to induce phenotypic changes in recipient cells [18–21]. One way that has been shown to reliably recover miRNA from animal cells and tissues, as well as exosomes, is to utilize kits that allow for the lysis of cells or exosomes, inhibition of RNases, separation and high-quality isolation of all RNA, or enrichment of miRNAs and other small RNAs from the sample of choice [47]. After isolation, quantitative real-time polymerase chain reaction (PCR) can be performed to identify the specific miRNA presence and abundance [47–50]. Examples of miRNA found in exosomes are miR150, miR155, and let7, along with miR128, which is abundant in neuronal exosomes [56, 57].

Another method for analyzing exosomes is through functional assays, which examine how exosomes affect recipient cells. These protocols, for example, look at changes in cytokine production in cells before and after exosome treatment from other cells that may be cancerous or infected with a pathogenic agent. One such test is the CTLL-2 assay. CTLL-2 cells are a line of murine cytotoxic T cells that are dependent upon IL-2 present in the growth media for their survival [51]. They can be used simply to assay for IL-2 [52], or have been used previously to determine the ability of Tax-containing exosomes from HTLV-1-infected T cells to promote a brief cell survival in the absence of IL-2 [16].

In addition to measuring exosomes in vitro, being able to track exosomes in vivo is also a common method. Labeling with fluorophores and dyes such as the amine-reactive TAMRA-NHS (carboxytetramethylrhodamine succinimidyl ester) and the lipophilic DiD (1,1′-Dioctadecyl-3,3,3′,3′-Tetramethylindodicarbocyanine Perchlorate) on isolated exosomes can allow the researcher to follow exosomes in in vivo models [54, 55]. In this way, the trafficking and transport of exosomes can be studied in more complex systems.

Due to the implication of exosomes in disease pathogenesis, we have decided to focus on a number of protocols related to exosomes and include them in the current book chapter. Presented below are a number of protocols that allow one to isolate, characterize, and quantify exosomes. Ultracentrifugation and gradient purification (*see* Fig. 1), and CTLL-2 assay are discussed in detail as well as several other previously described methods for further validation.

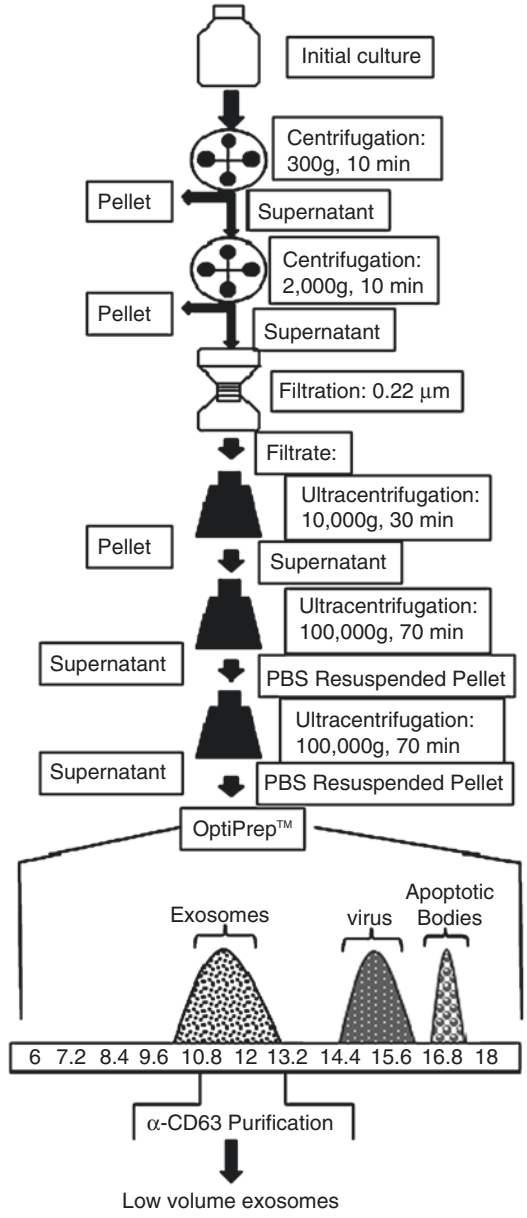

Fig. 1 Purification of exosomes using ultracentrifugation and a gradient. The procedure utilizes 100–200 mL of cell supernatants at 2.5–5 × 10^6 cells/mL (depending on exosome concentration) that have been incubated in exosome-free media for 5 days. Cells are spun at 300 × *g* and 2000 × *g* to remove the cells and debris. The supernatants, which contain exosomes and other vesicles, are filtered using a 0.22 μm filter before being ultracentrifuged at 10,000 × *g* for 30 min to remove any microvesicles, apoptotic bodies, and other debris. This is followed by two 100,000 × *g* ultracentrifugation spins to pellet the exosomes, which are washed with DPBS without Ca^{2+}/Mg^{2+} in between spins. The concentrated pellet can be resuspended in 50–200 μL and OptiPrep™, which utilizes an iodixanol gradient, can be run to separate particles by size. This will also separate most viruses from exosomes

2 Materials

2.1 Isolating Exosomes from Cell Culture

1. Pipettes.
2. 50 mL conical centrifugation tubes.
3. 0.22 μm polyethersulfone membrane.
4. Dulbecco's phosphate-buffered saline (DPBS) without Ca^{2+}/Mg^{2+}.
5. PBS without Ca^{2+}/Mg^{2+} + 0.1% Tween-20.
6. 25 mL high-speed centrifugation polycarbonate tubes.
7. 1.5 mL microcentrifuge tubes.
8. Fixed-angle centrifuge rotor.
9. 0.5% BSA in PBS+Tween-20.
10. Cell culture.

2.2 Isolating Exosomes from Brain Tissue

1. Brain tissue (can be one mouse hemibrain or 0.2 g of human brain tissue), either fresh or previously frozen at −80 °C.
2. Hibernate A (BrainBits, LLC, HA), which should be stored at 4 °C.
3. Papain vials (Worthington Biochemicals, Lakewood, NJ, USA). A solution of 20 units/mL papain in Hibernate A should be prepared and kept at 37 °C (each sample utilizes 3.5 mL).
4. Pipettes.
5. 15 and 50 mL conical centrifugation tubes.
6. Nylon mesh filters (40 μm).
7. 0.22 μm filter adapters with surfactant-free cellulose acetate membrane and 10 mL plunge syringes.
8. DPBS without Ca^{2+}/Mg^{2+} at pH 7.4, which should be stored at 4 °C.
9. 25 mL high-speed centrifugation polycarbonate tubes.
10. 1.5 mL microcentrifuge tubes.
11. Fixed-angle centrifuge rotor.

2.3 Isolating Exosomes by Nanotrap Pulldown

1. NT080 (Ceres Nanosciences, Manassas, VA, USA).
2. NT082 (Ceres Nanosciences).
3. DPBS without Ca^{2+}/Mg^{2+}.

2.4 Purifying Exosomes by Sucrose Gradient

1. 1 M at pH 7.5 HEPES buffer.
2. Prepare 2 mL each of 0.25 M, 0.6 M, 0.95 M, 1.3 M, 1.65 M, and 2.0 M sucrose solutions in 20 mM HEPES (per sample).
3. DPBS without Ca^{2+}/Mg^{2+}, which should be stored at 4 °C.
4. 13 mL high-speed ultra-clear centrifuge tubes.

5. 10 mL high-speed centrifugation tubes.
6. 1.5 mL microcentrifuge tubes.
7. Fixed-angle centrifuge rotor.
8. Swinging-bucket centrifuge rotor.

2.5 Purifying Exosomes by Iodixanol Gradient

1. Iodixanol solutions (OptiPrep™) in PBS ranging from 6 to 18% with 1.2% increments.
2. PBS without Ca^{2+}/Mg^{2+}.
3. Exosome samples.
4. Fixed rotor centrifuge.
5. Swinging bucket centrifuge rotor.
6. Polycarbonate centrifuge tubes.

2.6 ELISA

1. Exosome Antibodies Array & ELISA Kit (SBI, Palo Alto, CA, USA).
2. Distilled water.

2.7 AchE Assay

1. The Amplex Red Acetylcholine/Acetylcholinesterase Assay Kit (Invitrogen/ThermoFisherScientific, Waltham, MA, USA).
2. Stock 1: 20 mM Amplex Red reagent for 100 assays.
   - Leave the Amplex Red reagent (Component A) and DMSO (Component B) to warm at room temperature.
   - Measure 200 µL of DMSO (Component B).
   - Dissolve one vial of component A (1 mg) in the DMSO.
   - Store frozen at −20 °C away from light.
3. Stock 2: 1× reaction Buffer.
   - Measure 20 mL of dH_2O.
   - Add 5 mL of 5× Reaction Buffer (Component E).
4. Stock 3: 200 U/mL HRP.
   - Measure 1.0 mL of 1× Rx Buffer (Stock 2).
   - Add all components of the HRP vial (Component C).
   - Aliquot and store at −20 °C.
5. Stock 4: 20 mM H2O2. **HAS TO BE PROMPTLY USED DUE TO LOW STABILITY**.
   - Measure 977 µL of dH_2O.
   - Add 23 µL of 3% H_2O_2 (Component D).
6. Stock 5: 20 U/mL Choline Oxidase.
   - Measure 600 µL of 1× Rx Buffer (Stock 2).
   - Add contents of the Choline Oxidase Vial (Component F).
   - Aliquot and store at −20 °C.

7. Stock6: 100 mM Acetylcholine. **PREPARE ONLY BEFORE EACH EXPERIMENT**.
   - Measure 275 µL of dH_2O.
   - Add 5 mg of Acetylcholine-chloride (Component G).
   - The remaining solid should be stored desiccated at −20 °C (hygroscopic).
8. Stock 7: 100 U/mL Acetylcholine Esterase.
   - Measure 600 µL of 1× Rx Buffer (Stock 2).
   - Add all contents of Acetylcholine Esterase (Component H).
   - Aliquot and store at −20 °C.

2.8 Exosome Tracking Dye

1. Purified exosome solution.
2. 0.1 M sodium bicarbonate buffer at pH 8.3.
3. TAMRA-NHS.
4. 100 kDa ultrafiltration tube.
5. Fixed-rotor centrifuge.
6. DPBS without Ca^{2+}/Mg^{2+}.

2.9 TLR (3, 7, or 8) Assay

1. HEK-Blue hTLR3 Cells, HEK-Blue hTLR7 Cells, or HEK-Blue hTLR8 Cells.
2. Complete D-MEM with 10% FBS.
3. Blasticidn.
4. Zeocin.
5. Normacin.
6. T-75 Flask.
7. Poly I:C.
8. Sterile Water.
9. HEK-Blue™ Detection medium.
10. DPBS without Ca^{2+}/Mg^{2+}.

2.10 CTLL 2 Assay

1. CTLL 2 cell line.
2. RPMI-1640 with 10% FBS.
3. 96 flat-bottom well plate.
4. MTT Solution 5 mg/mL, stock in PBS kept at room temperature and protect from light.
5. MTT Lysing Solution (20% SDS and 50% DMF).

2.11 Isolating miRNA

1. RNeasy® Mini Spin Columns (Qiagen, Hilden, Germany).
2. Collection tubes (1.5 and 2 mL).
3. QIAzol lysis reagent.

4. Buffer RWT.
5. RNase-free water.

3 Methods

3.1 Isolating Exosomes from Cell Culture via Ultracentrifugation

1. Centrifuge cell culture supernatant at 300 × *g* for 10 min at 4 °C; collect supernatant and discard pellet.
2. Centrifuge supernatant at 2000 × *g* 4 °C for 10 min.
3. Filter supernatant with a 0.22 μm polyethersulfone membrane (blocked with 10 mL of 0.5% BSA in PBS/Tween prior to use).
4. Fill polycarbonate ultracentrifuge tube to 22.5 mL with filtrate.
5. Ultracentrifuge filtrate at 10,000 × *g* using a fixed-angled rotor (Ti-70) for 30 min at 4 °C; collect supernatant and discard pellet.
6. Ultracentrifuge supernatant at 100,000 × *g* using a fixed-angle rotor (Ti-70) for 70 min at 4 °C. Discard supernatant.
7. Wash and resuspend exosome pellet in 22.5 mL of DPBS without Ca^{2+}/Mg^{2+}.
8. Ultracentrifuge with a fixed-angle rotor (Ti-70) at 100,000 × *g* for 70 min at 4 °C.
9. Discard the supernatant and resuspend the exosome pellet in 100 μL of PBS; store at 4 °C (*see* Fig. 1).

3.2 Isolating Exosomes from Cell Culture via Nanotrap Particles

1. Take nanotrap particle NT080 and NT082 and create a 30% slurry:33% NT080, 33% NT082, and 33% DPBS without Ca^{2+}/Mg^{2+} (*see* **Note 1**).
2. Add to sample aliquot containing target of interest. For every mL of sample, add 25–30 μL of NT slurry.
3. Allow samples to incubate while rotating at 4 °C for 24–72 h (*see* **Note 2**).
4. Centrifuge sample at 14,000 × *g* for 5 min.
5. Wash nanoparticle-treated samples with PBS twice and resuspend in working buffer compatible with downstream assays.

3.3 Isolating Exosomes from Brain Tissue

1. Mince brain tissue in a few drops of 20 units/mL papain in Hibernate A.
2. Transfer the brain tissue into a 15 mL conical centrifugation tube containing 3.5 mL of 20 units/mL papain in Hibernate A.
3. Incubate at 37 °C for 20 min and gently shake the tube every 5 min.
4. Deactivate papain by adding 6.5 mL of cold Hibernate A.

5. Pipette up and down until the solution is homogenous (about 15–20 times).
6. Centrifuge at 300 × *g* for 10 min at 4 °C; recover supernatant and discard pellet.
7. Pass supernatant through a 40 μm mesh filter and collect the filtrate in a 50 μm conical centrifugation tube.
8. Centrifuge at 2000 × *g* for 10 min at 4 °C; recover supernatant and discard pellet.
9. Filter supernatant using a 0.22 μm filter adapter and collect the filtrate in a polycarbonate tube; fill the tube to 22.5 mL.
10. Ultracentrifuge the filtrate at 10,000 × *g* for 30 min at 4 °C using a fixed-angle rotor (Ti-70).
11. Pull off the supernatant and place it in another polycarbonate tube.
12. Ultracentrifuge the sample at 100,000 × *g* for 70 min at 4 °C using a fixed-angle rotor (Ti-70).
13. Discard the supernatant, being careful not to disturb the pellet, and then resuspend the pellet with 22.5 mL of PBS.
14. Ultracentrifuge the sample at 100,000 × *g* for 70 min at 4 °C using a fixed-angle rotor (Ti-70).
15. Pull off the sup, being careful not to disturb the pellet, and then resuspend the pellet with 100 μL of PBS.

3.4 Purifying Exosomes Using Sucrose Gradient

1. Resuspend exosome pellet in 2 mL of 0.95 M sucrose solution (*see* **Note 3**).
2. Lay 2 mL of 2.0 M sucrose solution at the bottom of a 13 mL high-speed ultra-clear centrifuge tube.
3. Add the remaining sucrose solutions in 2 mL increments atop the 2.0 M in decreasing molarity, beginning with the 1.65 M solution and ending with the 0.25 M solution (*see* **Note 4**).
4. Ultracentrifuge the tubes at 200,000 × *g* for 16 h using a swinging-bucket rotor (SW41 Ti).
5. Collect 1 mL fraction from the top of the gradient; then, collect 2 mL fractions from between two adjacent layers and place them in 10 mL high-speed centrifugation tubes.
6. Ultracentrifuge at 100,000 × *g* for 1 h with a fixed-angle rotor (Ti-70).
7. Discard the supernatant without disturbing the exosome pellet.
8. Resuspend the pellet in 30 μL of PBS, transfer into an Eppendorf tube, and store at 4 °C.

3.5 Purifying Exosomes Using Iodixanol Gradient

1. Prepare iodixanol solutions in PBS ranging from 6 to 18% with 1.2% increments.
2. Add 210 μL of exosome sample to the top of the gradient.
3. Ultracentrifuge the gradient at 250,000 × *g* for 1.5 h in a SW41 Ti rotor (or other swinging bucket rotor).
4. Collect 1 mL fractions from the top of each gradient and place them in polycarbonate ultracentrifuge tubes.
5. Dilute to 22.5 mL with PBS.
6. Ultracentrifuge at 100,000 × *g* for 70 min with a Ti-70 rotor (or other fixed rotor centrifuge).
7. Discard the supernatant and resuspend the exosome pellet in 30 μL of PBS.

3.6 Characterizing Exosomes by ELISA

1. To the appropriate well of the micro-titer plate, 50 μL of the prepared standards and exosome protein sample should be added.
2. Incubate the plate at 37 °C for at least 2 h after covering the plate with a sealing film/cover (*see* **Note 5**).
3. After the incubation, empty all contents.
4. The plate should be washed three times for 5 min each with 100 μL 1× Wash buffer (*see* **Note 6**).
5. Exosome specific primary antibody (*see* Table 1) (1:100–1:500 depending on the strength of the antibody) should be diluted in 1× blocking buffer and 50 μl of it should be added to each well.
6. Incubate at room temperature for 1 h with shaking.
7. Wash the plate with 100 μL 1× Wash buffer three times for 5 min each.
8. Dilute exosome validated secondary antibody 1:5000 in 1× blocking buffer and add 50 μL to each well; incubate at room temperature for 1 h with shaking.
9. Wash the plate with 100 μL 1× Wash buffer three times for 5 min each.
10. Add 50 μL of Super-Sensitive TMB ELISA substrate and incubate at room temperature for 15–45 min with shaking – 15–45 min substrate incubation time is optimized for the recommended exosome protein standard curve (*see* **Note 7**).
11. Add 50 μL of Stop buffer to provide a fixed endpoint for the assay. The initial color of a positive sample is blue and the color changes to yellow when Stop buffer is added.
12. Quantitate results with a spectrophotometric plate reader at 450 nm absorbance.

Table 1
Protein markers specifically present on various cell types

	Human DC	Human B	Human IEC	DC	Mature DC	M	U	IEC	MC	Mov	B	Mast	P	HEK	Ret	T	Ref.
Alix				X		X	X										[67, 69, 71]
Annexin II				X		X	X	X	X	X							[65, 67]
B7–2				X							X	X					[70]
CD9				X			X	X					X				[60, 62]
CD63	X	X	X														[70, 72]
CD81	X	X	X														[70, 72]
Clathrin				X				X			X			X			[62, 66]
Flotillin-1				X			X			X					X		[61, 62, 64, 65]
Gi2α				X			X			X	X				X		[61, 62, 65, 66]
Hsc70				X		X	X		X	X	X	X			X		[61, 62, 65, 67, 70]
ICAM-1					X						X						[69, 71]
Lamp-1 or 2				X							X						[68, 69, 71]
MFG-E8				X				X		X							[65]
MHC I				X			X	X	X		X			X		X	[62, 64]
MHC II				X				X			X	X				X	[63, 64, 70]
Transferrin receptor				X						X					X		[62, 65]
Tsg101				X			X			X							[65]

3.7 Quantifying Exosomes by AchE Assay

1. In the wells, dilute the acetylcholine esterase samples in Stock 2 (100 µL/each).
2. Use 100 µL of the 1× Reaction Buffer without AchE as negative control (in wells).
3. Make a first positive control by measuring 10 µL of Stock 7 and dilute it in 90 µL of the 1× Reaction Buffer. Take 10 µL of the new dilution and dilute in 90 µL of 1× Reaction Buffer. Take 20 µL of the new dilution in 80 µL of 1× Reaction Buffer in the wells to make a 0.2 U/mL of AchE solution.
4. Make a second positive control by diluting 5 µL of Stock 4 in 95 µL of Stock 2. Measure 10 µL of this dilution in 90 µL of Stock 2. Measure 10 µL of the new dilution in 90 µL of Stock 2 in the H_2O_2 wells to a final concentration of 10 µM.
5. Prepare the working solution mixing 9.59 mL of Stock 2 to 200 µL of Stock 1, 100 µL of Stock 3, 100 µL of Stock 5, and 10 µL of Stock 6. Add 100 µL to each reaction well.
6. Incubate at room temperature away from light for 30 min to let the reaction occur. Then, measure the fluorescence at different time intervals at an excitation between 530 and 560 nm and an emission of 590 nm.
7. For each point, correct for background fluorescence by subtracting from the negative control.

3.8 Functional Assay: Exosome Tracking Dye

1. Take 1 mL of $NaHCO_3$ at a pH of about 8.3 and dissolve 100 µg of TAMRA-NHS into it.
2. Take approximately 200 µL of purified exosomes and add them to the $NaHCO_3$ solution.
3. Incubate at room temperature for 1 h to allow reaction to proceed.
4. Remove unincorporated TAMRA-NHS by using a 100 kDa ultrafiltration tube.
5. Wash exosomes with DPBS without Ca^{2+}/Mg^{2+}.
6. Ultracentrifuge at 200,000 × *g* for 70 min.
7. Discard supernatant and resuspend pellet with about 200 µL of PBS.

3.9 Functional Assay: TLR

1. All cells should be passaged at 70–80% confluency and be maintained and subcultured in a growth medium supplemented with 15 µL of Blasticidin, 5 µL of Zeocin and 10 µL of Normacin for every 5 mL of media (*see* **Note 8**).
2. To prepare the cells for an experiment in 3 days, remove the cells of interest from the incubator and discard the growth medium.
3. In a T-75 flask, rinse cells gently with 5 mL of DPBS without Ca^{2+}/Mg^{2+}, which was pre-warmed to 37 °C.

4. Add 1 mL of the pre-warmed PBS and place the cells at 37 °C for 3 min before detaching the cells by tapping the flask (*see* **Note 9**). The cell clumps can be dissociated by gently pipetting up and down.
5. Pipette out 125 μL into a new T-75 flask based on the $1/2^n$ equation (n = number of days), and add 4.9 mL of D-MEM before labeling and incubation.
6. To detect SEAP, add 20 μL of each sample, positive control (poly (I:C),1 μg/mL) and negative control (sterile water) to corresponding wells.
7. Remove the cells from the incubator and discard the growth medium.
8. For a T-75 flask, rinse cells gently with 5 mL PBS, pre-warmed to 37 °C.
9. Add 1 mL of the pre-warmed PBS and place the cells at 37 °C for 3 min; detach the cells by tapping the flask. Dissociate cell clumps by gently pipetting up and down (*see* **Note 9**).
10. Count the cells that have been resuspended in pre-warmed PBS.
11. Prepare a cell suspension ~280,000 cells/mL in HEK-Blue™ Detection medium (220,000 for TLR7 and 8) and immediately add 180 mL of the cell suspension (~50,000 cells for TLR3 and ~40,000 cells for TLR 7 and 8) per well.
12. Incubate the plate at 37 °C in 5% CO_2 for 6–16 h.
13. SEAP can be observed with naked eye and determined using a spectrophotometer at 620–655 nm.

3.10 Functional Assay: CTLL 2

1. Add 100 μL of RPMI culture media to each well of a 96-well plate.
2. Using the Quick Chart Guide from eBioscience [53], dilute samples and standards by twofold serial dilution in the plate from Rows 2 through 12.
3. Wash CTLL 2 cells three times with RPMI and resuspend in the culture media at a density of about 2.75×10^5 cells/mL.
4. Plate 100 μL of cells in each well.
5. Add exosomes to cells.
6. Incubate cells for 48 h at 37 °C and 5% CO_2.
7. Add 10 μL of 5 mg/mL MTT solution to each well before incubating for 4 h.
8. Add 50 μL of MTT Lysing Solution to each well before incubating overnight.
9. Read plate at 570–650 nm using a spectrophotometer.

3.11 miRNA Isolation from Exosomes

1. Lyse the exosomes by adding 700 µL of QIAzol Lysis Reagent to the cell culture.
2. Vortex the cells for 1 min (*see* **Note 10**).
3. Incubate at room temperature for 5 min to allow disassociation of nucleoprotein complexes.
4. Add 140 µL of chloroform to the homogenate and vortex for 15 s; then, leave the tube at room temperature for 2 min.
5. Centrifuge at 12,000 × *g* for 15 min in 4 °C (*see* **Note 11**).
6. Transfer the upper phase to a collection tube and add about 350 µl of 70% ethanol; vortex.
7. At room temperature, add the sample into a RNeasy mini spin column in the collection tube and centrifuge at 8000 × *g* for 15 s; then, transfer the flow-through into a 2 mL tube.
8. Add 450 µL of pure ethanol to the flow-through and vortex.
9. Transfer 700 µL of the sample to a RNeasy MinElute spin column. At room temperature, centrifuge for 15 s at 8000 × *g*; discard the flow-through.
10. Add 500 µL of Buffer RPE to the RNeasy MinElute spin column. Centrifuge at 8000 × *g* for 15 s at room temperature; throw away the flow-through.
11. Add 500 µL of 80% of ethanol to the RNeasy MinElute spin column. Then, centrifuge for 2 min at 8000 × *g* at room temperature.
12. Carefully remove the RNeasy MinElute spin column from the collection tube and discard both the collection tube and the flow-through.
13. Transfer the RNeasy MinElute spin column into a 2 mL collection tube and centrifuge for 5 min at 8000 × *g* with the lid open.
14. Move the RNeasy MinElute spin column to a 1.5 mL collection tube and add 14 µL of RNase free water to the spin column.
15. Centrifuge for 1 min at 8000 × *g* to elute the miRNA.

4 Notes

1. Use this method if cell culture volume is less than 2 mL [73].
2. The incubation time is dependent by exosome concentration.
3. If the pellet is already suspended in PBS, add enough sucrose solution to reach 2 mL.
4. The 0.95 M solution containing the exosomes should sit atop the 1.3 M sucrose solution but below the 0.6 M solution.
5. We recommend an overnight incubation.

6. A plate shaker is recommended for subsequent washes and incubations. Hard-tap the plate on a fresh paper towel to remove residual liquid while making sure the wells do not dry out completely.
7. Further optimization may be required by the user for individual sample.
8. The cells should not be frozen but must be thawed immediately upon receipt and grown. All cell types should not be passaged more than 20 times.
9. We recommend not using Trypsin.
10. Failure to homogenize completely can reduce RNA yield.
11. After this step, the sample separates into three phases—an upper phase containing the RNA, an interphase, and a lower phase.

Acknowledgments

We would like to thank the members of the Kashanchi lab for any and all assistance with the manuscript. In addition, we would like to thank Dr. Benjamin Lepene, Ceres Biosciences, for providing reagents and expertise on the NT080 and NT082. This work was supported by National Institutes of Health grants (AI078859, AI074410, and AI043894) to F.K.

References

1. Keller S, Sanderson MP, Stoeck A, Altevogt P (2006) Exosomes: from biogenesis and secretion to biological function. Immunol Lett 107(2):102–108
2. Colombo M, Raposo G, Théry C (2014) Biogenesis, secretion, and intercellular interactions of exosomes and other extracellular vesicles. Annu Rev Cell Dev Biol 30:255–289. doi:10.1146/annurev-cellbio-101512-122326
3. Fleming A, Sampey G, Chung MC et al (2014) The carrying pigeons of the cell: exosomes and their role in infectious diseases caused by human pathogens. Pathog Dis 71(2):109–120. doi:10.1111/2049-632X.12135
4. Vlassov AV, Magdaleno S, Setterquist R, Conrad R (2012) Exosomes: current knowledge of their composition, biological functions, and diagnostic and therapeutic potentials. Biochim Biophys Acta 1820(7):940–948. doi:10.1016/j.bbagen.2012.03.017
5. Akers JC, Gonda D, Kim R et al (2013) Biogenesis of extracellular vesicles (EV): exosomes, microvesicles, retrovirus-like vesicles, and apoptotic bodies. J Neurooncol 113:1–11. doi:10.1007/s11060-013-1084-8
6. Sampey GC, Meyering SS, Asad Zadeh M et al (2014) Exosomes and their role in CNS viral infections. J Neurovirol 20(3):199–208. doi:10.1007/s13365-014-0238-6
7. Naito Y, Yoshioka Y, Ochiya T (2015) The functional role of exosomes in cancer biology and their potential as biomarkers and therapeutic targets of cancer. Gan To Kagaku Ryoho 42(6):647–655
8. Dreux M, Garaigorta U, Boyd B et al (2012) Short-range exosomal transfer of viral RNA from infected cells to plasmacytoid dendritic cells triggers innate immunity. Cell Host Microbe 12(4):558–570. doi:10.1016/j.chom.2012.08.010
9. Hu G, Yao H, Chaudhuri AD et al (2012) Exosome-mediated shuttling of microRNA-29 regulates HIV Tat and morphine-mediated neuronal dysfunction. Cell Death Dis 3:e381. doi:10.1038/cddis.2012.114
10. Luga V, Zhang L, Viloria-Petit AM et al (2012) Exosomes mediate stromal mobilization of

autocrine Wnt-PCP signaling in breast cancer cell migration. Cell 151(7):1542–1556. doi:10.1016/j.cell.2012.11.024

11. Suetsugu A, Honma K, Saji S et al (2013) Imaging exosome transfer from breast cancer cells to stroma at metastatic sites in orthotopic nude-mouse models. Adv Drug Deliv Rev 65(3):383–390. doi:10.1016/j.addr.2012.08.007
12. Peinado H, Alečković M, Lavotshkin S et al (2012) Melanoma exosomes educate bone marrow progenitor cells toward a pro-metastatic phenotype through MET. Nat Med 18(6):883–891. doi:10.1038/nm.2753
13. Honegger A, Leitz J, Bulkescher J et al (2013) Silencing of human papillomavirus (HPV) E6/E7 oncogene expression affects both the contents and the amounts of extracellular microvesicles released from HPV-positive cancer cells. Int J Cancer 133(7):1631–1642. doi:10.1002/ijc.28164
14. Kadiu I, Narayanasamy P, Dash PK et al (2012) Biochemical and biologic characterization of exosomes and microvesicles as facilitators of HIV-1 infection in macrophages. J Immunol 189(2):744–754. doi:10.4049/jimmunol.1102244
15. Khatua AK, Taylor HE, Hildreth JE, Popik W (2009) Exosomes packaging APOBEC3G confer human immunodeficiency virus resistance to recipient cells. J Virol 83(2):512–521. doi:10.1128/JVI.01658-08
16. Jaworski E, Narayanan A, Van Duyne R et al (2014) Human T-lymphotropic virus type 1-infected cells secrete exosomes that contain Tax protein. J Biol Chem 289(32):22284–22305. doi:10.1074/jbc.M114.549659
17. Mori Y, Koike M, Moriishi E et al (2008) Human herpesvirus-6 induces MVB formation, and virus egress occurs by an exosomal release pathway. Traffic 9(10):1728–1742. doi:10.1111/j.1600-0854.2008.00796.x
18. Pegtel DM, Cosmopoulos K, Thorley-Lawson DA et al (2010) Functional delivery of viral miRNAs via exosomes. Proc Natl Acad Sci U S A 107(14):6328–6333. doi:10.1073/pnas.0914843107
19. Lenassi M, Cagney G, Liao M et al (2010) HIV Nef is secreted in exosomes and triggers apoptosis in bystander CD4+ T cells. Traffic 11(1):110–122. doi:10.1111/j.1600-0854.2009.01006.x
20. Meckes DG Jr, Raab-Traub N (2011) Microvesicles and viral infection. J Virol 85(24):12844–12854. doi:10.1128/JVI.05853-11
21. Ceccarelli S, Visco V, Raffa S et al (2007) Epstein-Barr virus latent membrane protein 1 promotes concentration in multivesicular bodies of fibroblast growth factor 2 and its release through exosomes. Int J Cancer 121(7):1494–1506
22. Kastelowitz N, Ying H (2014) Exosomes and microvesicles: identification and targeting by particle size and lipid chemical probes. Chembiochem 15(7):923–928. doi:10.1002/cbic.201400043
23. Raposo G, Stoorvogel W (2013) Extracellular vesicles: Exosomes microvesicles, and friends. JCB 200(4):373–383. doi:10.1083/jcb.201211138
24. Vader P, Breakefield XO, Wood MJA (2014) Extracellular vesicles: emerging targets for cancer therapy. Trends Mol Med 20(7):385–393. doi:10.1016/j.molmed.2014.03.002
25. Zlotogorski-Hurvitz A, Dayan D, Chaushu G et al (2015) Human saliva-derived exosomes: comparing methods of isolation. J Histochem Cytochem 63(3):181–189. doi:10.1369/0022155414564219
26. Narayanan A, Iordanskiy S, Das R et al (2013) Exosomes derived from HIV-1-infected cells contain trans-activation response element RNA. J Biol Chem 288(27):20014–20033. doi:10.1074/jbc.M112.438895
27. Fertig ET, Gherghiceanu M, Popescu LM (2014) Extracellular vesicles release by cardiac telocytes: electron microscopy and electron tomography. J Cell Mol Med 18(10):1938–1943. doi:10.1111/jcmm.12436
28. Brydson R, Brown A, Hodges C et al (2015) Microscopy of nanoparticulate dispersions. J Microsc. doi:10.1111/jmi.12290
29. van der Pol E, Coumans FA, Grootemaat AE et al (2014) Particle size distribution of exosomes and microvesicles determined by transmission electron microscopy, flow cytometry, nanoparticle tracking analysis, and resistive pulse sensing. J Thromb Haemost 12(7):1182–1192. doi:10.1111/jth.12602
30. Sokolova V, Ludwig AK, Hornung S et al (2011) Characterisation of exosomes derived from human cells by nanoparticle tracking analysis and scanning electron microscopy. Colloids Surf B Biointerfaces 87(1):146–150. doi:10.1016/j.colsurfb.2011.05.013
31. Oosthuyzen W, Sime NE, Ivy JR et al (2013) Quantification of human urinary exosomes by nanoparticle tracking analysis. J Physiol 591(Pt 23):5833–5842. doi:10.1113/jphysiol.2013.264069
32. Gassmann M, Grenacher B, Rohde B, Vogel J (2009) Quantifying Western blots: pitfalls of densitometry. Electrophoresis 30:1845–1855. doi:10.1002/elps.200800720

33. Taylor SC, Posch A (2014) The design of a quantitative western blot experiment. Biomed Res Int 2014:361590. doi:10.1155/2014/361590
34. Savina A, Furlán M, Vidal M, Colombo MI (2003) Exosome release is regulated by a calcium-dependent mechanism in K562 cells. J Biol Chem 278(22):20083–20090. doi:10.1074/jbc.M301642200
35. Cantin R, Diou J, Bélanger D et al (2008) Discrimination between exosomes and HIV-1: Purification of both vesicles from cell-free supernatants. J Immunol Methods 338(1–2):21–30. doi:10.1016/j.jim.2008.07.007
36. Liu Z, Zhang X, Yu Q, He JJ (2014) Exosome-associated hepatitis C virus in cell cultures and patient plasma. Biochem Biophys Res Commun 455(3–4):218–222. doi:10.1016/j.bbrc.2014.10.146
37. Luo X, Fan Y, Park IW, He JJ (2015) Exosomes are unlikely involved in intercellular Nef transfer. PLoS One 10(4):e0124436. doi:10.1371/journal.pone.0124436
38. Oksvold MP, Neurauter A, Pedersen KW (2015) Magnetic bead-based isolation of exosomes. Methods Mol Biol 1218:465–481. doi:10.1007/978-1-4939-1538-5_27
39. Pospichalova V, Svoboda J, Dave Z et al (2015) Simplified protocol for flow cytometry analysis of fluorescently labeled exosomes and microvesicles using dedicated flow cytometer. J Extracell Ves 4:25530. doi:10.3402/jev.v4.25530
40. van der Pol E, van Gemert MJ, Sturk A et al (2012) Single vs. swarm detection of microparticles and exosomes by flow cytometry. J Thromb Haemost 10(5):919–930. doi:10.1111/j.1538-7836.2012.04683.x
41. Garza-Licudine E, Deo D, Yu S et al (2010) Portable nanoparticle quantization using a resizable nanopore instrument – the IZON qNano™. Conf Proc IEEE Eng Med Biol Soc 2010:5736–5739. doi:10.1109/IEMBS.2010.5627861
42. Choi DH, Kwon YM, Chiura HX et al (2015) Extracellular Vesicles of the Hyperthermophilic Archaeon "Thermococcus onnurineus" NA1T. Appl Environ Microbiol 81(14):4591–4599. doi:10.1128/AEM.00428-15
43. Coumans FA, van der Pol E, Böing AN et al (2014) Reproducible extracellular vesicle size and concentration determination with tunable resistive pulse sensing. J Extracell Ves 3:25922. doi:10.3402/jev.v3.25922
44. Maas SL, De Vrij J, Broekman ML (2014) Quantification and size-profiling of extracellular vesicles using tunable resistive pulse sensing. J Vis Exp 92:e51623. doi:10.3791/51623
45. SBI (2015) Quantitate exosomes by ELISA. System Biosciences, Mountain View, CA. Updated 2015. https://www.systembio.com/microrna-research/exosome-antibody/elisas. Accessed 17 Aug 2015
46. Franquesa M, Hoogduijn MJ, Ripoll E et al (2014) Update on controls for isolation and quantification methodology of extracellular vesicles derived from adipose tissue mesenchymal stem cells. Front Immunol 5:525. doi:10.3389/fimmu.2014.00525
47. Qiagen (2013) miRNeasy Mini Kit. Updated 2013,March, https://www.qiagen.com/us/shop/sample-technologies/rna-sample-technologies/mirna/mirneasy-mini-kit/, Accessed 13 Oct 2015
48. Yeh Y-Y, Ozer HG, Lehman AM et al (2015) Characterization of CLL exosomes reveals a distinct microRNA signature and enhanced secretion by activation of BCR signaling. Blood 125(21):3297–3305. doi:10.1182/blood-2014-12-618470
49. Chevillet JR, Kang Q, Ruf IK et al (2014) Quantitative and stoichiometric analysis of the microRNA content of exosomes. Proc Natl Acad Sci U S A 111(41):14888–14893. doi:10.1073/pnas.1408301111
50. Kroh EM, Parkin RK, Mitchell PS, Tewari M (2010) Analysis of circulating microRNA biomarkers in plasma and serum using quantitative reverse transcription-PCR (qRT-PCR). Methods (San Diego, CA) 50(4):298–301. doi:10.1016/j.ymeth.2010.01.032
51. ATCC (2014) CTLL-2 (ATCC® TIB-214™). American Type Culture Collection, Manassas, VA. Updated 2014. http://www.atcc.org/products/all/TIB-214.aspx#characteristics. Accessed 13 Oct 2015
52. Weston L, Geczy A, Farrell C (1998) A convenient and reliable IL-2 bioassay using frozen CTLL-2 to improve the detection of helper T lymphocyte precursors. Immunol Cell Biol 76(2):190–192
53. eBioscience, San Diego, CA. Updated 2010. https://www.ebioscience.com/media/pdf/best-protocols/cytokine-bioassays.pdf. Accessed 14 Oct 2015
54. Tian T et al (2010) Visualizing of the cellular uptake and intracellular trafficking of exosomes by live-cell microscopy. J Cell Biochem 111:488–496
55. Tian T, Zhu YL, Hu FH, Wang YY, Huang NP, Xiao ZD (2013) Dynamics of exosome internalization and trafficking. J Cell Physiol 228(7):1487–1495
56. Zhang J et al (2015) Exosome and exosomal mircroRNA: trafficking, sorting, and function.

Genomics Proteomics Bioinformatics 13(1):17–24

57. Bellingham SA, Coleman BM, Hill AF (2012) Small RNA deep sequencing reveals a distinct miRNA signature released in exosomes from prion-infected neuronal cells. Nucleic Acids Res 40(21):10937–10949
58. Schwab A., et al. (2015) Extracellular vesicles from infected cells: potential for direct pathogenesis. Front Microbiol. eCollection
59. Bard MP et al (2004) Proteomic analysis of exosomes isolated from human malignant pleural effusions. Am J Respir Cell Mol Biol 31:114–121
60. Blanchard N et al (2002) TCR activation of human T cells induces the production of exosomes bearing the TCR/CD3/zeta complex. J Immunol 168:3235–3241
61. Caby MP et al (2005) Exosomal like vesicles are present in human blood plasma. Int Immunol 17:879–887
62. Clayton A et al (2001) Analysis of antigen presenting cell derived exosomes, based on immuno-magnetic isolation and flow cytometry. J Immunol Methods 247:163–174
63. De Gassart A et al (2003) Lipid raft- associated protein sorting in exosomes. Blood 102: 4336–4344
64. Fevrier B et al (2004) Cells release prions in association with exosomes. Proc Natl Acad Sci U S A 101:9683–9688
65. Heijnen H et al (1999) Activated platelets release two types of membrane vesicles: Microvesicles by surface shedding and exosomes derived from exocytosis of multivesicular bodies and alpha-granules. Blood 94:3791–3799
66. Mears R et al (2004) Proteomic analysis of melanoma-derived exosomes by two dimensional polyacrylamide gel electrophoresis and mass spectrometry. Proteomics 4:4019–4031
67. Pisitkun T, Shen RF, Knepper MA (2004) Identification and proteomic profiling of exosomes in human urine. Proc Natl Acad Sci U S A 101:13368–13373
68. Segura E et al (2005) ICAM-1 on exosomes from mature dendritic cells is critical for efficient naive T cell priming. Blood 106: 216–223
69. Skokos D et al (2001) Mast cell-dependent B and T lymphocyte activation is mediated by the secretion of immunologically active exosomes. J Immunol 166:868–876
70. Thery C et al (2002) Indirect activation of naive CD4+ T cells by dendritic cell-derived exosomes. Nat Immunol 3:1156–1162
71. van Niel G et al (2003) Intestinal epithelial exosomes carry MHC class II/peptides able to inform the immune system in mice. Gut 52:1690–1697
72. Wubbolts R et al (2003) Proteomic and biochemical analyses of human B cell-derived exosomes. Potential implications for their function and multivesicular body. J Biol Chem 278(13):10963–10972
73. Jaworski E et al (2014) The use of nanotrap particles technology in capturing HIV-1 virions and viral proteins from infected cells. PLoS One 9(5):e96778
74. Chahar HS, Bao X, Casola A (2015) Exosomes and their role in the life cycle and pathogenesis of RNA viruses. Viruses 7(6):3204–3225
75. Lai FW, Lichty BD, Bowidsh DM (2015) Microvesicles: ubiquitous contributors to infection and immunity. J Leukoc Biol 97(2):237–245

Part II

Promoter Activity of HTLV Proteins

Chapter 6

A Luciferase Functional Quantitative Assay for Measuring NF-κB Promoter Transactivation Mediated by HTLV-1 and HTLV-2 Tax Proteins

Elisa Bergamo, Erica Diani, Umberto Bertazzoni, and Maria Grazia Romanelli

Abstract

HTLV-1 and HTLV-2 viruses express Tax transactivator proteins required for viral genome transcription and capable of transforming cells in vivo and in vitro. Although Tax oncogenic potential needs to be further elucidated, it is well established that Tax proteins activate, among others, transcription factors of the NF-κB family, which are involved in immune and inflammatory responses, cell growth, apoptosis, stress responses and oncogenesis. Here, we describe a reporter gene assay applied for quantitative analysis of Tax-dependent NF-κB activation. The procedure is based on co-transfection of two individual vectors containing the cDNA for firefly and *Renilla* luciferase enzymes and vectors expressing Tax proteins. The luciferase expression is driven by *cis*-NF-κB promoter regulatory elements responsive to Tax transactivating factor. This assay is particularly useful to investigate Tax influence on NF-κB activation mediated by viral or host factors.

Key words HTLV, Tax, Transfection, Luciferase, NF-κB, Expressing vectors, Gene reporter assay

1 Introduction

Activation of the NF-κB transcription factors by viral protein Tax plays a critical role in the pathogenesis of diseases associated with Human T-cell lymphotropic virus type 1 (HTLV-1) [1–5]. HTLV-1 is the etiological agent of adult T-cell leukemia/lymphoma (ATLL) and is associated with an inflammatory disease, the neurological disorder HTLV-1-associated myelopathy/tropical spastic paraparesis (HAM/TSP). The pathogenesis of these HTLV-1-associated diseases, principally the development of ATLL, is mainly mediated by the viral regulatory proteins Tax and HBZ, as reviewed by [6].

Numerous studies have demonstrated that HTLV-1 and HTLV-2 Tax proteins (Tax-1 and Tax-2) exert their pathogenic effect through persistent activation of NF-κB transcription factors [2, 7, 8]. Tax activates NF-κB by interacting with the IκB kinase

Claudio Casoli (ed.), *Human T-Lymphotropic Viruses: Methods and Protocols*, Methods in Molecular Biology, vol. 1582, DOI 10.1007/978-1-4939-6872-5_6,

(IKK) complex, which contains two catalytic components, IKKα and IKKβ, and a regulatory component, IKKγ, also known as NEMO. Tax interacts in the cytoplasm with NEMO leading to a persistent IKK and NF-κB activation [9] and with TAK1-binding protein 2 in calreticulin-containing complexes [10]. More recently, we have demonstrated that Tax proteins interact also with two closely related serine–threonine kinases, the TANK-binding kinase-1 (TBK1) and the inducible I-κB kinase epsilon (IKKε) involved in innate immune response to viral infection and able to modulate the NF-κB signalling [11].

In the nucleus, Tax has been reported to recruit RelA (also known as p65) as well as other cellular factors present in nuclear bodies leading to NF-κB transcriptional activation [12]. Several studies have been devoted to understanding the mechanism underlying Tax-mediated NF-κB activation in recent years. Noteworthy, the contribution of Tax ubiquitination and sumoylation on IKK activation and RelA nuclear translocation has been investigated [10, 13, 14]. Both post-translational modifications, ubiquitination and sumoylation, are involved in Tax-mediated NF-κB activation, although Tax sumoylation requirement is still controversial [15, 16]. More recently, a direct role of the anti-sense protein of HTLV-1, HBZ, on NF-κB activation has also been demonstrated. NF-κB activation, induced by Tax expression, correlates with senescence progression, whereas HBZ down-regulates NF-κB expression and transactivation by Tax, thus delaying or preventing the onset of Tax-induced senescence [17].

The experimental protocol described here illustrates the methodology applied for the quantification of Tax-1 and Tax-2 activities on NF-κB promoter. The assay can be very useful to obtain novel results aimed at understanding further the mechanism of Tax-dependent NF-κB activation and the role of HBZ in modulating the NF-κB activation.

2 Materials

2.1 Cell Culture

1. HEK293T cells.
2. Dulbecco's modified Eagle's medium (DMEM) supplemented with 10% fetal calf serum (FCS), 2 mM L-glutamine, with Penicillin G(100 U/L)/Streptomycin (100 μg/L).
3. Cells cultured in 12-well plates treated to obtain an adherent cell line.
4. Sterile pipettes and tips.

2.2 DNA Preparation and Transient Transfection

1. Plasmid DNA. To obtain high-quality DNA, NucleoBond Xtra Midi (Macherey-Nagel, Düren, Germany) is used (*see* **Note 1**).
2. Transfection reagent: TransIT-LT1 transfection reagent (Mirus, Madison, WI, USA) (*see* **Note 2**). Store at 4 °C, prewarm at room temperature, and mix well before use.

3. DMEM without serum to dilute DNA and transfection reagent.
4. DMEM supplemented with 10% FCS, L-glutamine, without antibiotics during cell growth of transfected cells.
5. Sterile 1.5 ml polypropylene tubes.
6. Sterile pipettes and tips.

2.3 Dual Luciferase Reporter Assay System

To evaluate the transactivation effect of Tax-1 or Tax-2 proteins on NF-κB promoter the Dual-Luciferase® Reporter (DLR™) Assay System (Promega, Madison, WI, USA) is used.

1. Luciferase Assay Reagent II (LAR II): dissolve the Luciferase Assay Substrate lyophilized in the bottle with 10 ml of Luciferase Assay Buffer included in the kit (*see* **Note 3**). Aliquot LAR II in 400 μl to avoid repetitive thawing that decreases its reactivity and store at −80 °C. Use LAR II at room temperature and protect from light.
2. Passive Lysis Buffer (PLB); dilute the PLB 5× in sterile water 1:5, and store at 4 °C for a few days.
3. Stop & Glo Reagent: Store at −20 °C and prepare it just before use, dilute a part of 50× Stop & Glo substrate with 50 parts of Stop & Glo buffer, and keep the solution protected from light and use at room temperature.
4. Refrigerated microcentrifuge.
5. Luminometer TD-20/20 (Turner Designs).
6. 1.5 ml polypropylene tubes, pipettes, and tips.

3 Methods

The luciferase assay provides a rapid, sensitive, and quantitative measurement of the activity of the reporter firefly (*Photinus pyralis*) luciferase enzyme expressed in transfected mammalian cell cultures. The assay is designed to be used in combination with a co-transfected reporter vector expressing the luciferase enzyme derived by the coelenterate *Renilla reniformis* as a control to normalize transfection efficiency.

The luciferase assay is highly sensitive, as ~1×10^{-20} moles of luciferase (1×10^5 luciferase molecules) are detected with a luminometer under optimal conditions. Background activity is very low because mammalian cells do not contain endogenous luciferase. The luciferase reporter gene assays are useful for studying the modulation of gene expression by *cis*- or *trans*-activating factors, or for analyzing the activation of cell signaling pathways. We use Dual-Luciferase Reporter Assay System to quantify Tax-1 and Tax-2 transactivating activity on a NF-κB promoter inserted in the vector pNF-κB-Luc (Stratagene, San Diego, CA, USA). To analyze the

transactivation effect of Tax proteins on NF-κB promoter, we use increasing amounts of Tax proteins and evaluate the fold induction of luciferase activity of each sample relative to NF-κB promoter alone.

3.1 Transient Transfection

1. The day before transfection, 2×10^5 HEK 293 T cells are seeded in 12-well plates (*see* **Note 4**).
2. For a high transfection efficiency the cells need to be 70–80% confluent at the time of transfection (*see* **Note 5**).
3. 500 ng of reporter plasmid NF-κB-Luc (NF-κB promoter driving the expression of luciferase reporter gene) is used to measure NF-κB levels in the presence of increasing amounts of plasmids coding for Tax-1 or Tax-2 [11, 18, 19] (*see* **Note 6**). 100 ng of phRG-TK plasmid (Promega) is utilized to normalize the transfection efficiency (*see* **Note 7**) in each sample. To make equal the total amount of DNA, an empty vector is added in each sample (i.e., pSGM5).
4. Prepare DNA dilutions in 100 μl of pre-warmed DMEM without antibiotics or serum. Mix well by pipetting (*see* **Note 8**).
5. Prepare transfection solution by mixing 2 μl of TransIT-LT1 for each μg of DNA (*see* **Note 9**) in 100 μl of DMEM without antibiotics or serum (*see* **Note 10**).
6. Mix gently the DNAs and the transfection solutions and incubate for 20 min at room temperature.
7. Remove the growth medium and replace with 800 μl of pre-warmed DMEM containing serum without antibiotics.
8. After 20 min incubation, mix gently the transfection/DNA mixture by pipetting and add, drop by drop, 200 μl of solution in each well.
9. Incubate the cells at 37 °C in the CO_2 humidified incubator for at least 4 h (*see* **Note 11**).
10. Perform Dual Luciferase Assay after 24 h of incubation.

3.2 Dual Luciferase Assay

1. Remove the growth medium from each well and wash twice with 1 ml of cold PBS.
2. Discard gently the PBS, add 150 μl of Passive Lysis Buffer (1×) in each well and incubate at room temperature for 10 min with gentle agitation.
3. Scrape the cells, pipet several times, and transfer in 1.5 ml tube.
4. Freeze and thaw on ice the cell suspensions at −20 °C.
5. Centrifuge the lysed cells for 2 min at 14,000 (20,817 × *g*) at 4 °C.
6. Collect the supernatant in a new tube, and then proceed with reporter enzymes analysis (Fig. 1). Maintain the lysates on ice.

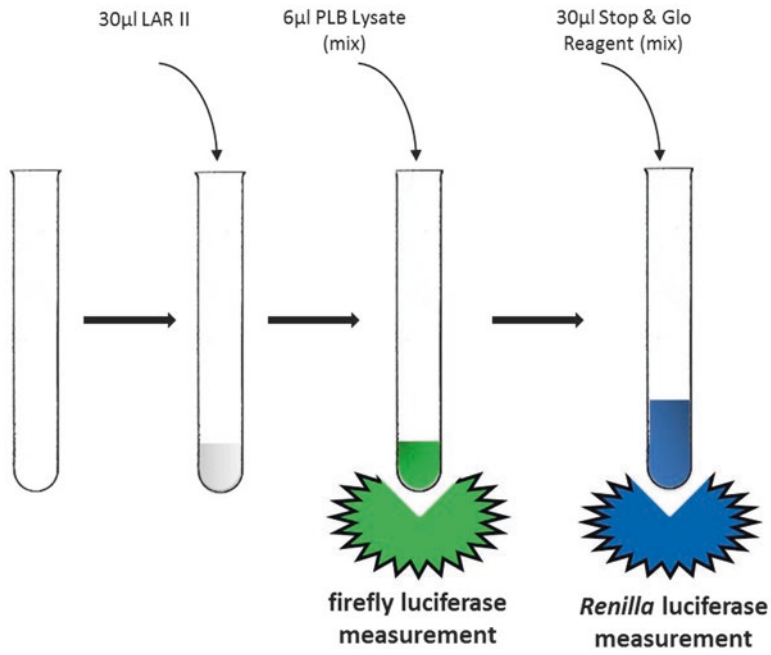

Fig. 1 Dual firefly and *Renilla* luciferases measurement

7. To perform the reporter enzyme assay, all kit reagents must be warmed at room temperature. Add 6 µl of cell lysate in 30 µl of LAR II and mix by pipetting ten times.
8. Place the tube in the luminometer and set the program to provide a 2-s preread delay, followed by a 10-s measurement period (as recommended by the manufacturer) and read the firefly luciferase activity.
9. Add 30 µl of Stop & Glo Reagent, mix well by rapidly pipetting ten times (*see* **Note 12**) and read immediately the *Renilla* luciferase activity.
10. Remove the tube from the luminometer and proceed with the next sample.
11. The luminometer gives the ratio between firefly and *Renilla* luciferase. To calculate fold induction, the mean value of each triplicate must be reported as fold induction relative to the luciferase activity quantified in the lysed sample derived by cell transfected only with the NF-κB-Luc vector and an empty vector (*see* **Note 13**). Results of the assay are analyzed by calculating the mean of at least three independent experiments performed in triplicate, as shown in Fig. 2 (*see* **Note 14**). Results are presented as mean ± standard deviation.

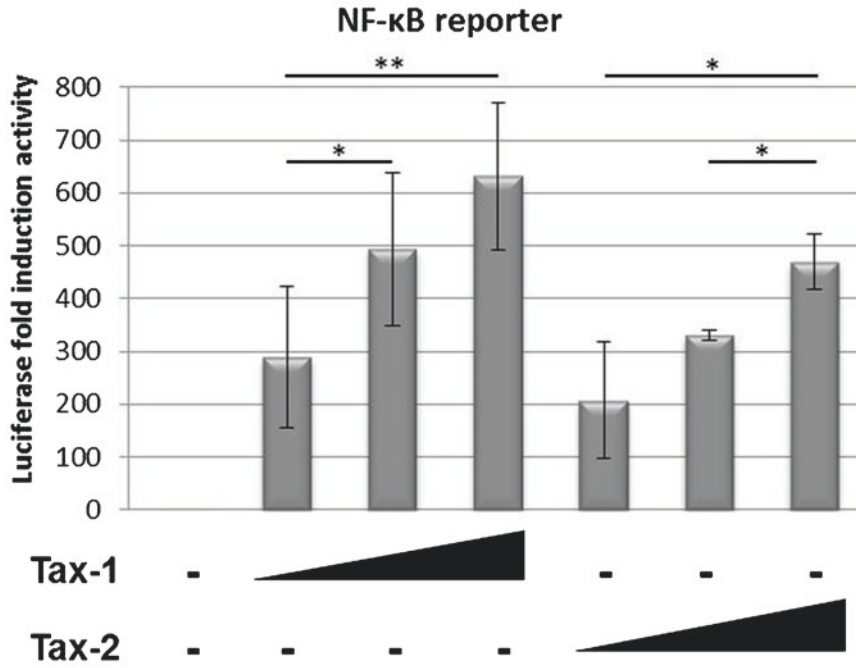

Fig. 2 Effect of overexpression of Tax-1 and Tax-2 on NF-κB reporter activity. Increasing amounts of Tax-1 or Tax-2 plasmids were co-transfected in HEK293T cells with NF-κB-Luc promoter vector. Luciferase reporter assay was performed 24 h after transfection. The transfection efficiency was normalized with *Renilla* luciferase and the induction on NF-κB promoter was calculated with respect to the promoter alone. Significant differences are shown as *asterisks* for $p < 0.05$, *Student's t*-test

4 Notes

1. The quality of DNA is essential to obtain good transfection efficiency. Contaminants, such as proteins, carbohydrates and lipids, may reduce transfection efficiency and modify gene expression levels. Use a purification kit (e.g., NucleoBond Xtra Midi produced by Macherey-Nagel) that gives a high-quality DNA.
2. We use TransIT-LT1 Transfection Reagent because it is a low toxicity, serum-compatible transfection reagent. Low cellular toxicity is required to achieve reliable experimental results. TransIT-LT1 gives high transfection efficiency and a high level of transactivation, thanks to a good viability of transfected cells.
3. To avoid loss of material, resuspend lyophilized Luciferase Assay Substrate in 10 ml of Luciferase Assay Buffer II with a sterile syringe, prepare aliquots in suitable amounts and store at −80 °C until use.
4. Split the cell cultures 18–24 h before transfection to ensure active cell division at the time of transfection.

5. To increase both expression and transfection efficiency and to minimize cytotoxicity, a cell confluence at 70–80% at the time of transfection is recommended. The type of cell line, the number of cells seeded, and the transfection reagent may influence the results of experiment. For different cell lines, an optimization step may be necessary.
6. We use NF-κB-Luc promoter as a reporter plasmid (pNF-κB-Luc, Stratagene). This inducible reporter plasmid contains the luciferase reporter gene driven by a basic promoter element (TATA box) plus a defined inducible *cis*-enhancer element, five copies of the NF-kB enhancer elements (TGGG GACTTTCCGC).
7. To normalize the transfection efficiency, we routinely used phRG-TK plasmid (Promega) coding for *Renilla* luciferase enzyme. It carries the *Renilla* luciferase gene under the control of the HSV-1 thymidine kinase (HSV-1 TK) promoter [20]. It is recommended not to use *Renilla* luciferase reporter plasmids driven by CMV immediate-early enhancer/promoter (i.e., phRL-CMV), which may be induced by Tax [21].
8. To minimize experimental error, we recommend preparing DNA solution for each triplicate in a single tube.
9. The optimal TransIT-LT1 reagent: DNA ratio for HEK293T is 2:1. For other cell types, the concentration of TransIT-LT1 reagent may vary from 2 to 8 μl per 1 μg of DNA.
10. Warm TransIT-LT1 to room temperature and vortex gently before use. Avoid any contact of the TransIT-LT1 with the sides of the plastic tube while adding transfection reagent to the diluted DNA mixture.
11. There is no need to change fresh culture medium after transfection. If required for further treatment, perform a medium change at least 4 h post-transfection.
12. Carefully transfer the lysate in the tube containing LAR II and mix by pipetting ten times, avoiding the vortex.
13. Firefly and *Renilla* luciferases have different enzyme structures and substrate requirements. These differences allow the distinction of the corresponding bioluminescent reactions. In the DLR™ Assay System, the luminescence from the firefly luciferase reaction is quenched, while the luminescent reaction of *Renilla* luciferase is simultaneously activated. Firefly luciferase is a 61 kDa monomeric protein that does not require post-translational modification for enzyme activity. Photon emission is achieved through oxidation of beetle luciferin in a reaction that requires ATP, Mg^{2+}, and Oxigen. *Renilla* luciferase, a 36 kDa monomeric protein, catalyzes the luminescent reaction utilizing Oxigen and coelenterate-luciferin. Luciferases are enzymes that generate light through the release of chemical energy in their substrates as photons. This is a luminescence

process that differs from fluorescence since a chemical reaction occurs and no light is needed to excite the molecules involved (excitation). Firefly and *Renilla* luciferase emissions occur at 560 nm and 480 nm, respectively. The ratio between firefly and *Renilla* luminescence represents the normalized value of luciferase activity driven by the promoter analyzed. The ratio between the value of luciferase activity of the sample analyzed and the value of the promoter alone gives the luciferase fold induction.

14. The expression of Tax may be confirmed by analyzing the cell lysates on SDS PAGE and western blots.

Acknowledgment

This work was supported by the following grants to M.G.R.: AIRC-Cariverona-2008 "An integrated approach to chronic lymphoproliferative disorders: B-CLL and virus related neoplasia", FUR 2014 University of Verona.

References

1. Ciminale V, Rende F, Bertazzoni U, Romanelli MG (2014) HTLV-1 and HTLV-2: highly similar viruses with distinct oncogenic properties. Front Microbiol 29(5):398. doi:10.3389/fmicb.2014.00398
2. Romanelli MG, Diani E, Bergamo E, Casoli C, Ciminale V, Bex F, Bertazzoni U (2013) Highlights on distinctive structural and functional properties of HTLV Tax proteins. Front Microbiol 9(4):271. doi:10.3389/fmicb.2013.00271
3. Rende F, Cavallari I, Romanelli MG, Diani E, Bertazzoni U, Ciminale V (2012) Comparison of the genetic organization, expression strategies and oncogenic potential of HTLV-1 and HTLV-2. Leuk Res Treatment 2012:876153. doi:10.1155/2012/876153.2012
4. Bertazzoni U, Turci M, Avesani F, Di Gennaro G, Bidoia C, Romanelli MG (2011) Intracellular localization and cellular factors interaction of HTLV-1 and HTLV-2 Tax proteins: similarities and functional differences. Viruses. 3:541–560. doi:10.3390/v3050541
5. Pilotti E, Bianchi MV, De Maria A, Bozzano F, Romanelli MG, Bertazzoni U, Casoli C (2013) HTLV-1/–2 and HIV-1 co-infections: retroviral interference on host immune status. Front Microbiol 23(4):372. doi:10.3389/fmicb.2013.00372
6. Matsuoka M, Yasunaga J (2013) Human T-cell leukemia virus type 1: replication, proliferation and propagation by Tax and HTLV-1 bZIP factor. Curr Opin Virol 3:684–691. doi:10.1016/j.coviro. 2013.08.010
7. Yasunaga J, Matsuoka M (2011) Molecular mechanisms of HTLV-1 infection and pathogenesis. Int J Hematol 94:435–442. doi:10.1007/s12185-011-0937-1
8. Qu Z, Xiao G (2011) Human T-cell lymphotropic virus: a model of NF-κB-associated tumorigenesis. Viruses 3:714–749. doi:10.3390/v3060714
9. Harhaj EW, Sun SC (1999) IKKgamma serves as a docking subunit of the IkappaB kinase (IKK) and mediates interaction of IKK with the human T-cell leukemia virus Tax protein. J Biol Chem 274:22911–22914
10. Avesani F, Romanelli MG, Turci M, Di Gennaro G, Sampaio C, Bidoia C, Bertazzoni U, Bex F (2010) Association of HTLV Tax proteins with TAK1-binding protein 2 and RelA in calreticulin-containing cytoplasmic structures participates in Tax-mediated NF-κB activation. Virology 408:39–48. doi:10.1016/j

11. Diani E, Avesani F, Bergamo E, Cremonese G, Bertazzoni U, Romanelli MG (2015) HTLV-1 Tax protein recruitment into IKKε and TBK1 kinase complexes enhances IFN-I expression. Virology 476:92–99. doi:10.1016/j
12. Bex F, McDowall A, Burny A, Gaynor R (1997) The human T-cell leukemia virus type 1 transactivator protein tax colocalizes in unique nuclear structures with NF-kB proteins. J Virol 71:3484–3497
13. Shibata Y, Tanaka Y, Gohda J, Inoue J (2011) Activation of the IκB kinase complex by HTLV-1 tax requires cytosolic factors involved in tax-induced polyubiquitination. J Biochem 150:679–686
14. Xiao G (2012) NF-kappaB activation: Tax sumoylation is out, but what about Tax ubiquitination? Retrovirology **25**(9):78. doi:10.1186/1742-4690-9-78
15. Turci M, Lodewick J, Di Gennaro G, Rinaldi AS, Marin O, Diani E, Sampaio C, Bex F, Bertazzoni U, Romanelli MG (2012) Ubiquitination and sumoylation of the HTLV-2 Tax-2B protein regulate its NF-κB activity: a comparative study with the HTLV-1 Tax-1 protein. Retrovirology 7(9):102. doi:10.1186/1742-4690-9-102.2012
16. Journo C, Bonnet A, Favre-Bonvin A, Turpin J, Vinera J, Côté E, Chevalier SA, Kfoury Y, Bazarbachi A, Pique C, Mahieux R (2013) Human T cell leukemia virus type 2 tax-mediated NF-κB activation involves a mechanism independent of Tax conjugation to ubiquitin and SUMO. J Virol 87:1123–1136. doi:10.1128/JVI.01792-12
17. Zhi H, Yang L, Kuo YL, Ho YK, Shih HM, Giam CZ (2011) NF-κB hyperactivation by HTLV-1 tax induces cellular senescence, but can be alleviated by the viral anti-sense protein HBZ. PLoS Pathog 7:e1002025. doi:10.1371/journal.ppat.1002025
18. Turci M, Romanelli MG, Lorenzi P, Righi P, Bertazzoni U (2006) Localization of human T-cell lymphotropic virus type II Tax protein is dependent upon a nuclear localization determinant in the N-terminal region. Gene 365:119–124
19. Turci M, Lodewick J, Righi P, Polania A, Romanelli MG, Bex F, Bertazzoni U (2009) HTLV-2B Tax oncoprotein is modified by ubiquitination and sumoylation and display intracellular localization similar to its homologue HTLV-1 Tax. Virology 30:6–11. doi:10.1016/j.virol.2009.01.003
20. Shifera AS, Hardin JA (2010) Factors modulating expression of Renilla luciferase from control plasmids used in luciferase reporter gene assays. Anal Biochem 396:167–172. doi:10.1016/j.ab
21. Lwa TR, Lee J, Ng CH, Lew QJ, Hia HC, Chao SH (2011) Human T-lymphotropic virus tax activates human cytomegalovirus major-immediate early promoter and improves production of recombinant proteins in HEK293 cells. Biotechnol Prog 27:751–756. doi:10.1002/btpr.571

Chapter 7

Generation of a Tet-On Expression System to Study Transactivation Ability of Tax-2

Fabio Bignami, Riccardo Alessio Sozzi, and Elisabetta Pilotti

Abstract

HTLV Tax proteins (Tax-1 and Tax-2) are known to be able to transactivate several host cellular genes involved in complex molecular pathways. Here, we describe a stable and regulated high-level expression model based on Tet-On system, to study the capacity of Tax-2 to transactivate host genes. In particular, the Jurkat Tet-On cell line suitable for evaluating the ability of Tax-2 to stimulate transactivation of a specific host gene, CCL3L1 (C-C motif chemokine ligand 3 like 1 gene), was selected. Then, a plasmid expressing *tax-2* gene under control of a tetracycline-response element was constructed. To avoid the production of a fusion protein between the report gene and the inserted gene, a bidirectional plasmid was designed. Maximum expression and fast response time were achieved by using nucleofection technology as transfection method. After developing an optimized protocol for efficiently transferring *tax-2* gene in Jurkat Tet-On cellular model and exposing transfected cells to Dox (doxycycline, a tetracycline derivate), a kinetics of *tax*-2 expression through TaqMan Real-time PCR assay was determined.

Key words HTLV Tax-2, Nucleofection, Bidirectional vectors, Tet-On systems, TaqMan Real-Time PCR, $2^{-\Delta\Delta CT}$ method

1 Introduction

The role of HTLVs during HIV-1 infection has been extensively studied. It is noteworthy that microbes, infecting the same host, may influence each other's replication [1, 2]. In particular, HTLV-2 seems to counteract HIV-1 progression by modulating cytokine-chemokine network [3]. After observing that up-regulation of CCR5-binding chemokine expression is significantly higher in cultured PBMCs of HTLV-2/HIV-1-co-infected individuals than in HIV-1-single-infected individuals [4], we demonstrated that CCL3 secretion is responsible for anti-HIV-1 activity in PBMC cultures from co-infected subjects [3]. Later, we found that an isoform of CCL3, namely CCL3L1, which is considered the most potent anti-R5 HIV-1 chemokine, was preferentially induced by HTLV-2 [5]. HTLVs Tax proteins play a key role in inducing modifications of

Claudio Casoli (ed.), *Human T-Lymphotropic Viruses: Methods and Protocols*, Methods in Molecular Biology, vol. 1582,
DOI 10.1007/978-1-4939-6872-5_7,

cellular molecular pathways [6–11]. Since some authors reported that both recombinant Tax-1 and Tax-2 induce high levels of CC-chemokines which in turn cause CCR5 down-regulation in cultured PBMCs [8], and that Tax-2 transactivates CC-chemokines production in cultured monocyte-derived macrophages [6], we designed an in vitro inducible model to study Tax-2 ability in activating CCL3L1 expression.

Tet inducible systems provide powerful tools to control the expression of genes of interest. After cloning these genes in a specific vector that will be stably integrated into a Tet- responsive cell line, their expression can be switched on or off in a controlled, dose-dependent, manner [12, 13]. Specifically, the expression system can be activated in the absence (Tet-Off©) or in the presence (Tet-On©) of doxycycline (Dox). While in the Tet-Off system Dox must be constantly kept in the medium to maintain the off state, in Tet-On system the off-state is maintained until when Dox is added to the medium. Besides exhibiting a tight on/off regulation, both systems are characterized by the absence of pleiotropic effects, high induction levels, and rapid induction times [14, 15].

Additionally, pTRE-Tight vectors [16, 17] are designed and optimized for obtaining an inducible expression system. The integration of genes of interest into this vector permits activating a tetracycline responsive construct by the Tet—controlled transactivator (tTA) in the absence of Dox (Tet-Off) or by the reverse tTA in the presence of Dox (Tet-On or Tet-On Advanced) [18]. The use of this vector is particularly suitable because it ensures a very low basal level of gene expression. The use of pTRE-Tight-BI bidirectional vectors [19] allows to co-regulate the expression of two genes, namely the gene of interest and a fluorescent reporter. In detail, this vector contains a bidirectional promoter composed of a modified Tetracycline Response Element (TREmod), between two copies of minimal CMV promoter (P_{minCMV}) in opposite directions. The co-expression of a fluorescent protein permits rapidly detecting the relative expression of a gene of interest using fluorescence microscopy, or flow cytometry [20]. Furthermore, the use of a bidirectional vector avoids the expression of fusion proteins or the need of an internal ribosomal entry site for the simultaneous expression of two elements from a single transcript. As a selectable marker, the vector includes an antibiotic resistance cassette (i.e., neomycin resistance gene) for the selection of stable transfected cells using Geneticin (G418).

As cellular model Jurkat cell line has been selected since it harbors only one copy per diploid genome of CCL3L1 gene and it does not express CCL3L1 transcript. For the transfection of Jurkat Tet-On with pTRE-Tight-BI-Tax-2Gu-AcGFP1 construct, the Nucleofector™ technology (Lonza group Ltd.) was used. Among the advantages offered by this technology, there are a high efficiency

of transfection and a fast protein expression. In fact, the nucleofected DNA can directly enter the nucleus of most cell types, and the transfected gene can be analyzed just after 2–4 h.

Using this approach, an uncorrected interpretation of results due to pleiotropic effects or nonspecific induction is minimized.

Given the importance of studying the transactivation ability of Tax-2, a protocol for switching *tax-2* expression in a tightly regulated manner and also for performing a kinetics analysis of gene expression in response to Tax-2 action is provided.

2 Materials

2.1 Mammalian Cell Culture Supplies

1. Jurkat Tet-On® Cell line (Clontech Laboratories, Mountain View, CA, USA) (*see* **Note 1**).
2. RPMI-1640 (Euroclone, Pero, Milan, Italy).
3. Fetal Bovine serum (FBS), tetracycline (Tc)-free approved for Tet inducible system (Clontech) (*see* **Note 2**).
4. L-glutamine solution, 200 mM (Euroclone).
5. Penicillin and Streptomycin solution, 10,000 U/mL (Euroclone).
6. Trypan Blue solution 0.4% (Euroclone).
7. Dimethylsulfoxide (DMSO) (Sigma-Aldrich, Milano, Italy).
8. Tissue culture flasks/plates.
9. Cryovials.
10. TopeSafe™ Class II safety cabinet (Euroclone).
11. Inverted microscope (Carl Zeiss AG, Oberkochem, Germany).

2.2 Nucleofection and Inducible Expression System

1. pTRE-Tight-BI-AcGFP1 Vector (Clontech).
2. Geneticin, G418 (Sigma-Aldrich).
3. Linear Puromycin Marker, 50 ng/μL (Clontech).
4. Puromycin dihydrochloride (Sigma-Aldrich).
5. Doxycycline hyclate (Sigma-Aldrich).
6. Cell Line Nucleofector® kit V (Lonza Group Ltd., Basel, Switzerland) (*see* **Note 3**).
7. Nucleofector™2b Device (Lonza Group Ltd). It is a single cuvette-based system (low-throughput platform). It efficiently transfects from 2×10^6 up to 2×10^7 cell number, by using 1–5 μg DNA vector amount/sample.
8. Fluorescence microscope or flow cytometer.

2.3 RNA Purification

1. RNA extraction system (*see* **Note 4**).
2. DNase I treatment system (*see* **Note 5**).

3. To measure RNA concentration Nanodrop™ 1000 Spectrophotometer was used (Thermo Fischer Scientific, Wilmington, DE, USA).
4. Microcentrifuges.
5. Vortex mixer.

2.4 Real-Time RT-PCR Assay

1. cDNA synthesis system (*see* **Note 6**).
2. Primer Express® software v 2.0 (Applied Biosystems, Carlsbad, California) was used to design primers and probes of Tax and housekeeping genes (*see* **Note 7**). Primers and probe for HTLV-2 *tax* cDNA were selected on *tax* gene of HTLV-IIGu strain (GenBank accession number: X89270), while primers and probe for *human beta-globin (HBB)* cDNA amplification were designed on HBB sequence (GenBank accession number: AF007546). To check for their specificity, all sequences were aligned using BLAST program (http://blast.ncbi.nlm.nih.gov). The primers and probe sequences for *tax-2* and *HBB* genes are reported in Table 1.
3. TaqMan PCR master mix is a premix of all components except for primer pairs and probe. The assay was performed by using FluoCycle™ probe (Euroclone, Milan, Italy) master mix.
4. Nuclease-free PCR-grade water.
5. Real-time PCR thermal cycler. The qPCR reactions were performed using Chromo4^{T} Continuous Fluorescence Detector (MJ GeneWorks Inc., Waltham, MA, USA).
6. Plasticware: reaction optical tube in the 8-tube strips format (*see* **Note 8**), flat optical caps, microcentrifuges tubes, and pipette tips with filter plugs.

Table 1
Primers and probes sets for qPCR analysis

Gene	Primers/ Probes	Sequences (5′–3′)	Melting T (°C)
tax-2GU	FW	TTCCAATCAATGCGAAAGCA	62
	RV	GATCCCCGAGGGTTGGTT	61
	PR	FAM-ACCCCCTATCGCAATGGATGCCTG-BHQ1	71
β-globin	FW	GCTGGCCCATCACTTTGG	62
	RV	CCAGCCACCACTTTCTGATAGG	61
	PR	TXR–AAGAATTCACCCCACCAGTGCAGGC-BHQ2	71

FW forward primer, *RV* reverse primer, *PR* probe, *T* temperature

3 Methods

Cell cultures are grown under controlled conditions. To maintain a sterile environment and prevent cross-contamination, an area specifically dedicated to cellular biology and supplied of a laminar flow biohazard cabinet (Class II) is needed. Other essential equipments (i.e., humidified CO_2 incubator, inverted microscope, water bath, and cryopreservation system) and disposable plasticware for cell culture are necessary.

A separate area should be used for molecular biology experiments. Use clean gloves before performing each step. Use DNA surface decontaminant to clean work area and micropipettes dedicated to PCR setup. For all experimental procedures use pipette tips with filter plugs.

3.1 Nucleofection of Tet-On Cells with the Vector of Interest and Monitor Responses to Dox

1. Seed Jurkat Tet-On cells at the final concentration of about 1–1.5 × 10^5 cells/mL in culture flasks in the presence of appropriate medium and incubate at 37 °C with 5% CO_2. Use RPMI-1640 medium supplemented with 10% FBS Tet-approved, 4 mM L-glutamine, penicillin/streptomycin (10,000 U/mL), and 0.2 mg/mL G418 for maintaining cell line selection.
2. Clone *tax*-2 cDNA into the pTRE-Tight-BI-AcGFP1 (*see* **Note 9**). This vector contains the reverse transactivator rTA. As a result of Dox addition the "reverse" Tet repressor (rTetR) domain of rTA binds the TRE and activates transcription.
3. Culture the cells for 2–3 days in appropriate conditions, as described above, prior to transfection (*see* **Note 10**).
4. Initially, transfect the Jurkat Tet-On cells with pmaxGFP as control, and change, when necessary, one or more of the following reaction parameters: cells concentration, vector amount, and nucleofection program. Centrifuge 1–2 × 10^6 cells and resuspend the pellet in 100 μL of Cell line Nucleofector solution V. Proceed with nucleofecting the cells with 2 or 3 μg of vector using three different protocols (C16; I10; T14).
5. Immediately after nucleofection, add 500 μL of fresh medium to the tube containing the transfect cells, gently resuspend, and seed the entire cell suspension in a single well of a 12-well plate. Put the plate in an incubator at 37 °C with 5% CO_2.
6. Monitor the transfection efficiency by analyzing maxGFP expression through flow cytometry after 24 h as it follows: centrifuge 2 × 10^5 transfected cells, wash twice with phosphate buffer saline (PBS), resuspend the pellet in 1 mL of PBS, and analyze fluorescent properties of the cell suspension by flow cytometer (Fig. 1a, b).

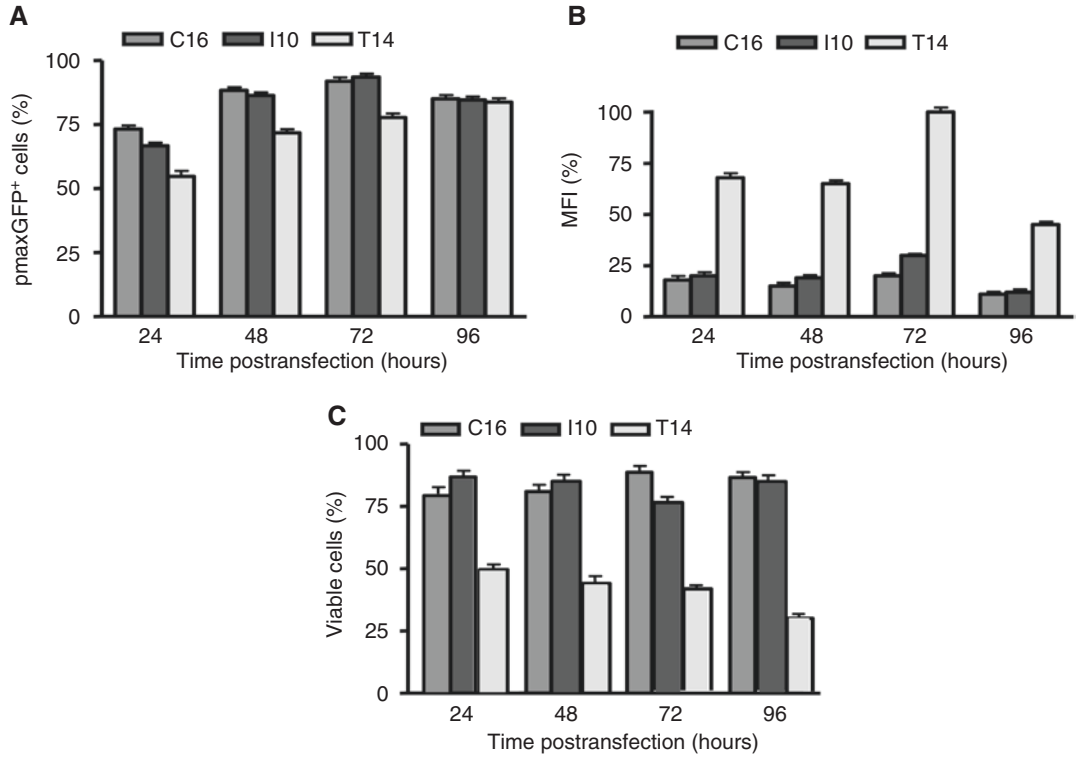

Fig. 1 Nucleofection efficiency monitoring with the pmaxGFP control vector. (**a**) Evaluation of three different nucleofection programs (C16, I10, and T14) by flow cytometry analysis of the maxGFP reporter expression at 24, 48, 72, and 96 h after transfection. (**b**) Measure of mean fluorescence intensity (MFI) of the Jurkat Tet-On cells transfected with the GFP reporter vector. (**c**) Evaluation of cell viability by inverted microscope analysis

7. Determine cellular toxicity by counting viable cells after having stained an aliquot of cell suspension, from transfected and control samples, with Trypan Blue solution 0.4% according to manufacturer's instruction and observed them at an inverted microscope (Fig. 1c).
8. Repeat the above experiment by transfecting Jurkat Tet-On cells with pTRE-Tight-Tax-2Gu-AcGFP1. Optimize the experimental conditions for a high nucleofection efficiency and a low cellular toxicity (*see* **Note 11**).
9. After 72 h, treat the transfected cells with Dox at different concentrations (*see* **Note 12**). Plan a kinetics analysis to monitor transfection efficiency through the determination of AcGFP1 expression by flow cytometer (Fig. 2) (*see* **Note 13**).

3.2 Development of a Stable Tet Transfected Cell Line

1. To identify stable transfected clones, co-transfect 2×10^6 Jurkat Tet-On cells with both pTRE-Tight-Tax-2Gu-AcGFP1 and pPur vectors. A 1:10 ratio of puromycin marker to expression vector DNA is recommended.

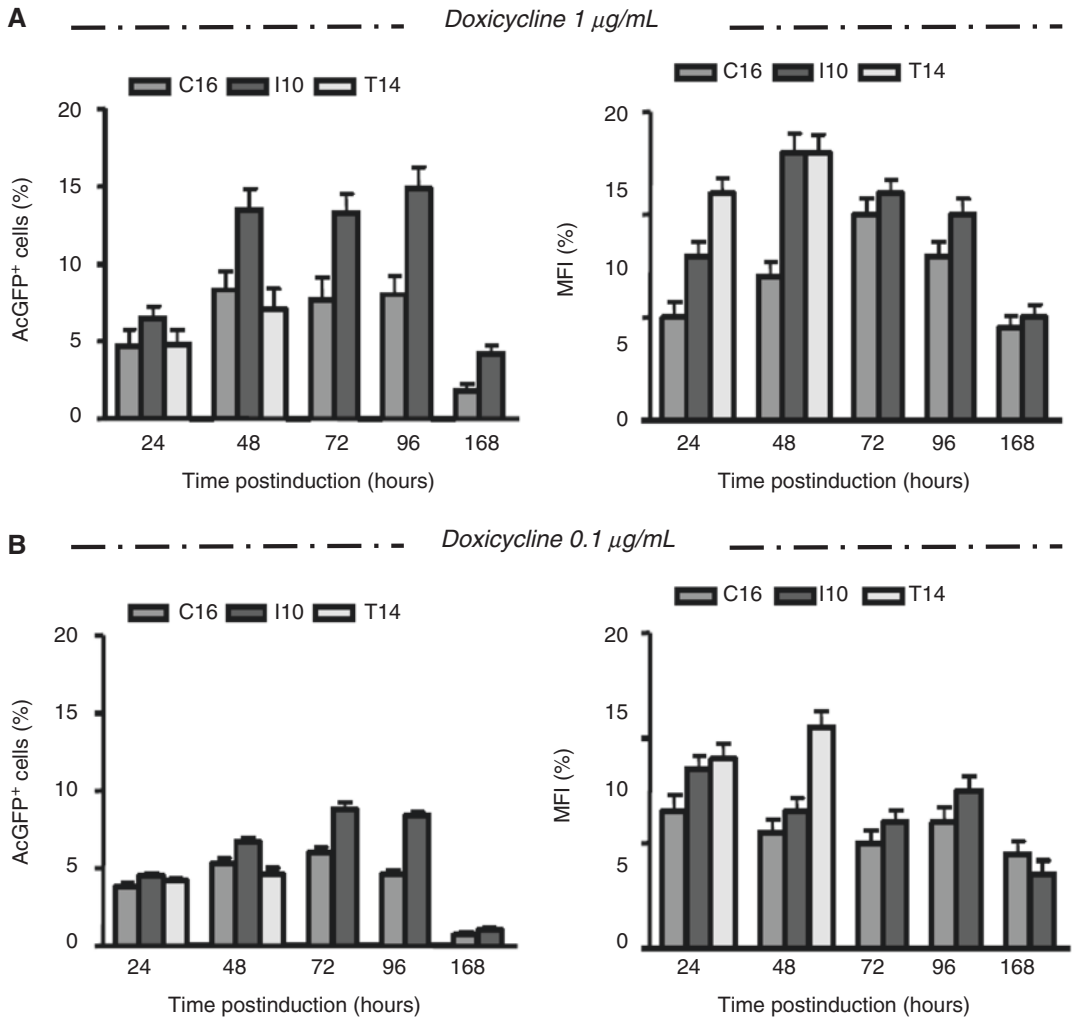

Fig. 2 Nucleofection efficiency monitoring of the pTRE-Tight-BI-AcGFP1 vector, after doxycycline treatment. Flow cytometric evaluation of the AcGFP1 reporter expression and its mean fluorescence intensity (MFI) in Jurkat Tet-On cells, using three different nucleofection programs (C16, I10, and T14), at different time points postinduction with doxycycline 1 μg/mL (**a**) or 0.1 μg/mL (**b**) The T14 nucleofection program was not tested in all time points because it extremely reduced the cell viability after 48 h, as previously demonstrated

2. At 48 h following nucleofection, add the puromycin to the culture medium at a final concentration of 0.5 μg/mL. Maintain the cells under selective conditions by adding the antibiotic in fresh medium every 4 days during the next 3 weeks (*see* **Note 14**). To avoid massive proliferation that results in death cell, split the suspension when necessary.
3. To select drug-resistant cells in the mixed cell population, perform a limiting dilution procedure as it follows: after 10 days of culture with G418 at 0.2 mg/mL, 4×10^5 cells are seeded in a 96-well plate in the presence of conditioned medium (*see* **Note 15**). More precisely, preplate 50 μL of conditioned

medium in each well. At A1 add 100 μL of cell suspension containing 4×10^5 cells and carry over 50 μL of this to the next well of the same column after gentle up and down pipetting, thereby diluting to a 1:2 ratio. Repeat the procedure for each consecutive well. Complete by adding 50 μL of fresh medium in each well. Then add 50 μL of cell suspension from the first to the following columns, by using a multichannel pipette. Repeat this procedure until the last column and add 50 μL of medium to each well. Incubate the cells under standard conditions (Fig. 3).

4. Analyze cell growth by an inverted microscope.
5. Determine nucleofection efficacy by flow cytometry analysis. Harvest 2×10^5 cells and wash with PBS buffer. After centrifugation, resuspend the pellet in 1 mL of PBS and analyze the AcGFP expression by flow cytometer.
6. Freeze stocks of transfected clones before expanding the cultures (*see* **Note 16**).

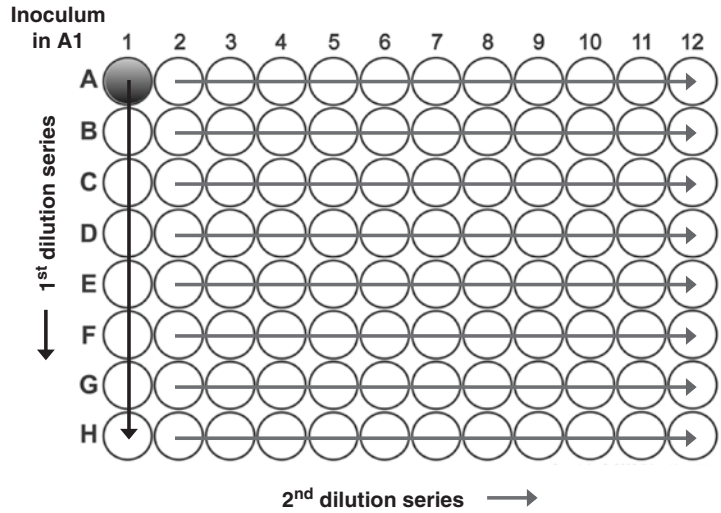

Fig. 3 Scheme of limiting dilution procedure for the selection of stable-transfected cells. After filling the 96-well plate with 50 μL conditioned medium per well (except well A1), add 100 μL of 4×10^5 preconditioned cells to well A1 (*inoculum*). Transfer 50 μL from the well A1 to B1 and mix. Repeat these 1:2 dilutions down the entire column, discarding 50 μL from H1 (*first dilution series*). Then, add an additional 50 μL conditioned medium to each well in column 1 and transfer 50 μL from column 1 to column 2 and mix. Repeat these 1:2 dilutions across the entire plate, discarding 50 μL from the last column (*second dilution series*). Finally, add an additional 50 μL of conditioned medium to all wells (final volume: 100 μL). Clones should be visible by microscopy after 4–5 days, depending on the cell growth rate

3.3 Evaluation of tax-2 Expression by Real-Time RT-PCR Assay

1. Extract total RNA from transfected and control cells (e.g., from 2×10^5 cells) at different time points (e.g., 8, 24, 48, and 96 h postinduction) (*see* **Note 17**). To remove contaminating DNA, treat the RNA samples with DNAse I prior to reverse transcription (*see* **Note 18**).
2. Perform RT-PCR in two sequential reactions (*see* **Note 19**). First, the RNA template (250 ng) is reversed transcribed using random primers (*see* **Note 20**). Positive and negative reaction products should be visualized on an ethidium bromide-stained agarose gel according to routine protocols. Second, the newly synthesized cDNA is amplified by specific primers through TaqMan Real-time PCR Assay.
3. Design Real-time PCR assay by considering the following points:
   (a) No template control (NTC) is a sample that does not contain DNA template; samples should be tested in triplicate;
   (b) The reactions must be in a monoplexed format (the target amplicon and the housekeeping amplicon are in separate tubes/wells).
4. Prepare a working solution of primers and probes at 10× final concentration (*see* **Note 21**).
5. Prepare a PCR master mix according to Table 2. The final total volume per reaction is 25 μL.
6. Add 20 μL of master mix to each tube, by mixing gently with micropipette and avoiding bubbles.
7. Add 5 μL of cDNA template to the appropriate PCR tube or well.
8. Cap the reaction tubes.
9. Place the reaction tubes on the Real-time PCR thermal cycler and start the appropriate cycling for *tax-2* assay (Table 3).
10. Analyze the data by setting the threshold and by calculating $\Delta\Delta C_T$ values as follows:
    $\Delta C_T = C_T$ [target] − C_T [housekeeping].
    $\Delta\Delta C_T = \Delta C_T$ [sample] − ΔC_T [calibrator].

Table 2
Preparation of qPCR mix in a final reaction volume of 25 μL

	Final concentration per reaction		
Assay	**PCR Master MIX**	**FW/RV primers (nM)**	**Probe (nM)**
tax-2GU	1×	300	200
β-globin	1×	600	200

Table 3
Conditions of qPCR reactions

Assay	No.cycles	Temperature, time	Step
tax-2GU *β-globin*	1	95 °C for 10 min[a]	DNA polymerase activation
	45	95 °C for 15 s	Denaturation
		56 °C for 30 s	Annealing
		72 °C for 30 s	Extension

[a]Optimum temperature and time are dependent on enzyme's features

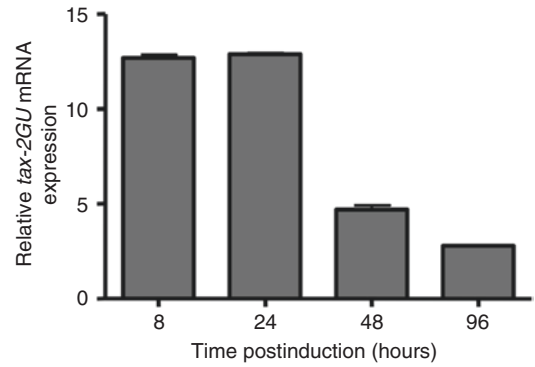

Fig. 4 Relative mRNA *tax-2GU* expression in Jurkat Tet-On cells after doxycycline treatment. After nucleofection of Jurkat Tet-On cells with pTRE-Tight-BI-Tax-2Gu-AcGFP1 (I10 program) and stimulation with 1 μg/mL doxycycline, *tax-2GU* expression kinetics was monitored by Real-time RT-PCR assay at different time points (8, 24, 48, and 96 h postinduction). The relative quantification was determined using the $\Delta\Delta C_T$ method, the *β-globin* as housekeeping gene, and the unstimulated transfected cells as calibrator. The *tax-2GU* expression increased more than ten times in 24 h

(target: *tax-2*; housekeeping: *β-globin*; calibrator: unstimulated transfected cells).

11. Express normalized target gene expression level as $2^{(-\Delta\Delta CT)}$ (Fig. 4).

4 Notes

1. Jurkat Tet-On is a human T-cell leukemia-derived cell line (E 6.1), which constitutively expresses the reverse tetracycline-controlled transctivator.
2. FBS Tet-approved does not contain trace levels of tetracycline, known to interfere with proper regulation of TRE-controlled gene expression (Clontech-Certificate of Analysis).

3. The kit contains a specific solution to assure high transfection efficiency and cell viability. The kit also provides disposable sterile vessels, pipettes, and the pmaxGFP™ control vector.
4. A protocol for phenol-free total RNA isolation using a guanidinium-based lysis/denaturant and glass fiber separation technology is suggested.
5. After removing DNA contamination, the DNase-I should also be removed by DNase inactivation reagent.
6. To obtain cDNA, the following reagents are needed: nuclease-free water, 10× RT-PCR buffer, dNTP mix (2.5 mM each), random (50 μM) or oligo(dT) (50 μM) primers, RNase inhibitor (10 U/μL), M-MLV-RT enzyme. Positive and negative (minus-RT or minus template) control reactions should be planned in the same assay.
7. Each oligonucleotide is ordered as lyophilized salt HPLC purified. Stock solutions of primers or probes have to be prepared in nuclease-free PCR-grade water at 100 μM and stored at −20 °C. Multiple freezing/thawing are to be avoided by making single-use aliquots of stock solutions
8. Use polypropylene tubes/plates and avoid polystyrene plasticware to reduce fluorescence background.
9. Tax-2Gu-X89270 was produced from GeneArt™ Gene Synthesis Service (Thermo Fisher Scientific), which also cloned the gene into the plasmid pTRE-Tight-BI-AcGFP1 and verified it by sequencing. The coding sequence of the *tax-2* gene contains 1071 bp and is flanked by a Kozak consensus translation initiation site at 5′ terminus and two stop codons at 3′ terminus to further increase translation efficacy in eukaryotic cells. The final sequence also includes two restriction sites on both 3′ (for EcoRV) and 5′ (for KpnI) termini.
10. In order to obtain high transfection efficiency, cells should be in active growth phase before being processed.
11. The transfection of 2×10^6 target cells with 2 μg of pTRE-Tight-Tax-2Gu-AcGFP1 using C16, I10, and T14 programs is suggested.
12. Doxycycline concentrations should be tested at 0.1–2 μg/mL.
13. Since Tc and Dox have a half-life not longer than 24 or 12 h, respectively, it is necessary to add fresh Tc or Dox to the medium at least every 48 h.
14. Isolated colonies of transfected cells should appear after 2–4 weeks of culture.
15. The conditioned medium is obtained by culturing $2–4 \times 10^6$ PBMCs per mL for 24 h in RPMI-1640 supplemented with 10% FBS Tet-approved, 4 mM L-glutamine, and penicillin/

streptomicin (10,000 U/mL). After separating the cells by centrifugation, both G418 (at 0.2 mg/mL) and puromycin (at 0.5 μg/mL) were added to the medium.

16. Sterilized conditions are recommended. Prepare freezing medium with 10% DMSO and 90% FBS Tet-approved. 2–5 × 10^6 cells per cryovial should be freezed and transferred to liquid nitrogen.
17. The extracted RNA, if not immediately processed, must be stored at −80 °C.
18. A dedicated set of micropipettes that are used solely for PCR setup is needed.
19. To improve sensitivity and range of detection of gene expression by Real-time PCR assay, two separate reactions need to be performed.
20. When the sample contains partially degraded RNA strands, the use of random primers allows obtaining a higher recovery of cDNA with respect to oligo(dT) or specific primers.
21. Each oligonucleotide is ordered as lyophilized salt HPLC purified. Stock solutions of primers or probes have to be prepared in nuclease-free PCR-grade water at 100 μM and stored at −20 °C. Multiple freezing/thawing are to be avoided by making single-use aliquots of stock solutions.

Acknowledgments

This work was supported by Istituto Superiore di Sanità, National Research Project on AIDS (grants 40D.14 and 40D.62, ELVIS Italian Network on LTNP), and EC Project number LSHP-CT-2007-037616 (Genetic and Immunological Studies of European and African HIV-1+ Long Term Non-Progressors, GISHEAL) (to C. Casoli).

References

1. Margolis L (2003) Cytokines: strategic weapons in germ warfare? Nat Biotechnol 21:15–16
2. Kannangara S, DeSimone JA, Pomerantz RJ (2005) Attenuation of HIV-1 infection by other microbial agents. J Infect Dis 192: 1003–1009
3. Casoli C, Vicenzi E, Cimarelli A, Magnani G, Ciancianaini P, Cattaneo E, Dall'Aglio P, Poli G, Bertazzoni U (2000) HTLV-II down-regulates HIV-1 replication in IL-2-stimulated primary PBMC of coinfected individuals through expression of MIP-1alpha. Blood 95(9):2760–2769
4. Lewis MJ, Gautier VW, Wang XP, Kaplan MH, Hall WW (2000) Spontaneous production of C-C chemokines by individuals infected with human T lymphotropic virus type II (HTLV-II) alone and HTLV-II/HIV-1 coinfected individuals. J Immunol 165(7):4127–4132
5. Pilotti E, Elviri L, Vicenzi E, Bertazzoni U, Re MC, Allibardi S, Poli G, Casoli C (2007) Postgenomic up-regulation of CCL3L1

expression in HTLV-2-infected persons curtails HIV-1 replication. Blood 109(5):1850–1856

6. Balistrieri G, Barrios C, Castillo L, Umunakwe TC, Giam CZ, Zhi H, Beilke MA (2013) Induction of CC-chemokines with antiviral function in macrophages by the human T lymphotropic virus type 2 transactivating protein, Tax2. Viral Immunol 26(1):3–12
7. Banerjee P, Rochford R, Antel J, Canute G, Wrzesinski S, Sieburg M, Feuer G (2007) Proinflammatory cytokine gene induction by human T-cell leukemia virus type 1 (HTLV-1) and HTLV-2 Tax in primary human glial cells. J Virol 81(4):1690–1700
8. Barrios CS, Abuerreish M, Lairmore MD, Castillo L, Giam CZ, Beilke MA (2011) Recombinant human T-cell leukemia virus types 1 and 2 Tax proteins induce high levels of CC-chemokines and downregulate CCR5 in human peripheral blood mononuclear cells. Viral Immunol 24(6):429–439
9. Boxus M, Twizere JC, Legros S, Dewulf JF, Kettmann R, Willems L (2008) The HTLV-1 Tax interactome. Retrovirology 5:76
10. Charoenthongtrakul S, Zhou Q, Shembade N, Harhaj NS, Harhaj EW (2011) Human T cell leukemia virus type 1 Tax inhibits innate antiviral signaling via NF-kappaB-dependent induction of SOCS1. J Virol 85(14):6955–6962
11. Franchini G, Streicher H (1995) Human T-cell leukaemia virus. Baillieres Clin Haematol 8(1):131–148
12. Gossen M, Bujard H (1992) Tight control of gene expression in mammalian cells by tetracycline-responsive promoters. Proc Natl Acad Sci U S A 89(12):5547–5551
13. Gossen M, Freundlieb S, Bender G, Muller G, Hillen W, Bujard H (1995) Transcriptional activation by tetracyclines in mammalian cells. Science 268(5218):1766–1769
14. Gossen M, Bonin AL, Bujard H (1993) Control of gene activity in higher eukaryotic cells by prokaryotic regulatory elements. Trends Biochem Sci 18(12):471–475
15. Gossen M, Bonin AL, Freundlieb S, Bujard H (1994) Inducible gene expression systems for higher eukaryotic cells. Curr Opin Biotechnol 5(5):516–520
16. HT1080 Cell Line & pTRE2 Vector (Jan 1999) Clontechniques XIV(1):23
17. pTRE-Tight Vectors (Apr 2003) Clonetechniques XVIII(2):10
18. Furth PA, St Onge L, Boger H, Gruss P, Gossen M, Kistner A, Bujard H, Hennighausen L (1994) Temporal control of gene expression in transgenic mice by a tetracycline-responsive promoter. Proc Natl Acad Sci U S A 91(20):9302–9306
19. Baron U, Freundlieb S, Gossen M, Bujard H (1995) Co-regulation of two gene activities by tetracycline via a bidirectional promoter. Nucleic Acids Res 23(17):3605–3606
20. BD Living Clors AcGFP1 fluorescent protein (Jan 2005) Clontechniques XX (1):5–6

Chapter 8

EGF Uptake and Degradation Assay to Determine the Effect of HTLV Regulatory Proteins on the ESCRT-Dependent MVB Pathway

Colin Murphy and Noreen Sheehy

Abstract

The endosomal sorting complex required for transport (ESCRT) pathway plays key roles in multivesicular bodies (MVBs) formation and lysosomal degradation of membrane receptors, viral budding, and midbody abscission during cytokinesis. The epidermal growth factor receptor (EGFR) is regarded as a prototypical cargo of the MVB/ESCRT pathway and following stimulation by epidermal growth factor (EGF) EGFR/EGF complexes are internalized, sorted into MVBs, and degraded by lysosomes or recycled back to the cell membrane. Here, we describe an assay to analyze the effect of human T-cell leukemia (HTLV) regulatory proteins on the functionality of ESCRT-dependent MVB/lysosomal trafficking of EGFR/EGF complexes. This is performed by direct visualization and quantification of the rate of EGF-Alexa595/EGFR internalization and degradation in HeLa cells expressing HTLV regulatory proteins by immunofluorescence and western blot.

Key words HTLV, EGF, ESCRT, Tax1, HBZ, APH-2, MVBs

1 Introduction

Human T-cell leukemia virus type 1 and type 2 (HTLV-1; HTLV-2) are highly related retroviruses [1]. While HTLV-1 is the causative agent of adult T-cell leukemia (ATL) and a chronic inflammatory neurodegenerative disorder termed HTLV-1-associated myelopathy/tropical spastic paraparesis (HAM/TSP), HTLV-2 infection is not linked to the development of cancer but is associated with non-malignant lymphocyte proliferation, elevated platelet counts, and milder neurological disorders [2–4]. HTLV-1 and -2 infections are governed by regulatory proteins, the most widely studied of which are Tax1 and HBZ or Tax2 and APH-2, respectively [5, 6]. Tax1 and Tax2 are pivotal transcriptional regulators of both viral and cellular gene expression, which is linked to their ability to modulate several cellular signaling pathways including CREB, NFkB, and AP1. HBZ and APH-2 appear to oppose the activities of their

Claudio Casoli (ed.), *Human T-Lymphotropic Viruses: Methods and Protocols*, Methods in Molecular Biology, vol. 1582,
DOI 10.1007/978-1-4939-6872-5_8,

respective Tax proteins and inhibit Tax-mediated activation of the CREB, NFkB, and AP-1 pathways.

The ESCRT pathway plays key roles in multivesicular bodies (MVBs) formation and lysosomal degradation of membrane receptors, viral budding, and midbody abscission during cytokinesis [7]. These distinct processes all involve equivalent membrane fission events that are governed by multi-subunit ESCRT complexes termed ESCRT-0, -I, -II, -III together with Vps4-Vta1 and ALIX. During MVB formation, the ESCRT machinery is recruited to endosomes by the ESCRT-0 subunit HRS that forms a complex with ubiquitinated cargos and the ESCRT-I subunit Tsg101. These interactions together with those of ESCRT-II and ESCRT-III and Vps4 culminate in the formation of MVBs and the lysosomal degradation of internalized cargos. Budding of enveloped viruses possessing "late domains" such as PTAP or YPDL in their matrix proteins depends on the recruitment of ESCRT-I subunit Tsg101 or ALIX, respectively and ESCRT-III to cell membranes to facilitate their final egress from cells [8]. During cytokinesis the 55 kDa centromere protein CEP55 recruits the ESCRT-I subunit Tsg101 and ALIX to the midbodies of separating cells to facilitate their final separation [9, 10].

To date, the role of the ESCRT pathway in HTLV infection has not been investigated. However, there is evidence to suggest that this pathway may play a role in HTLV-1 budding. The HTLV-1 Matrix protein contains two adjacent late motifs "PPPYEPTAP" that interact with Nedd4.1 and the ESCRT-I component TSG101, respectively to mediate viral budding [11, 12]. The impact of HTLV infection on ESCRT-dependent MVB formation and lysosomal degradation of cellular receptors or in cytokinesis has not been reported.

In this protocol, we describe an assay to determine the effect of the HTLV regulatory proteins Tax1, Tax2, HBZ, and APH-2 on the ESCRT-dependent MVB pathway. The Epidermal Growth Factor Receptor (EGFR) has been extensively studied as a prototype cargo of the MVB pathway [13]. Following activation, ubiquitination, and internalization by endocytosis, EGF/EGFRs are sorted into MVBs, which ultimately fuse with lysosomes resulting in their degradation and termination of the signal. Thus, the EGF/EGFR uptake and degradation assay described here can be used to determine the effect of HTLV regulatory proteins on the functionality of ESCRT-dependent MVB pathway.

2 Materials

1. HeLa cell line (ATCC CCL-2) or any other EGFR expressing cell line.
2. DMEM (1×) + GlutaMax (Gibco Life Technologies/Thermo Fisher Scientific, Waltham, MA, USA).

3. Phosphate Buffered Saline (PBS).
4. 0.05% Trypsin-EDTA Phosphate buffered saline (PBS).
5. Fetal Bovine Serum (FBS).
6. Glass chamber slides.
7. T75 flasks.
8. Epidermal Growth Factor complexed to Texas Red (Molecular Probes/Thermo Fisher Scientific).
9. Unlabeled Epidermal Growth Factor (Molecular probes/Thermo Fisher Scientific).
10. TurboFect (Thermo Fisher Scientific).
11. Paraformaldehyde and DAPI (4′,6-diamidino-2-phenylindole).
12. Labeled and unlabeled EGF components: dissolve EGF-Texas Red or unlabeled EGF in 100 μl of sterile deionized water to give a final concentration of 1 μg/μl. Once completely dissolved aliquot into 10 μl volumes and store at −20 °C.
13. DMEM growth medium: Add 50 ml of Fetal Bovine Serum (FBS) to 450 ml DMEM (1×) + GlutaMax to give a final concentration of 10% FBS.
14. 4% Paraformaldehyde: Add 80 ml of PBS to a glass beaker on a stir plate in a Fume Hood. Heat while stirring to approximately 60 °C. Take care that the solution does not boil. Add 4 g of Paraformaldehyde powder to the heated PBS (*see* **Note 1**). Slowly raise the pH of the solution by adding 1 N NaOH dropwise until the solution clears. Once the Paraformaldehyde has dissolved allow the solution to cool down and adjust the volume to 100 ml with PBS. Finally, check the pH and adjust to approximately pH 7 with dilute HCL. Aliquot the solution and store at −20 °C.

3 Methods

All cell culture is carried out in a Biosafety Level 2 laboratory.

3.1 Sub-culturing of HeLa Cells (ATCC CCL-2)

Volumes used in this protocol are for a 75 cm^2 flask; proportionally reduce or increase amount of dissociation medium for culture vessels of other sizes.

1. Remove and discard cell culture medium.
2. Wash the monolayer with 10 ml of sterile PBS.
3. Add 1 ml of Trypsin/EDTA and place flask in 37 °C incubator for 2–3 min. Observe cells under an inverted microscope to ensure all cells are detached from the flask.
4. Add 9 ml of complete growth medium and pipette up and down to ensure complete dispersal of cells.

5. Add 1 ml of cell suspension into new flask and an appropriate volume of DMEM growth medium.
6. Incubate cultures at 37 °C in the presence of 5% CO_2. Cells are usually sub-cultured two to three times per week.

3.2 Transfection of Cells

1. Dislodge cells from confluent flask as described in Subheading 3.1.
2. Seed each well of a two-well glass chamber slide with 100,000 HeLa cells/ml.
3. Incubate slides in a humidified incubator at 37 °C overnight.
4. Each well of a two-well slide is transfected with 500 ng of the following plasmids: pEGFP empty, pEGFP Tax1, pEGFP Tax2, pEGFP HBZ or pEGFP APH-2 (*see* **Note 2**).
5. Dilute plasmid DNA in 100 μl of serum-free DMEM.
6. Add 1 μl of Turbofect reagent, mix and allow to stand at room temperature for 20–30 min (*see* **Note 3**).
7. Drop entire mixture onto each well, rotate and place at 37 °C for a further 24 h.

3.3 EGF Uptake and Degradation Assay

1. Remove and discard medium from slides.
2. Wash cells three times with PBS.
3. Serum starve the cells by adding 1 ml of serum-free DMEM (SFM) to each well and incubate at 37 °C for 3 h.
4. Toward the end of the incubation period dilute EGF-Texas Red in serum-free medium to give a final concentration of 2 μg/ml (*see* **Note 4**).
5. Discard the SFM from wells and wash twice with PBS.
6. Add 1 ml of diluted EGF-Texas Red (2 μg/ml) to each well and incubate at 4 °C for 30 min.
7. During the incubation dilute unlabeled EGF in SFM to a final concentration of 2 μg/ml.
8. Wash cells three times with cold PBS (*see* **Note 5**).
9. Add 1 ml of diluted unlabeled EGF to each well and incubate at 37 °C for the desired amounts of time (*see* **Note 5**).
10. Following incubation wash cells in PBS and fix cells using 4% Paraformaldehyde for 10 min at room temperature.
11. Permeabilise the cells using 0.5% Triton® X-100/PBS for 5 min at room temperature and wash two times in 0.05% Triton® X-100/PBS.
12. Stain the nuclei by immersing the slides in DAPI (20 μg/ml) for 10 s and wash once in water followed by one wash in PBS.

13. Mount coverslips in Prolong Gold anti-fade (Life Technologies/Thermo Fisher Scientific) and visualize images using a suitable Fluorescent Microscope.
14. Quantification of EGF-595 signal in GFP positive cells is performed by measurement of signal intensity using Fiji Image Processor in cells that had been acquired using the same exposure times (*see* **Note 6**).

4 Notes

1. Formaldehyde is toxic. Read the Material Safety Data Sheet before working with this chemical. Gloves and safety glasses should be worn and solutions should be made inside a fume hood.
2. For best results confluency of cells should be 80–90% on the day of transfection. The quality of the plasmid DNA is critical for achieving good transfection efficiency. Use a kit such as Nucleo Bond Xtra Midi endotoxin free (Macherey-Nagel, Duren, Germany) to perform plasmid preps.
3. Even though there are a great variety of transfection reagents available Turbofect appears to be the least toxic for HeLa cells.
4. EGF-Texas Red is light sensitive and should be protected from light.
5. Use cold PBS (4 °C) to wash away unincorporated EGF-Texas Red as this prevents uptake of EGF/EGFR by the cells before the start of the incubation period at 37 °C. Using the method described here 15, 30, 60, and 120 min incubation periods at 37 °C give the best visualization of EGF/EGFR uptake and degradation with the maximum signal generally being observed at 30 or 60 min followed by loss of signal at 120 min.
6. Depending on the strength of the signal, use 3 or 5 s exposure times to measure and compare the EGF-Texas Red signal intensities in GFP positive cells using the Fiji Image Processor or equivalent programme.

Acknowledgment

This work was supported by the National Virus Reference Laboratory (NVRL), University College Dublin, Ireland and by the UCD School of Medicine and Medical Science Student Summer Research Award (SSRA) programme.

References

1. Ciminale V, Rende F, Bertazzoni U, Romanelli MG (2014) HTLV-1 and HTLV-2: highly similar viruses with distinct oncogenic properties. Front Microbiol 5:398
2. Araujo A, Hall WW (2004) Human T-lymphotropic virus type II and neurological disease. Ann Neurol 56:10–19
3. Roucoux DF, Murphy EL (2004) The epidemiology and disease outcomes of human T-lymphotropic virus type II. AIDS Rev 6:144–154
4. Bartman MT, Kaidarova Z, Hirschkorn D, Sacher RA, Fridey J, Garratty G et al (2008) Long-term increases in lymphocytes and platelets in human T-lymphotropic virus type II infection. Blood 112:3995–4002
5. Romanelli MG, Diani E, Bergamo E, Casoli C, Ciminale V, Bex F, Bertazzoni U (2013) Highlights on distinctive structural and functional properties of HTLV Tax proteins. Front Microbiol 4:271
6. Barbeau B, Peloponese JM, Mesnard JM (2013) Functional comparison of antisense proteins of HTLV-1 and HTLV-2 in viral pathogenesis. Front Microbiol 4:226
7. Wollert T, Yang D, Ren X, Lee HH, Im YJ, Hurley JH (2009) The ESCRT machinery at a glance. J Cell Sci 122:2163–2166
8. Votteler J, Sundquist WI (2013) Virus budding and the ESCRT pathway. Cell Host Microbe 14(3):232–241
9. Carlton JG, Martin-Serrano J (2007) Parallels between cytokinesis and retroviral budding: a role for the ESCRT machinery. Science 316:1908–1912
10. Morita E, Sandrin V, Chung HY, Morham SG, Gygi SP, Rodesch CK, Sundquist WI (2007) Human ESCRT and ALIX proteins interact with proteins of the midbody and function in cytokinesis. EMBO J 26:4215–4227 Erratum in: EMBO J. 2012 31:3228
11. Blot V, Perugi F, Gay B, Prévost MC, Briant L, Tangy F et al (2004) Nedd4.1-mediated ubiquitination and subsequent recruitment of Tsg101 ensure HTLV-1 Gag trafficking towards the multivesicular body pathway prior to virus budding. J Cell Sci 117:2357–2367
12. Bouamr, F., Melillo, J.A., Wang, M.Q., Nagashima, K., de Los Santos, M, Rein, A., and Goff, S.P. (2003) PPPYVEPTAP motif is the late domain of human T-cell leukemia virus type 1 Gag and mediates its functional interaction with cellular proteins Nedd4 and Tsg101 [corrected]. J Virol 77: 11882–11895. Erratum in: J Virol. 2004 Apr; 78(8):4383
13. Eden ER, White IJ, Futter CE (2009) Down-regulation of epidermal growth factor receptor signalling within multivesicular bodies. Biochem Soc Trans 37:173–177

Part III

Genotyping and Gene Expression

Chapter 9

Methods for Identifying and Examining HTLV-1 HBZ Post-translational Modifications

Jacob Al-Saleem, Mamuka Kvaratskhelia, and Patrick L. Green

Abstract

Post-translational modifications (PTMs) are chemical alterations to individual amino acids that alter a protein's conformation, stability, and/or function. Several pathogenic viruses have been shown to encode proteins with PTMs, including human T-cell leukemia virus type 1 (HTLV-1) Tax and Rex regulatory proteins. HTLV-1 basic leucine zipper protein (HBZ) was hypothesized to feature PTMs due to its functional activities and interactions with cellular transcription factors and acetyltransferases. Here, we describe the approach used to identify, via mass spectrometry, the PTMs of HBZ. In addition, we describe methods to determine the functional relevance of the identified PTMs.

Key words HTLV-1, Post-translational modifications, HBZ, Mass spectrometry, NF-κB, c-Jun, IRF-1

1 Introduction

HTLV-1 was the first discovered pathogenic human retrovirus and was shown to cause several human diseases including Adult T-cell Leukemia/Lymphoma (ATLL) and HTLV-1 Associated Myelopathy/Tropic Spastic Paraparesis (HAM/TSP) [1–4]. As a complex retrovirus, HTLV-1 expresses several regulatory and accessory genes along with the structural and enzymatic proteins common among all retroviruses [5]. Tax, the HTLV-1 regulatory gene product, drives transcription of the viral gene products via interaction with cellular transcription factors and the viral promoter [6]. In addition, studies have shown Tax to be a key viral oncogene because its expression is required for primary T-cell transformation in vitro and induces leukemia/lymphoma development in Tax-transgenic mice [7–9]. HBZ is the only HTLV-1 gene product encoded by the antisense strand of the viral genome [10, 11]. HBZ promotes cell growth and viral persistence in vitro and regulates several cellular transcription factors, including CREB, Jun family members, p65 (NF-κB), and IRF-1 [12–15]. Additional studies have demonstrated that HBZ, in both its mRNA and protein forms, can induce

Claudio Casoli (ed.), *Human T-Lymphotropic Viruses: Methods and Protocols*, Methods in Molecular Biology, vol. 1582,
DOI 10.1007/978-1-4939-6872-5_9,

cellular proliferation; moreover, transgenic expression of HBZ in mice leads to development of a T-cell lymphoma similar to ATLL [16–18]. Interestingly, as a result of either a deletion or methylation of the 5′ viral LTR, HBZ remains the only gene product constitutively expressed in all ATLL patients [19–21]. Collectively, these studies have suggested that HBZ has a larger role in the pathogenesis of HTLV-1, and have led to the hypothesis that HBZ, in cooperation with Tax, is critical for HTLV-1-induced disease.

PTMs include phosphorylation, methylation, and/or acetylation of amino acids within a protein [22]. These modifications can result in conformation shifts in a protein, which changes protein function, localization, and in some cases, stability. PTMs are transitional (can be added or removed), which allows diverse feedback mechanisms where proteins can respond to the state of the cell, and change their activity or localization as needed. Several HTLV-1 proteins, including Tax and Rex, are post-translationally modified. Tax features phosphorylation, acetylation, and sumoylation. These modifications affect the ability of Tax to activate viral transcription and the classical NF-κB pathway, and to induce the formation nuclear bodies [23–25]. Rex also is phosphorylated; these phosphorylation events are critical for its ability to localize to the nucleus and bind target RNA, ultimately resulting in its export to the cytoplasm [26]. HBZ was predicted to contain PTMs when the protein sequence was analyzed with phosphorylation and acetylation prediction tools. This chapter describes the methods used to identify PTMs in HBZ to address what effect these PTMs have on protein stability and known protein functions. To quantitate the effects of PTMs, mutational analysis was performed where the amino acids identified to be post-translationally modified were changed to mimic either the presence or absence of the PTM on that amino acid. For phosphorylation events, the amino acid that was modified was changed to aspartate to mimic phosphorylation, and to alanine to mimic the lack of phosphorylation. For acetylation events, the amino acid was replaced with glutamine to mimic acetylation and arginine to mimic the lack of acetylation.

2 Materials

2.1 HBZ Protein Purification

1. 10-cm tissue culture dishes.
2. HEK293T cells (ATCC).
3. Flag-HBZ expression vector.
4. Empty Flag-Tag expression vector (Sigma-Aldrich/MERCK Millipore, Billerica, MA, USA).
5. Phosphate Buffered Saline (PBS).

6. DMEM supplemented with 10% Fetal Bovine Serum, 2 mM glutamine, penicillin (100 U/mL), and streptomycin (100 mg/mL).
7. Optimem medium.
8. Lipofectamine reagent.
9. Cell scrapers.
10. Pipets and tips.
11. 15-mL conical tubes.
12. 1.5-mL microcentrifuge tubes.
13. Flag M Purification Kit (Sigma-Aldrich/Merck Millipore).
14. 6× SDS Loading Dye: 0.375 M Tris–HCl pH 6.8, 12% SDS, 60% glycerol, 0.6 M DTT, 0.06% bromophenol blue.
15. Tube rotator.

2.2 Mass Spectrometry Sample Preparation

1. 4–20% polyacrylamide precast gel.
2. Benchmark protein standard.
3. 1× SDS running buffer: 3.5 mM SDS, 25 mM Tris, 192 mM glycine.
4. Gel Code Blue (ThermoFisher Scientific, Waltham, MA, USA).
5. Water (Optima™ LC/MS, ThermoFisherScientific).
6. Acetonitrile.
7. 50 mM ammonium bicarbonate.
8. Sequencing-grade modified trypsin Gel apparatus.
9. Western blot power supply.
10. Clean trays for staining SDS-PAGE gels.
11. DNA SpeedVac Concentrator DNA120-115 (ThermoFisher-Scientific) or equivalent.

2.3 Mass Spectrometry

1. Buffer A: 2% acetonitrile, 0.2% formic acid.
2. Buffer B: 80% acetonitrile, 19.8% water, and 0.2% formic acid.
3. 15 cm × 0.075 mm reversed phase column.
4. 3 μm ReproSil-Pur C18AQ resin (Dr. Maisch GmbH, Ammerbuch, Germany).
5. Orbitrap Mass Spectrometer (ThermoFisherScientific) or equivalent.
6. 1525u Binary HPLC (Waters, Milford, MA, USA) or equivalent.
7. MASCOT (Matrix Sciences, London, UK).

2.4 Mimetic/Ablative Mutation Generation

1. DH5α Competent *E. coli* or equivalent.

2. QuickChange Site Directed Mutagenesis PCR Kit (Agilent, Santa Clara, CA, USA).
3. Carbenicillin.
4. LB Agar Plates (supplemented with 100 mg/L. carbenicillin).
5. LB Liquid Medium.
6. Plasmid DNA Purification Kits.
7. Oligonucleotides for sequencing.
8. PCR thermal cycler.
9. Access to a sequencing facility.

2.5 HBZ Functional Assays

1. HEK293T cells (ATCC).
2. PBS.
3. DMEM supplemented with 10% Fetal Bovine Serum, 2 mM glutamine, penicillin (100 U/mL), and streptomycin (100 mg/mL).
4. Optimem medium.
5. Lipofectamine reagent.
6. Cell scrapers.
7. Pipets and tips.
8. Dual Glo Luciferase System Assay Kit (Promega, Madison,WI, USA).
9. Reporter plasmids:
   (a) Renilla-TK plasmid.
   (b) HTLV-1 LTR-Luciferase reporter plasmid.
   (c) κB-Luciferase reporter plasmid.
   (d) AP1-Luciferase reporter plasmid.
   (e) IRF1-Luciferase reporter plasmid.
10. Expression vectors:
   (a) Flag HBZ expression vector.
   (b) Mutant Flag HBZ expression vectors.
   (c) Empty Flag expression vector.
   (d) Tax-1 expression vector.
   (e) p65 expression vector.
   (f) c-Jun expression vector.
   (g) IRF-1 expression vector.
11. 6× SDS loading dye:0.375 M Tris–HCl pH 6.8, 12% SDS, 60% glycerol, 0.6 M DTT, 0.06% bromophenol blue.
12. 1× SDS running buffer: 3.5 mM SDS, 25 mM Tris base, 192 mM glycine.

13. 1× transfer buffer: 25 mM Tris base, 192 mM glycine, 20% methanol.
14. Benchmark protein standard.
15. Precast 4–20% PAGE gel.
16. 3 mm Whatman paper.
17. Dried milk.
18. Tween-20.
19. PBS containing 0.1% Tween-20 (PBST).
20. Nitrocellulose blotting membrane 0.45 μm.
21. Enhanced chemiluminescent (ECL) detection reagent.
22. Antibodies:
    (a) Flag (M2, Sigma-Aldrich).
    (b) Goat Anti-Mouse HRP.
23. Fluorescence microplate reader.
24. Mini gel apparatus.
25. Western blot transfer apparatus.
26. Western power supply.
27. Western blot imagining and analysis.

3 Methods

PTMs can be predicted using a multitude of online tools. We utilize tools to identify the amino acids that could be potentially phosphorylated and acetylated. Use of these will help gauge the likelihood that a protein features PTMs, but further analyses will be needed to ensure that these residues are actually modified:

(a) NetPhos 2.0 Server can be used to identify potential phosphorylation events: http://www.cbs.dtu.dk/services/NetPhos/

(b) PAIL (Prediction of Acetylation on Internal Lysines) can be used to identify potential acetylation events: http://bdmpail.biocuckoo.org/prediction.php

3.1 HBZ Protein Purification (See Note 1)

1. Seed six 10-cm tissue culture plates with 2.5 × 10^6 HEK293T cells in DMEM medium.
2. After 18 h, check plates for confluence (70% is ideal for transfection).
3. Transfect three plates with Flag-HBZ and the other three with empty Flag expression vector using Lipofectamine reagent as follows. Transfection reaction for one plate: in a sterile 1.5-mL tube, dilute 10 μg of either Flag-HBZ or empty Flag expres-

sion vector in 500 μL of Optimem. In a separate 1.5 mL tube, dilute 30 μL Lipofectamine reagent in 500 μL of Optimem. Combine the two dilutions and incubate at room temperature for 30 min.

4. During incubation, aspirate growth medium from cells. Wash gently with 1× PBS.
5. Add 9 mL of Optimem medium to each plate.
6. Add the transfection reaction dropwise to the plate. Gently swirl the plate to ensure equal distribution of transfection complexes.
7. Incubate at 37 °C in a tissue culture incubator for 3 h.
8. Aspirate Optimem/transfection reactions.
9. Gently replenish plate with DMEM.
10. After 24 h, collect cell samples. Aspirate growth medium and wash plates with 3 mL ice cold PBS. Add 1 mL of ice cold CelLytic M from the Flag M Purification Kit and scrape cells off plate. Collect like samples into a 15 mL conical tube.
11. Rotate conical vials at 15 rpm on tube rotator for 25 min at 4 °C to lyse cells (*see* **Note 2**).
12. During rotation, prepare Flag beads as follows: thoroughly suspend the ANTI-FLAG M2 affinity gel by inverting, and dispense 150 μL of resin to a 1.5 mL tube. Spin beads out of liquid at 800 × *g* in a tabletop centrifuge. Remove supernatant and wash beads three times in 500 μL of ice cold 1× Wash Buffer (from Flag M Purification Kit). Keep beads on ice while sample preparation is finished.
13. For complete lysis, briefly vortex conical vials containing cells and then incubate on ice for 10 min.
14. Spin down cell lysate at 13,000 × *g* for 10 min at 4 °C.
15. Transfer the supernatant to a clean 15 mL conical tube (*see* **Note 3**).
16. Suspend Flag beads in 100 μL of cell lysate; then add beads to remaining lysates.
17. Rotate samples at 10 rpm on tube rotator overnight at 4 °C.
18. Split samples evenly into three separate 1.5 mL tubes, and centrifuge at 800 × *g* for 1 min at 4 °C.
19. Remove and keep supernatant as a flow-through control (*see* **Note 3**). Resuspend beads in 500 μL of ice cold 1× Wash Buffer.
20. Centrifuge beads at 800 × *g* for 1 min at 4 °C and aspirate wash buffer. Repeat wash twice.

21. Add 70 μL of 1× SDS loading buffer to beads and place in a heat block at 95 °C for 10 min. Agitate beads by flicking tubes halfway through heating.
22. Spin samples briefly and transfer supernatants to clean 1.5 mL tubes.

3.2 Mass Spectrometry

It is important to avoid possible contamination during MS sample preparation. Skin contact with objects that contact the gel can result in high levels of keratin picked up during MS. If possible, work in a laminar hood specifically for MS sample generation and wear a lab coat with full-length sleeves.

1. Load samples onto a 4–20% acrylamide SDS-PAGE gel and perform PAGE at a constant 55 mA for 2 h or until dye front exits gel.
2. Carefully remove gel from plastic plates and place in a clean tray.
3. Rinse gel three times with 100 mL of deionized water.
4. Add Code Blue reagent to cover gel completely and place on orbital shaker overnight at room temperature (*see* **Note 4**).
5. Remove Code Blue reagent carefully by pipetting. Destain the gel by adding 100 mL of deionized water to gel and agitating gently for 1–2 h until bands fully develop. Replace water two to three times during destaining (*see* Fig. 1 for representative gel).
6. Excise the HBZ protein band with a clean scalpel, slice into several small pieces, and place into a 1.5 mL tube.
7. Add 450 μL water and 500 μL 100% acetonitrile to each 1.5 mL tube, and shake at 250 rpm overnight to destain.
8. Carefully remove the destain solution without touching the gel slices. Add 0.8 mL of water to each tube. Vortex for 1 min, spin briefly, and discard the solution. Repeat this step.
9. Add 300 μL 100% acetonitrile to each sample. Shake the samples for 15 min or until the gel slices are white and shrunken. Centrifuge the samples and carefully remove the acetonitrile. Lyophilize the gel slices in a SpeedVac at 45 °C for 15 min or until dry.
10. While drying the samples, prepare the trypsin solution. First, prepare a stock solution (0.2 μg/μL) of sequencing-grade modified trypsin in trypsin resuspension buffer (50 mM acetic acid). Immediately prior to use, dilute the stock solution 40-fold with 50 mM ammonium bicarbonate.
11. Add 50 μL of trypsin solution to each dried gel slice. Allow ~15 min for the gel slices to soak up the solution. If needed, add 50 mM ammonium bicarbonate to fully cover the gel slices.

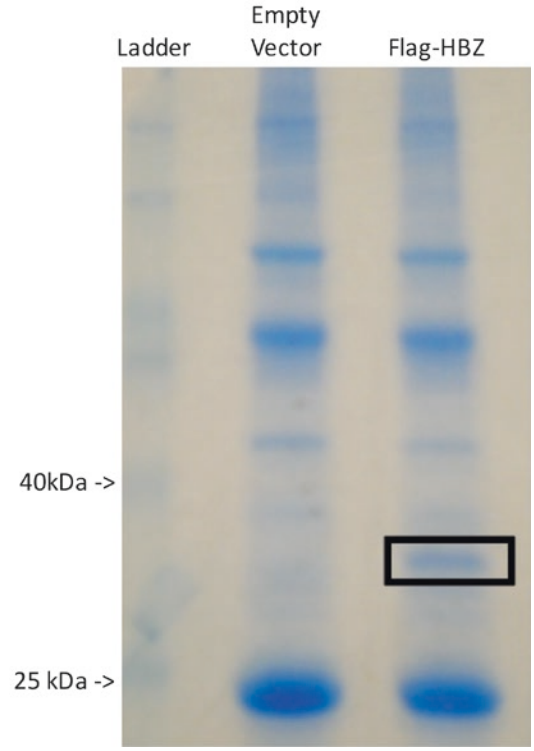

Fig. 1 Flag-HBZ protein expression on a Gel Code Blue stained gel. Representative PAGE gel showing Flag-HBZ expression inside *black box*. Gel was stained with Gel Code Blue

12. Spin briefly, place the samples on a shaker, and incubate overnight at room temperature.
13. The next day, add 150 μL pure acetonitrile to each digestion, and immediately vortex the samples for ~10 min.
14. Centrifuge the tubes at 1000 × *g* for 2 min, and carefully remove 180 μL of supernatant from each tube and transfer into 500 μL tubes.
15. Dry the peptide mixtures completely using vacuum desiccation at medium heat (~2 h at 45 °C).
16. Resuspend each dried sample in 6 μL buffer A and load 5 μL onto a 15 cm × 0.075 mm reversed phase column packed with 3 μm ReproSil-Pur C18AQ resin.
17. Elute peptides over 50 min by applying a 0–30% linear gradient of buffer B at a flow rate of 350 nL/min in an EASY-nLC HPLC.
18. Analyze samples using the Orbitrap mass spectrometer in data-dependent mode with ten data-dependent scan events for each full MS scan. Set normalized collision energy at 35, and activation

Q at 0.250. Set dynamic exclusion to 60 s and disable early expiration.

19. Analyze the MS and MS/MS results with MASCOT software using an indexed human subset Swiss-Prot database, supplemented with HTLV, 263 contaminants, and 114,960 decoy sequences.

3.3 Mimetic/Ablative Mutation Generation

To generate the amino acid mutations, we use the Stratagene QuickChange kit to perform site directed mutagenesis (SDM). Considerations while designing your primers include (kit manual has full details of primer design):

1. Both primers must feature the mutation and cover the same sequence on opposite strands.
2. We have the best success with primers that are ~30 nucleotides in length, with 12–15 nucleotides on both sides of the mutations to be introduced.
3. The melting temperature of the primers should be ≥78 °C. Melting temperatures should be verified by the calculator at the Stratagene website: http://www.genomics.agilent.com/primerDesignProgram.jsp

3.3.1 Site-Directed Mutagenesis Protocol

1. Prepare PCR reaction by mixing 5 μL of the 10× reaction buffer, 50 ng of template DNA, 125 ng of each primer, 1 μL of dNTP mix, and water to a final volume of 50 μL. Add 1 μL of PfuTurbo DNA Polymerase (2.5 U/μL).
2. Place reaction in thermocycler with the following cycling program:
   (a) 95 °C for 30 s.
   (b) 95 °C for 30 s.
   (c) 55 °C for 1 min.
   (d) 68 °C for 1 min per 1 kb of template plasmid length.
   (e) Repeat b–d 17 times.
   (f) 67 °C for 5 min.
   (g) Hold at 4 °C.
3. Add 1 μL DpnI enzyme to each PCR reaction and incubate at 37 °C for 1 h.
4. Analyze 10 μL of sample on an agarose gel to ensure a band equal in size to the full-length template plasmid is present. If no band is present, the PCR conditions should be optimized (*see* **Note 5**).
5. Perform PCR purification using PCR Purification Kit; elute sample with 40 μL water.

6. Transform competent *E. coli* with 20 μL of sample. Plate transformations on LB agar plates supplemented with carbenicillin and incubate at 37 °C overnight.
7. Isolate 3–5 individual colonies and culture for plasmid mini prep.
8. Isolate plasmid from each culture using the MiniPrep Kit (Qiagen).
9. Confirm presence of mutation via sequencing.

3.4 HBZ Functional Assays

For HBZ functional assays we use plasmid DNA isolated with a purification kit. Working solutions of all plasmids are prepared at 100 ng/μL. Functional assays are performed using both Jurkat and HEK293T cells. In this section, we describe the HEK293T experiments. All functional assays should be performed in triplicate. When describing our transfections, volumes/amounts used to transfect one well of a 6-well plate are shown. To determine what effect HBZ PTMs have on protein steady-state levels, we measure HBZ protein expression via western blot, and normalized expression to transfection efficiency measured via luciferase expression (*see* **Note 6**).

1. In 6-well plates, seed 3×10^5 HEK293T cells/well in complete DMEM.
2. After 18 h, check plates for confluence, ideally cells will be 50–70% confluent at the time of transfection. If cells are at optimal confluence, continue with transfection.
3. Dilute 900 ng of HBZ mutant plasmid and 100 ng of CMV-Luc plasmid with 50 μL Optimem medium.
4. Dilute 3 μL Lipofectamine reagent with 50 μL Optimem in a separate tube. (Lipofectamine reagent to DNA ratio is 3 μL:1 μg).
5. Combine DNA and Lipofectamine dilutions in one tube and pipet up and down five times. Incubate at room temperature for 30 min.
6. During incubation, aspirate growth medium from the HEK293T cells. Add 1 mL of Optimem onto cells carefully to avoid disturbing cell adhesion.
7. Add the transfection mixture to the well dropwise, and then gently swirl the plate to ensure equal distribution.
8. Place plates at 37 °C in a tissue culture incubator for 3 h.
9. After 3 h, aspirate Optimem/transfection medium from the cells. Carefully replenish 2 mL of complete DMEM for each well. Return plates to the tissue culture incubator.
10. At 48 h post-transfection, collect the cells by removing the growth medium and then adding 1 mL of ice cold PBS to each

well. Scrape cells from the wells and transfer to a 1.5 mL tube on ice.

11. Pellet the cells by centrifuging at 800 × *g* for 5 min at 4 °C.
12. Remove supernatant.
13. Add 100 μL 1× Passive Lysis Buffer. Vortex to suspend the pellet and rotate at 15 RPM on tube rotator for 30 min at 4 °C.
14. Clear lysates of debris by centrifugation at 16,300 × *g* for 10 min. Transfer supernatants to new 1.5 mL tubes on ice.
15. Transfer 30 μL of lysate to a fresh tube and add 6 μL of 6× SDS loading dye.
16. Boil samples at 95 °C for 10 min. After boiling, briefly spin down samples.
17. Load samples onto a precast 4–20% SDS-PAGE gel and electrophorese at 150 V for 30–60 min, or until dye front exits gel.
18. Transfer gel to nitrocellulose membrane via wet Western blotting transfer at 110 V for 30 min.
19. Incubate membrane in 5% milk diluted in PBST for 1 h at room temperature.
20. Incubate membrane in Flag M2 antibody diluted in 5% milk-TBST (1:1000) overnight with gentle agitation at 4 °C.
21. Wash membrane three times in PBST for 10 min with gentle agitation at room temperature.
22. Incubate membrane in goat anti-mouse HRP antibody diluted in 5% milk TBST (1:5000) and incubate for 2 h with gentle agitation at room temperature.
23. Wash membrane three times in PBST for 10 min with gentle agitation at room temperature.
24. Add ECL reagent to membrane and incubate at room temperature for 1 min. Remove excess ECL reagent.
25. Image the membrane.
26. Analyze image by densitometry.
27. Analyze sample lysate for luciferase expression using the Luciferase Assay System (Promega, Madison). Add 10 μL of lysate into one well of a 96-well plate. Add 100 μL of Luciferase Assay Reagent (LAR) and mix by pipetting three times. Read sample on luminometer.
28. Use luciferase levels to normalize densitometry data for experimental variability and transfection efficiency. These corrected numbers reflect steady-state levels of HBZ expression. Perform each experiment in triplicate to ensure statistically relevant data.

3.5 Effect of HBZ on Transcription of Tax and Cellular Factors

HBZ promotes viral persistence and survival through several different functions in infected cells. HBZ inhibits Tax transactivation via direct competition for binding with CREB/p300 and by promoting Tax degradation [12]. HBZ further inhibits HTLV-1 gene expression by limiting AP-1 activation. Tax promotes AP-1 activity, which up-regulates basal viral gene expression, while HBZ down-regulates AP-1 via inhibition of c-Jun transactivation [13, 27]. Inhibition of Tax expression allows immune evasion and blocks a phenomenon known as Tax-induced senescence (TIS), which occurs due to Tax-driven hyper-activation of the classical NF-κB pathway [28]. HBZ further blocks TIS by directly inhibiting the classical NF-κB pathway via promoting the degradation of p65 [14]. HBZ also functions directly in immune evasion by interaction with interferon regulatory factor 1 (IRF-1). IRF-1 is a tumor suppressor that can promote cell growth arrest and apoptosis. HBZ inhibits IRF-1 activity by lowering IRF-1 DNA binding ability and promoting IRF-1 degradation [15].

HBZ mutants can be analyzed for their ability to affect Tax, p65, c-Jun, and IRF-1-mediated transcription via luciferase reporter assays. We use the Dual-Glo Luciferase Assay System (Promega) to quantify promoter activity. This system analyzes the firefly luciferase values produced by the luciferase reporter plasmid and Renilla luciferase levels from the Renilla-TK plasmid as an internal control. Normalizing firefly luciferase levels to the Renilla luciferase levels will account for differences in transfection efficiency and reduce experimental variability. All experiments should be performed with two amounts of HBZ (100 and 500 ng) for transfection to determine any dose-dependent changes in transcription.

1. Seed HEK293T cells as in Subheading 3.4, **step 1**. Ensure three wells per condition.
2. Transfect cells as in Subheading 3.4, **steps 3–9**, using the following plasmids (*see* **Note 7**):
   (a) Tax transactivation assay: 100 ng LTR1-luciferase, 10 ng Renilla-TK, 100 ng S-tagged Tax-1, and either 0, 100, or 500 ng of the Flag-HBZ mutant, and empty Flag expression vector for a total of 1 μg of DNA.
   (b) p65 transcriptional assay: 100 ng κB-luciferase, 10 ng Renilla-TK, 50 ng p65 expression vector, and either 0, 100, or 500 ng of the Flag-HBZ mutant, and empty Flag expression vector for a total of 1 μg of DNA.
   (c) c-Jun transcriptional assay: 50 ng 6× AP1-luciferase, 10 ng Renilla-TK, 25 ng c-Jun expression vector, and either 0, 100, or 500 ng Flag-HBZ mutant, and empty Flag expression vector for a total of 1 μg of DNA.
   (d) IRF-1 transcriptional assay: 50 ng pIRF-1-luciferase, 10 ng Renilla-TK, 100 ng IRF-1 expression vector, and either 0, 100, or 500 ng Flag-HBZ mutant, and empty flag expression vector for a total of 1 μg of DNA.

3. Collect and lyse cells as in Subheading 3.1, **steps 10–14**.
4. Place 10 μL of lysate into one well of a 96-well plate.
5. Add 100 μL of LARII to the lysates and pipet up and down three times.
6. Read plate in FilterMax F5 microplate reader and obtain firefly luciferase levels.
7. Add 100 μL of Stop & Glo reagent to wells and pipet up and down three times.
8. Read plate in FilterMax F5 microplate reader and obtain Renilla luciferase levels.
9. Perform statistical analysis to obtain mean firefly luciferase levels normalized to Renilla luciferase values. Show data as a fold-change over the negative control (*see* Fig. 2 for representative data).

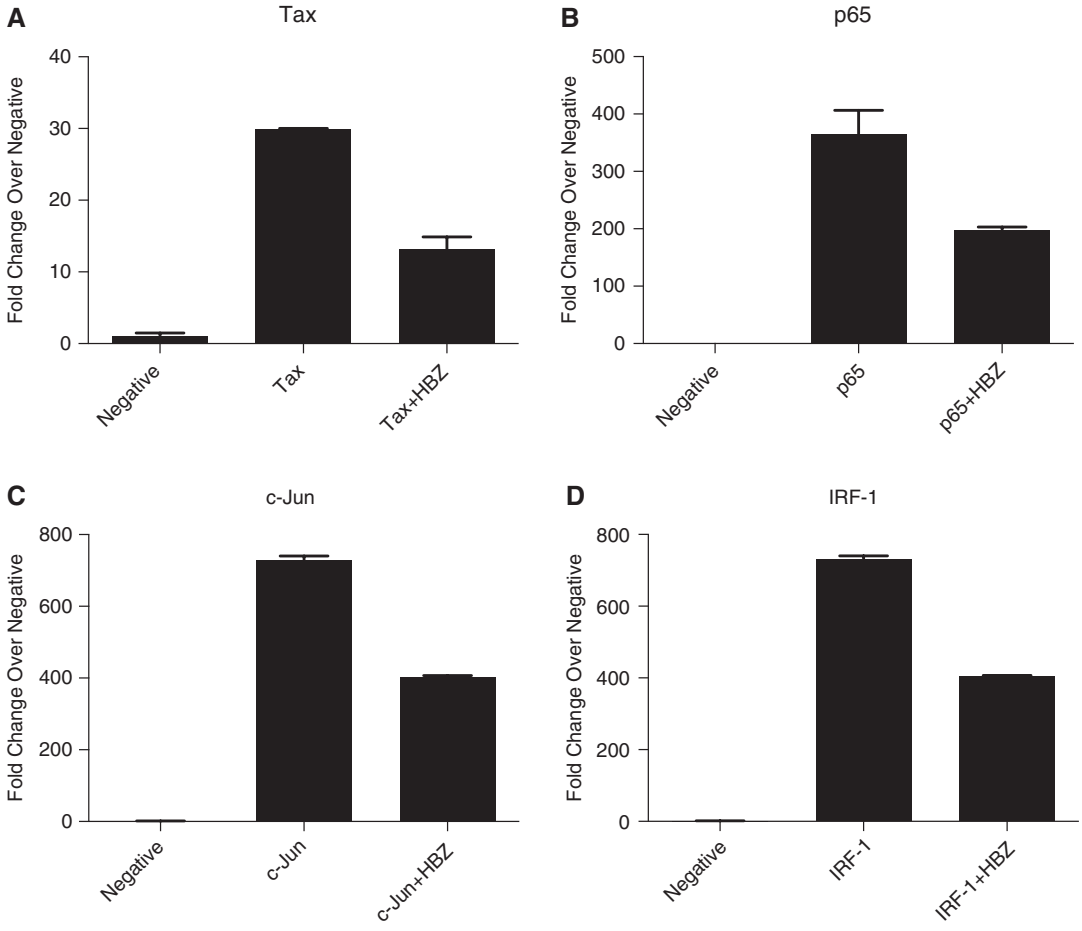

Fig. 2 Transcriptional Repression by HBZ. Representative data of HBZ functional assays for repression of (**a**) Tax transactivation, (**b**) p65 transactivation, (**c**) c-Jun transactivation, and (**d**) IRF-1 transactivation. For all experiments, 293 T cells were transfected in triplicate as described in Subheading 3.5, **step 2** using 500 μg of Flag-HBZ

10. To ensure successful transfection, samples should be analyzed for HBZ protein expression. Sample remaining after luciferase assays should be subjected to western blotting as done in Subheading 3.4, **steps 13–26**.

4 Notes

1. We performed most steps of the protein purification procedure at room temperature unless otherwise stated. If protein degradation is a problem, perform purification at 4 °C.
2. To avoid protein degradation, lysis buffer is supplemented with a protease inhibitor cocktail; we keep 10× aliquots of this cocktail in the freezer at −20 °C.
3. During the protein purification procedure, it is wise to collect some of the cellular lysate prior to the addition of the Flag beads as an input control and collect the flow-through supernatant after IP. These samples can then be tested for the expression of the Flag-tagged construct to determine the efficiency of expression and IP.
4. The container used to stain the gel should have a cover. If not, use foil to cover during staining to prevent exposure of the gel to light and debris.
5. PCR conditions that can be modified include the annealing temperature, extension cycle length, number of cycles, and $MgCl_2$ concentration.
6. HBZ protein half-life could also be determined. After transfecting HBZ into HEK293T cells add cycloheximide (10 μg/mL) to transfected cells. Collect samples at multiple time points post-cycloheximide addition, and analyze via western blotting as done in Subheading 3.4, **steps 13–26**. Calculate the half-life of the HBZ protein via analysis of densitometry [29].
7. Positive and negative controls should be included for the HBZ functional assays.
   (a) For the positive control the Flag-HBZ expression vector should be removed from the transfection mix, and all other constructs should be added as normal. The positive control demonstrates uninhibited reporter activity by the activating protein (i.e., Tax-1).
   (b) For the negative control the activating protein (i.e., Tax-1) and Flag-HBZ should be removed from the transfection mix, and all other constructs should be added as normal. The negative control demonstrates the background activity level of the reporter construct.

References

1. Poiesz BJ, Ruscetti FW, Gazdar AF et al (1980) Detection and isolation of type C retrovirus particles from fresh and cultured lymphocytes of a patient with cutaneous T-cell lymphoma. Proc Natl Acad Sci U S A 77:7415–7419
2. Yoshida M, Miyoshi I, Hinuma Y (1982) Isolation and characterization of retrovirus from cell lines of human adult T-cell leukemia and its implication in the disease. Proc Natl Acad Sci U S A 79:2031–2035. doi:10.1186/s12985-015-0398-x
3. Osame M, Usuku K, Izumo S et al (1986) HTLV-I associated myelopathy, a new clinical entity. Lancet 1:1031–1032
4. Matsuoka M (2005) Human T-cell leukemia virus type I (HTLV-I) infection and the onset of adult T-cell leukemia (ATL). Retrovirology 2:27. doi:10.1186/1742-4690-2-27
5. Nicot C, Harrod RL, Ciminale V, Franchini G (2005) Human T-cell leukemia/lymphoma virus type 1 nonstructural genes and their functions. Oncogene 24:6026–6034. doi:10.1038/sj.onc.1208977
6. Felber BK, Paskalis H, Kleinman-Ewing C et al (1985) The pX protein of HTLV-I is a transcriptional activator of its long terminal repeats. Science 229:675–679
7. Grassmann R, Berchtold S, Radant I et al (1992) Role of human T-cell leukemia virus type 1 X region proteins in immortalization of primary human lymphocytes in culture. J Virol 66:4570–4575
8. Grossman WJ, Kimata JT, Wong FH et al (1995) Development of leukemia in mice transgenic for the tax gene of human T-cell leukemia virus type I. Proc Natl Acad Sci U S A 92:1057–1061
9. Michael D, Robek LR (1999) Immortalization of CD4(+) and CD8(+) T lymphocytes by human T-cell leukemia virus type 1 Tax mutants expressed in a functional molecular clone. J Virol 73:4856–4865
10. Gaudray G, Gachon F, Basbous J et al (2002) The complementary strand of the human T-cell leukemia virus type 1 RNA genome encodes a bZIP transcription factor that down-regulates viral transcription. J Virol 76:12813–12822. doi:10.1128/JVI.76.24.12813-12822.2002
11. Larocca D, Chao LA, Seto MH, Brunck TK (1989) Human T-cell leukemia virus minus strand transcription in infected T-cells. Biochem Biophys Res Commun 163:1006–1013
12. Lemasson I, Lewis MR, Polakowski N et al (2007) Human T-cell leukemia virus type 1 (HTLV-1) bZIP protein interacts with the cellular transcription factor CREB to inhibit HTLV-1 transcription. J Virol 81:1543–1553. doi:10.1128/JVI.00480-06
13. Basbous J, Arpin C, Gaudray G et al (2003) The HBZ factor of human T-cell leukemia virus type I dimerizes with transcription factors JunB and c-Jun and modulates their transcriptional activity. J Biol Chem 278:43620–43627. doi:10.1074/jbc.M307275200
14. Zhao T, Yasunaga J-I, Satou Y et al (2009) Human T-cell leukemia virus type 1 bZIP factor selectively suppresses the classical pathway of NF-kappaB. Blood 113:2755–2764. doi:10.1182/blood-2008-06-161729
15. Mukai R, Ohshima T (2011) Dual effects of HTLV-1 bZIP factor in suppression of interferon regulatory factor 1. Biochem Biophys Res Commun 409:328–332. doi:10.1016/j.bbrc.2011.05.014
16. Satou Y, Yasunaga J-I, Yoshida M, Matsuoka M (2006) HTLV-I basic leucine zipper factor gene mRNA supports proliferation of adult T cell leukemia cells. Proc Natl Acad Sci U S A 103:720–725. doi:10.1073/pnas.0507631103
17. Arnold J, Zimmerman B, Li M et al (2008) Human T-cell leukemia virus type-1 antisense-encoded gene, Hbz, promotes T-lymphocyte proliferation. Blood 112:3788–3797. doi:10.1182/blood-2008-04-154286
18. Satou Y, Yasunaga J-I, Zhao T et al (2011) HTLV-1 bZIP factor induces T-cell lymphoma and systemic inflammation in vivo. PLoS Pathog 7:e1001274. doi:10.1371/journal.ppat.1001274
19. Takeda S, Maeda M, Morikawa S et al (2004) Genetic and epigenetic inactivation of tax gene in adult T-cell leukemia cells. Int J Cancer 109:559–567. doi:10.1002/ijc.20007
20. Koiwa T, Hamano-Usami A, Ishida T et al (2002) 5'-long terminal repeat-selective CpG methylation of latent human T-cell leukemia virus type 1 provirus in vitro and in vivo. J Virol 76:9389–9397. doi:10.1128/JVI.76.18.9389-9397.2002
21. Furukawa Y, Kubota R, Tara M et al (2001) Existence of escape mutant in HTLV-I tax during the development of adult T-cell leukemia. Blood 97:987–993
22. Prabakaran S, Lippens G, Steen H, Gunawardena J (2012) Post-translational modification: nature's escape from genetic imprisonment and the basis for dynamic information encoding. Wiley Interdiscip Rev Syst Biol Med 4:565–583. doi:10.1002/wsbm.1185

23. Bex F, Murphy K, Wattiez R et al (1999) Phosphorylation of the human T-cell leukemia virus type 1 transactivator tax on adjacent serine residues is critical for tax activation. J Virol 73:738–745
24. Lodewick J, Lamsoul I, Polania A et al (2009) Acetylation of the human T-cell leukemia virus type 1 Tax oncoprotein by p300 promotes activation of the NF-κB pathway. Virology 386:68–78. doi:10.1016/j.virol.2008.12.043
25. Fryrear KA, Guo X, Kerscher O, Semmes OJ (2012) The Sumo-targeted ubiquitin ligase RNF4 regulates the localization and function of the HTLV-1 oncoprotein Tax. Blood 119:1173–1181. doi:10.1182/blood-2011-06-358564
26. Kesic M, Doueiri R, Ward M et al (2009) Phosphorylation regulates human T-cell leukemia virus type 1 Rex function. Retrovirology 6:105. doi:10.1186/1742-4690-6-105
27. Matsumoto J, Ohshima T, Isono O, Shimotohno K (2005) HTLV-1 HBZ suppresses AP-1 activity by impairing both the DNA-binding ability and the stability of c-Jun protein. Oncogene 24:1001–1010. doi:10.1038/sj.onc.1208297
28. Zhi H, Yang L, Kuo Y-L et al (2011) NF-κB hyper-activation by HTLV-1 Tax induces cellular senescence, but can be alleviated by the viral antisense protein HBZ. PLoS Pathog 7:e1002025. doi:10.1371/journal.ppat.1002025.g007
29. Kelly JJ, Shao Q, Jagger DJ, Laird DW (2015) Cx30 exhibits unique characteristics including a long half-life when assembled into gap junctions. J Cell Sci 128(21):3947–3960. doi:10.1242/jcs.174698

Chapter 10

High-Throughput Mapping and Clonal Quantification of Retroviral Integration Sites

Nicolas A. Gillet, Anat Melamed, and Charles R.M. Bangham

Abstract

We describe here a method to identify the position of retroviral insertion sites and simultaneously to quantify the absolute abundance of each clone, i.e., the number of cells having the provirus inserted at a given place in the host genome. The method is based on random shearing of the host cell DNA, followed by a linker-mediated PCR to amplify the genomic regions flanking the proviruses, and high-throughput sequencing of the amplicons. The quantification of the abundance of each infected clone allowed us to develop two new metrics: i. the oligoclonality index, which quantifies the nonuniformity of the distribution of clone abundance, and ii. an estimator of the total number of clones in the body of the host. These new tools are valuable for the study of retroviral infections and can also be adapted for the tracking of gene-edited cells.

Key words Retroviral integration sites, Insertion sites, Clonality, Clonal distribution, Oligoclonal, Clonal expansion, Number of clones, Gene therapy, Gene-edited cells, Off-target insertion

1 Introduction

Retroviral integration into the host genome is not random but is biased by several sequential events. First, the preintegration complex favors euchromatin, where the open conformation enables access to the host DNA. Concomitantly, the nucleotide sequence of the host DNA and interactions between the preintegration complex and specific host factors also bias the targeting of insertion [1, 2]. Once inserted, the virus propagates by producing new infectious virions and by driving clonal expansion of the infected cell. At this stage, the abundance of the infected clone will be influenced by the nature of the host genome surrounding the proviral DNA. By developing a technique that allows the precise quantification of the abundance of each clone, we observed that the host genomic environment surrounding the HTLV-1 or 2 (Human T lymphotropic Virus 1 or 2) and BLV (Bovine Leukemia Virus) proviruses has important effects on clonal expansion [3–9].

Claudio Casoli (ed.), *Human T-Lymphotropic Viruses: Methods and Protocols*, Methods in Molecular Biology, vol. 1582,
DOI 10.1007/978-1-4939-6872-5_10,

Our protocol of high-throughput mapping and quantification of retroviral integration sites is based on PCR amplification between the end of the proviral LTR and a DNA linker, followed by massively parallel sequencing [3, 10]. Crucially, instead of using restriction enzymes to cut the host DNA prior linker ligation, the DNA is sheared almost randomly [3, 10] by nebulization or sonication. This confers two critical advantages compared to the previous high-throughput retroviral mapping techniques. First, the proviruses inserted close to a given restriction site were over-estimated by the previous methods owing to the inherent PCR bias for amplification of short fragments; this is no longer the case with this protocol. Second, since the DNA is randomly cut, two different cells from a given clone can be distinguished by the different lengths of the amplicons from the two respective cells, allowing the quantification of the abundance of each infected clone. Knowing the distribution of clonal abundance, we were able to develop two new metrics:

1. The oligoclonality index (OCI), based on the Gini coefficient, which quantifies the nonuniformity of the distribution of clone abundance: the index ranges from 0 (all the infected clones having the same abundance, i.e., perfect polyclonality) to 1 (only one infected clone constitutes the total proviral load, i.e., perfect monoclonality).
2. An estimator of the total number of clones in the body of the host [11].

Using this protocol, we showed that initial integration of HTLV-1 and BLV favored transcriptionally active chromatin [3, 5, 6]. In the BLV animal model, we also demonstrated that the initial host selection occurring during primary infection specifically targets cells that carry a provirus inserted in genomic transcribed regions [6]. We observed that the HTLV-1 clonal abundance is positively correlated with the transcriptional potential of the host genome surrounding the provirus [3, 5] but inversely correlated with the level of expression of the HTLV-1 transcriptional transactivator protein Tax [5], highlighting the complex relationship between viral expression and exposure of the infected cell to the host immune response. In contrast to the common belief that oligoclonal expansion is a hallmark of a pre-leukemic state, we showed that HTLV-2 clonal distribution is highly oligoclonal despite the fact that HTLV-2 has never been linked to a malignant disease [7]. Similarly, we demonstrated in a large cohort of HTLV-1 leukemic patients that oligoclonal proliferation per se does not cause malignant transformation, because the presumed malignant clones resembled low-abundance clones and differed from clones that had undergone strong oligoclonal proliferation [8]. We therefore pro-

posed that the major determinant of the risk of HTLV-1-associated leukemia is the absolute number of clones: the larger the number, the greater the chance of malignant transformation [8].

HIV infection is another field where the study of the proviral clones is revealing new lessons about how the virus persists. Indeed, it has been recently demonstrated, using the approach we describe here, that HIV-infected cells persisting under antiretroviral therapy were clonally expanded and were more likely to contain the provirus integrated in particular genes [12]. Stem-cell gene therapy based on lentiviral vectors had already produced several important successes in treating certain genetic diseases [13]. Nevertheless, insertional mutagenesis and subsequent tumor development highlighted the fact that gene-edited cells must be monitored at the clone level. Finally, the newly developed gene-editing techniques using zinc finger nucleases, TALENs or CRISPR, despite being targeted approaches [14], can also cause off-target effects. Our approach can be easily adapted to identify and quantify the clones that arise from both beneficial and potentially harmful insertion events.

2 Materials

2.1 DNA Extraction System

1. Elution buffer: 10 mM Tris–HCl, pH 8.5.
2. Heat block.

2.2 DNA Shearing by Nebulization or by Sonication in Closed Tubes

1. Nebulizer (Life Technologies/ThermoFisherScientific, Waltham, MA, USA) (*see* **Note 1**).
2. Nitrogen tank with pressure regulator.
3. Shearing buffer: 10 mM Tris–HCl pH 8, 1 mM EDTA, with 10% glycerol.
4. Silica membrane-based column procedure.
5. DNA sonicator.

2.3 Vectorette Unit (VU) Construction

1. 10× annealing buffer: 100 mM Tris–HCl pH 7.5 to 8, 500 mM NaCl, 10 mM EDTA.
2. VU "upper arm": 5′ p-GATCGGAAGAGCGAAAAAAAAAA AAA 3′ at 1 nmol/μl in water.
3. VU "lower arm" with 8 bp tag (NNNNNNNN): 5′ T C A T G A T C A A T G G G A C G A T C A C A G C A G A A G A C G G C A T A C G A G A T N N N N N N N N C G G T C T C G G C A T T C C T G C T G A A C C G C T C T TCCGATCT 3′ at 1 nmol/μl in water

2.4 DNA Ends Repair

1. T4 DNA ligase buffer 10× (New England Biolabs, Ipswich, MA, USA).
2. T4 DNA polymerase 3 U/μl (New England Biolabs).
3. DNA polymerase I Klenow fragment 5 U/μl (New England Biolabs).
4. T4 polynucleotide kinase 10 U/μl (New England Biolabs).
5. dNTP 10 mM (Sigma Aldrich/Merck Millipore, Billerica, MA, USA).
6. Silica membrane-based column procedure.

2.5 Deoxyadenosine Addition to the DNA 3′ Ends

1. 10X buffer: 500 mM NaCl, 100 mM Tris–HCl, 100 mM $MgCl_2$, 10 mM DTT, pH 7.9).
2. Klenow Fragment (3′ to 5′ exo-) 5 U/μl (New England Biolabs).
3. ATP 1 mM (Sigma Aldrich).
4. Silica membrane-based column procedure.

2.6 Ligation of the Vectorette Unit to the DNA Fragments

1. Quick Ligation Reaction buffer 2× (New England Biolabs).
2. Quick T4 DNA Ligase 2000 U/μl (New England Biolabs).
3. Silica membrane-based column procedure.

2.7 PCR

1. Phusion High Fidelity DNA polymerase 2 U/μl (New England Bioloabs).
2. High Fidelity PCR buffer 5× (New England Bioloabs).
3. dNTP 10 mM (Sigma Aldrich).
4. Primer specific to the proviral LTR named “LTR primer” (20 pmol/μl) (*see* Fig. 1 and **Note 2**).
5. Primer specific to the vectorette unit named “VU primer” (10 pmol/μl), 5′ TCATGATCAATGGGACGATCA 3′.
6. PCR purification system.

2.8 Nested PCR

1. Phusion High Fidelity DNA polymerase 2 U/μl (New England Bioloabs).
2. High Fidelity PCR buffer 5× (New England Bioloabs).
3. dNTP 10 mM (Sigma Aldrich).
4. Nested primer specific to the proviral LTR named “P5_nLTR primer” (10 pmol/μl) (*see* Fig. 1 and **Note 2**).
5. Nested primer specific to the vectorette unit named “P7 primer” (10 pmol/μl), 5′ CAAGCAGAAGACGGCATACGA 3′.
6. PCR purification kit.

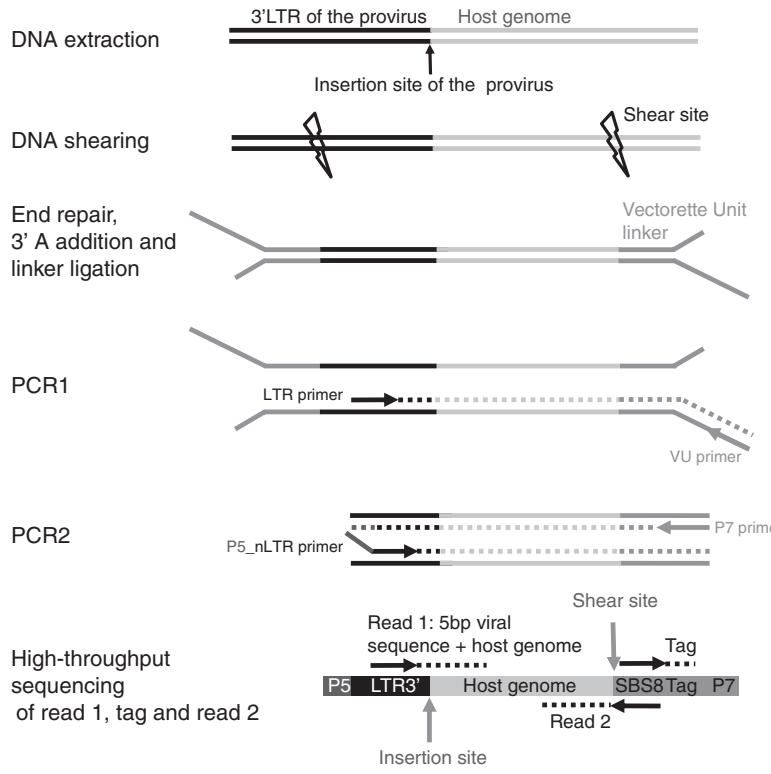

Fig. 1 Mapping of proviral insertion sites and quantification of clone abundance. DNA is extracted and sheared by either nebulization or sonication. DNA ends are repaired, polyadenylated, and ligated to a tagged double-stranded linker with mismatched ends (this linker is also known as a vectorette unit). Nested PCR is performed between the end of the viral long terminal repeat and the linker. A paired-end read (read 1 and read 2) plus a tag read are acquired on a high-throughput sequencer. Read 1 and read 2 are then mapped on the host genome

2.9 Library Quantification by qPCR

1. P5 primer 5′ AATGATACGGCGACCACCGAGAT 3′.
2. P7 primer 5′ CAAGCAGAAGACGGCATACGA 3′.
3. qPCR control template library PhiX 10 nM (Illumina, San Diego, CA, USA).
4. Mesa green qPCR master mix 2× (Eurogentec, Liège, Belgium).
5. Real-time thermocycler.

2.10 Library Sequencing

1. Illumina clustering and sequencing reagents (Illumina).
2. Custom sequencing primer for read 1 acquisition, around 40 bp long (not shorter), leaving about 5 bp at the end of the LTR. This short sequence of 5 bp will constitute the beginning of read 1 and serves as quality control to make sure that we actually sequence a proper proviral insertion site (*see* Figs. 1 and 2).

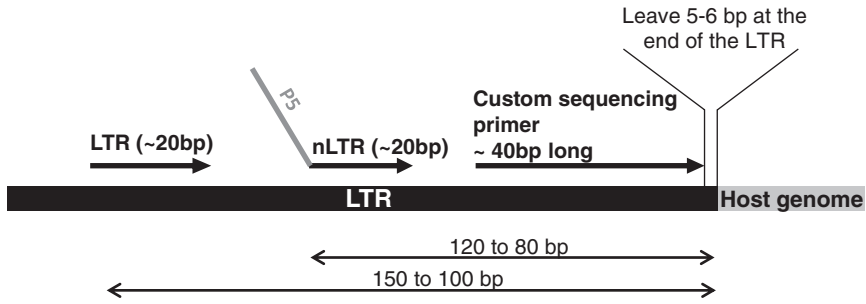

Fig. 2 Positioning of the different primers on the viral LTR

3. SBS8+T primer 5′ CGGTCTCGGCATTCCTGCTGAACCGC TCTTCCGATCT 3′ for read 2 acquisition.
4. SBS8rev primer 5′ GATCGGAAGAGCGGTTCAGCAGGA ATGCCGAGACCG 3′ for tag acquisition.

3 Methods

3.1 DNA Extraction

The first step of the protocol is the extraction of genomic DNA from a mixture of uninfected and infected cells. DNA will be eluted in 100 µl of elution buffer (*see* **Note 3**).

3.2 DNA Shearing (See Note 4) by Nebulization

1. Place 20 µg of DNA in 750 µl of shearing buffer at the bottom of the nebulizer.
2. Place the nebulizer in an ice bucket to keep the DNA cold and shear the DNA at 2 bars during 4 min.
3. Recover the DNA and re-concentrate using PCR purification kit and elute in 100 µl elution buffer.

3.3 DNA Shearing (See Note 4) by Sonication in Closed Tubes

1. Ten microgram of DNA in 100 µl of 10 mM Tris–HCl, pH 8.5 will be sheared:
   - with a Covaris S2 instrument with the following operating conditions: water bath at 6–8 °C, 5 s at 20% duty cycle, intensity level 5 and 200 cycles per burst and 90 s at 5% duty cycle, intensity level 3 and 200 cycles per burst.
   - or with a Diagenode Bioruptor instrument using the following protocol: 15 s ON, 90 s OFF, four cycles in a 4 °C water bath.

3.4 Vectorette Unit (VU) Construction

1. Mix in a thin-wall pcr tube: 5 µl of VU "upper arm" (1 nmol/µl), 5 µl of VU "lower arm" (1 nmol/µl), 5 µl of 10× annealing buffer, 35 µl of water.
2. Incubate in a thermo-cycler using the following protocol for annealing: 95 °C for 3 min, then decrease temperature at a rate of 0.1 °C/min to 4 °C.

3. Design several VU "lower arm" with different tags, this will allow multiplexing during high-throughput sequencing.
4. Store the vectorette unit stocks at −80 °C.

3.5 DNA Ends Repair

1. The sheared DNA will be end-repaired as follows: mix the 100 µl of sheared DNA with 12 µl of T4 DNA ligase buffer 10×, 4 µl of dNTP 10 mM, 5 µl of T4 DNA polymerase 3 U/µl, 1 µl of DNA polymerase I Klenow fragment 5 U/µl, 5 µl of T4 polynucleotide kinase 10 U/µl.
2. Incubate 30 min at 20 °C.
3. Clean using PCR purification kit and elute in 32 µl elution buffer.

3.6 Deoxyadenosine Addition to the DNA 3′ Ends

1. Mix the 32 µl of sheared DNA with 5 µl of NEB2 buffer 10×, 10 µl 1 mM ATP, 3 µl Klenow (3′ to 5′ exo-).
2. Incubate for 30 min at 37 °C.
3. Clean using PCR purification kit and elute in 40 ul elution buffer.

3.7 Ligation of the Vectorette Unit to the DNA Fragments

1. Mix the 40 µl of DNA with 50 µl of Quick Ligation buffer 2×, 5 µl of vectorette unit diluted at 20 pmol/µl, 5 µl of Quick T4 DNA ligase.
2. Incubate 30 min at room temperature.
3. Clean using PCR purification kit and elute in 60 µl elution buffer.

3.8 PCR

1. This step will perform a first amplification between the end of the proviral LTR and the linker. As a result, half of the PCR products will be generated between the 5′LTR and the linker and contain only viral sequences. The other half will be generated between the 3′LTR and the linker and contain host genomic sequences, only these products will be informative (*see* **Note 5**).
2. Split equally the 60 µl of ligated DNA into three thin-wall PCR tubes and mix with 10 µl of PCR buffer 5×, 1 µl of dNTP 10 mM, 2.5 µl of LTR primer (20 pmol/µl), 1 µl of VU primer (10 pmol/µl), 0.5 µl of Phusion DNA polymerase, 15 µl of water.
3. The following thermal protocol will be used: 30 s at 98 °C; then 30 cycles (5 s at 98 °C, 10 s at 60 °C, 30 s at 72 °C); followed by 10 min at 72 °C; and finally cooled at 4 °C. The 3 PCR products, derived from the same sample, will be pooled.
4. The DNA will be cleaned using a PCR purification kit and eluted in 150 µl of elution buffer.

3.9 Nested PCR

1. This step is necessary to increase the signal/noise ratio.
2. Take 1 µl of the cleaned PCR product and mix with 10 µl of PCR buffer 5×, 1 µl of dNTP 10 mM, 2.5 µl of P7_nLTR primer (10 pmol/µl), 2.5 µl of P5 primer (10 pmol/µl), 0.5 µl of Phusion DNA polymerase, 32.5 µl of water.
3. The following thermal protocol will be used: 30 s at 98 °C; then 30 cycles (5 s at 98 °C, 10 s at 60 °C, 30 s at 72 °C); followed by 10 min at 72 °C; and finally cooled at 4 °C.
4. The DNA will be cleaned using a Qiaquick PCR purification kit and eluted in 50 µl of elution buffer. These PCR products will be named library as they are amplicons that can be sequenced on Illumina sequencers.

3.10 Library Quantification by qPCR

1. The different libraries (the cleaned nested PCR products) will be quantified by qPCR using the Illumina PhiX reference library.
2. A standard curve will be generated by serial dilution of the PhiX library to achieve concentration from 10 pM to 10 fM in the working aliquotes.
3. The libraries will be diluted as follows: Tube A: 1 µl of library in 1000 µl of water, Tube B: 10 µl of tube A + 90 µl of water, Tube C: 10 µl of tube B + 90 µl of water, Tube D: 10 µl of tube C + 90 µl of water.
4. The setting of the PCR reaction will be the following: 2 µl of template (diluted PhiX control or diluted library), 2 µl of P5 primer at 3 µM, 2 µl of P7 primer at 3 µM, 10 µl of Mesa green qPCR master mix, 4 µl of water.
5. The following thermal protocol will be used: denaturation/DNA polymerase activation for 5 minutes at 95 °C; then 40 cycles (15 s at 95 °C, 20 s at 60 °C, 40 s at 72 °C); followed by a melting curve.

3.11 Library Sequencing

1. Use the Custom sequencing primer for read 1 acquisition (*see* **Note 2**).
2. Use the SBS8rev primer for tag acquisition.
3. Use SBS8+T primer for read 2 acquisition.
4. Sequencing platform: for efficient sequencing (*see* **Note 6**), several adaptations need to be considered. We recommend using the Illumina sequencing platform. This is currently widely used, allows considerable flexibility in the number of samples sequenced, and is cost effective [15].
5. Uneven clusters: because the protocol described here does not contain a size selection step, the clusters on the flow cell are more diverse in quality and length than in a standard sequencing protocol. To ensure correct cluster identification we recommend

loading on the flow cell a lower concentration of the DNA library than is normally required. A titration experiment may be required to determine the optimum concentration. Thus, we recommend the clustering of a library at different concentrations (from 0.5 pM up to 20 pM) to select the optimal concentration that will be used throughout your experiment. The library tested will be kept and used as reference in the qPCR assay for library titration (3:10) instead of PhiX.

6. Low diversity libraries: the use of a sequencing primer binding site that ends before the LTR terminus (*see* Fig. 2) results in a low-diversity library, because all amplicons share the same initial sequence. This low diversity can reduce the sequencing efficiency [16]. To solve this problem, we recommend using one of the following two approaches:
   (a) Spiking the integration site DNA with a high-diversity library of unrelated sequences, e.g., from phiX DNA. This may require optimization to identify the ideal concentration to ensure sufficient diversity as well as maximal recovery of integration site data.
   (b) Dark cycles. The sequencing program is modified such that the first five sequencing cycles are not acquired, and therefore are not used for the cluster calling by the sequencer. After the sequencing of read 1 (*see* Fig. 1) is completed, the new strand can be denatured, and the same LTR-specific sequencing primer can be re-annealed to sequence the first five bases. We recommend this approach.
7. The read length used in the sequencing should be carefully considered for each application.
8. A longer read length may improve the mapping but may also result in a large proportion of read-through into the linker sequence.

3.12 Sequence Data Analysis

1. Multiplexing: use of barcodes to multiplex samples on a single sequencing lane.
2. Barcode choice: in each lane, it is recommended to use barcode sequences that are as distinct as possible from each other, in order to minimize the impact of barcode errors. When using a small number of barcodes on the Illumina platform, it is important to consider the required base composition of the barcodes (see Illumina pooling guidelines, http://support.illumina.com/sequencing/sequencing_kits/nextera_rapid_capture_custom_kit/best_practices.html#Pool).
3. Demultiplexing: the sequences of the barcode, read 1 and read 2, are assigned to a single cluster by matching their coordinates on the flowcell. The sequencing data from read 1 and read 2 are divided into different datasets based on the barcode sequence.

4. Barcode error: PCR or sequencing errors may result in samples being mis-attributed to the wrong barcode. This can be minimized by the usage of highly distinct barcodes, but may still occur. It is advisable not to multiplex samples if there is a reasonable expectation that two or more samples will share a common integration site (e.g., integration sites from two different time-points from one individual). In such cases, a single integration site can be represented by a very low number of reads—typically one or two—in one of the samples (and a large number in the other sample). We then assume that the low read-number represents cross-contamination or barcode error: we therefore introduce a filtering step to remove integration sites mapped to the less frequent position.

3.13 Alignment: The Mapping of Sequence Data to the Host Genome Reference

1. Choice of alignment algorithm: paired-end reads can be aligned to an appropriate reference using a suitable large-scale aligner such as ELAND (Illumina) or Bowtie [17]. It is advisable to consider how the aligner deals with reads that map to multiple locations, so that ambiguous genomic mapping sites can be filtered out.
2. Alignment to a modified reference sequence: we recommend using a reference sequence that contains the proviral sequence (*see* Fig. 3) as an additional reference file ("chromosome") to facilitate the filtering out of these reads. If the reads include 5 bp viral sequence, this sequence must be separated from the rest of the read prior to alignment, because it should not align to the host reference chromosome.

3.14 Filter Data

1. Quality—reads must pass the standard platform-specific quality control criteria.
2. Specificity—reads must begin with the terminal five bases of the proviral LTR (excluding mispriming products).
3. Both reads must represent a proper pair, aligned to the same chromosome on the host genome in opposite orientation, with a plausible distance (e.g., <1 kb) between the mapped positions of

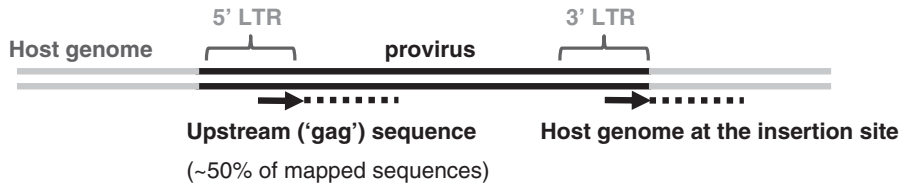

Fig. 3 Products amplified from the integrated provirus. In this protocol, products are amplified from both the 5′ and the 3′ LTRs (~50% from each LTR). The amplicons from the 5′ LTR contain "upstream" sequence from the proviral *gag* region: the *gag* sequence allows these amplicons to be identified by alignment to the provirus reference sequence, and so to be excluded

read 1 and read 2. Longer products are not efficiently amplified using the PCR conditions specified here.

4. Alignment must be of sufficiently high score (this will vary according to the alignment tool used) to ensure a unique mapping position. Nonunique mapping positions can be considered (as they are likely to represent integration into genome repeats), but they should be used with care and not used for downstream analysis. Integration sites that appear to map to adjacent positions on the reference genome (e.g., within 1–2 bases) should be considered with caution: such sites may represent the same integration event mapping to two locations as a result of ambiguous ("N") bases.

3.15 Quantification

1. Integration site frequency: the reads are grouped by the unique integration site (the first base position following the LTR terminus, sequenced by read 1). The shear site is calculated from the aligned position of read 2. Note that some aligners report the starting position of the reverse complemented sequence (if the read maps to the negative strand of the genome), and this should be corrected appropriately based on the read length.
2. Sonicant length is defined as follows:

$$\text{sonicant length} = \left|\text{Shear site position} - \text{Integration site position}\right|$$

3. The quantification of integration site abundance is performed in two steps. First, all reads corresponding to a given unique integration site are grouped together. Second, the number of unique sonicant lengths (see above) is counted for that integration site (*see* Fig. 4).

   The total number of reads per integration site should be recorded but this number should be interpreted with great care, because it is likely to be skewed by the PCR bias for amplification of short products.

4. Calibration: the maximum observable number of sonicant lengths is limited by the length distribution and, in the case of highly frequent integration sites, the probability of repeated shearing at the same genomic position. To account for these experiment-specific factors, three approaches may be used: calibration curves (quantification of serially diluted samples), statistical approaches (e.g., [10]), or an additional quantification method such as random tags [18].
5. Relative frequency

   The relative frequency of a given integration site is calculated as follows:

$$p_i = \frac{n_i}{\sum_{i=1}^{S} n_{i.}}$$

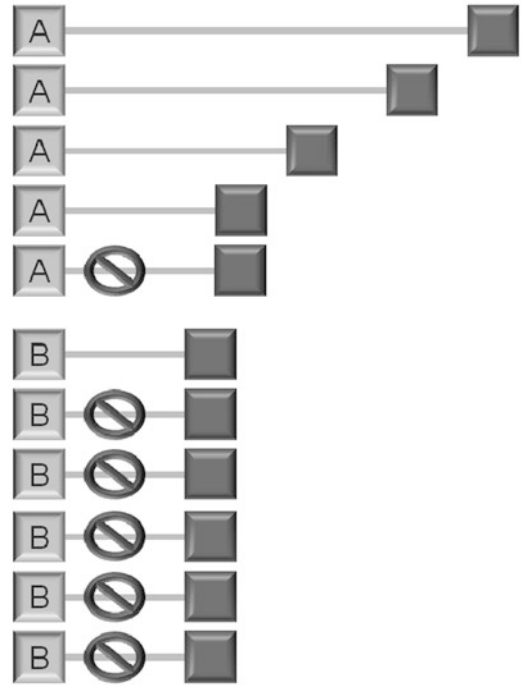

Fig. 4 Quantification of integration sites by amplicon length analysis. Sequencing reads are grouped by the unique integration site (read 1 sequence position). The frequency of each integration site is quantified by the number of distinct amplicon lengths (distinct read 2 positions); identical-length reads are discarded because they represent PCR duplicates

where n_i is the frequency of the ith integration site, and S is the total number of integration sites identified.

6. Oligoclonality index (OCI): the oligoclonality index (*see* Fig. 5) is a useful single measure of the dispersion (i.e., nonuniformity) of clone frequencies. It is based on the Gini index [19] and is calculated by the following formula:

$$OCI = 2 \times \left\{ \sum_{k=1}^{S} \frac{X_{\mathrm{k}}}{S} - 0.5 \right\}$$

where X_{k} is the cumulative frequency of the integration sites in decreasing order of frequency:

$$X_{\mathrm{k}} = \sum_{i=1}^{k} P_i$$

OCI can also be calculated using the Gini function in the "reldist" R package [20].

7. To estimate of total integration site (clonal) diversity the use of DiVE [11].

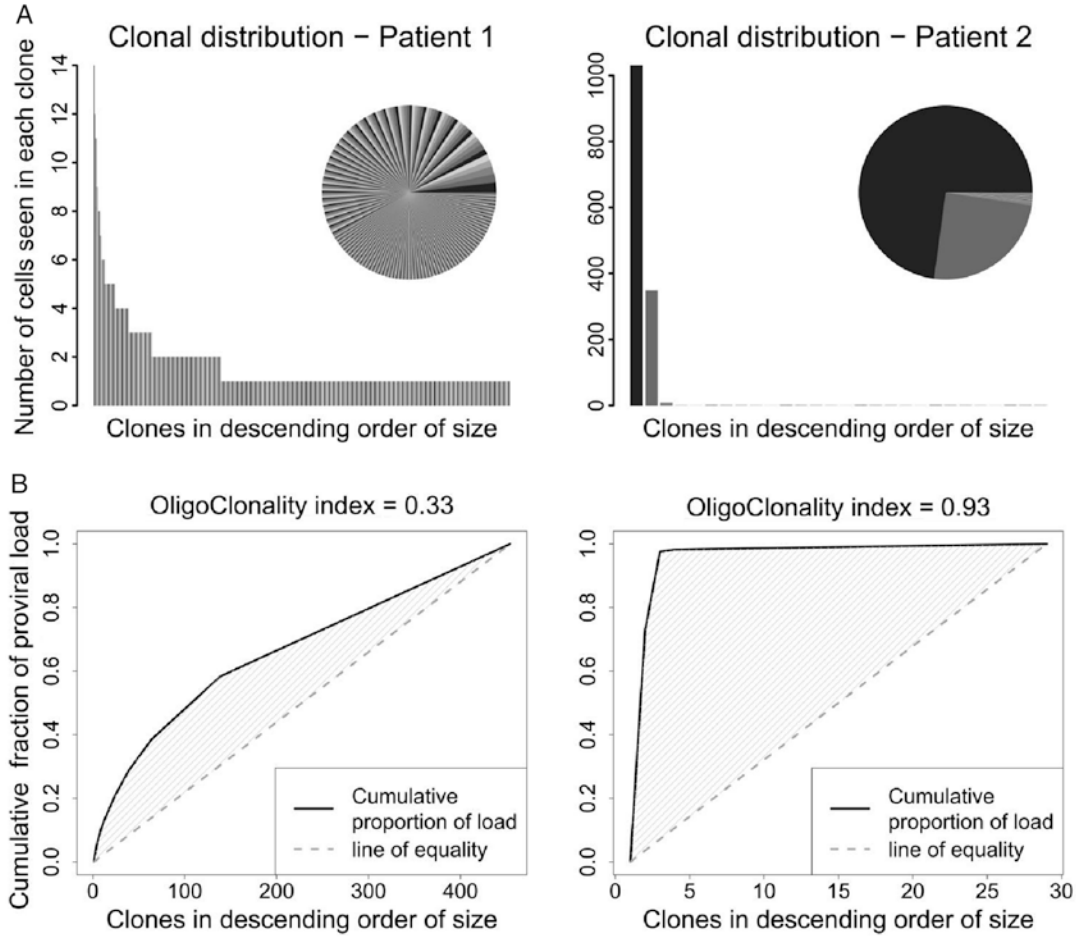

Fig. 5 Quantifying dispersion in the integration site frequency distribution. (A) Two examples of an integration site distribution are shown: a high diversity sample (left) and a low diversity sample (right). (B) The degree of dispersion (nonuniformity) in the integration site frequency distribution can be quantified by the oligoclonality index [3], which is calculated as the ratio between the shaded area and the triangle that contains the shaded area. Figure adapted from [9] by permission of the publisher

4 Notes

1. DNA shearing by nebulization causes a substantial loss of DNA (up to 50%) and nebulization also carries the risk of cross-contamination between samples. When possible we recommend using sonication in closed vessels to avoid contamination and DNA loss and to ensure high reproducibility.

   The shearing conditions will vary with the device and must be optimized to generate DNA fragments from 500 bp to 1 kb.

2. The design of primers is crucial. Figure 2 illustrates the positioning and requirement for the different primers. The LTR region of a retrovirus is typically more variable in nucleotide sequence

than the protein-coding regions of the provirus. We therefore recommend the use of classical PCR to amplify the end of the LTR, followed by cloning and (conventional) sequencing, to verify the nucleotide sequence of the LTR in each host. PCR primers based on the consensus sequence, which may differ in one or two nucleotides from the target sequence, can lead to poor efficiency of the PCR or sequencing steps. The sequencing primer is particularly sensitive and a mismatch can dramatically decrease the sequencing output. Where the LTR sequence is known to vary between samples, the primers LTR and P5_nLTR should be adapted to each particular sample. If the polymorphism involves the binding site of the sequencing primer, several sequencing primers can be mixed during the sequencing step, to match every indexed sample (we have used this procedure successfully on the Illumina Hiseq platform).

3. Before beginning, we recommend measuring the proviral load of the starting DNA material, i.e., the number of proviruses per μg of DNA, to guide the amount of genomic DNA to be used in the procedure, and to allow estimation of the absolute clone abundance.
4. To set up the DNA shearing conditions, the distribution of fragment sizes in the sheared DNA should be analyzed on a 2% agarose gel or using the Agilent Bioanalyzer.
5. It is important to avoid the generation of short fragments (less than 500 bp) because these can dominate longer sequences during the PCR steps, resulting in a loss of informative sequences.
6. The resulting clusters on the flow cell are variable in size: this is expected, because there is no size selection of clusters prior to sequencing (such selection would preclude accurate clonal quantification). We recommend running a titration flow cell with the same library clustered at different densities to find the ideal concentration of the library, so maximizing the sequencing output without overloading the flow cell.

Acknowledgments

Nicolas A. Gillet and Anat Melamed contributed equally to this paper.

References

1. Lewinski MK, Yamashita M, Emerman M, Ciuffi A, Marshall H et al (2006) Retroviral DNA integration: viral and cellular determinants of target-site selection. PLoS Pathog 2:e60
2. Craigie R, Bushman FD (2012) HIV DNA integration. Cold Spring Harb Perspect Med 2:a006890
3. Gillet NA, Malani N, Melamed A, Gormley N, Carter R et al (2011) The host genomic

environment of the provirus determines the abundance of HTLV-1-infected T-cell clones. Blood 117:3113–3122

4. Cook LB, Rowan AG, Melamed A, Taylor GP, Bangham CR (2012) HTLV-1-infected T cells contain a single integrated provirus in natural infection. Blood 120:3488–3490
5. Melamed A, Laydon D, Gillet N, Tanaka Y, Taylor G et al (2013) Genome-wide determinants of proviral targeting, clonal abundance and expression in natural HTLV-1 Infection. PLoS Pathog 9
6. Gillet NA, Gutierrez G, Rodriguez SM, de Brogniez A, Renotte N et al (2013) Massive depletion of bovine leukemia virus proviral clones located in genomic transcriptionally active sites during primary infection. PLoS Pathog 9:e1003687
7. Melamed A, Witkover AD, Laydon DJ, Brown R, Ladell K et al (2014) Clonality of HTLV-2 in natural infection. PLoS Pathog 10:e1004006
8. Cook LB, Melamed A, Niederer H, Valganon M, Laydon D et al (2014) The role of HTLV-1 clonality, proviral structure, and genomic integration site in adult T-cell leukemia/lymphoma. Blood 123:3925–3931
9. Bangham CR, Cook LB, Melamed A (2014) HTLV-1 clonality in adult T-cell leukaemia and non-malignant HTLV-1 infection. Semin Cancer Biol 26C:89–98
10. Berry CC, Gillet NA, Melamed A, Gormley N, Bangham CR et al (2012) Estimating abundances of retroviral insertion sites from DNA fragment length data. Bioinformatics 28:755–762
11. Laydon DJ, Melamed A, Sim A, Gillet NA, Sim K et al (2014) Quantification of HTLV-1 clonality and TCR diversity. PLoS Comput Biol 10:e1003646
12. Maldarelli F, Wu X, Su L, Simonetti FR, Shao W et al (2014) Specific HIV integration sites are linked to clonal expansion and persistence of infected cells. Science 345(6193):179–183
13. Trobridge GD (2011) Genotoxicity of retroviral hematopoietic stem cell gene therapy. Expert Opin Biol Ther 11:581–593
14. Gaj T, Gersbach CA, Barbas CF 3rd (2013) ZFN, TALEN, and CRISPR/Cas-based methods for genome engineering. Trends Biotechnol 31:397–405
15. Bahassi EM, Stambrook PJ (2014) Next-generation sequencing technologies: breaking the sound barrier of human genetics. Mutagenesis 29:303–310
16. Krueger F, Andrews SR, Osborne CS (2011) Large scale loss of data in low-diversity illumina sequencing libraries can be recovered by deferred cluster calling. PLoS One 6:e16607
17. Langmead B, Trapnell C, Pop M, Salzberg SL (2009) Ultrafast and memory-efficient alignment of short DNA sequences to the human genome. Genome Biol 10:R25
18. Firouzi S, Lopez Y, Suzuki Y, Nakai K, Sugano S et al (2014) Development and validation of a new high-throughput method to investigate the clonality of HTLV-1-infected cells based on provirus integration sites. Genome Med 6:46
19. Gini (1914) Sulla misura della concentrazione e della variabilita dei caratteri: transactions of the real istituto veneto di scienze
20. Handcock MS, Morris M (1999) Relative distribution methods in the social sciences. Springer, New York, NY

Chapter 11

STR Profiling of HTLV-1-Infected Cell Lines

Vittoria Raimondi, Sonia Minuzzo, Vincenzo Ciminale, and Donna M. D'Agostino

Abstract

Many investigations of the replication and pathogenesis of human T-cell leukemia virus type 1 (HTLV-1) employ chronically infected cell lines, cell lines stabilized from primary adult T-cell leukemia cells, and noninfected T-cell lines. The validity of data obtained from such studies depends on the unambiguous identification of each cell line, which can be performed by short-tandem-repeat (STR) profiling (DNA fingerprinting). While kit-based profiling represents the standard method for cell line authentication, not all labs have ready access to the required capillary electrophoresis equipment, and the costs of such tests can become substantial, especially if the cell lines are to be tested frequently. We analyzed DNA from a panel of HTLV-1-infected cell lines and noninfected T-cell lines using a commercial STR kit and then analyzed the same DNA for individual STR markers followed by nondenaturing polyacrylamide gel electrophoresis. This simplified method should facilitate routine confirmation of cell line identity in diverse laboratory settings.

Key words HTLV-1, ATLL, STR profiling, Nondenaturing polyacrylamide gel electrophoresis, Combined DNA Index System (CODIS)

1 Introduction

Research into the replication and pathogenesis of HTLV-1 has relied considerably on the use of continuous cell lines, including cell lines derived from tumor cell samples of patients with ATLL (adult T-cell leukemia) and cell lines generated by transmission of the virus from infected donor cells to uninfected cells through co-cultivation. The validity of data obtained from studies of cell lines depends on their purity and authenticity. Unfortunately, misidentification and contamination of cell lines occurs frequently [1]. A list of contaminated and misidentified cell lines [2] is published by the International Cell Line Authentication Committee (ICLAC) (http://iclac.org/databases/cross-contaminations/). Aside from problems caused by human error, cell lines that have been in culture in multiple labs for many years may undergo genetic drift or selection for lab-specific tissue culture methods. The identity of cell

Claudio Casoli (ed.), *Human T-Lymphotropic Viruses: Methods and Protocols*, Methods in Molecular Biology, vol. 1582, DOI 10.1007/978-1-4939-6872-5_11,

lines should therefore be periodically checked to avoid generation of false or unreproducible results.

Cell lines can be unequivocally identified by genetic profiling of short tandem repeats (STRs) [3], which are highly polymorphic repeats of 2–7 bp located in different gene loci [4]. STRs can be composed of one type of repeat sequence ("simple" repeats, e.g., AGAA in STR D18S51) or more than one type of repeat sequence ("complex" repeats, e.g., TCTA$[TCTG]_n[TCTA]_n$ in D3S1358), sometimes with intervening sequences.

To perform STR profiling, genomic DNA is isolated and PCR-amplified using sets of primers specific for individual STRs plus a set of primers to amplify a segment of the amelogenin gene, which permits sex identification. The technique originally relied on polyacrylamide gel electrophoresis (PAGE) to separate the PCR products. Refinements of the method resulted in the development of commercial kits that employ fluorescent-labeled PCR primers in multiplex PCR and capillary electrophoresis to separate and identify the products. Allele identification numbers are assigned based on the number of repeat sequences. Alleles that contain partial repeats (microvariants) are named according to the full number of repeats and number of nucleotides in the partial repeat.

STR profiling was originally developed for forensic analysis. To facilitate standardization between laboratories, genetic profiling makes use of 13 "core" tetranucleotide STRs specified by the Combined DNA Index System (CODIS) operated by the U.S. Federal Bureau of Investigation (*see* STRs in bold type in Table 1). Most of the CODIS STRs are located on different chromosomes, so they are unlikely to co-segregate during meiosis, a feature that increases the power of the technique to discriminate between individuals. The American Type Culture Collection (ATCC) provides STR profiles of eight of the CODIS STRs plus the amelogenin gene for its human cell lines (http://www.lgcstandards-atcc.org/en/STR_Database.aspx). Several other databases of human cell line STR profiles are also available for online consultation. The Leibniz Institute DSMZ-German Collection of Microorganisms and Cell Cultures provides an online search engine for cell line identification that uses the same markers as the ATCC (http://www.dsmz.de/fp/cgi-bin/str.html). The National Center for Biotechnology Information (NCBI) BioSample website provides a list of misidentified cell lines and a searchable database of STR profiles (http://www.ncbi.nlm.nih.gov/biosample?term=human+str+profile[Filter]). In the interest of good research, several journals require recent STR genotyping or use of authenticated cell lines that have been purchased within a certain timeframe.

Only a small number of HTLV-1-transformed cell lines are commercially available, and the profiles of only few of the commonly

used cell lines are present in online databases. We obtained STR profiles of the HTLV-1-infected cell lines C91PL [5], MT-2 [6], C8166–45 [7], HUT-102 [8], and the noninfected T-ALL cell line Jurkat [9], using the Promega Powerplex 16 HS kit [10], which amplifies the 13 CODIS STRs plus amelogenin and 2 pentanucleotide STRs named Penta D and Penta E. Table 1 reports the genetic profiles of the five cell lines. To our knowledge, the profiles for C91PL and C8166 have not been described elsewhere and must therefore be considered provisional; the profiles of the other cell lines match those reported in online databases (Table 1).

Multiplex STR amplification is the most accurate method for cell line genotyping and identification, but requires special equipment, kits, and expertise that are not readily on hand in all labs. Our objective was to determine whether analysis of STR products

Table 1
Genetic profiles of HTLV-1-infected cell lines and the Jurkat cell line obtained with the Powerplex 16 HS kit

STR	Chromosome location	C91PL	MT-2	C8166	HUT-102	Jurkat
TPOX	2p25.3	8	10,11	11	6	8,10
D3S1358	3p21.31	15,19	16,17	15,16	15,16	15,17
FGA	4q31.3	19,23	23,24	21,22	24	20,21
D5S818	5q23.2	13	13	12	8,13	9
CSF1PO	5q32	10	10,11	10,11	8,11	11,12
D7S5820	7q21.11	10,11	8,13	9,10	8,10	8,12
D8S1179	8q24.13	13,14	11,14	11,14	13,15	13,14
TH01	11p15.5	8,9	6,10	6,9.3	7,8	6,9.3
vWA	12p13.31	17	16	15,16	16,19	18
D13S317	13q31.1	8,11	9,13	10,11	11,13	8,12
Penta E	15q26.2	16,20	15,16	7,11	7,8	10,12
D16S539	16q24.1	9,12	9,11	12,13	12	11
D18S51	18q21.33	12,13	12,14	14,17	20	13,21
D21S11	21q21.1	29,31.2	29,30	27,30	28,29	31.2,33.2
Penta D	21q22.3	10,13	10,11	11,15	8,10	11,13
Amelogenin	X (p22.2) Y (p11.2)	X,Y	X,Y	X,Y	X,Y	X,Y

CODIS STRs are in bold type. Listed are the number of repeat sequences identified for each STR. Profiles for HUT-102 and Jurkat (Clone E6–1) are reported in the ATCC and DSMZ databases. The profile for MT-2 is reported in the DSMZ database. These databases list the following loci: TPOX, D5S818, CSF1PO, D7S5820, TH01, vWA, D13S317, D16S539, and amelogenin

by conventional nondenaturing PAGE would provide sufficient information for routine monitoring of cell lines currently in use in our laboratory. This method does not require special equipment and is useful for routine cell line monitoring.

2 Materials

2.1 STR Amplification

1. DNA Isolation system.
2. AmpliTaq Gold DNA polymerase.
3. 10× GeneAmp PCR Buffer without magnesium (Applied Biosystems (Applied Biosystems)).
4. 25-mM $MgCl_2$.
5. dNTP stock solution.
6. PCR primers.
7. Ultrapure dH_2O.
8. Low-aerosol filter tips.
9. 200 μl PCR tubes (sterile, free of nucleases and nucleic acids).
10. Thermocycler.
11. Microcentrifuge.
12. Heat block.

2.2 Nondenaturing Polyacrylamide Gel Electrophoresis

1. 6× DNA loading dye: 0.24% bromophenol blue, 0.24% xylene cyanol, 15% Ficoll-400, 100 mM EDTA (ethylenediamine tetraacetic acid, prepared as a 500 mM stock, pH 8.0).
2. Acrylamide:bis-acrylamide solution (19:1 and 29:1 ratios).
3. TEMED (N,N,N',N'-tetramethylethylenediamine) and ammonium persulfate (10% w/v stock prepared in dH_2O).
4. 10×TBE (Tris-Borate electrophoresis buffer): 500 mM Tris, 500 mM boric acid, 10 mM EDTA, pH 8.3.
5. DNA ladder suitable for PAGE analysis of PCR products (e.g., PCR 20 bp Low Ladder, Sigma-Aldrich). The stock preparation of PCR 20 bp Low ladder should be diluted eightfold in DNA loading dye; 6 μl are loaded on gels.
6. High-sensitivity nucleic acid stain.
7. Spectrophotometer.
8. Glass plates for vertical PAGE.
9. 0.75-mm spacers.
10. Gel Combs.
11. Gel rig suitable for 12-cm-long gels.
12. Power supply.
13. Imaging system for photographing gels.

3 Methods

3.1 Primer Sets and PCR

1. We PCR-amplified the 16 loci listed in Table 1 using as template the same preparations of genomic DNA (*see* **Notes 1–3**) that had been analyzed with the Powerplex 16 HS kit. This kit uses the same primer sets that were employed in a previous version of the kit [10] (Powerplex 16); the sequences of these primers have been published [11].
2. Table 2 lists the primers that we tested. With the exception of the primers for FGA, D8S1179, and D18S51, all of the primer sets were identical or similar to the primers used in the Powerplex kit.
3. We shortened some of the primers at the 3′ end to reduce the melting temperature (Tm), and changed the 5′ end of some primers to eliminate mismatches with the human genome reference sequence (Table 2).

Table 2
PCR primers

Marker	Primers	Ref.	Annealing temp., °C
TPOX	F GGCACAGAACAGGCACTTAGG R GAACTGGGAACCCCACAGGTT	[17][a]	62
D3S1358	F ACTGCAGTCCAATCTGGGT R ATGAAATCAACAGAGGCTTGC	[11]	62
FGA	F GCCCCATAGGTTTTGAACTCA R TGATTTGTCTGTAATTGCCAGC	[18]	62
D5S818	F GGTGATTTTCCTCTTTGGTATCC R AGCCACAGTTTACAACATTTGTATCT	[11]	62
CSF1PO	F CCGGAGGTAAAGGTGTCTTAAAGT R ATTTCCTGTGTCAGACCCTGTT	[11]	62
D7S5820	F ATGTTGGTCAGGCTGACTATG R GATTCCACATTTATCCTCATTGAC	[11]	60
D8S1179	F TTTTTGTATTTCATGTGTACATTCG R CGTAGCTATAATTAGTTCATTTTCA	[19]	60
TH01	F GTGATTCCCATTGGCCTGTTC R CCTCCTGTGGGCTGAAAAGCTC	[11][a]	64
vWA	F GCCCTAGTGGATGATAAGAATAATC R GGACAGATGATAAATACATAGGATG	[11][a]	62
D13S317	F ATCACAGAAGTCTGGGATGTGG R GGCAGCCCAAAAAGACAGAC	[11][a]	62
Penta E	F TTTACCAACATGAAAGGGTACCAATA R TGGGTTATTAATTGAGAAAACTCCTTAC	[11][a]	60

(continued)

Table 2
(continued)

Marker	Primers	Ref.	Annealing temp., °C
D16S539	F GGGGGTCTAAGAGCTTGTAAAAAG R GTTTGTGTGTGCATCTGTAAGC	[11][a]	62
D18S51	F CAAACCCGACTACCAGCAAC R GAGCCATGTTCATGCCACTG	[19]	62
D21S11	F ATATGTGAGTCAATTCCCCAAG R TGTATTAGTCAATGTTCTCCAGAGAC	[11]	60
Penta D	F GAAGGTCGAAGCTGAAGTG R GAATTCTTTAATCTGGACACAAG	[11][a]	60
Amelogenin	F CCCTGGGCTCTGTAAAGAATAGTG R ATCAGAGCTTAAACTGGGAAGCTG	[20]	62

[a]Primer sequences were modified from published primers

4. Primer sets were tested in PCR reactions performed in a final 25 µl volume.
5. A mastermix containing all reaction components except the genomic DNA was prepared for the number of samples to be amplified plus an H_2O control (*see* **Note 4**).
6. The 25 µl PCR volume contained 1× GeneAmp PCR buffer (from a 10× stock), 1.5 mM $MgCl_2$ (from a 25 mM stock), 200 µmoles dNTP mix (from a 10 mM stock), 0.5 µmole of each primer (from 10 µM stocks), 0.65 U AmpliTaq Gold DNA polymerase (from a 5 U/µl stock), and 20 ng genomic DNA (added last).
7. The cycling conditions were as follows: 95 °C for 5 min (hot-start); 32 cycles of [95 °C for 30 s, annealing temp. (Table 2) for 30 s, 72 °C for 45 s]; 72 °C for 10 min (final extension); 4 °C (hold).
8. Amplified samples were stored at −20 °C until PAGE analysis.
9. In initial trials, PCR reactions were performed on genomic DNA from C91PL and MT-2 cells at 4–6 annealing temperatures differing by 2 °C.
10. Table 2 lists the annealing temperatures that yielded readily detectable bands of the expected sizes and minimal amounts of higher molecular weight bands detected by PAGE.

3.2 PAGE

1. The lengths of PCR products produced with the STR primers listed in Table 2 range from less than 100 bp to more than 400 bp.
2. We attempted to resolve STRs with standard vertical nondenaturing PAGE using 12-cm-long, 14.5-cm-wide gels with 20 wells, which is a commonly used, easy-to-handle format.

3. Gels were prepared using 0.75-mm spacers with acrylamide:bis acrylamide ratios of 19:1 or 29:1 and various total percentages of acrylamide (*see* **Note 5**).
4. The gels were prepared using 30 ml mixtures containing the desired percentage of acrylamide-bis acrylamide and 1× TBE, and 300 µl ammonium persulfate (10% stock) and 30 µl TEMED to catalyze polymerization.
5. After polymerization for at least 30 min, gels were loaded and electrophoresed at 100 V for 3 h or until the bromophenol blue dye front reached the bottom of the gel (*see* **Notes 6** and **7**).
6. Gels were stained for 20 minutes using DNA stain solution, rinsed briefly in dH_2O, and photographed using a digital imaging system (*see* **Notes 8**).

We observed that STRs with amplicon sizes of ≤200 bp were resolved in 6% polyacrylamide gels prepared with a 19:1

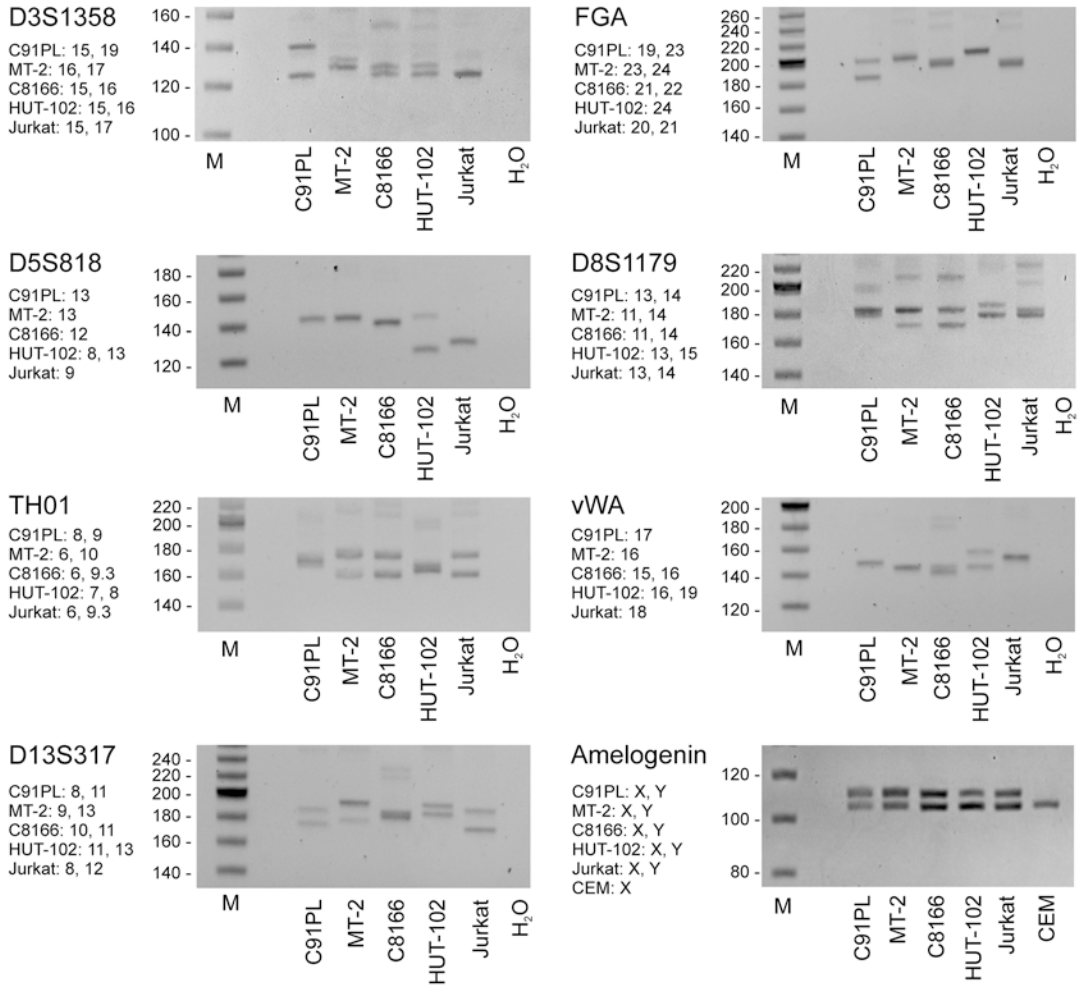

Fig. 1 Nondenaturing PAGE of STR and amelogenin amplicons using 6% (19:1) gels. PAGE was performed as described in the text. The lanes labeled M contained PCR 20 bp Low Ladder (Sigma-Aldrich)

acrylamide:bis acrylamide ratio (Fig. 1), while larger amplicons were resolved better in 6 or 7% gels prepared with a 29:1 ratio. In general, the sizes of the amplicons detected for the different STRs matched the profiles obtained with the Powerplex kit, which are indicated to the left of each photo. Among the 15 STRs tested, five were resolved sufficiently to show a 1-repeat difference. Four of these amplicons were in the ≤ 200 bp category (Fig. 1): D5S818 (compare MT-2 and C8166, with alleles 13 and 12, respectively), D8S1179 (*see* C91PL and Jurkat, each with alleles 13 and 14), vWA (compare C91PL and MT-2, with alleles 17 and 16, respectively, and C8166, with alleles 15 and 16), D13S317 (*see* C8166, with alleles 10 and 11). Among the STRs with larger amplicons (Fig. 2), only Penta D showed one-repeat resolution (*see* MT-2, alleles 10, 11). CSF1PO yielded the poorest resolution (Fig. 2).

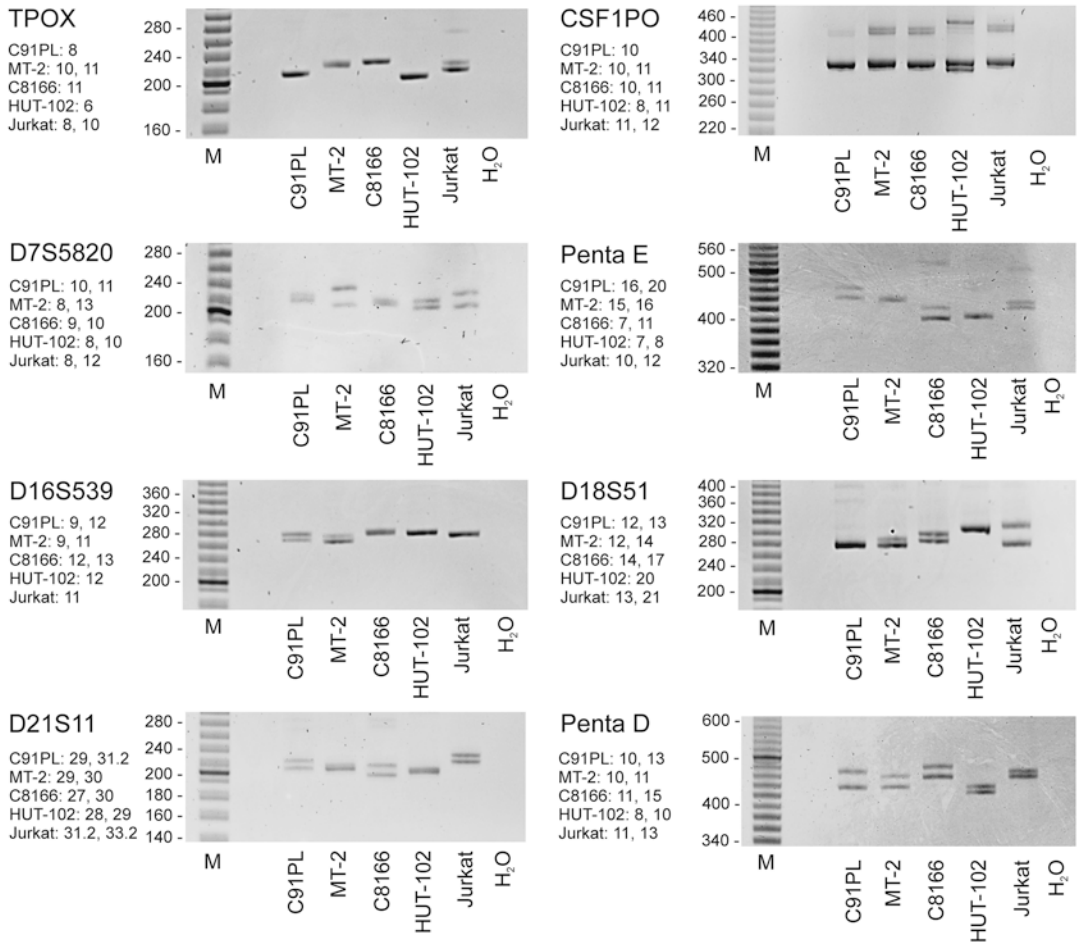

Fig. 2. Nondenaturing PAGE of STR amplicons using 6% or 7% (29:1) gels. PAGE was performed as described in the text. D7S5820, Penta E, and Penta D were separated in 6% gels; all other gels were 7%. The lanes labeled M contained PCR 20 bp Low Ladder (Sigma-Aldrich)

The STRs used for profiling have a high frequency of heterozygosity in the human population, a desirable property for forensic applications. The two alleles detected in normal diploid cells should have equivalent peak heights in the capillary electropherogram or band intensities on gels. The pattern obtained for Jurkat cells using STR D3S1358 (Fig. 1) suggested the presence of a single allele (allele 15, inferred from its comigration with the amplicons obtained for the other cell lines), whereas two alleles were expected according to the Powerplex profile (i.e., alleles 15 and 17). Interestingly, there was a large difference in the peak heights of these two alleles in the original capillary electropherogram, with the allele 15 peak nearly fivefold higher than allele 17 (not shown). Such peak height imbalance is not uncommon among cell lines [3], and may result from gene duplication, aneuploidy, or the presence of mutations in one allele that affect binding of the PCR primers. Among the five cell lines tested, we noted a low frequency of heterozygosity for D5S818 (1/5 cell lines), vWA (2/5 cell lines), and TPOX (2/5 cell lines). Such loss of heterozygosity may reflect the genetic instability associated with the transformed phenotype [3]. The appearance of three or more alleles is more rare, and should raise the suspicion of a mixed cell line. None of the cell lines analyzed here showed more than two alleles.

Figure 1 also shows the PCR amplicons obtained for the amelogenin alleles located on the X and Y chromosomes, which differ by 6 bp (these amplicons can also be separated on 5-cm-long gels). As expected from the Powerplex profiles, all the cell lines had a male genotype; the T-ALL cell line CCRF-CEM [12] is shown to provide an example of a "female" cell line. It is noteworthy that several subclones or variants of the Jurkat cell line yield a single amelogenin (X) amplicon rather than the expected XY pattern.

This standard PAGE system allows one to confirm cell line identity by comparing patterns of different cell lines whose genetic profiles were previously established by multiplex PCR, especially if amplicons from "authenticated" DNA are included on the gel as markers. However, its level of resolution is not sufficient for establishing the genetic profile of a previously uncharacterized cell line.

Longer gels would undoubtedly aid in resolving closely spaced STR alleles. For example, Azari et al. were able to analyze the 13 CODIS STR loci and amelogenin amplicons from a large panel of cell lines using 26-cm, 10% polyacrylamide gels [13]. In alternative, the separation of small DNA fragments by conventional small-format PAGE may be improved by reducing the concentration of crosslinker, adding a stacking gel and preparing the gel with a lower pH compared to the running buffer [14]. A recent report described 6.5-cm, 10% acrylamide gels prepared with a low-pH stacking gel and a polymer additive (EnhanceIt, Elchrom Scientific) that yielded very high resolution of amplicons ranging from 100 to 40 bp [15]; gels of this format with a lower concentration of acrylamide might be suited for separation of STR amplicons.

4 Notes

1. The STR detection method described here requires the availability of genomic DNA from cell lines that have been authenticated by multiplex STR analysis. Aliquots of this genomic DNA should be stored for use as a positive control/marker for end-point PCR and PAGE.
2. Genomic DNA can be isolated from cell lines using classic techniques such as phenol-chloroform extraction or with a variety of kits, which offer the advantages of being more rapid and standardized. We routinely use the Flexigene DNA Kit (Qiagen) and isolate DNA from 1×10^6 cells.
3. The last step of many DNA isolation protocols and kits calls for precipitation of DNA with isopropanol or ethanol followed by washing in 70% ethanol, drying, and resuspension in ultrapure H_2O or TE (Tris/EDTA buffer). DNA may be difficult to resuspend if the number of starting cells is too high or if the DNA pellet is left to dry for too long. Resuspension may be accomplished by increasing the volume of resuspension solution and incubation at 65 °C for 30 min. If TE is used, it should be prepared with a low EDTA concentration (≤0.1 mM) to avoid chelating magnesium ions that are needed by the DNA polymerase during the PCR reaction. Resuspended DNA can be stored at 4 °C for a short time or at ≤−20 °C for long-term storage.
4. PCR reagents should be stored and aliquoted in an area free of DNA templates and PCR products. Taq polymerase adds an extra A to the 3′ end of DNA. Ending the PCR method with a long final extension time will increase the probability that all DNA molecules have this modification. This is important, since the STR alleles differ by only four or five nucleotides (or fewer in the case of microvariants).
5. Acrylamide is a neurotoxin. Purchase premixed stock solutions instead of dissolving acrylamide powder. Prepare gels under a fume hood and wear gloves at all stages of gel preparation and handling.
6. DNA loading dye generally contains either sucrose, glycerol or Ficoll-400 to increase the density of the sample. As described by Umetsu et al. [15], glycerol can form complexes with borate present in the TBE running buffer, which may affect migration of the DNA. We observed that DNA loading dye containing Ficoll-400 yielded better resolution of DNA bands compared to dye prepared with glycerol or sucrose (data not shown).
7. The electrophoretic migration of DNA molecules is increased when more molecules are loaded, due to the increased mechanical force that they exert on the gel matrix [16]. It is therefore important to load small, approximately equal amounts of the STR amplicons and DNA ladder.

8. We recommend staining gels with a noncarcinogenic fluorescent DNA stain (e.g., EuroClone EuroSafe Nucleic Acid Staining Solution, diluted 1:20,000 in dH2O) instead of ethidium bromide.

Acknowledgments

We thank Luca Persano for the Jurkat and CCRF-CEM cell lines. This work was supported by an investigator grant from the Associazione per la Ricerca sul Cancro (AIRC, awarded to V.C.).

References

1. American Type Culture Collection Standards Development Organization Workgroup ASN (2010) Cell line misidentification: the beginning of the end. Nat Rev Cancer 10:441–448
2. Capes-Davis A, Theodosopoulos G, Atkin I, Drexler HG, Kohara A, MacLeod RA, Masters JR, Nakamura Y, Reid YA, Reddel RR, Freshney RI (2010) Check your cultures! A list of cross-contaminated or misidentified cell lines. Int J Cancer 127:1–8
3. Masters JR, Thomson JA, Daly-Burns B, Reid YA, Dirks WG, Packer P, Toji LH, Ohno T, Tanabe H, Arlett CF, Kelland LR, Harrison M, Virmani A, Ward TH, Ayres KL, Debenham PG (2001) Short tandem repeat profiling provides an international reference standard for human cell lines. Proc Natl Acad Sci U S A 98:8012–8017
4. Butler JM (2006) Genetics and genomics of core short tandem repeat loci used in human identity testing. J Forensic Sci 51:253–265
5. Popovic M, Lange-Wantzin G, Sarin PS, Mann D, Gallo RC (1983) Transformation of human umbilical cord blood T cells by human T-cell leukemia/lymphoma virus. Proc Natl Acad Sci U S A 80:5402–5406
6. Miyoshi I, Kubonishi I, Yoshimoto S, Akagi T, Ohtsuki Y, Shiraishi Y, Nagata K, Hinuma Y (1981) Type C virus particles in a cord T-cell line derived by co-cultivating normal human cord leukocytes and human leukaemic T cells. Nature 294:770–771
7. Salahuddin SZ, Markham PD, Wong-Staal F, Franchini G, Kalyanaraman VS, Gallo RC (1983) Restricted expression of human T-cell leukemia-lymphoma virus (HTLV) in transformed human umbilical cord blood lymphocytes. Virology 129:51–64
8. Poiesz BJ, Ruscetti FW, Gazdar AF, Bunn PA, Minna JD, Gallo RC (1980) Detection and isolation of type C retrovirus particles from fresh and cultured lymphocytes of a patient with cutaneous T-cell lymphoma. Proc Natl Acad Sci U S A 77:7415–7419
9. Schneider U, Schwenk HU, Bornkamm G (1977) Characterization of EBV-genome negative "null" and "T" cell lines derived from children with acute lymphoblastic leukemia and leukemic transformed non-Hodgkin lymphoma. Int J Cancer 19:621–626
10. Ensenberger MG, Thompson J, Hill B, Homick K, Kearney V, Mayntz-Press KA, Mazur P, McGuckian A, Myers J, Raley K, Raley SG, Rothove R, Wilson J, Wieczorek D, Fulmer PM, Storts DR, Krenke BE (2010) Developmental validation of the PowerPlex 16 HS System: an improved 16-locus fluorescent STR multiplex. Forensic Sci Int Genet 4:257–264
11. Krenke BE, Tereba A, Anderson SJ, Buel E, Culhane S, Finis CJ, Tomsey CS, Zachetti JM, Masibay A, Rabbach DR, Amiott EA, Sprecher CJ (2002) Validation of a 16-locus fluorescent multiplex system. J Forensic Sci 47:773–785
12. Norman MR, Thompson EB (1977) Characterization of a glucocorticoid-sensitive human lymphoid cell line. Cancer Res 37:3785–3791
13. Azari S, Ahmadi N, Tehrani MJ, Shokri F (2007) Profiling and authentication of human cell lines using short tandem repeat (STR) loci: *Report from the National Cell Bank of Iran*. Biologicals 35:195–202
14. Sajantila A, Lukka M (1993) Improved separation of PCR amplified VNTR alleles by a vertical polyacrylamide gel electrophoresis. Int J Leg Med 105:355–359
15. Umetsu K, Yuasa I, Hashiyada M, Adachi N, Watanabe G, Haneda T, Yamazaki K (2016) The art of traditional native PAGE: The APLP 48-ID assay for human identification. Leg Med (Tokyo) 19:28–31

16. Kozulic B (1995) Models of gel electrophoresis. Anal Biochem 231:1–12
17. Huang NE, Schumm J, Budowle B (1995) Chinese population data on three tetrameric short tandem repeat loci-HUMTHO1, TPOX, and CSF1PO-derived using multiplex PCR and manual typing. Forensic Sci Int 71:131–136
18. Urquhart A, Kimpton CP, Downes TJ, Gill P (1994) Variation in short tandem repeat sequences—a survey of twelve microsatellite loci for use as forensic identification markers. Int J Leg Med 107:13–20
19. Barber MD, Parkin BH (1996) Sequence analysis and allelic designation of the two short tandem repeat loci D18S51 and D8S1179. Int J Leg Med 109:62–65
20. Mannucci A, Sullivan KM, Ivanov PL, Gill P (1994) Forensic application of a rapid and quantitative DNA sex test by amplification of the X-Y homologous gene amelogenin. Int J Leg Med 106:190–193

Chapter 12

Expression of HTLV-1 Genes in T-Cells Using RNA Electroporation

Mariangela Manicone*, Francesca Rende*, Ilaria Cavallari, Andrea K. Thoma-Kress, and Vincenzo Ciminale

Abstract

Human T-cell leukemia virus type 1 (HTLV-1) infects about 20 million people world-wide. Around 5% of the infected individuals develop adult T-cell leukemia (ATL) or a neurological disease termed tropical spastic paraparesis (TSP) after a clinical latency of years to decades. Through the use of two promoters and alternative splicing HTLV-1 expresses at least 12 different proteins. HTLV-1 establishes a life-long persistent infection by inducing the clonal expansion of infected cells, a property largely ascribed to the viral genes Tax and HBZ. However, the fact that ATL arises in a minority of infected individuals after a long clinical latency suggests the existence of factors counterbalancing the oncogenic potential of HTLV-1 in the context of natural infection.

To study the role of the different HTLV-1 gene products in the HTLV-1 life cycle, we optimized a transfection protocol for primary T-cells using an approach based on the electroporation of in vitro-transcribed RNA. Results showed that the RNA transfection technique combines a high transfection efficiency with low toxicity, not only in Jurkat T-cells but also in primary T-cells. These findings suggest that RNA electroporation is preferable for experiments aimed at investigating the role of HTLV-1 gene products in the context of primary T-cells, which represent the main target of HTLV-1 in vivo.

Key words HTLV-1, ATL, In vitro transcription, RNA electroporation, Peripheral blood mononuclear cells (PBMCs)

1 Introduction

Human T-cell leukemia virus type 1 (HTLV-1) infects about 20 million people world-wide. Around 5% of infected individuals develop adult T-cell leukemia (ATL) or a neurological disease termed tropical spastic paraparesis (TSP) after a clinical latency of years to decades. Current ATL therapies have limited success, there is no vaccine against HTLV-1, and infected patients are unable to eradicate the virus [1].

*These authors contributed equally to this work.

Claudio Casoli (ed.), *Human T-Lymphotropic Viruses: Methods and Protocols*, Methods in Molecular Biology, vol. 1582,
DOI 10.1007/978-1-4939-6872-5_12, © Springer Science+Business Media LLC 2017

The HTLV-1 expression strategy is characterized by the production of plus and minus-strand transcripts, alternative splicing (producing over ten alternatively spliced mRNAs), and polycistronic translation [1]. This strategy greatly increases the coding potential of the virus, resulting in expression of several regulatory and accessory genes in addition to the structural proteins and virion-associated enzymes common to all retroviruses (Gag, Pro, Pol, Env). These additional proteins, named Tax, Rex, p12/p8, p13, p21Rex, and p30Tof, are coded by the X region of the genome [2, 3]. An additional protein, named HBZ, is coded by minus-strand transcripts that overlap with the X region [4–6].

HTLV-1 establishes a life-long persistent infection through induction of clonal expansion of infected cells, a property largely ascribed to the viral genes Tax and HBZ. However, the fact that ATL arises in a minority of infected individuals after a long clinical latency suggests the existence of factors (i.e., other viral proteins) curbing HTLV-1's oncogenic potential in the context of natural infection.

With the aim of investigating the role of the different HTLV-1 gene products in some aspects of the HTLV-1 life cycle and pathogenicity, that remain unclear, we optimized a transfection protocol for primary T-cells using an innovative approach based on the electroporation of in vitro transcribed RNA. The coding sequences of GFP and p13 were cloned into the pST1-vector (Fig. 1),

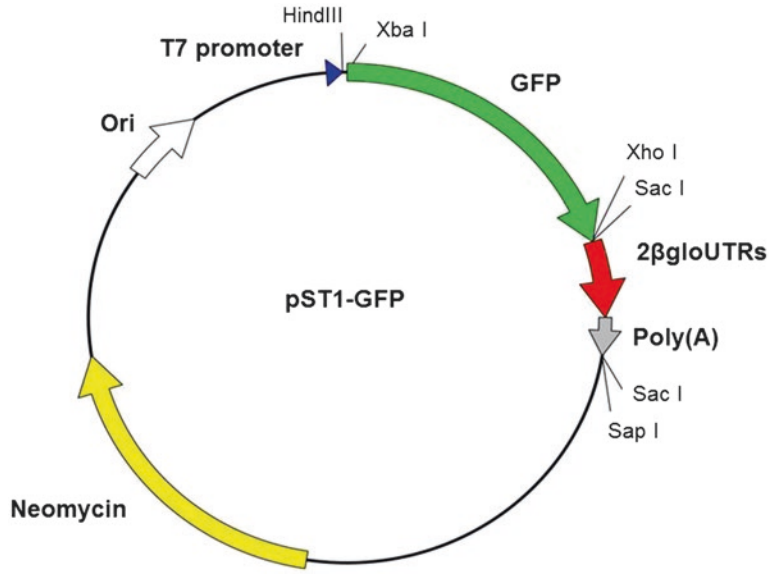

Fig. 1 The pST1-GFP plasmid. The vector contains the T7 phage promoter and a 120 base pair-long poly(A) tail (*gray arrow*) flanking the coding sequence of the green fluorescent protein (GFP, *green arrow*). Two tandemly repeated human β-globin UTRs (2βgloUTRs, *red arrow*) located between the GFP coding sequence and the poly(A) tail increase the stability of the in vitro transcribed RNA. The unique Sap I site, located downstream of the poly(A) tail, can be used to linearize the vector (Adapted from (7))

which allows efficient production of highly stable in vitro-transcribed RNA [7]. Transfection of in vitro-transcribed RNA has emerged in recent years as a promising technique for gene transfer in cells refractory to standard methods of DNA transfection, including primary T-cells and dendritic cells [7–10]. We first tested the protocol in Jurkat T-cells, and then applied it to freshly isolated peripheral blood mononuclear cells (PBMCs).

Our experiments indicated that the RNA transfection technique combines a high transfection efficiency with low transfection-related toxicity, not only in Jurkat T-cells, but also in primary T-cells, which are usually refractory to standard DNA transfection techniques; in particular, electroporation of DNA often results in high toxicity combined with a low transfection efficiency, thus rendering subsequent analyses extremely difficult. The obtained results suggest that RNA electroporation is preferable for experiments aimed at investigating the role of HTLV-1 gene products in the context of Jurkat T-cells and primary T-cells, which represent the main target of HTLV-1 in vivo.

2 Materials

1. pST1-GFP vector, originally referred to as pST1-eGFPmut-2ßglobinUTR-A(120) [7].
2. pCR-Blunt Kit (Invitrogen/ThermoFisherScientific, Waltham, MA, USA).
3. *Hind* III and *Xho* I restriction enzymes (New England BioLabs, Ipswich, MA, USA).
4. FastDigest *Sap* I (*Lgu* I) restriction enzyme (Fermentas/ThermoFisherScientific).
5. 10×FastDigestionBuffer(Fermentas/ThermoFisherScientific).
6. GENECLEAN Turbo kit (MP Biomedicals, Santa Ana, CA, USA).
7. UltraPure Agarose.
8. mMESSAGE mMACHINE T7 kit (ThermoFisherScientific).
9. TURBO DNase (ThermoFisherScientific).
10. RNeasy MinElute Cleanup kit (Qiagen, Hilden, Germany).
11. pmaxGFP plasmid (Amaxa/LONZA, Basel, Switzerland).
12. Jurkat T-cell line.
13. Peripheral blood mononuclear cells (PBMCs) from healthy donors.
14. Ficoll-Hypaque.
15. RPMI 1640 medium.
16. Phosphate-buffered saline (PBS).

17. Fetal calf serum (FCS).
18. L-Glutamine.
19. Penicillin, Streptomycin.
20. Neon transfection system (Invitrogen).
21. MicroPorator (DigitalBio/ThermoFisherScientific).
22. Nanodrop ND-1000 (ThermoFisherScientific) or equivalent.
23. BD LSRII flow cytometer or equivalent (BD Biosciences, San Jose, CA, USA) equipped with 488-nm lasers.
24. Heat block.
25. Refrigerated centrifuge.

3 Methods

3.1 Plasmid Construction and Linearization

RNA to be transfected was transcribed in vitro using a system based on the vector pST1-GFP (Fig. 1) [7–9]. pST1-GFP contains the T7 phage promoter sequence at the 5′ end and a 120 base pair-long poly(A) tail at the 3′ of the coding sequence of interest. In addition, the pST1-vector contains two tandemly repeated human β-globin untranslated regions (UTRs) between the coding sequence and the poly(A) tail that increase the stability of the in vitro transcribed RNA. This vector can be used to in vitro transcribe genes of interest, ensuring high transcript stability and translational efficiency [7]. The vector can be linearized by digestion with the Sap I enzyme, whose unique recognition site is located downstream of the poly(A) tail.

For our experiments, the coding sequence of p13-GFP was obtained from the plasmid pcDNAp13-GFP [11] through Hind III-Xho I restriction digestion. The p13-GFP fragment was cloned in the intermediate pCR-Blunt Vector (Invitrogen) and cut with Hind III and Xho I to generate the Hind III-p13GFP-Xho I fragment. This fragment was then ligated to the pST1-delta-GFP vector obtained by digesting pST1-GFP with Hind III and Xho I.

1. Linearize the pST1-p13-GFP plasmid and the control pST1-GFP plasmid (*see* **Note 1**) with the FastDigest Sap I (Lgu I) restriction enzyme, using the following reaction in the indicated order:
   - nuclease-free water to a final volume of 50 μl.
   - 10× Fast Digestion Buffer (5 μl).
   - DNA (15 μg).
   - Sap I enzyme (5 μl).
2. Digest for 1 h at 37 °C.

3. Purify the linearized plasmids from a 1% UltraPure Agarose gel (ThermoFisher) using the GENECLEAN Turbo kit (MP Biomedicals) (*see* **Note 2**), and quantitate using a Nanodrop ND-1000 spectrophotometer (ThermoFisherScientific). The expected yield is approximately 10 μg; to maximize yields, DNA should be relatively free of contaminating proteins.

3.2 In Vitro Transcription and Capping

The Sap I-linearized pST1-p13-GFP and pST1-GFP plasmids were subjected to in vitro transcription and capped using the mMESSAGE mMACHINE T7 kit (Ambion, Life Technologies) that contains all the necessary buffers and reagents (*see* **Note 3**). All four ribonucleotides and cap analog [m7G(5′)ppp(5′)G] are mixed in a single solution. A cap analog:GTP ratio of 4:1 is optimal for maximizing both RNA yield and the proportion of capped transcripts. In addition, a RNase inhibitor (a component of the Enzyme Mix) protects the RNA synthesized from degradation by contaminating ribonucleases that may be present. The DNA template must contain upstream of the sequence to be transcribed the correct RNA polymerase promoter site (T7, T3, or SP6 depending on the RNA polymerase used; T7 in our case). The suggested template concentration is 0.5 μg/μl in water or TE buffer. Using T7 RNA polymerase, the expected yield is approximately 20–30 μg of RNA per reaction.

1. Thaw the frozen reagents and place the RNA Polymerase Enzyme Mix on ice; vortex the 10× Reaction Buffer and the 2× NTP/CAP until they are completely in solution. All reagents should be centrifuged briefly before opening to prevent loss and/or contamination of material that may be present around the rim of the tube. While assembling the reaction, keep the ribonucleotides (2× NTP/CAP) on ice and the 10× Reaction Buffer at room temperature.
2. Assemble the transcription reaction at room temperature; otherwise, the spermidine in the 10× Reaction Buffer may precipitate; add water and then the 10× Reaction Buffer (the ribonucleotides are already in the tube).

   The following amounts are for a single 20-μl in vitro transcription reaction:

   – Nuclease-free water to 20 μl.
   – 2× NTP/CAP (10 μl).
   – 10× Reaction Buffer (2 μl).
   – Linear template DNA (use 0.1–0.2 μg PCR-product template or 0.1–1 μg linearized plasmid template) in a maximum volume of 6 μl (the template DNA should have a good starting concentration).

3. Mix thoroughly: gently flick the tube or pipette the mixture up and down, and then centrifuge briefly to collect the reaction mixture at the bottom of the tube.
4. Incubate at 37 °C for 2 h.
5. Add 1 μl of TURBO DNase (Ambion, Life Technologies), and incubate samples for 15 min at 37 °C to remove DNA templates.
6. For troubleshooting, *see* **Notes 4–7**.

3.3 Purification of the In Vitro Transcribed RNA

For the purification of the in vitro-transcribed RNA different methods can be used (i.e., MEGAclear Kit -Ambion, Life Technologies-; lithium chloride precipitation, spin column chromatography, phenol:chloroform extraction and isopropanol precipitation). We used the RNeasy MinElute Cleanup kit (Qiagen). This kit is designed for cleaning up RNA from enzymatic reactions, for desalting RNA samples, and for concentrating RNA isolated by various methods.

Consider the following important points before starting:

1. A maximum of 45 μg RNA in a maximum volume of 200 μl can be purified with this protocol. This amount corresponds to the binding capacity of the RNeasy MinElute spin column and overloading the column will significantly reduce RNA yield and purity.
2. All steps of the procedure have to be performed at room temperature (15–25 °C) and during the procedure it is important to work quickly.
3. In the procedure described below, the indicated volumes refer to a starting volume ≤100 μl.
   (a) Adjust the sample to a volume of 100 μl with RNase-free water. Add 350 μl of Buffer RLT and mix well (we recommend adding β-mercaptoethanol to Buffer RLT −10 μl per 1 ml; if Buffer RLT forms a precipitate during the storage, redissolve by warming and then place at room temperature).
   (b) Add 250 μl of 96–100% ethanol to the diluted RNA and mix well by pipetting (do not centrifuge).
   (c) Transfer the sample to an RNeasy MinElute spin column placed in a 2-ml collection tube. Close the lid gently, and centrifuge for 15 s at ≥8000 × *g*. Discard the flow-through.
   (d) Place the RNeasy MinElute spin column in a new 2-ml collection tube, and add 500 μl of Buffer RPE [as Buffer RPE is supplied as a concentrate, before using it for the first time, add 4 volumes of ethanol (96–100%) to obtain the working solution]. Close the lid gently, and centrifuge for

15 s at ≥8000 × *g* to wash the spin column membrane. Discard the flow-through.

(e) Add 500 µl of 80% ethanol to the RNeasy MinElute spin column. Close the lid gently, and centrifuge for 2 min at ≥8000 × *g* to wash the spin column membrane. Discard the flow-through and collection tube (after centrifugation, carefully remove the RNeasy MinElute spin column from the collection tube so that the column does not contact the flow-through, otherwise, ethanol carryover will occur).

(f) Place the RNeasy MinElute spin column in a new 2-ml collection tube, open the lid of the spin column, and centrifuge at full speed for 5 min. Discard the flow-through and collection tube (it is important to dry the spin column membrane since residual ethanol may interfere with downstream reactions. Centrifugation with the lids open ensures that no ethanol is carried over during RNA elution).

(g) Place the RNeasy MinElute spin column in a new 1.5-ml collection tube and add 14 µl RNase-free water directly to the center of the spin column membrane. Close the lid gently and centrifuge for 1 min at full speed to elute the RNA (as little as 10 µl RNase-free water can be used for elution if a higher RNA concentration is required, but the yield will be reduced by approximately 20%; do not elute with less than 10 µl RNase-free water as the spin column membrane will not be sufficiently hydrated). The dead volume of the RNeasy MinElute spin column is 2 µl.

(h) Quantitate the purified RNA using a Nanodrop ND-1000 spectrophotometer (ThermoFisherScientific). The expected yield is approximately 20–30 µg of RNA per reaction. For troubleshooting *see* **Notes 8–12**.

3.4 Transfections

The RNA transfection protocol was set up in Jurkat T-cells and freshly isolated PBMCs using the Neon transfection system (Life Technologies) (*see* **Note 13**).

1. At the day of the transfection, cells were counted and washed in PBS. Jurkat cells were resuspended in aliquots of 5×10^6 cells in 100 µl of R buffer for each electroporation.
2. Transfections were carried out in 100-µl tip-electrodes of the Neon transfection system with one 1410-V, 30-ms pulse.
3. PBMCs were resuspended in aliquots of 3×10^6 cells in 10 µl of T buffer (Neon, Life Technologies/ThermoFisherScientific) for each electroporation, and transfections were carried out in 10 µl tip-electrodes of the Neon transfection system with one 1910-V, 30-ms pulse. A total of 4 µg of in vitro-transcribed RNA for Jurkat cells and 3 µg for PBMCs were transfected.

Alternatively 5 μg of DNA plasmid for Jurkat cells and 4 μg for PBMCs were transfected to compare transfection efficiency.

4. After transfection, cells were cultured in RPMI 1640 supplemented with 10% FCS and 2 mM L-glutamine without antibiotics, to a final density of 1.25×10^6 cells/ml for Jurkat cells and 1×10^6 cells/ml for PBMCs and harvested after 24 h. It is also possible to transfect Jurkat cells and PBMCs with in vitro-transcribed RNA using a transfection system from BioRad (data not shown; *see* **Note 19**), which gave comparable results.

In our experiments, pmaxGFP DNA was transfected to compare the efficiency of RNA vs. DNA transfection, in parallel in Jurkat cells and in PBMCs. The in vitro-transcribed GFP RNA and p13-GFP RNA were transfected in freshly isolated PBMCs, after optimizing the transfection efficiency and viability. At the day of the transfection, cells were counted, centrifuged, and resuspended as described above. RNA was prepared for the following transfection mixtures: (1) pST1-GFP and (2) pST1-p13-GFP (*see* **Notes 15–19**).

3.5 Analysis by Flow Cytometry

Cell viability and transfection efficiency (percentage of transfected cells among the viable fraction) were evaluated by flow cytometry, by measuring the changes in side scatter (SSC)/forward scatter (FSC) and the GFP fluorescence signal 24 h after the transfection of the pmaxGFP DNA (used as DNA control) and pST1-GFP RNA in Jurkat T-cells (Fig. 2), or pmaxGFP DNA, pST1-GFP RNA, and pST1-p13-GFP RNA in freshly isolated PBMCs (Fig. 3).

Results obtained in Jurkat cells showed that the percentage of viable cells in the RNA-transfected population was comparable to the untransfected sample (Fig. 2a, c, left). On the contrary, pmaxGFP DNA transfection dramatically reduced cell viability (Fig. 2b, left). Moreover, RNA electroporation reached a higher transfection efficiency (>90% GFP-positive cells), compared to DNA transfection (~70% GFP-positive cells) (Fig. 2c, b, right). Furthermore, RNA transfection produced a more homogeneous level of expression, with the GFP fluorescence signal spanning one log of the intensity scale (Fig. 2c, right), while the pmaxGFP DNA transfection resulted in a broad distribution of the signal that spanned more than three orders of magnitude (Fig. 2b, right). These results indicated that the RNA transfection technique combines a high transfection efficiency with low toxicity.

The RNA transfection protocol was then tested on freshly isolated PBMCs, which are refractory to standard DNA transfection techniques. In particular, electroporation of DNA often results in a high toxicity combined with a low transfection efficiency, thus, rendering subsequent analyses extremely difficult. Freshly isolated PBMCs were electroporated with pmaxGFP DNA, in vitro-transcribed GFP RNA, or in vitro-transcribed p13-GFP RNA, and viability and transfection efficiency were assessed, as described for

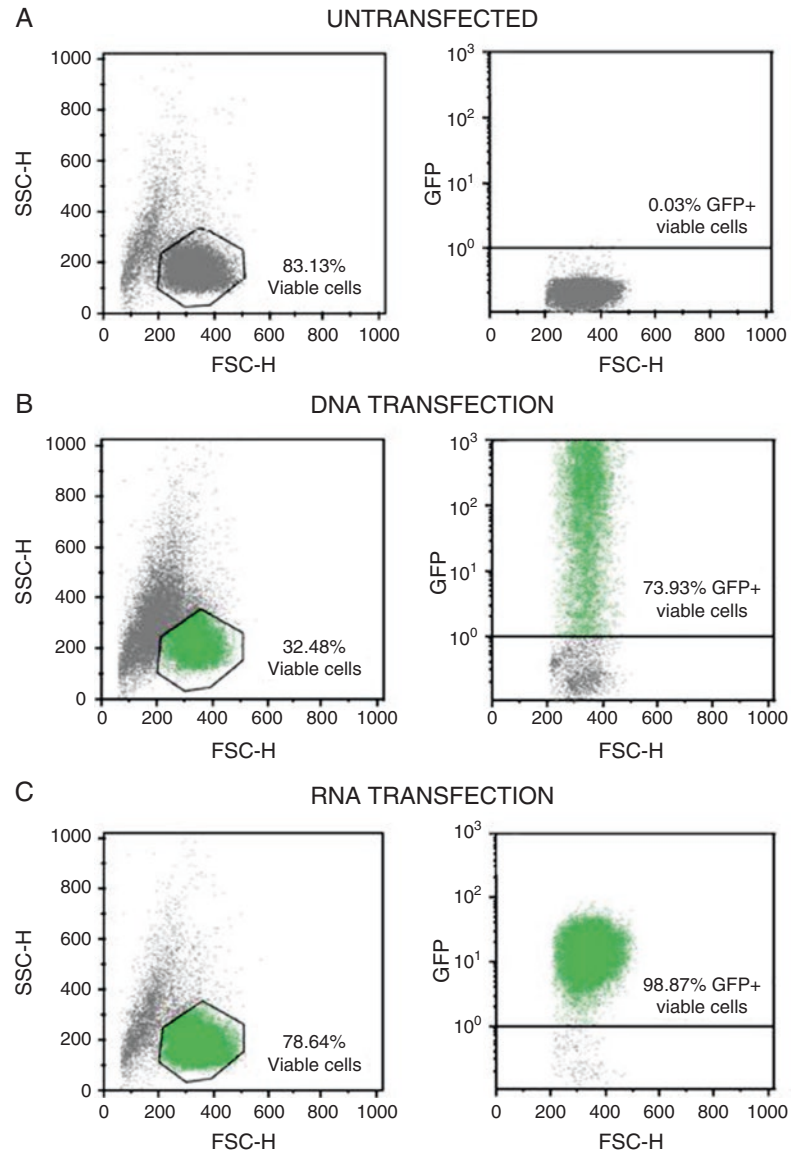

Fig. 2 pmaxGFP DNA and GFP RNA transfection in Jurkat T-cells. Dot plot of the side/forward scatter (*left*) and GFP fluorescence (*right*) of untransfected (**a**), pmaxGFP DNA- (**b**), and GFP RNA-transfected cells (**c**) 24 h after electroporation. In the side/forward scatter plots (*left*) viable cells are gated and their percentage is shown. GFP-positive viable cells are indicated as *green dots* and their percentage is shown (*right*)

Jurkat cells. Figure 3 shows the side scatter (SSC)/forward scatter (FSC) (left) and the GFP fluorescence (right) of untransfected (Fig. 3a), pmaxGFP DNA (Fig. 3b), GFP RNA (Fig. 3c), or p13-GFP RNA (Fig. 3d) in transfected PBMCs 24 h after electroporation. As previously observed for Jurkat cells, RNA transfection yielded

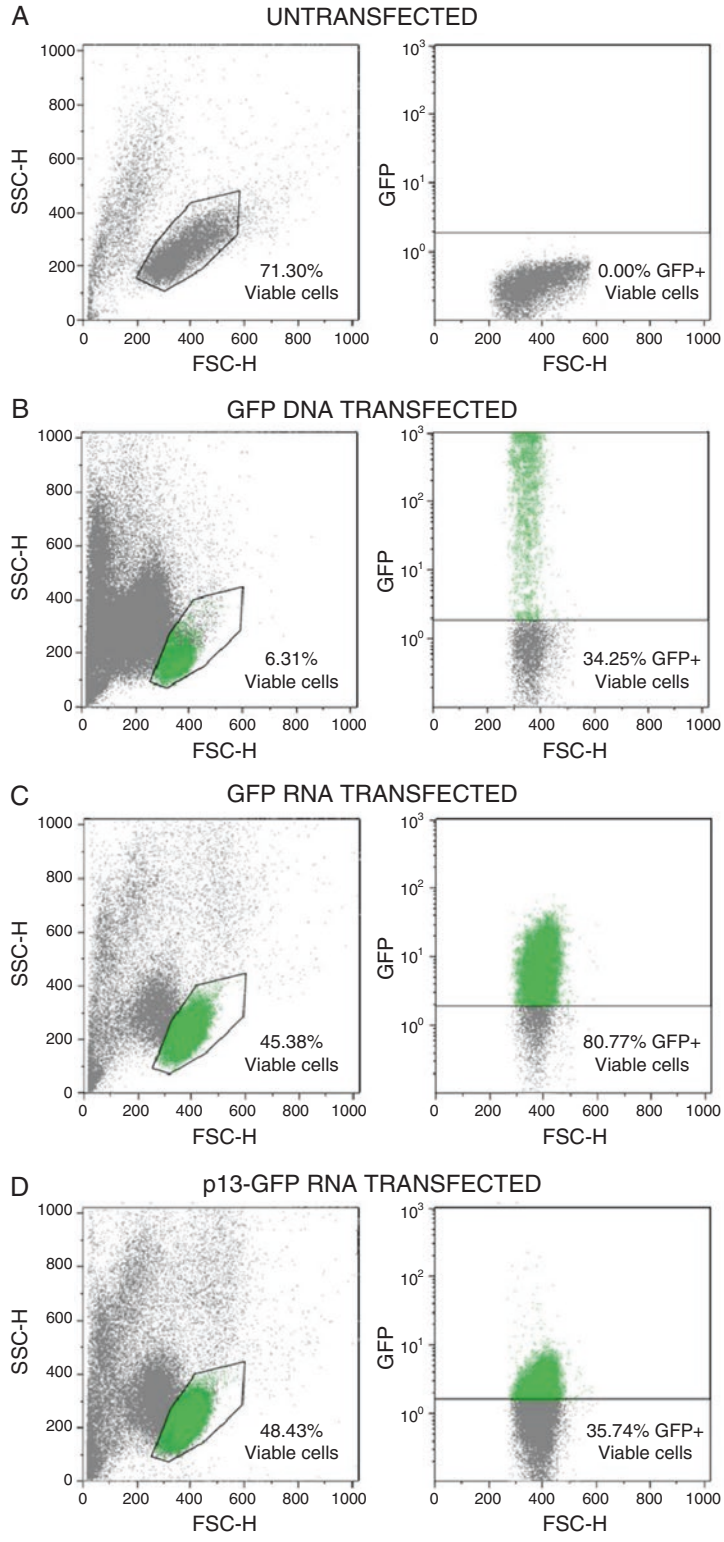

Fig. 3 pmaxGFP DNA, GFP RNA, and p13-GFP RNA transfection in PBMCs. Dot plot of the side/forward scatter (*left*) and GFP fluorescence (*right*) of untransfected (**a**), pmaxGFP (**b**), GFP RNA (**c**), and p13-GFP RNA (**d**) transfected cells 24 h after electroporation. In the side/forward scatter plots (*left*) viable cells are gated and their percentage is shown. GFP-positive viable cells are indicated as *green dots* and their percentage is shown (*right*)

superior results compared to plasmid DNA transfection, both in terms of cell viability and transfection efficiency. The viability of RNA transfected cells was 45.38% for GFP RNA (Fig. 3c, left) and 48.43% for p13-GFP RNA (Fig. 3d, left) versus 6.31% for DNA transfection (Fig. 3b, left). The transfection efficiency was 80.77% for GFP RNA (Fig. 3c, right) and 35.74% for p13-GFP RNA (Fig. 3d, right) versus 34.25% for DNA transfection (Fig. 3b, right). The percentage of viable cells was dramatically reduced in the DNA-transfected cells compared to either GFP RNA or p13-GFP RNA. Again, RNA transfection led to a more homogeneous level of expression, with the GFP fluorescence signal spanning one log of the intensity scale (Fig. 3c–d, right) compared to more than three logs in the DNA-transfected sample (Fig. 3b, right).

These results confirmed that RNA electroporation was preferable for experiments aimed at investigating the functional interaction in the context of primary T-cells, which represent the main target of HTLV-1 in vivo.

4 Notes

1. Plasmid DNA must be linearized with a restriction enzyme downstream of the sequence to be transcribed. It is worthwhile examining the linearized template DNA on a gel to confirm that cleavage is complete. Even a small amount of circular plasmid in a template prep will generate a large proportion of heterogeneous RNA transcripts because RNA polymerases are very processive.
2. We used ethidium bromide to visualize the linearized DNA. In our experiments, other fluorescent DNA stains impaired the efficiency of the subsequent in vitro transcription.
3. Linearized plasmid DNA, PCR products, and in general, any DNA with a RNA polymerase promoter site, that is pure enough to be easily digested with restriction enzymes can be used for in vitro transcription with the mMESSAGE mMACHINE Kit. This kit works best with templates that code for RNA transcripts in the 0.3–5 kb range. We used linearized plasmid DNA as template for the in vitro transcription reaction (*see* Subheading 3.1).
4. *Low yield*: the amount of RNA synthesized in a standard 20-μl mMESSAGE mMACHINE reaction should be 15–20 μg; however, there is a great range of variation from different templates. If the yield is low, the first step in troubleshooting the reaction is to use the pTRI-Xef control template (included in the kit) in a standard reaction: if the control reaction works, and your template generates full-length, intact RNA, but

with a low yield, it is possible that contaminants in the DNA are inhibiting the RNA polymerase. A mixing experiment can help to differentiate between problems caused by inhibitors of transcription and problems caused by the sequence of the template. You could include three reactions in the mixing experiment, using the following DNA templates:

(a) pTRI-Xef control template (1 μl).

(b) Experimental DNA template (0.5 μg plasmid or 2–6 μl PCR product).

(c) A mixture of (a) and (b).

Assess the results of the mixing experiment by running 0.5–1 μl of each transcription reaction on a denaturing gel. You can get two different results:

(a) The transcription of the control template could be inhibited by the template itself if inhibitors are present in the experimental reaction. Typical inhibitors include residual SDS, salts, EDTA, and RNases. Treatment with Proteinase K (100–200 μg/ml) and 0.5% SDS for 30 min at 50 °C, followed by phenol/chloroform extraction (using an equal volume) and ethanol precipitation, frequently improves template quality. Carry-over of SDS can be minimized by diluting the DNA several fold before ethanol precipitation, and excess salts and EDTA can be removed by vigorously rinsing DNA pellets with cold 70% ethanol before resuspension. Alternatively, drop dialysis could be performed to remove SDS or excess salts.

(b) If addition of the experimental template does not inhibit synthesis of the control RNA, the problem may be inherent to your template. In this case:

- Use a different RNA polymerase for transcription; templates differ in transcription efficiency depending on the initiation efficiency of their promoter, the presence of internal termination signals, and their length.
- Check the amount and quality of the template on an agarose gel to make sure it is intact and that it is the expected size. If quantitation was based on UV absorbance and the DNA prep had substantial amounts of RNA or chromosomal DNA, the amount of template DNA may be substantially less than the calculated value.
- Extend the reaction time; extending the standard 2 h incubation to 4–6 h or even overnight may improve yield.

5. *Multiple reaction products, transcripts of the wrong size*:

(a) Reaction products produce a smear when run on a denaturing gel: if the RNA appears degraded, remove residual

RNase from the DNA template preparation before in vitro transcription with Proteinase K. The RNase inhibitor that is present in the transcription reaction can only inactivate trace RNase contamination.

(b) Reaction products run as more than one band, or as a single band that is smaller than expected:

- Sample is not adequately denatured in the gel: if the amount of RNA produced is acceptable, but the size of the product is different than expected, the RNA may be running aberrantly due to secondary structure. Sometimes, the RNA will run as two distinct bands on a native agarose gel, but when the same RNA is run on a denaturing gel, it will migrate as a single band of the expected size.
- Premature termination of transcription: if denaturing gel analysis shows the presence of multiple bands or of a single band smaller than the expected size, there may be problems with premature termination by the polymerase. Possible causes of this are: (1) sequences that resemble the phage polymerase termination signals: as different phage polymerases recognize different termination signals, using a different polymerase, and promoter may help; (2) stretches of single nucleotides: termination at single polynucleotide stretches can sometimes be minimized by decreasing the reaction temperature [12]. We suggest testing 30, 20, and 10 °C. However, decreasing the reaction temperature will also significantly decrease the yield of the reaction; (3) GC-rich templates: the transcription efficiency of a GC-rich template could be improved by adding single-stranded binding (SSB) protein to the reaction [13].

(c) Reaction products are larger than expected:

- Persistent secondary structure: in vitro transcribed RNA occasionally run as two bands, one larger than the expected size, and one of the expected size, because of persistent secondary structure. To verify this, the band that migrates at the expected size can be excised from the gel and run in a second denaturing gel. If the RNA runs as a doublet in the second gel also, it is a good indication that the larger band is simply an artifact of electrophoresis.
- Circular templates: longer-than-expected transcription products will be seen if any of the template molecules are circular. This is typically caused by incomplete digestion of a plasmid template.

6. *Optimizing yield of long transcripts*: when synthesizing transcripts that are larger than 5 or 6 kb, GTP will become rate limiting and may result in low yield, premature termination of transcription, or both. To circumvent this, we suggest supplementing the reaction with extra GTP. For templates in the 5–8 kb range we suggest initially testing the addition of 1 μl of GTP. For larger templates you should add more GTP to determine the minimum amount needed. However, remember that the fraction of capped transcripts is proportional to the ratio of Cap Analog to GTP in the reaction, therefore, adding GTP will decrease the fraction of capped transcripts, but it will increase the yields of full-length products.
7. *Optimizing yield of short transcripts*:
   (a) Reaction time is the first variable to change: increasing the incubation time to 4–6 h allows each RNA polymerase molecule to engage in more initiation events.
   (b) Increasing the template concentration is the next variable that should be tested: as with short templates, the initiation step of the transcription reaction is rate-limiting. In general, for optimum yield of short transcripts, use about 0.5–2 pmol of template. For very short templates (i.e., ~20–30 nt), use the upper end of this range.
   (c) Increasing the RNA polymerase concentration should be the last variable tested: adding additional RNA polymerase allows more initiation events to occur in a given amount of time. We suggest adding a separate high concentration polymerase rather than increasing the concentration of the 10× Enzyme Mix from the mMESSAGE mMACHINE Kit.
8. *Low or no recovery of RNA*:
   (a) RNase-free water incorrectly dispensed: pipet RNase-free water to the center of the RNeasy MinElute spin column membrane to completely cover it.
   (b) Ethanol carryover: be sure to centrifuge at full speed for 5 min to dry the RNeasy MinElute spin column membrane after washing with 80% ethanol, and, after centrifugation, carefully remove the RNeasy MinElute spin column from the collection tube so that the column does not contact the flow-through.
9. *Clogged RNeasy MinElute spin column*:
   (a) Too much starting RNA: reduce the amount of starting RNA; a maximum of 45 μg RNA (including any carrier RNA), corresponding to the binding capacity of an RNeasy MinElute spin column, can be used.
   (b) Centrifugation temperature too low: the centrifugation temperature should be 20–25 °C; temperatures below

20 °C can cause formation of precipitates that may result in clogging the spin column.

10. *Low A_{260}/A_{280} value*: water used to dilute RNA for A_{260}/A_{280} measurement: try to use 10 mM Tris–Cl, pH 7.5 instead of RNase-free water to dilute the sample before measuring purity.
11. *RNA degraded*: although all RNeasy buffers are guaranteed to be RNase-free, RNases can be introduced during use; for example do not place RNA samples into a centrifuge that has been used in DNA preparations where RNases may have been used. Adding β-mercaptoethanol to Buffer RLT may be helpful.
12. *DNA contamination in downstream experiments*: if DNA contamination is detected in downstream experiments, digest the RNA sample with DNase before RNA cleanup.
13. With the Neon transfection system, a Neon Pipette with a Neon Tip is inserted into the Neon Tube equipped with an electrode that transfers the electric field inside the Neon Tip. The Neon Tube holds the Electrolytic Buffer during electroporation and is inserted into the Neon Pipette Station; compared to standard cuvette-based electroporation, the Neon transfection system generates a more uniform electric field [14].
14. To avoid contamination, the Neon Tubes should be used for a maximum of ten times. We recommend changing the tube and buffer when switching to a different DNA/RNA or cell type.
15. To ensure-reproducibility and eliminate intra/inter-variation of the transfection conditions, the Neon Tip must be used more than three times. Oxide formation at the piston surface area can be generated if the tips are used repeatedly, which decreases its function as an electrode.
16. Fill the Neon Tube with 4 ml of Electrolytic Buffer, and use Buffer E for the 10 µl Neon Tip and Buffer E2 for the 100 µl Neon Tip, making sure that the electrode on the side of the tube is completely covered by the buffer.
17. After resuspension of cells in R or T buffer, avoid storing the cell suspension for more than 15–30 min at room temperature, as this reduces cell viability and transfection efficiency; also avoid air bubbles during pipetting, as air bubbles cause arcing during electroporation. If you notice air bubbles in the tip, eject the sample and carefully aspirate it into the tip again without any air bubbles.
18. Electroporated cells should be cultivated without antibiotics as these greatly reduce cell viability.
19. It is also possible to use other transfection systems. We tested the Gene Pulser Xcell from BioRad (500 V, 5-ms square-wave pulse, 4 mm cuvette), which gave comparable results. We used

cell culture medium without phenol red (e.g., GIBCO Optimem I Reduced Serum medium) in this case.

Acknowledgment

The authors are grateful to Prof. Ugur Sahin (Research Center for Immunotherapy (FZI), Mainz, Germany; TRON—Translational Oncology at the University Medical Center of Johannes Gutenberg University, Mainz, Germany; Biopharmaceutical New Technologies (BioNTech) Corporation, Mainz, Germany) for providing the plasmid pST1-eGFPmut-2hBgUTR-A120. We are grateful to Armin Ensser and Benjamin Vogel (Institute of Clinical and Molecular Virology, Erlangen, Germany) for helpful discussions.

References

1. Lairmore M, Franchini G (2007) Human T-cell leukemia virus types 1 and 2. In: Knipe DM, Howley PM (eds) Fields virology, 5th edn. Williams and Wilkins, Lippincott, Philadelphia, PA, pp 2071–2106
2. Ciminale V et al (1992) Complex splicing in the human T-cell leukemia virus (HTLV) family of retroviruses: novel mRNAs and proteins produced by HTLV type I. J Virol 66(3):1737–1745
3. Koralnik IJ et al (1992) Protein isoforms encoded by the pX region of human T-cell leukemia/lymphotropic virus type I. Proc Natl Acad Sci U S A 89(18):8813–8817
4. Larocca D et al (1989) Human T-cell leukemia virus minus strand transcription in infected T-cells. Biochem Biophys Res Commun 163(2):1006–1013
5. Murata K et al (2006) A novel alternative splicing isoform of human T-cell leukemia virus type 1 bZIP factor (HBZ-SI) targets distinct subnuclear localization. J Virol 80(5): 2495–2505
6. Cavanagh MH et al (2006) HTLV-I antisense transcripts initiating in the 3'LTR are alternatively spliced and polyadenylated. Retrovirology 3:15
7. Holtkamp S et al (2006) Modification of antigen-encoding RNA increases stability, translational efficacy, and T-cell stimulatory capacity of dendritic cells. Blood 108(13): 4009–4017
8. Van Tendeloo VF et al (2001) Highly efficient gene delivery by mRNA electroporation in human hematopoietic cells: superiority to lipofection and passive pulsing of mRNA and to electroporation of plasmid cDNA for tumor antigen loading of dendritic cells. Blood 98(1):49–56
9. Zhao Y et al (2006) High-efficiency transfection of primary human and mouse T lymphocytes using RNA electroporation. Mol Ther 13(1): 151–159
10. Rowley J et al (2009) Expression of IL-15RA or an IL-15/IL-15RA fusion on CD8+ T cells modifies adoptively transferred T-cell function in cis. Eur J Immunol 39(2):491–506
11. Silic-Benussi M et al (2010) Redox regulation of T-cell turnover by the p13 protein of human T-cell leukemia virus type 1: distinct effects in primary versus transformed cells. Blood 116(1):54–62
12. Krieg PA (1990) Improved synthesis of full-length RNA probe at reduced incubation temperatures. Nucleic Acids Res 18(21):6463
13. Ben Aziz R, Soreq H Improving poor *in vitro* transcription from G,C-rich genes. Nucleic Acids Res 18(11):3418
14. Kim JA et al (2008) A novel electroporation method using a capillary and wire-type electrode. Biosens Bioelectron 23(9):1353–1360

Part IV

Cellular Dynamics

Chapter 13

Quantification of Cell Turnover in the Bovine Leukemia Virus Model

Alix de Brogniez, Pierre-Yves Barez, Alexandre Carpentier, Geronimo Gutierrez, Michal Reichert, Karina Trono, and Luc Willems

Abstract

In a perspective of a comparative virology approach, characterization of the bovine leukemia virus (BLV) model may be helpful to better understand infection by the related human T-lymphotropic virus type 1 (HTLV-1). In this paper, we first provide detailed protocols to inoculate cloned BLV proviruses into sheep or cattle. We also describe methods to quantify apoptosis ex vivo and cell turnover in vivo.

Key words Deltaretrovirus, Bovine leukemia virus, HTLV-1, Apoptosis, Proliferation, CFDA-SE

1 Introduction

Bovine leukemia virus (BLV) and human T-lymphotropic virus type 1 (HTLV-1) are two evolutionary-related deltaretroviruses that induce hematological diseases in ruminants and human, respectively [1–3]. In particular, BLV naturally infects cattle and induces major economical losses worldwide due to custom restrictions, decrease in production, and direct death. BLV induces a chronic lymphoproliferative disease (persistent lymphocytosis) and a leukemia/lymphoma (enzootic bovine leukemia). Experimental transmission of BLV to sheep induces a more acute leukemia characterized by shorter latency periods. Unraveling the mechanisms of persistence, replication and pathogenesis in the BLV model may therefore also be informative to better understand HTLV-1 physiopathology.

In this chapter, we describe the techniques of BLV inoculation and methods to quantify cell turnover in vivo.

Claudio Casoli (ed.), *Human T-Lymphotropic Viruses: Methods and Protocols*, Methods in Molecular Biology, vol. 1582, DOI 10.1007/978-1-4939-6872-5_13,

2 Materials

2.1 Virus Inoculation

1. *Preparation of polyethylenimine (PEI) stock solution*: dissolve the PEI powder in water preheated to 60 °C. Mix thoroughly. Adjust pH to 7.0 with HCl. Mix thoroughly. Adjust the volume with water to the final concentration (1 mg/mL) and incubate overnight in a water bath at 56 °C. Mix thoroughly. Filter through 0.22 μm filter (*see* **Note 1**). Make 0.1–1 mL aliquots and store at −80 °C for long-term preservation (*see* **Note 2**).
2. *Transfection and inoculation*:
   - 25 cm^2 cell culture flask (T25).
   - 1.5 mL microfuge tubes.
   - Dubelcco modified eagle medium (DMEM).
   - DMEM supplemented with 10% (v/v) Fetal bovine serum (FBS) and 1% (v/v) Penicillin/Streptomycin 10,000 U/mL.
   - Incubator at 37 °C, 5% CO_2, and 100% humidity.
   - PEI.
   - Phosphate Buffer Saline (PBS).
   - Trehalose.
   - Needles 18 G × 1″ for cow and 25 G × 5/8″ for sheep.

2.2 Isolation of Peripheral Blood Mononuclear Cells (PBMCs)

1. PBS.
2. Percoll solution: 54 mL Percoll (GE Healthcare, Cleveland, USA), 6 mL NaCl 9%, 40 mL PBS per 100 mL.
3. Ethylenediaminetetraacetic acid (EDTA).
4. FBS.
5. Cryovials.
6. 50 mL centrifuge tubes.
7. Dimethylsulfoxyde (DMSO).
8. Needles, 18 G × 1 ½″ for sheep or cows and 21 G × 1 ½″ for calves.

2.3 Quantification of B Cell Apoptosis Ex Vivo

1. RPMI 1640 medium supplemented with 10% (v/v) FBS and 1% (v/v) Penicillin/Streptomycin 10,000 U/mL.
2. FBS.
3. PBS.
4. 96-well conical bottom (V) plates.
5. Centrifuge.
6. Primary monoclonal antibody: 1H4 (IgG_1) directed against the IgMs of ovine and bovine B lymphocytes. This antibody is

expressed in the culture supernatant of 1H4 hybridoma cells. The working solution is a 100-fold dilution of this supernatant in PBS-FBS 10% (v/v) solution. The commercially available antibody (PIG45A, IgG_{2b}) directed against the anti-porcine IgMs can also be used.

7. Secondary antibody: Alexa Fluor 488 conjugated goat anti-mouse IgG. The working solution is a 1000-fold dilution of the secondary antibody in PBS-FBS 10% (v/v).
8. 15 mL centrifuge tubes.
9. Ethanol.
10. Tween 20.
11. 10 mg/mL RNase A.
12. Propidium iodide (PI).
13. FACS tubes.
14. Flow cytometer.

2.4 Quantification of B Cell Kinetics in Vivo

1. Carboxyfluorescein diacetate succinimidyl ester (CFDA-SE).
2. DMSO.
3. Heparin (1000 U/mL).
4. Needles 18 G × 1 ½" for sheep or cows and 21 G × 1 ½" for calves.
5. 96-well conical bottom (V) plates.
6. Primary monoclonal antibody: The working solution used for the experiment consists of a 100-fold dilution of the 1H4 or PIG45A anti-IgM antibodies in PBS-FBS 10% (v/v) solution.
7. Secondary antibody: Alexa Fluor 647 conjugated goat anti-mouse IgG. The working solution is a 1000-fold dilution of the secondary antibody in PBS-FBS 10% (v/v).
8. Flow cytometer.

3 Methods

3.1 Virus Inoculation

All these steps must be performed under sterile conditions.

3.1.1 Transfection and Inoculation

1. Twenty four hours before transfection, seed cells in T25 tissue culture flasks to obtain 80% confluency the next day.
2. Prepare a transfection mix in a microfuge tube. Per sample, add 5.2 µL of PEI (1 mg/mL) to 260 µL of DMEM medium without FBS or antibiotics (*see* **Note 3**).
3. Add the transfection mix onto 2.6 µg of proviral DNA (*see* **Note 4**), mix and incubate for 10 min.
4. Prepare the cells during this incubation time.

5. For each T25 cell culture flask, wash the cells with PBS.
6. Add 3 mL of DMEM medium without FBS and antibiotics.
7. Add the transfection mix dropwise onto the cell monolayer.
8. Cultivate cells in an incubator at 37 °C for at least 4 h.
9. Add 3 mL of DMEM medium containing 10% FBS (v/v) and 3% trehalose (m/v).
10. Three days post transfection, add trehalose to a final concentration of 15% (*m/v*) and freeze the flask to lyse the cells at −80 °C.
11. Thaw lysate and inject small volumes (≈100 μL) subcutaneously in the back of the calves (*see* **Note 5**) (Fig. 1a).

3.2 Isolation of Peripheral Blood Mononuclear Cells (PBMCs)

All these steps must be performed under sterile conditions.

1. Collect venous blood by jugular venipuncture in a tube containing 0.3% (m/v) EDTA used as anticoagulant. Blood flow is restricted with a rope surrounding the neck. Using a sterile needle, blood is collected from the jugular vein (Fig. 1b–d).
2. Transfer blood into a new tube and adjust volume to 50 mL.
3. Centrifuge during 25 min at 1880 × *g* at room temperature. After this step, three phases are obtained: the red blood cells in the bottom of the tube, the plasma in the upper part, and a ring of white blood cells at the interface between the red blood cells and the plasma, called buffy coat (*see* **Note 6**) (Fig. 1e).
4. Carefully recover about 2–3 mL of buffy coat (*see* **Note 7**).
5. Add PBS containing 0.075% (m/v) EDTA up to a final volume of 35 mL.
6. Carefully add, without mixing, the 35 mL of cell suspension on top of 15 mL of Percoll (*see* **Notes 7** and **8**) (Fig. 1f, g).
7. Centrifuge 25 min at 1880 × *g* at room temperature. Red blood cells and granulocytes sediment in the bottom of the tube and a ring of white blood cells equilibrate at the PBS-Percoll interface (*see* **Note 6**) (Fig. 1h).
8. Carefully recover this buffy coat, add 50 mL PBS containing 0.075% (m/v) EDTA and centrifuge at 260 × *g* during 10 min to remove platelets. Discard supernatant and repeat the wash with 50 mL PBS containing 0.075% (m/v) EDTA.
9. Wash the cells at least twice with 50 mL PBS 1× (*see* **Note 9**).
10. Enumerate viable cells (as identified by trypan blue exclusion) under a microscope using a cell counter.
11. Resuspend cell pellet in a cold (i.e., 4 °C) freezing solution of FBS containing 10% DMSO (v/v) at a concentration of maximum ten million cells per mL per cryovial (*see* **Note 10**).
12. Transfer cryovials to a polystyrene box into a −80 °C freezer (*see* **Note 11**).

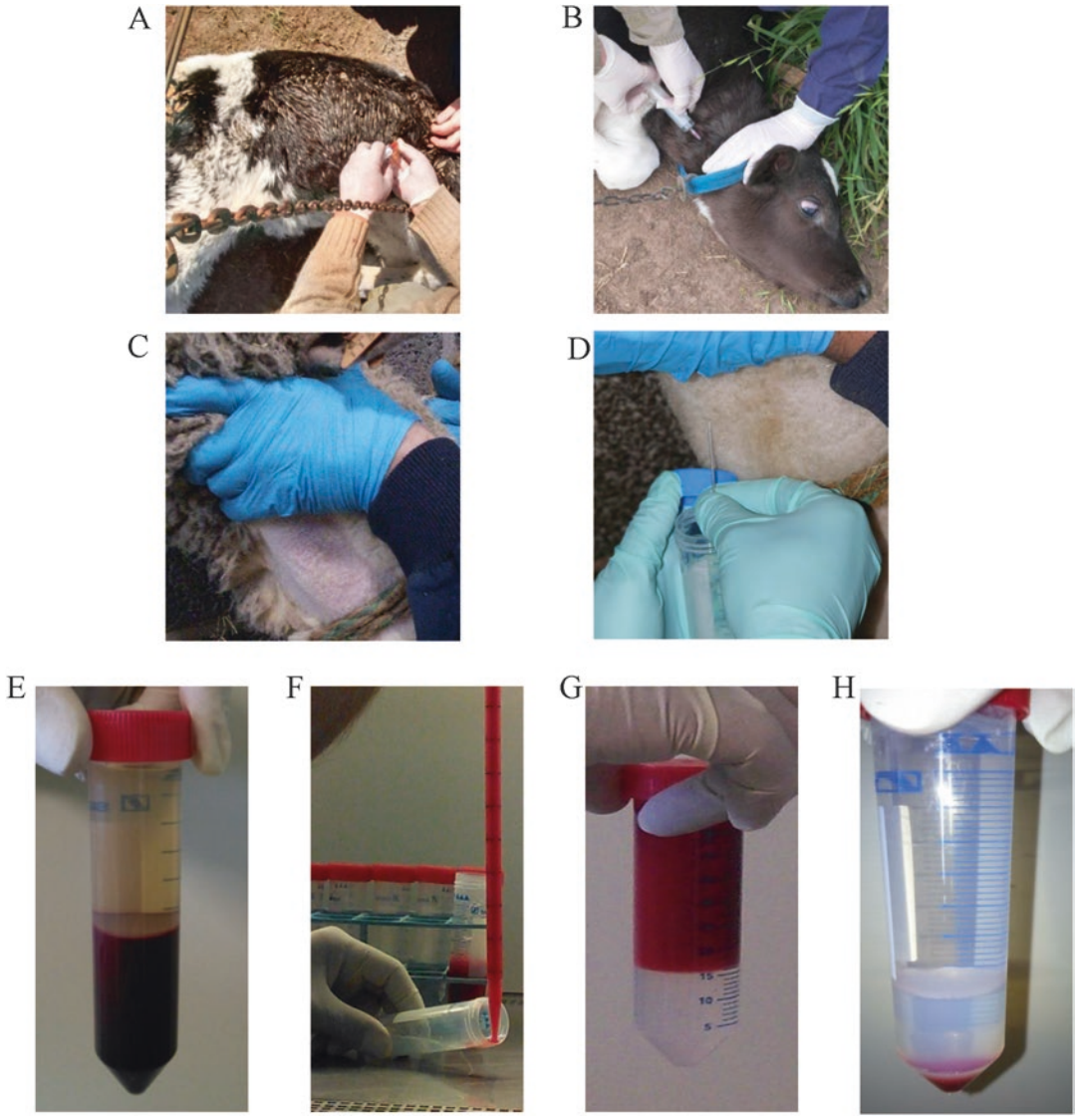

Fig. 1 (**a**) Viral inoculation by subcutaneous injection. (**b**) Jugular venipuncture of a calf. (**c**) Jugular vein of a sheep. (**d**) Jugular venipuncture of a sheep. (**e**) Isolation of peripheral blood mononuclear cells by Percoll gradient centrifugation. The picture shows the three phases obtained after the first centrifugation step. The red blood cells in the bottom of the tube, the plasma in the upper part, and a ring of white blood cells (buffy coat) at the interface between the red blood cells and the plasma. (**f**) and (**g**) Overlay of the buffy coat on the Percoll solution. (**h**) Phases obtained after the second centrifugation step with the ring of white blood cells at the interface between the Percoll solution and the PBS

3.3 Quantification of B Cell Apoptosis Ex Vivo

1. Thaw PBMCs by incubating the vials a few seconds in a water bath at 37 °C and gently resuspend the cells in 10 mL of PBS.
2. Centrifuge cells at room temperature during 5 min at 485 × *g* and resuspend the pellet in RPMI medium supplemented with 10% (v/v) FBS, 1% (v/v) penicillin/streptomycin at two million cells per mL.

3. Transfer maximum 3 mL of cell suspension into a sterile 15 mL centrifuge tube.
4. Cultivate cells in an incubator (5% CO_2 and 100% relative humidity) at 37 °C during 16 h (*see* **Note 12**).
5. Centrifuge PBMCs for 5 min at 485 × *g* and add 10 mL of PBS-FBS 10% (v/v).
6. Centrifuge for 5 min at 485 × *g* and resuspend the cell pellet in 200 µL of PBS-FBS 10% (v/v).
7. Transfer cell suspension into a well of a 96-well V bottom plate.
8. Centrifuge 96-well plate for 5 min at 450 × *g* and resuspend the pellet in 100 µL of primary antibody.
9. Incubate 30 min at 4 °C.
10. Add 100 µL of PBS-FBS 10% (v/v).
11. Centrifuge for 5 min at 450 × *g* and resuspend the pellet in 100 µL of secondary antibody.
12. Incubate during 30 min at 4 °C.
13. Wash with 200 µL of PBS-FBS 10% (v/v), centrifuge for 5 min at 450 × *g*, and resuspend the pellet in 300 µL of PBS-FBS 10% (v/v), then transfer the cells to a 15 mL centrifuge tube (*see* **Note 13**).
14. Add dropwise 700 µL of ethanol chilled at −20 °C under vigorous vortexing.
15. Store the samples at −20 °C for at least 1 h.
16. Centrifuge tubes at 4 °C for 10 min at 485 × *g* (*see* **Note 14**).
17. Wash with PBS-FBS 10% (v/v).
18. Centrifuge 5 min at 485 × *g* and resuspend the pellet in 100 µL of PBS containing RNase A (50 µg/mL) and Tween 0.1% (v/v).
19. Incubate samples for 30 min at 37 °C (*see* **Note 15**).
20. Transfer cells into a FACS tube containing 400 µL of propidium iodide (20 µg/mL diluted in PBS).
21. Analyze the cells by flow cytometry.

The principle of the assay is based on quantification of DNA fragmentation in apoptotic cells. The DNA content can be quantified by flow cytometry upon labeling with a DNA intercalating dye such as propidium iodide. Cells in G_0/G_1 and G_2/M contain 2N and 4N chromosomes, respectively (Fig. 2). Cells in S have an intermediate DNA content. Small DNA fragments generated during apoptosis will exit cells upon ethanol fixation. Cells undergoing apoptosis will thus fluoresce with a sub-G1 intensity. This particularly inexpensive technique that quantifies a major hallmark of

apoptosis has two limitations. First, inadequate fixation (e.g., using ethanol at room temperature) or excessive DNA fragmentation (e.g., due to prolonged cell culture) will generate cell debris lacking significant fluorescence. Secondly, aggregates of apoptotic cells will potentially stain in G_0/G_1 or in S. It is therefore required to limit aggregates during fixation by adequate vortexing and to remove cell doublets from the flow cytometry analysis.

The principle of doublet exclusion is the following. When a cell crosses the laser beam, it creates a pulse of photon emission overtime characterized by its area (*A*), height (*H*), and width (*W*) (Fig. 2a). Width (*W*) is the time taken by a cell to pass through the laser beam and is thus proportional to the cell size. Height (*H*) is the intensity of the signal that depends on the amount of fluorescence. Disproportions between *W*, *H* and the area ($A = H \times W$)

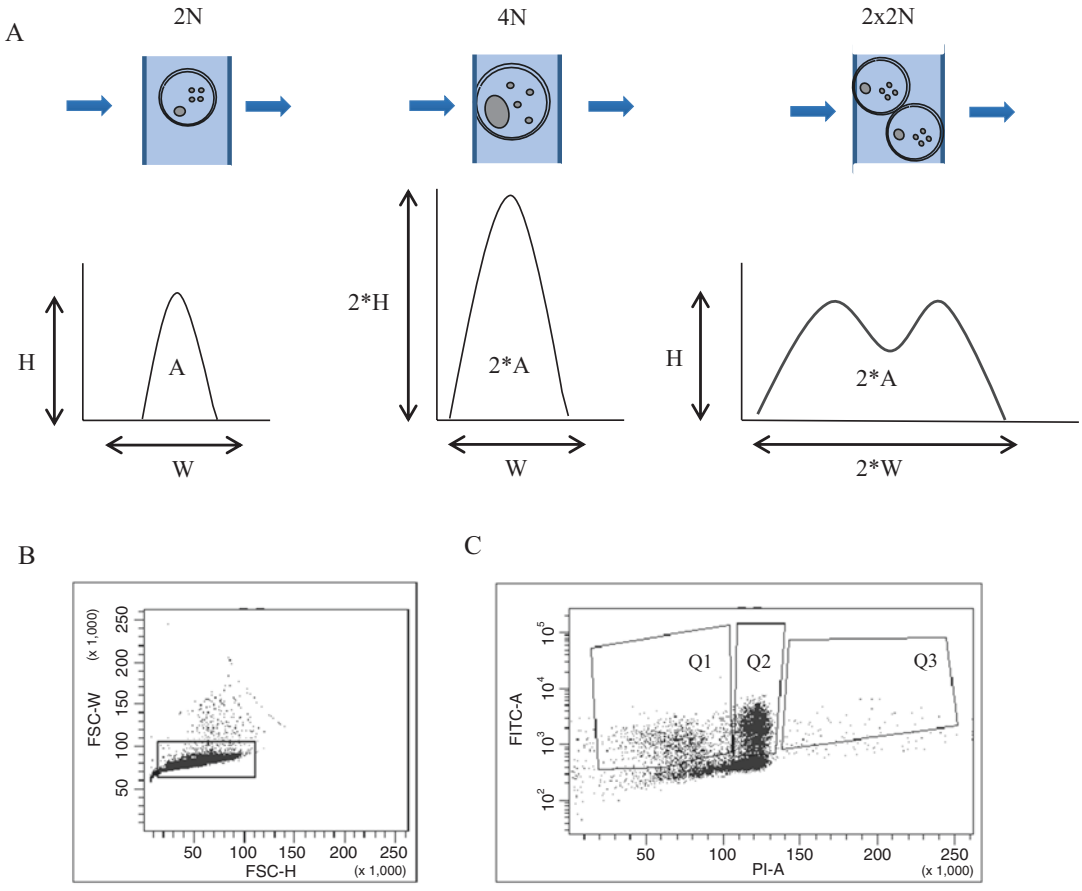

Fig. 2 (**a**) Principle of doublet exclusion based on the identification of disproportion between the fluorescence intensity (**h**), the flight time (*W*), and the Area (*A*). (**b**) Biparametric diagram allowing cell doublet discrimination based on the width (FSC-W) and the height (FSC-H). (**b**) and (**c**) Example of scattergram obtained by flow cytometry after labeling with propidium iodide (PI, *X* axis) and anti-IgM antibodies (1H4) coupled with an Alexa 488 conjugate (*Y* axis). B lymphocytes in Q1, Q2, and Q3 are apoptotic, in G0/G1 and in S+G2/M, respectively

allow doublet discrimination. Compared to single cells, doublets have a longer flight time (two peaks) but a similar intensity (*H*) (Fig. 2a). In contrast, cells in G2/M have a twofold increase in H but a similar W. Although different options are possible to exclude doublets the most straightforward strategy is based on the selection of cells based on the *W* and *H* parameters. Doublets appearing with a higher width on the scattergram are excluded from the analysis as depicted in Fig. 2b. This strategy is the most accurate since it is based on cell dimension only.

After doublet exclusion, an example of propidium iodide (*X* axis) versus IgM (*Y* axis) scattergrams is shown in Fig. 2c. Cells in areas Q2 and Q3 are in phases G0/G1 and S+G2/M, respectively. The cells in Q1 (sub-G1) are apoptotic B lymphocytes.

3.4 Quantification of B Cell Kinetics in Vivo

Cell turnover can be quantified by intravenous injection of CFDA-SE (commonly but inappropriately called CFSE), a cell permeant fluorochrome coupled by esters bonds to a succinimidyl group and two acetates. Cleavage of acetate groups by intracellular esterases converts the molecule in a fluorescent dye [4]. The succinimidyl group reacts covalently with aminoterminal ends of cellular proteins. Upon mitosis, half of the fluorescence is transmitted to the daughter cells.

3.4.1 CFDA-SE Preparation and Injection

1. CFDA-SE (25 mg) is dissolved at room temperature in 4 mL of DMSO containing 40 µL of heparin (1000 U/mL) [5].
2. Immediately, inject the CFDA-SE solution into the jugular vein (*see* **Note 16**).

3.4.2 B Cell Labeling and Flow Cytometry Analysis

1. Collect blood by jugular venipuncture at regular intervals of time (up to several weeks).
2. Isolate the PBMCs by Percoll gradient centrifugation as described in Subheading 3.2.
3. Add 2–4 million PBMCs resuspended in PBS-FBS 10% (v/v) to a well of a 96-well V bottom plate.
4. Centrifuge for 5 min at 450 × *g*.
5. Add 100 µL of primary antibody.
6. Incubate during 30 min at 4 °C.
7. Add 100 µL of PBS-FBS 10% (v/v) and centrifuge for 5 min at 450 × *g*.
8. Discard supernatant and add 200 µL of PBS-FBS 10% (v/v) and centrifuge for 5 min at 450 × *g*.
9. Resuspend the pellet in 100 µL of secondary antibody and incubate during 30 min at 4 °C.
10. Add 100 µL of PBS-FBS 10% (v/v) and centrifuge for 5 min at 450 × *g*.

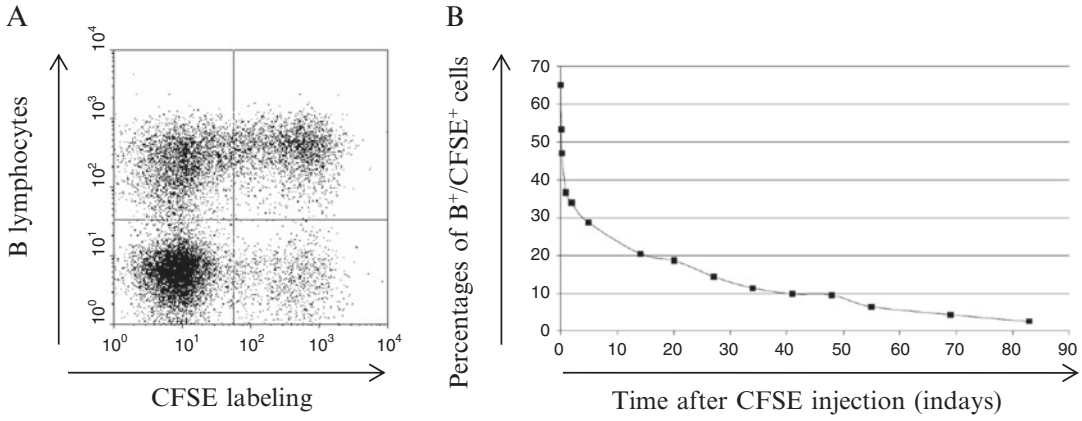

Fig. 3 (**a**) Flow cytometry scattergram of peripheral blood mononuclear cells labeled with CFDA-SE (*X* axis) and anti-IgM antibodies (1H4) coupled with an Alexa 488 conjugate (*Y* axis). (**b**) Percentages of $B^+/CFDA\text{-}SE^+$ lymphocytes in the peripheral blood over time

11. Discard supernatant, wash the pellet again with 200 µL of PBS-FBS 10% and centrifuge for 5 min at 450 × *g*.
12. Resuspend the pellet in 200 µL of PBS, transfer to a FACS tube, and analyze the cells by flow cytometry.

This protocol fluorescently labels up to 98% of lymphocytes present in the peripheral blood in a very limited period of time due to the instability of unbound CFDA-SE [5]. The percentage of CFDA-SE-labeled B cells and the mean fluorescence intensity can then be monitored over time by flow cytometry (Fig. 3). Decrease of the fluorescence parameters results from (1) cell death, (2) reduction in the labeling intensity under the detection threshold due to cell proliferation, (3) de novo production of cells by the lymphoid organs, and (4) cell recirculation from the blood to the lymphatic compartment. Cell proliferation and disappearance can be calculated using a mathematical model described by Asquith et al. [6].

4 Notes

1. Filtration ensures sterility and eliminates undissolved PEI that inhibits transfection.
2. PEI can be stored at 4 °C up to 1 month.
3. Although less efficient, it is possible to directly inject the proviral DNA complexed with PEI in 1 mL of pre-warmed PBS.
4. DNA provirus corresponds to a plasmid containing a cloned BLV provirus (pBLV344) as described by Willems et al. [7].
5. Sheep are inoculated with the cell lysate from one 150-mm diameter Petri dish.

6. During this centrifugation step, switch off the brake of the centrifuge to avoid mixing of the phases.
7. Place a 10 mL pipette perpendicularly to the ring of white blood cells.
8. For the isolation of PBMCs from human blood, a Lymphoprep™ ready-to-use solution (Stemcell Technologies) must be used instead of the Percoll solution.
9. Wash the cells at least three times with PBS until a clean supernatant is obtained.
10. Since DMSO is toxic, immediately transfer cell vials on ice and maintain freezing solution cold at all times.
11. Good cell viability is maintained for 6 months at −80 °C. For longer term storage, it is recommended to store vials in liquid nitrogen.
12. The cap of the tube should be slightly loosened to allow gas exchange.
13. FBS is essential at this stage to allow recovery of cells after ethanol fixation.
14. At this step, a particular attention will be paid to recover the cell pellet.
15. DNases should be inactivated by boiling RNase A solution for 15 min. Adjust pH 7.4 by adding 0.1 volume of 1 M Tris–HCl, pH 7.4. Aliquots are then stored at −20 °C.
16. To obtain optimal labeling, CFDA-SE should be injected less than 1 min after solubilization.

References

1. Rodríguez SM, Florins A, Gillet N, de Brogniez A, Sánchez-Alcaraz MT, Boxus M, Boulanger F, Gutiérrez G, Trono K, Alvarez I, Vagnoni L, Willems L (2011) Preventive and therapeutic strategies for bovine leukemia virus: lessons for HTLV. Viruses 3(7):1210–1248
2. Gillet N, Florins A, Boxus M, Burteau C, Nigro A, Vandermeers F, Balon H, Bouzar A-B, Defoiche J, Burny A, Reichert M, Kettmann R, Willems L (2007) Mechanisms of leukemogenesis induced by bovine leukemia virus: prospects for novel anti-retroviral therapies in human. Retrovirology 4:18
3. Gutiérrez G, Rodríguez SM, De Brogniez A, Gillet N, Golime R, Burny A, Jaworski JP, Alvarez I, Vagnoni L, Trono K, Willems L (2014) Vaccination against δ-retroviruses: the bovine leukemia virus paradigm. Viruses 6(6):2416–2427
4. Lyons AB (2000) Analysing cell division in vivo and in vitro using flow cytometric measurement of CFSE dye dilution. J Immunol Methods 243:147–154
5. Ristevski B (2003) Tracking dendritic cells: use of an in situ method to label all blood leukocytes. Int Immunol 15:159–165
6. Asquith B, Debacq C, Florins A, Gillet N, Sanchez-Alcaraz T, Mosley A, Willems L (2006) Quantifying lymphocyte kinetics in vivo using carboxyfluorescein diacetate succinimidyl ester. Proc R Soc B Biol Sci 273: 1165–1171
7. Willems L, Kettmann R, Dequiedt F, Portetelle D, Vonèche V, Cornil I, Kerkhofs P, Burny A, Mammerickx M (1993) In vivo infection of sheep by bovine leukemia virus mutants. J Virol 67:4078–4085

Chapter 14

Analysis of NK Cell Function and Receptor Expression During HTLV-1 and HTLV-2 Infection

Federica Bozzano, Francesco Marras, and Andrea De Maria

Abstract

Cytofluorimetric analysis is a typical method in immunology to evaluate phenotype and function of Natural Killer (NK) cells derived from HTLV-1/2 infected patients and healthy donors. Here, we described protocols to NK cells phenotypical and cytotoxicity assay, performed by flow cytometry on fresh and immunemagnetically or flow cytometry sorted NK cells. A new developed protocol able to evaluate IFNγ production has been included.

Key words NK, HTLV-1, HTLV-2, Inhibitory receptors, NK cell functional analysis

1 Introduction

NK cells belong to the innate arm of the immune system. They circulate in peripheral blood where they represent 5–15% of peripheral blood mononuclear cells and peripheral tissues, and may be recovered in secondary lymphoid organs and in some non-lymphoid organs (e.g., the liver) [1–3]. A vast array of molecules are expressed on NK cell surface, and in general their recognition is based on their expression on the surface of CD56 and/or CD16 with the absence of T-cell receptor complexes (CD3-CD56^{+}CD16^{+}) [4, 5]. At least three major subsets can be readily identified using these three markers, i.e., CD16$^{+/-}$CD56^{bright}, CD16^{+}CD56^{dull}, and CD16^{+}CD56^{-} NK cells. The vast majority of NK cells are resident in lymphoid organs (95%) where they express a CD56bright phenotype, while CD56dull NK cells predominate in the peripheral blood [6, 7]. Analysis of peripheral blood NK cells thus pictures only a small fraction of total NK cells, and is not representative of what is taking place in secondary lymphoid organs but rather represent a dynamic window depicting their transit toward and from peripheral tissues/organs [8]. It should be kept in mind that the historic arbitrary subdivision in three main subsets based on CD56 and CD16 represents an oversimplification. Mass flow cytometry

Claudio Casoli (ed.), *Human T-Lymphotropic Viruses: Methods and Protocols*, Methods in Molecular Biology, vol. 1582,
DOI 10.1007/978-1-4939-6872-5_14,

using additional mAbs specific for other molecules present on NK cells has recently shown that up to 30,000 different NK cell phenotypes may be present in a single individual [9, 10] and that their total number in small groups of individuals is estimated to exceed 100,000 different phenotypes [11].

For flow cytometric analysis of peripheral blood NK cells for example in patients with HTLV infection or co-infection, standard identification is performed on CD3-14-19-20- PBMC using anti-CD16 and anti CD56 mAbs. This mAb combination is suitable for the study of human samples, while for nonhuman primates different mAbs and rules apply.

A set of activating receptors preferentially, but not exclusively, expressed on NK cells may be identified using specific mAbs. Natural Cytotoxicity Receptors (NCR) NKp46 and NKp30 are expressed to variable extent on resting circulating NK cells [4, 5, 11, 12]. A third NCR, NKp44, is expressed in vitro upon activation, and may be sometimes expressed in vivo on NK cells [13]. Caution should be used since NKp44 may be expressed also by pDC and ILC in tissues [14, 15]. Other Activating receptors commonly present on flow cytometric analysis are NKG2D, DNAM, NKp80 [16]. CD16, the FcgRIII receptor, represents an activating receptor, which is responsible for NK cell antibody dependent cell cytotoxicity (ADCC) [17].

Toll-like receptors are expressed by NK cells including TLR-3, TLR-7/8, TLR-9, and TLR-2 and have activating effects alone or in combination with other activating receptors [16].

NK cells express cytokine receptors for IL-2, IL-7. IL-12, IL-15, and IL-21. Optimal triggering of NK cells may be observed with high concentrations of IL-2, or with combinations of IL-2 and IL-12 and of IL-12 and IL-15 [17].

Inhibitory receptors are represented by Killer Ig-like NK cell receptors (KIR) with long intracytoplasmatic tails specific for HLA class I molecules, NKG2A specific for HLA-E molecules and IRP-60 that recognizes non-HLA molecules. NK cells may also express KIR with short intracytoplasmatic chains and an activating activity [18, 19].

NK cells are characterized by considerable cytotoxic activity, which is due to their constitutive expression of perforin and granzyme, which may be promptly released upon cell triggering. In addition to this unique feature, which contributes to the high efficiency with which NK cells are suited to kill virally infected or tumor cells, their function also includes the production of cytokines, such as IFN-g, tumor necrosis factor (TNFa) and G-CSF, and the early release of chemokines (MIP-1a/b, RANTES). NK cell function is finely regulated by the interplay of a wide array of activating and inhibitory receptors expressed on their surface [20]. In general, signaling through inhibitory NK cell receptors that are mostly but not exclusively HLA class I specific may dampen or

override the signals transduced by the interaction of activating receptors with their ligands [16]. These characteristics can be exploited to test NK cell function in vitro. Accordingly, when studying NK cell function, receptor expression and density should be first evaluated before proceeding to NK cell function assays. In the present section, we describe standard protocol, to assess NK cell phenotype and function are described. A recently developed stimulation protocol to evaluate differential IFNg production on both CD56bright and CD56dull NK cells subsets is included [7].

2 Materials

Prepare all reagents and manipulate biological samples under Biohazard Safety Cabinet level II and diligently use Individual Protection Equipment (gloves, glasses, etc.) (*see* **Note 1**).

Follow all waste disposal country regulations when disposing waste biological biohazardous material.

2.1 Plastic Disposable

1. 50 ml conical tubes.
2. 14 ml round tubes.
3. 4.5 ml sterile round tubes.
4. Filter system.
5. Cell Counting Chamber Slides.
6. MS and/or LS Columns (Miltenyi, Bergisch Gladbach, Germany).

2.2 Reagents

1. Lympholyte Ficoll Hypaque.
2. RPMI 1640 w/o L-glutamine.
3. PBS (Phosphate Buffer Saline w/o Ca and Mg).
4. Pen-Streptomicin Mixture 5 mg/ml stock solution.
5. L-glutamine.
6. Fetal Calf Serum (FCS).
7. Trypan Blue.
8. rhIL2 (Peprotech, Rocky Hill, NJ, USA).
9. BSA (Bovine Serum Albumine).
10. Saponin.
11. Golgi Plug (BD Biosciences, San Jose, CA, USA).
12. Golgi Stop (BD Biosciences).
13. NK Isolation Kit (human; Miltenyi, Bergisch Gladbach, Germany).
14. PKH26 (Sigma Aldrich, MERCK Millipore, Billerica, MA, USA).
15. TOPRO-3 (Invitrogen/ThermoSherScientific, Waltham, MA, USA).

2.3 Monoclonal Antibodies Fluorochrome Unconjugated

1. Anti-human NKp46, IgG1, clone BAB281.
2. Anti-human NKp30, IgG1, clone 7A6.
3. Anti-human DNAM-1-1 (CD226) IgG1, clone F22.
4. Anti- human LIR-1/Cd85j IgG1, clone F278.
5. Anti-human KIRs mixture IgG1, clone 11pb6, Z27, and GL183.

2.4 Direct Monoclonal Antibodies Fluorochrome Conjugate

1. Anti-human CD3.
2. Anti-human CD14.
3. Anti-human CD19.
4. Anti-human CD56.
5. Anti-human CD16.
6. Anti-human NKp44.
7. Anti-human NKG2D.
8. Anti-human CD107a.
9. Anti-human IFNg.

2.5 Complete Medium

1. Add to RPMI 1620 w/o L-glutamine, 10% FCS, 2 mM glutamine, and 1% antibiotic mixture; Pen-Strep 5 mg/ml stock solution).
2. Filter complete medium before to use by 0.22 μm filter system.
3. Store to 4 °C.

2.6 2% BSA in PBS Solution

1. Add to 500 ml of PBS, 10 g of BSA.
2. Sterile filter.
3. Store to 4 °C.

2.7 Isolation Buffer

1. Mix 74: 6 ml PBS, 25 ml 2%BSA in PBS, and 0.4 ml EDTA pH 8.
2. Sterile Filter.
3. Store at 4 °C.

2.8 IL2 Medium

1. Complement RPMI complete medium, recombinant human (rh)IL2 (Peprotech) at 200 U/ml as final concentration.
2. Sterile filter.
3. Store to 4 °C.

2.9 10% Saponin Stock Solution

1. Heat 50 ml of PBS, in conical 50 ml tube, to 37 °C.
2. Add 5 mg of Saponin and vortex.
3. Sterile filter.
4. Store to 4 °C.

3 Methods

3.1 Peripheral Blood Mononuclear Cells Separation by Density Gradient Centrifugation [21]

1. Collect 15 ml of Peripheral blood (PB) from patients and/or healthy donors in sterile vacuum tubes in the presence of EDTA.
2. Decant collected PB in 50 ml sterile conical tubes and dilute 1:2 with RPMI 1620 w/o L-glutamine (final volume in 50 ml V bottom will be 30 ml).
3. Add 15 ml of Ficoll Hypaque Lympholyte at room temperature in a new 50 ml tube V bottom.
4. Carefully layer 15 ml of diluted PB over 15 ml Ficoll Hypaque in a 50 ml conical tube.
5. Centrifuge at 2000 rpm (931×*g* for Allegra 12R Beckman Coulter centrifuge) for 30 min at 20 °C in a swinging bucket rotor without brake.
6. Aspirate the upper ring containing peripheral blood mononuclear cells (PBMC) and transfer the mononuclear layer in 15 ml round-bottom tube.
7. Fill 15 ml containing PBMC with RPMI 1620 w/o L-glutamine and centrifuge at 1000 rpm for 7 min at 4 °C to remove platelets. Discharge the supernatant, resuspend the cell pellet, refill tubes with 10 ml of RPMI w/o L-glutamine, and centrifuge at 1500 rpm (626×*g* for Allegra 12R Beckman Coulter centrifuge) for 5 min at 4 °C.
8. Discharge the supernatant and refill tubes with 10 ml of sterile filtered complete medium containing RPMI added with 10% FCS, 2 mM glutamine and 1% antibiotic mixture (Pen-Strep 5 mg/ml stock solution).
9. Viability of cells will be evaluated with Trypan blue staining and observation at microscope. Blue cells are dead.

3.2 Immunomagnetic Isolation of Freshly Peripheral Blood-Derived NK Cell According to Protocol of NK Cell Isolation KIT, Human (Miltenyi, Bergisch Gladbach, Germany)

1. Collect 10×10^6 PBMC in 15 ml round-bottom tube.
2. Centrifuge at 1500 rpm for 5 min at 4 °C.
3. Discharge supernatant, resuspend cell pellet, and add 40 μl of Isolation Buffer and 10 μl of NK Cell Biotin-Antibody Cocktail.
4. Incubate at 4 °C for 5 min.
5. Add 30 μl of Isolation Buffer and 20 μl of NK Cell MicroBead Cocktail.
6. Incubate at 4 °C for 10 min.
7. Centrifuge at 1500 rpm for 5 min at 4 °C.
8. Discharge supernatant and resuspend cell pellet in 500 μl of Isolation Buffer.
9. Place column in magnetic field.

10. Place under the column a new 5 ml round-bottom tube labeled NK cell.
11. Prepare column by rinsing with 1 ml of Isolation Buffer.
12. Place in column 500 μl with cell suspension.
13. Wash the column three times with 500 μl of Isolation Buffer and collect NK cells that pass through the column in the 5 ml tube.
14. Fill the NK cell tube with Isolation Buffer.
15. Centrifuge; 1500 rpm at 4 °C for 5 min.
16. Discharge supernatant and add 2 ml of complete medium with (rh)IL2 200 U/ml.
17. Count cells and check viability with Trypan blue staining and microscope observation.

3.3 Flow Cytometric Isolation of NK Cells

1. Collect 10×10^6 PBMC in a 5 ml sterile round-bottom tube.
2. Centrifuge at 1500 rpm ($626 \times g$ for Allegra 12R Beckman Coulter centrifuge) for 5 min at 4 °C.
3. Discharge supernatant, resuspend cell pellet, and add 30 μl of anti-CD56, -CD16, -CD3, -CD14, CD19, monoclonal antibodies conjugated with appropriate fluorochrome based on your cytofluorimeter laser arrangement.
4. Sort NK cells in CD3negCd14negCD19negCD56pos CD16pos/neg gate into a 5 ml sterile round-bottom tube.

3.4 Activation of Freshly Sorted Purified NK Cell [22]

1. Collect freshly isolated NK cells in complete medium and rhIL2 as previously described.
2. Plate NK cells in 24-well plates at a concentration of 2×10^4 per well to 2×10^3 per well.
3. Incubate at 37 °C 5% CO_2 up to 6 days.

3.5 Indirect and Direct Immunofluorescence Analysis (Fig. 1)

1. Collect 5×10^5 PBMCs or 1×10^5 freshly isolated NK cells in a 5 ml sterile round tube.

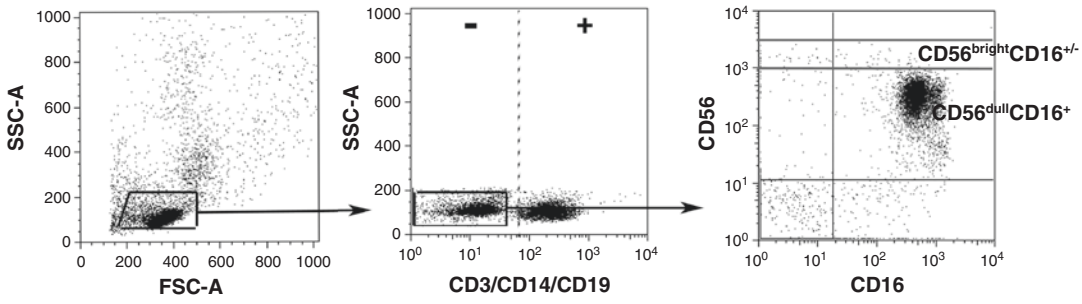

Fig. 1 Representative cytofluorometric analysis of NK cell subsets. Dot plots show CD3−CD14−CD19− gated PBMC expressing CD16 and CD56. The *dotted line* indicates the gate used to identify $CD16^{+/-}CD56^{bright}$ NK cells. 20,000 events were acquired in SSC/FCS/CD3−CD14−CD19− gate

2. Add 50 µl of primary mAbs at 0.1 µg/ml direct against activating and inhibitory NK cell receptors (e.g., NKp46, NKp30, NKp44, NKG2D, DNAM-1, KIRs, LIR-1/ILT2/CD185j).
3. Incubate at 4 °C for 20 min.
4. Wash with 2 ml of PBS and centrifuge at 1500 rpm (626×*g* for Allegra 12R Beckman Coulter centrifuge) for 5 min at 4 °C.
5. Discharge supernatant and resuspend cell pellet.
6. Add 50 µl PE- or FITC-conjugated anti-isotype-specific goat anti-mouse secondary reagents according to datasheets.
7. Incubate at 4 °C for 20 min.
8. Wash with 2 ml of PBS and centrifuge at 1500 rpm for 5 min at 4 °C.
9. Discharge supernatant and resuspend cell pellet.
10. Add fluorochrome-conjugated mAbs according to datasheets.
11. Wash with 2 ml of PBS and centrifuge at 1500 rpm for 5 min at 4 °C.
12. Discharge supernatant, resuspend cell pellet, and fix with 500 µl formaldehyde 0.7% in PBS.
13. Acquire sample on a flow cytometer (*see* **Note 2**).

3.6 NK Cell Functional Analysis: Reverse ADCC Assay with TOPRO3/PKH26 Staining [23] (Fig. 2)

1. Collect purified NK cell as effector, resuspend at 1 ×10^6 ml^{-1}.
2. Collect P815FcγR+ cells to be used as target cells at 1 ×10^6 ml^{-1}.
3. Dilute primary anti-NKp30 and -NKp46 mAbs at 0.1 µg/ml.
4. Stain P815 with PKH26.

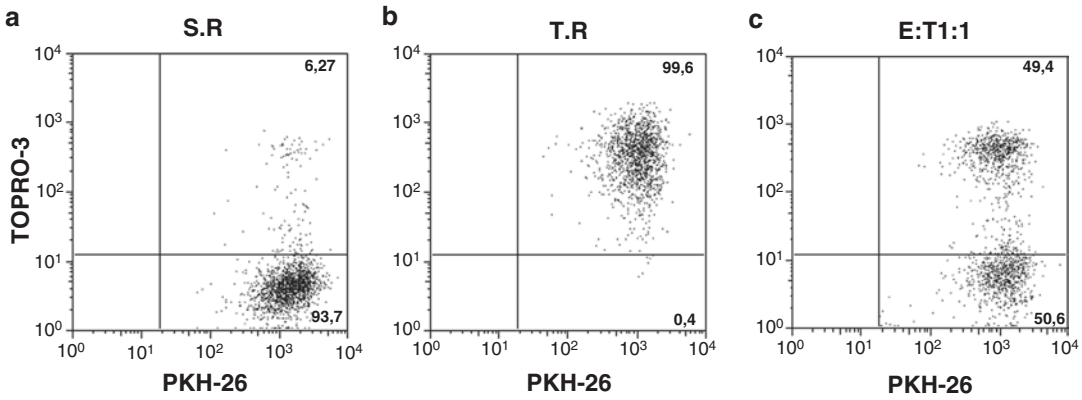

Fig. 2 Representative cytofluorimetric analysis of NK cells cytotoxicity assay. (**a**) Dot plot shows Spontaneous lysis of target cells (S.R.). In *upper right quadrant* dead target cells PKH26+TOPRO-3+ can be observed; (**b**) Dot plot shows maximal lysis of target cells (T.R. Total Release); (**c**) Representative dot plot of cytotoxicity assay where *E*/*T* ratio was 1:1. Proportion of target cell lysed by NK cells can be observed in upper right quadrant PHK26+TOPRO-3+. Twenty-thousand events were acquired in SSC/FSCA/PHK26+ gate

5. Prepare and label 4.5 ml sterile tubes as (1) P815 spontaneous release; (2) P815 Total release; (3) P815+NK; (4) NK+P815+NKp30+NKp46.
6. Add 100 µl P815 cell line suspension to each tube (1–4).
7. Add 100 µl NK cells suspension (E:T ratio 1:1, NK and P815 cells) to tubes 3 and 4.
8. Add 100 µl of monoclonal primary antibodies to tube 4.
9. Add 100 µl Cytofix/Cytoperm® (BD Pharmingen, San Jose, CA, USA) at tube 2.
10. Add complete medium prepared as previously described to tube 1, 2, 3 to 400 µl final volume.
11. Incubate at 37 °C, 5%CO2 for 4 h.
12. Add 5 µl of TOPRO-3 at final concentration to all tubes.
13. Acquire samples on a flow cytometer (*see* **Note 3**).

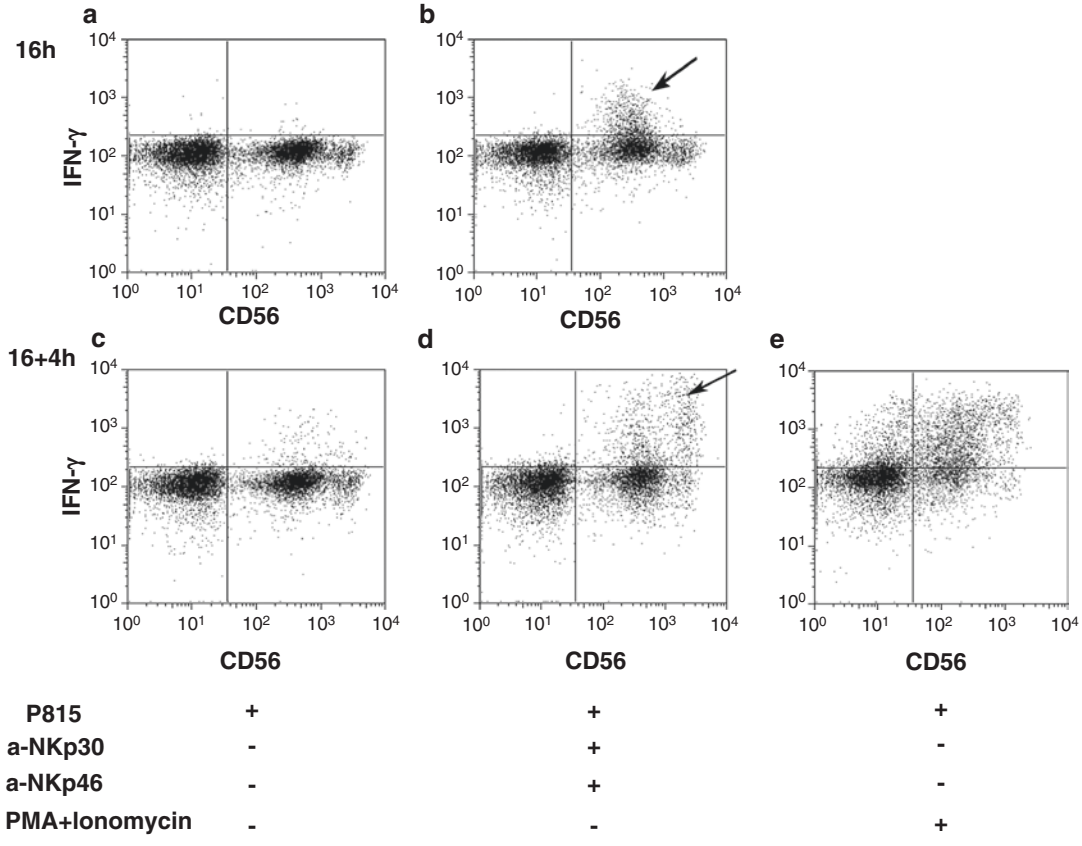

Fig. 3 Representative cytofluorimetric analysis of IFNg NK cells production. (**a**) and (**c**) Dot plots represent IFNg production after 16 and 16 + 4 h of stimulation with P815; (**b**) and (**d**) dot plots show IFNg production by NK cells in the presence of P815 and anti-NKp30, –NKp46 mAbs triggered; (**e**) Dot plot PMA plus Ionomycin stimulation to evaluate NK cells maximal IFNg production capability

3.7 Reverse ADCC Assay by CD107a Surface NK Cells Evaluation [24]

1. Collect freshly or activated isolated NK cell as effectors at 1×10^6 ml^{-1}.
2. Collect P815FcgR+ as target cells at 1×10^6 ml^{-1}.
3. Dilute anti NKp30 and-NKp46 mAbs at 0.1 μg/ml.
4. Dilute and label 4.5 ml sterile tubes as (1) P815+NK; (2) NK+P815+NKp30+NKp46; (3) P815+NK+PMA+Ionomycin.
5. Add 100 μl of P815 cell line suspension at each tube (1–3).
6. Add 100 μl of NK cell suspension (E:T ratio 1:1, NK and P815 cells) at each tubes (1–3).
7. Add 100 μl of monoclonal primary antibodies to tube 2.
8. Add 100 μl mixture of Phorbol Myristate Acetate (PMA)/ionomycin (0.5 ng/ml) for maximal stimulation to tube 3.
9. Add to GolgiStop according to datasheet.
10. Add complete medium prepared as previously described to tube 1; 400 μl final volume.
11. Incubate at 37 °C, 5% CO_2 for 1 h.
12. Add fluorochrome-conjugated mouse anti human CD107a to tubes 1–3.
13. Incubate at 37 °C, 5% CO_2 for 3 h.
14. Wash each tube with 2 ml of 0.1% saponin in sterile PBS and centrifuge at 1500 rpm ($626 \times g$ for Allegra 12R Beckman Coulter centrifuge) for 5 min at 4 °C.
15. Discharge supernatant and resuspend the cell pellet in 500 μl of sterile PBS.
16. Add anti-CD3 and anti-CD56 fluorochrome-conjugated mAbs for surface staining.
17. Incubate at 4 °C for 20 min.
18. Wash each tube with 2 ml of PBS and centrifuge at 1500 rpm for 5 min at 4 °C.
19. Discharge supernatant and resuspend the cell pellet in 500 μl of sterile PBS.
20. Acquire samples on a flow cytometer (*see* **Note 4**).

3.8 IFNg Production [7] (Fig. 3)

Collect purified NK cells or PBMC as effectors resuspend at 1×10^6 ml^{-1}.

1. Collect P815FcgR+ cells as targets, resuspend at 1×10^6 ml^{-1}.
2. Prepare anti NKp30 and-NKp46 mAbs at 0.1 μg/ml.
3. Prepare 200 μl of Phorbol Myristate Acetate (PMA) and Ionomycin mixture at 0.5 ng/ml concentration.
4. Prepare and label 4.5 ml sterile tubes as (1) P815+NK 4 h; (2) NK+P815+NKp30+NKp464h;(3)P815+NK+PMA+Ionomycin 4 h; (4) P815+NK 16 h; (5) NK+P815+NKp30+NKp46 16 h.

5. Add 100 µl of the P815 cell line suspension to each tube (1–3).
6. Add 100 µl of NK cell suspension (*E*:*T* ratio 1:1, NK and P815 cells) to tubes 1–5.
7. Add 100 µl of primary mAbs to tubes 2 and 5.
8. Add 100 µl of Phorbol myristate acetate (PMA)/Ionomycin (0,5 ng/ml) mixture for maximal stimulation to tube 3.
9. Add to GolgiPlug (BD Pharmingen, San Jose, CA, USA) according datasheet at tubes 4–5.
10. Add complete medium prepared as previously described at tube 1 to 400 µl final volume.
11. Incubate at 37 °C, 5% CO_2 for 16 h.
12. Add GolgiPlug (BD Pharmingen, San Jose, CA, USA) according to datasheet in tubes 1–3 and incubate at 37 °C, 5%CO_2 for another 4 h.
13. Wash tubes 4 and 5 with 2 ml of PBS and centrifuge at 1500 rpm for 5 min at 4 °C.
14. Discharge supernatant and resuspend cell pellet.
15. Proceed with intracellular staining protocol.
16. After 4 h of incubation wash tubes 1–3 with 2 ml of PBS and centrifuge at 1500 rpm (626×*g* for Allegra 12R Beckman Coulter centrifuge) for 5 min at 4 °C.
17. Discharge supernatant and resuspend cell pellet.
18. Proceed with the intracellular staining protocol.

3.9 Intracellular Staining [25]

1. Add directly fluorocrome-conjugated anti-CD3 and anti-CD56 mAbs for surface staining.
2. Incubate at 4 °C for 20 min.
3. Wash each tube with 2 ml of PBS and centrifuge at 1500 rpm (626×*g* for Allegra 12R Beckman Coulter centrifuge) for 5 min at 4 °C.
4. Follow permeabilization by Citoperm™ protocol/fixation according to datasheet.
5. Incubate at 4 °C for 20 min gently vortexing tubes.
6. Wash each tube with 2 ml of 0.1% saponin in PBS sterile solution and centrifuge at 1500 rpm for 5 min at 4 °C.
7. Discharge supernatant and resuspend cell pellet.
8. Add fluorocrome-conjugated anti-IFNγ mAbs.
9. Wash each tube with 2 ml of 0,1% saponin in PBS sterile solution and centrifuge at 1500 rpm for 5 min at 4 °C.
10. Discharge supernatant and resuspend the cell pellet in 500 µl of sterile PBS.
11. Acquire samples on a flow cytometer (*see* **Note 5**).

4 Notes

1. All reagents and plastic disposable must be sterile filtered. Store stock all reagent at 4 °C and peripheral blood samples at room temperature until to use.
2. For each analysis acquisition of 20,000 events is recommended.
3. For each sample 20,000 events in the PKH26 positive gate are recommended.
4. For each analysis acquire 20,000 events in the CD56posCd3neg gate.
5. For each analysis 20,000 events in CD56posCd3neg gate should be counted.

References

1. Cooper MA et al (2001) The biology of human natural killer-cell subsets. Trends Immunol 22(11):633–640
2. Corado J et al (1997) Impairment of natural killer (NK) cytotoxic activity in hepatitis C virus (HCV) infection. Clin Exp Immunol 109(3):451–457
3. Bozzano F et al (2012) Natural killer cells in hepatitis C virus infection. Expert Rev Clin Immunol 8(8):775–788. doi:10.1586/eci.12.71
4. Sivori S et al (1997) p46, a novel natural killer cell.specific surface molecule that mediates cell activation. J Exp Med 186(7):1129–1136
5. Biassoni R et al. (2002) Human natural killer receptors and their ligands. Curr Protoc Immunol Chapter 14:Unit 14.10. doi:10.1002/0471142735.im1410s46.
6. Caligiuri MA (2008) Human natural killer cells. Blood 112(3):461–469. doi:10.1182/blood-2007-09-077438
7. De Maria A et al (2011) Revisiting human natural killer cell subset function revealed cytolytic CD56dimCD16+ NK cells as rapid producers of abundant IFN-γ on activation. Proc Natl Acad Sci U S A 108(2):728–732
8. Freud AG et al (2014) Human natural killer cell development in secondary lymphoid tissues. Semin Immunol 26(2):132–137
9. Horowitz A et al Genetic and environmental determinants of human NK cell diversity revealed by mass cytometry. Sci Transl Med 5(208):208ra145. doi:10.1126/scitranslmed.3006702
10. Marras F et al (2014) Baseline and dynamic expression of activating NK cell receptors in the control of chronic viral infections: the paradigm of HIV-1 and HCV. Front Immunol 5:305. doi:10.3389/fimmu.2014.00305
11. Freud AG et al (2013) Expression of the activating receptor, NKp46 (CD335), in human natural killer and T-cell neoplasia. Am J Clin Pathol 140(6):853–866. doi:10.1309/AJCPWGG69MCZOWMM
12. Siewiera J et al (2015) Natural cytotoxicity receptor splice variants orchestrate the distinct functions of human natural killer cell subtypes. Nat Commun 6:10183. doi:10.1038/ncomms10183
13. Vitale M et al (1998) NKp44, a novel triggering surface molecule specifically expressed by activated natural killer cells, is involved in non-major histocompatibility complex-restricted tumor cell lysis. J Exp Med 187(12):2065–2072
14. Fuchs A et al (2005) Paradoxic inhibition of human natural interferon-producing cells by the activating receptor NKp44. Blood 106(6):2076–2082
15. Villanova F et al (2014) Characterization of innate lymphoid cells in human skin and blood demonstrates increase of NKp44+ ILC3 in psoriasis. J Invest Dermatol 134(4):984–991. doi:10.1038/jid.2013.477
16. Marras F et al (2011) Involvement of activating NK cell receptors and their modulation in pathogen immunity. J Biomed Biotechnol 2011:152430. doi:10.1155/2011/152430
17. Vivier E et al (2011) Innate or adaptive immunity? The example of natural killer cells. Science 331(6013):44–49. doi:10.1126/science.1198687 Review
18. Moretta L et al (2004) Killer immunoglobulin-like receptors. Curr Opin Immunol 16(5):626–633 Review

19. Sivori S et al (2014) TLR/NCR/KIR: which one to use and when? Front Immunol 5:617. doi:10.3389/fimmu.2014.00617
20. Della Chiesa M et al (2014) Human NK cell response to pathogens. Semin Immunol 26(2):152–160. doi:10.1016/j.smim.2014.02.001
21. Fuss IJ et al. (2009) Isolation of whole mononuclear cells from peripheral blood and cord blood. Curr Protoc Immunol Chapter 7:Unit 7.1. doi:10.1002/0471142735.im0701s85.
22. Caligiuri MA et al (1990) Functional consequences of interleukin 2 receptor expression on resting human lymphocytes. Identification of a novel natural killer cell subset with high affinity receptors. J Exp Med 171(5):1509–1526
23. Lee-MacAry AE et al (2001) Development of a novel flow cytometric cell-mediated cytotoxicity assay using the fluorophores PKH-26 and TO-PRO-3 iodide. J Immunol Methods 252(1–2):83–92
24. Alter G (2004) CD107a as a functional marker for the identification of natural killer cell activity. J Immunol Methods 294(1–2):15–22
25. Pala P et al (2000) Flow cytometric measurement of intracellular cytokines. J Immunol Methods 243(1–2):107–124 Review

Part V

Therapy

Chapter 15

Overview of Targeted Therapies for Adult T-Cell Leukemia/Lymphoma

Rihab Nasr, Ambroise Marçais, Olivier Hermine, and Ali Bazarbachi

Abstract

Adult T-Cell Leukemia/lymphoma (ATL) is the first human malignancy associated with a chronic infection by a retrovirus, the human T-cell lymphotropic virus type I (HTLV-I). ATL occurs, after a long latency period, only in about 5% of 10–20 millions infected individuals. ATL has a dismal prognosis with a median survival of less than 1 year, mainly due to its resistance to chemotherapy and to a profound immunosuppression. The viral oncoprotein, Tax, plays a major role in ATL oncogenic transformation by interfering with cell proliferation, cell cycle, apoptosis, and DNA repair. The diversity in ATL clinical features and prognosis led to Shimoyama classification of ATL into four clinical subtypes (acute, lymphoma, chronic, and smoldering) requiring different therapeutic strategies. Clinical trials, mainly conducted in Japan, demonstrated that combination of chemotherapy could induce acceptable response rate in the lymphoma subtype but not in acute ATL. However, long-term prognosis remains poor for both subtypes, due to a high relapse rate. Similarly, whether managed by a watchful waiting or treated with chemotherapy, the indolent forms (smoldering and chronic) have a poor long-term outcome. An international meta-analysis showed improved survival in the leukemic subtypes of ATL (chronic, smoldering as well as a subset of the acute subtype) with the use of two antiviral agents, zidovudine and interferon-alpha, and accordingly, this combination should be considered the standard first-line treatment in this context. ATL patients with lymphoma subtype benefit from induction chemotherapy, given simultaneously or sequentially with an antiviral combination of zidovudine and interferon-alpha. Allogeneic hematopoietic stem cells transplantation remains a promising and potentially curative approach but is limited to a small number of patients. Novel drugs such as arsenic trioxide in combination with interferon-alpha or monoclonal antibodies such as anti-CXCR4 have shown promising results and warrant further investigation.

Key words ATL, Therapeutic strategies, Antiviral drugs, Shimoyama classification

1 Introduction

In 1977, a group of Japanese researchers described a new clinical entity representing an atypical T-cell leukemia in adults in southern Japan [1]. Further studies revealed that the pathological features of this entity, later named Adult T-Cell Leukemia/Lymphoma (ATL), were quite distinct from those of other previously described lymphoproliferative disorders. Later, in 1980, the association of ATL

Claudio Casoli (ed.), *Human T-Lymphotropic Viruses: Methods and Protocols*, Methods in Molecular Biology, vol. 1582,
DOI 10.1007/978-1-4939-6872-5_15,

with the first oncogenic human retrovirus, Human T-Cell Leukemia Virus type I (HTLV-I), was clearly established [2, 3].

ATL is a T-cell lymphoproliferative malignancy characterized by the presence of atypical lymphocytes with multilobulated nuclei, named flower cells, in the peripheral blood and an aggressive clinical course mainly manifested in adulthood. Indeed, chronic HTLV-I infection induces clonal expansion and transformation of T cells [4, 5], leading to the development of ATL in about 5% of the 10–20 millions infected individuals after a long latency period, which is often greater than 50 years.

Few years later, the association between HTLV-I infection and tropical spastic paraparesis (TSP) or HTLV-I associated myelopathy (HAM) has been demonstrated [6]. TSP/HAM is a progressive myelopathy characterized by a chronic inflammatory and demyelinating process of the spinal cord. Furthermore, an epidemiological association has been established between HTLV-I and some autoimmune disorders [7] namely, uveitis, polymyositis, polyarthritis and Sjogren's Syndrome as well as infective dermatitis, a skin disease described in Jamaican children.

HTLV-I retrovirus is endemic in several regions of the world. It is indeed mainly present as small endemic foci in southern Japan, the Caribbean islands, Central America, South America, Intertropical Africa, Romania, and Northern Iran [8–11]. In Europe, outside Romania, few cases of ATL or HAM/TSP are mostly reported in patients originating from endemic areas mostly from West Indies or Africa.

1.1 How HTLV-I Is Transmitted?

HTLV-I retrovirus is mainly transmitted by infected cells through three main routes: breastfeeding, sexual transmission, and by transfusion of blood cells [12]. Several studies, especially from Japan, have shown that vertical transmission from mother to child via breastfeeding is the main route of HTLV-I transmission [13]. Indeed, early infection in childhood and breastfeeding contamination pathway are required for the development of ATL [14]. HTLV-I is also transmitted by sexual contact, more efficiently from men to women. Furthermore, blood transfusion has been established as the third route of transmission and can now be prevented by routine screening of anti-HTLV-I antibodies in blood donors [12]. However, only cellular products are infectious. In Japan, HTLV-I screening of blood donations has been conducted since 1985.

1.2 Molecular and Cellular Mechanisms Leading to ATL Pathogenesis

Although infection with HTLV-I is considered the first step of a multi-step oncogenic process culminating in ATL, the exact mechanism of leukemogenesis induced by this retrovirus is not yet fully elucidated. Many studies have consistently highlighted the crucial role of the retroviral oncoprotein Tax in cell transformation and consequently in the establishment of ATL [15]. Tax controls not only viral expression but also interferes with cellular functions by

activating the promoters of various cellular genes. Tax simultaneously activates the production of interleukins, specifically IL-2 and IL-15 and their receptors creating an autocrine stimulation loop [16, 17]. Tax also disrupts many cellular signaling pathways leading to the activation of several transcription factors, namely CREB, SRF, and NF-κB and to the inhibition of apoptosis by stimulating the expression of several anti-apoptotic proteins and inhibitors of apoptosis such as cIAP and XIAP. Tax impairs DNA repair mechanisms and induces genetic instability by suppressing the expression or function of p53, DNA polymerase β, nuclear proliferating cell antigen, and the mitotic spindle assembly checkpoint protein 1 (MAD1). Tax also perturbs cell cycle by altering the expression of cyclins and cyclin-dependent kinase inhibitors [15, 18–26]. Furthermore, posttranslational modifications of Tax, precisely ubiquitination and SUMOylation, are essential for its intracellular localization and constitutive activation of the NF-κB pathway [27–31]. Finally, Tax modulates the microenvironment not only by inducing angiogenesis and gap junction-dependent communication between infected cells and endothelial cells [32, 33], but also through affecting TGF-beta signaling [34]. Other factors related to the host and/or to the virus certainly play a role yet to be defined.

Since its discovery, several studies have shed light on Tax multiple effects and proposed it as the primary oncogene in ATL. However, Tax expression is almost undetectable in most circulating leukemic cells which raised some controversies [35]. In fact, freshly isolated HTLV-I infected or ATL cells express a low level of HTLV-I transcripts and antigens that begin to be detected, in most cases, after a few hours of culture in vitro [36–39]. This low expression of viral mRNA and viral proteins in vivo may be explained by the rapid elimination by the immune system, of cells expressing viral antigens on their surface, by the presence of a hidden viral reservoir located outside the blood compartment and/or by maintaining a low or transient Tax expression level almost undetectable by Western blotting [40].

The relatively low percentage of infected individuals who develop ATL as well as the long latency period of this disease suggest that secondary genetic events that may occur after infection are probably involved in the progression of HTLV-I-induced leukemia. Mutations, deletions or aberrant expression of tumor suppressor genes, such as p53 or p15INK4b/p16INK4a [41], end-to-end chromosomal fusions, and shortened telomeres [42], are among these secondary events leading to transformation. A recent integrated molecular study on 426 ATL cases identified alterations that overlap significantly with the Tax interactome and are highly enriched for T-cell receptor-NF-κB signaling, T-cell trafficking, and other T-cell-related pathways as well as immunosurveillance [43].

Tax expression in developing thymocytes of transgenic mice or in human CD34+ hematopoietic progenitor cells induces a leukemia that strikingly recapitulates the human ATL [44–46], providing a strong evidence that Tax plays a major role in ATL initiation. However, the role of continuous Tax expression in maintaining the leukemic phenotype remains disputed. The fact that fresh ATL leukemic cells have the same morphological and biochemical characteristics as Tax-expressing cells suggests that the former transiently express latent, transient, and/or low level of Tax expression in the skin, gastrointestinal tract, and/or in other lymphoid organs, all considered to be preferential sites infiltrated by tumor cells. The existence of anti-Tax cytotoxic lymphocytes in patients with ATL [47] and the multiplication of leukemic cells in ATL patients outside the bloodstream (Hermine et al., unpublished observations) support this hypothesis. In that sense, a recent report demonstrated that ATL-derived or HTLV-I transformed cells are addicted to continuous Tax expression [48] even when Tax protein is undetectable. Finally, the clinical efficacy of anti-Tax vaccination in inducing responses in ATL patients [49] strongly supports the concept that low levels of Tax are present in ATL and are mandatory for the maintenance of the leukemic phenotype.

Recently, the HTLV-1 bZIP factor gene (HBZ), an antisense mRNA transcribed from the 3′-LTR, was demonstrated to be consistently expressed in ATL cells [50, 51]. Indeed, HBZ expression level correlates with viral load. Furthermore, HBZ growth promoting activity in vivo and in vitro, as well as its capacity to induce immunosuppressive molecules [51, 52], suggests that this gene plays a role in the maintenance of the transformed clone, likely through maintaining low levels of Tax expression and through allowing escape from immune surveillance.

1.3 Clinical Subclassification

Essential diagnostic criteria of ATL include histological or cytological evidence of T-lymphoid malignancy with detectable anti HTLV-I antibodies. Abnormal T-lymphocytes are often present in peripheral blood, characteristically expressing a mature activated T-cell immunophenotype and are usually CD4+ CD25+ with absent CD7 expression.

The diversity in clinical presentation, evolution, and prognosis of ATL patients led to the classification of ATL into four major clinical subtypes as proposed by the Shimoyama classification: smoldering, chronic, lymphoma, and acute forms [53]. These clinical subtypes are all associated with a poor prognosis and a median survival of 6, 10, and 24 months for the acute, lymphoma, and chronic forms respectively.

(a) *Acute ATL*: The majority of ATL patients are diagnosed with the acute subtype. Lymphadenopathy, hepatosplenomegaly, and skin lesions characterize acute ATL but other visceral

lesions (lung, central nervous system, gastrointestinal tract, or bones) may be observed. Hypercalcemia, high lactate dehydrogenase (LDH), and opportunistic infections are frequent in these patients. Acute ATL patients present with a major lymphocytosis often with a high percentage of "flower cells," characteristics of typical ATL cells.

(b) *Smoldering ATL*: This clinical subtype is characterized by 5% or less leukemic flower cells and with the absence of lymphocytosis. Serum calcium level is normal and LDH can be increased up to 1.5 times the normal level. Specific skin or lung involvement is possible but without any other visceral involvement.

(c) *Chronic ATL*: This subtype is characterized by lymphocytosis, less frequently showing flower cells than the acute subtype. Chronic ATL is occasionally associated with skin lesions and visceral involvement with lymphadenopathy and hepatosplenomegaly. However, there is no associated hypercalcemia or infiltration of the central nervous system, bones, or the gastrointestinal tract. LDH level may be slightly increased (less than 2.5 times the upper limit of normal).

(d) *Lymphoma ATL*: This subtype accounts for about 25% of cases of ATL, and is characterized by the absence of peripheral blood involvement with the absence of lymphocytosis and less than 1% of circulating leukemia cells. Clinically, this subtype manifests with massive lymphadenopathy and hepatosplenomegaly, and frequently with high LDH and hypercalcemia.

1.4 Response Criteria

ATL clinical subclassification is quite important not only for predicting prognosis but also for tailoring the suitable treatment. In fact, evaluation of the therapeutic response is complicated by the heterogeneous clinical presentation of ATL clinical subtypes. Accordingly, new response criteria were introduced [54]. A complete response (CR) means that all measurable tumor lesions (including size of the lymph nodes) have disappeared and that the absolute lymphocyte count has been normalized ($<4 \times 10^9\ L^{-1}$). A 75% reduction of the tumor size and a normalization of the absolute lymphocyte count below 4×10^9 cells/L define an unconfirmed CR. A partial response (PR) is defined as a 50% reduction of tumor size and absolute lymphocyte count. A progressive disease is defined as a 50% increase of tumor size and/or absolute lymphocyte count. These response criteria require that each response criterion must be maintained for at least 4 weeks [54, 55].

1.5 Therapeutic Options for ATL

ATL is a heterogeneous disease and therefore, its management depends primarily on the ATL subtype and response to initial therapy. Patients with ATL aggressive forms of the disease (acute and lymphoma) have a dismal prognosis mainly because of a high tumor burden, an intrinsic resistance to chemotherapy,

hypercalcemia, and/or frequent opportunistic infections due to a severe immune deficiency. Several clinical trials conducted in Japan have clearly shown that although combinations of chemotherapeutic agents, specifically those used to treat aggressive non-Hodgkin lymphomas, have improved the response rate in aggressive ATL, particularly in the lymphoma subtype, they did not significantly impact long-term survival. Patients with indolent ATL (chronic or smoldering subtypes) have a better prognosis. However, recent data from Japan showed a poor long-term outcome when these patients are managed with a watchful-waiting policy until disease progression. The outcome of these patients was even worse when they were treated with chemotherapy [56].

1.6 Conventional Chemotherapy

The Japan Clinical Oncology Group (JCOG) has performed several prospective clinical studies since 1978 [55]. The first JCOG 7801 clinical trial investigated the efficacy of the VEPA protocol (a protocol similar to CHOP containing vincristine, cyclophosphamide, prednisolone, and doxorubicin) and showed that only a 17% CR rate was achieved with a median survival of 5 months [57]. The second trial, JCOG 8101, was a randomized phase III study that compared the VEPA protocol with VEPA-M (VEPA plus methotrexate) in 54 ATL patients [57]. Although a 36.7% CR rate was observed in the VEPA-M group, no significant differences were noted in terms of median survival (7.5 months) or overall survival (8% at 4 years). The third clinical trial, JCOG 8701, is a phase II study that used a more aggressive protocol (LSG4), which consisted of alternating treatment with three different chemotherapeutic regimens: VEPA-B (VEPA + bleomycin), M-FEPA (methotrexate, vindesine, cyclophosphamide, doxorubicin, and prednisolone), and VEPP-B (vincristine, etoposide, procarbazine, prednisolone, and bleomycin). Interestingly, the CR rate increased to 42%, however, early relapses occurred and the survival remained dismal with a median survival time of 8 months and an overall survival rate of 12% at 4 years [58]. These trials included also patients with other subtypes of Non-Hodgkin's lymphoma. The median survival time of these patients was much better (44 months) compared to ATL patients (8 months). The next study JCOG 9109 used a specific protocol for ATL developed by JCOG, in a Phase II study conducted between 1991 and 1993. The results were disappointing and indeed, this pentostatin-containing regimen did not show any improvement in survival (median survival time of 7.4 months and overall survival of 15% at 2 years) [59]. The following study, JCOG 9303, conducted between 1994 and 1996 used more intensive chemotherapy combinations, including VCAP (vincristine, cyclophosphamide, doxorubicin, and prednisolone), AMP (doxorubicin, ranimustine, and prednisolone), and VCEP (vindesine, etoposide, carboplatin, and prednisolone) in addition to intrathecal injection of methotrexate and cytarabine, as well as systematic use of granulocyte colony stimulating factor [60].

A significant improvement in CR rate (35%) and in survival was observed. The median survival time was 13 months compared to 8 months with the CHOP-like regimen. The overall survival was 31% at 2 years. Based on these promising results, the JCOG conducted a Phase III study (JCOG 9801) between 1998 and 2003. This trial compared this LSG15 regimen (VCAP-AMP-VECP) versus biweekly CHOP. One hundred and eighteen patients (81 patients with acute ATL and 26 patients with lymphoma subtype) were enrolled in the study [61]. Importantly, the study showed that the LSG15 is a more effective regimen as the response rate was higher in the experimental group (40% versus 25%). This was also accompanied by an improved overall survival rate at 3 years (24% against 13%). Overall, ATL lymphoma patients seem to benefit from this dose dense/dose intense regimen. However, in acute ATL, complete remission (CR) rates with LSG15 are less than 20% and 4 year OS is less than 10%.

1.7 Allogeneic Stem Cell Transplantation

Due to the high rate of relapse after conventional chemotherapy, allogeneic stem cells transplantation (alloSCT) remains a potentially curative option in ATL. Several retrospective studies, all conducted in Japan, have confirmed the feasibility of alloSCT using myeloablative or reduced-intensity conditioning in patients with ATL and also revealed promising results [62, 63]. Recently, a large Japanese retrospective study, published in 2010, reported the outcome of 386 patients who underwent allograft between 1995 and 2005 [64]. An overall survival rate of 33% at 3 years was observed, after a median follow-up of 41 months. However, donor HTLV-1 seropositivity aggravated the disease-associated mortality. Finally, for 30 patients who received a reduced intensity conditioning, the 5-year overall survival and progression free survival were 36% and 31%, respectively [65]. The EBMT registry recently reported 3-year OS rates of 34.3% in a cohort of 17 ATL patients [66], demonstrating that alloSCT is a feasible strategy outside Japan.

A recent study from Nagasaki, describing the results of ATL patients treated with donor lymphocyte infusion for relapse after allogeneic transplantation, reported durable responses, with three cases of long-term remission of more than 3 years [67]. This response to donor lymphocyte infusion is often seen as the best evidence for a graft versus leukemia (GVL) effect.

Unfortunately, poor performance status, severe immunosuppression, low CR rate, particularly in the acute form and low probability of finding a matched donor for patients from ethnic minorities are all important factors contributing to the limited use of alloSCT [55].

1.8 Antiviral Therapy: Combination of Interferon Alpha and Zidovudine

The combination of interferon alpha (IFN) and zidovudine (AZT) resulted in important advances in ATL therapy and it was first reported in two Phase II studies [68–70]. A high response rate was observed, particularly in patients with previously untreated

ATL. The high efficacy of AZT/IFN combination was later confirmed in several small clinical trials [71–75]. Recently, a worldwide meta-analysis reported the results of antiviral therapy in 254 ATL patients (116 acute ATL, 11 smoldering ATL, 18 chronic ATL, and 100 ATL lymphoma) treated between 1995 and 2008 [76]. This study compared the efficacy of different treatment strategies, namely, first-line antiviral therapy (AZT/IFN) alone, first-line chemotherapy alone, and chemotherapy followed by antiviral maintenance treatment. The overall survival rate at 5 years was 46% for 75 patients who received first-line antiviral therapy, 20% for 77 patients who received chemotherapy alone, and 12% for 55 patients who received chemotherapy followed by the antiviral treatment. First-line antiviral therapy was mainly beneficial in patients with the leukemic subtypes of ATL (acute, chronic, and smoldering), while patients with the lymphoma subtype benefited more from chemotherapy. Indeed, first-line antiviral treatment alone resulted in a significant prolonged survival in an important proportion of patients with acute ATL (5-year overall survival of 28%) compared with first-line chemotherapy with or without maintenance antiviral therapy (5-year overall survival of 10%). Interestingly, spectacular results were observed in acute ATL patients who achieved CR under antiviral treatment resulting in a 5-year survival rate of 82%. On the other hand, the 5-year survival in the indolent subtypes of ATL (chronic and smoldering) treated with antiviral therapy was 100%. Unfortunately, in the lymphoma subtype, the results of first-line antiviral treatment were disappointing (median overall survival of 7 months and 5-year overall survival of 0%). Finally, a multivariate analysis confirmed that the first-line antiviral therapy resulted in a better overall survival of ATL patients (hazard ratio 0.47; 95% confidence interval 0.27 to 0.83; $p = 0.021$).

Finally, a recent retrospective study confirmed the effectiveness of AZT/IFN in combination with chemotherapy in 73 patients with the aggressive acute and lymphoma subtypes of ATL (29 and 44 patients, respectively) [77]. Patients received either first-line chemotherapy (mainly a CHOP-like protocol), or AZT/IFN either as first-line treatment in combination with chemotherapy (concurrent or sequential), or on relapse. The response rate was 81% for combination therapy (chemotherapy plus AZT/IFN) compared to 49% for chemotherapy alone, which consequently resulted in a doubling of progression-free survival (8 months versus 4 months, respectively) but without reaching statistical significance. Subgroup analysis demonstrated that the median overall survival was significantly improved in acute ATL ($p = 0.0081$) and lymphoma ATL ($p = 0.001$), specifically in patients who received first-line combination treatment compared to those treated with chemotherapy alone. In addition, multivariate analysis showed that the combination of AZT/IFN resulted in a better overall survival in the two aggressive subtypes of ATL (hazard ratio 0.23; 95%

confidence interval 0.091–0.60; $p = 0.002$). However, toxicity, particularly on hematopoiesis, was not reported in this study, and a cautious attitude in this regard is recommended.

The mechanisms of action of this remarkably successful combination are not fully elucidated. Although several arguments are in favor of an antiviral effect of AZT/IFN combination, a potentially cytotoxic effect of this antiviral therapy cannot be excluded [40]. Indeed, AZT induces a persistent inhibition of telomerase, reactivation of p53 and accordingly cellular senescence, which may explain the lack of efficacy of AZT/IFN in patients with a p53 mutation [78].

1.8.1 Arsenic Trioxide

Arsenic trioxide synergizes with IFN to induce cell cycle arrest and apoptosis of HTLV-1 transformed cell lines as well as fresh ATL cells. At the molecular level, following the proteasomal degradation of Tax oncoprotein, this combination induces a rapid shut off of the transcription factor NF-κB and a delayed inhibition of genes associated with cell cycle [79–81], indicating the importance of continuous Tax expression for ATL cell survival. In preclinical studies using *tax*-transgenic mice, arsenic and IFN synergized to induce a specific depletion of leukemia-initiating cells (LIC) and accordingly leading to cure of Tax-driven murine ATL [82]. Therefore, continuous Tax expression is essential for ATL LIC activity. Thus, the addition of arsenic to AZT and IFN, by targeting LIC activity, may result in long-term disease eradication and ATL cure.

On the basis of these findings, a phase II prospective study was conducted to investigate the safety and efficacy of the triple combination (arsenic, IFN, and AZT) in ten patients, newly diagnosed with chronic ATL. Remarkable results were observed with 100% response rate including seven CR, two very good PR but with persistence of more than 5% of circulating atypical lymphocytes, and one PR. Side effects were mild and mainly hematologic [83]. Interestingly, this triple combination seems to play an important role in restoring the immune response by switching the ATL microenvironment from an immunodeficient (Treg and Th2 phenotype before treatment) to an immunocompetent status (Th1 phenotype after treatment) [84]. Furthermore, preliminary results were reported on 11 patients with ATL (three ATL lymphomas, three chronic ATL, and five acute ATL) treated with arsenic and IFN as a consolidation therapy after induction chemotherapy [85]. At the beginning of treatment with arsenic, four patients were in CR, two patients in PR, and five patients had progressive disease. While one patient has progressed 3 days after starting arsenic treatment, ten patients received the treatment for 3–8 weeks. Six patients died, including those who had progressive disease at the time of arsenic initiation, while five patients survived. The latter includes three patient with lymphoma subtype in CR (with a follow-up of

25, 31, and 46 months of follow-up), one with acute ATL in CR (with a follow-up of 9 months), and one with chronic ATL in PR (with a follow-up of 39 months). The toxicity profile was favorable. Four patients experienced peripheral neuropathy, three had hand-foot syndrome and had a rash including two with toxic epidermolysis.

Although preliminary, these results suggest that arsenic/IFN represents one of the most promising targeted therapies against ATL. Arsenic/IFN effectively target the activity of ATL stem cells and may accordingly be useful as consolidation treatment after achieving a satisfactory response with induction therapy.

1.8.2 Monoclonal Antibodies

(a) *Anti-CD25 antibody*: CD25 (the alpha chain of human interleukin-2) is expressed on ATL cells. Waldmann et al. conducted the first clinical trial testing the efficacy of an anti-CD25 antibody in 19 patients with ATL. Interestingly, six patients responded including two patients who achieved CR and four who achieved PR. The duration of the responses was from 9 weeks to more than 3 years [86]. Two years later, the results of the second clinical trial that used an anti-CD25 coupled with Yttrium-90 in 18 patients were reported. Seven patients (one patient with chronic ATL and six patients with acute ATL) achieved PR that lasted from 1.6 to 22.4 months (mean: 9.2 months), and two patients achieved CR (one patient died 36 months after initiation of treatment due to a secondary acute myeloid leukemia and one patient was still in CR at the time of publication) [87].

(b) *Anti-transferrin receptor antibody*: A24, a monoclonal antibody against the transferrin receptor, induces apoptosis in HTLV-I transformed cell lines and primary ATL cells [88]. However, only preclinical studies have been conducted.

(c) *Anti-CC chemokine receptor 4*: The CC chemokine receptor 4 (CCR4) is expressed on ATL cells. The clinical efficacy of mogamulizumab (KW-0761), a defucosylated humanized anti-CCR4 monoclonal antibody, was first tested in 13 patients with relapsed ATL. The overall response rate was 31% including two CR and two PR [89]. The results of a multicenter phase II study, published later, have confirmed the efficacy of KW-0761 in 28 patients with relapsed ATL [90]. Enrolled patients received weekly, an intravenous infusion KW-0761 (1 mg/kg) for 8 weeks. Among the 26 evaluable patients, the overall response rate was 50% including eight CR and five RP. The median progression-free survival and overall survival were 5.2 and 13.7 months, respectively. Toxicity profile was acceptable and manageable. Side effects were mainly infusion reactions (89%) and skin rash (63%). The potential of immunochemotherapy was explored in a randomized phase 2 trial:

the addition of Mogamulizumab to LSG15 combination chemotherapy improved response rates mainly in the peripheral blood, albeit with increased toxicity, but unfortunately with no effect on progression free and overall survival [91].

1.9 Watch and Wait Policy for Patients with Indolent ATL

The prognosis of patients with chronic or smoldering ATL is better than that of patients with acute and lymphoma subtypes. Accordingly, most of these patients are considered to have an indolent ATL and are thus managed by watch and wait policy without treatment, until disease progression, similarly to the management of patients with chronic lymphocytic leukemia. In contrast, patients with chronic ATL having poor prognostic factors are managed like patients with aggressive ATL subtypes and hence, treated with chemotherapy. A recent study in Japan reported long-term results of 90 enrolled patients with indolent ATL (65 with chronic ATL and 25 with smoldering subtype) [56]. Sixty-three patients died, and the reported median survival was 4.1 years. Forty-four patients (49%) progressed to an aggressive form after a median time to transformation of 18.8 months (0.3 months to 17.6 years). No difference was observed between smoldering and chronic subtypes. The estimated 10-year survival rate was only 25.4% and therefore the prognosis remains poor, even in these indolent ATL subtypes. Surprisingly, patients who received chemotherapy had an even more disappointing and worse prognosis than patients treated by watchful waiting strategy. These findings underscore the need to start treating ATL patients with indolent subtypes with the antiviral combination of AZT and IFN.

1.10 Promising New Therapeutic Options for T-Cell Lymphomas

(a) *Histone deacetylase Inhibitors*: Histone deacetylase (HDAC) Inhibitors represent a new class of compounds designed to alter epigenetic modifications. Vorinostat, Romidepsin are two HDAC inhibitors currently approved by FDA for the treatment of refractory and relapsed cutaneous T-cell lymphoma. The response rate is 30% for vorinostat and 34% for romidepsin [92, 93]. Moreover, the latter induces around 25–40% response rates in two Phase II studies in peripheral T-cell lymphomas (PTCL) [94, 95]. These drugs have not been evaluated in ATL, neither as monotherapy nor in combination with other drugs during induction treatment. However, Ramos et al. investigated the efficacy of AZT/IFN in combination with another HDAC inhibitor, valproic acid, as a maintenance therapy in 13 ATL patients [96]. One patient had a positive response (decrease in ATL clonal disease measured by PCR). However, it was also reported that fresh cells isolated from this patient and treated ex vivo with vorinostat demonstrated an increase of HTLV-1 expression and induction of apoptosis. Induction of an immune response against HTLV-I infected cells was not discussed in this study. However, the authors pro-

posed that inhibition of HDAC could lead to reactivation of latent HTLV-1 virus and therefore helping to eliminate residual disease [97].

(b) *Alemtuzumab*: A high response rate was shown with Alemtuzumab (Campath-1H), an anti-CD52 antibody approved for treatment of chronic lymphocytic leukemia and T-Cell prolymphocytic leukemia. The results of this prospective study that includes 39 enrolled patients treated with alemtuzumab [98] revealed an overall response rate of 76% and a median disease-free interval of 7 months. Responses were durable with 60% of the patients achieving CR and 16% PR. However, experience in ATL is limited to case reports [99] as well as to a CR in one patient with ATL enrolled in a study conducted to test the combination of alemtuzumab and pentostatin in various types of PTCL [100]. On the other hand, in PTCL, Alemtuzumab in combination with conventional chemotherapy showed a relative efficiency, but a high rate of infection.

(c) *SGN-35 (brentuximab vedotin)*: It is a chimeric monoclonal antibody that targets CD30, a cell-membrane protein bound to an anti-mitotic agent. SGN-35 is FDA approved for the treatment of CD30-positive anaplastic T-cell lymphoma and Hodgkin lymphoma. Recent in vitro and in vivo studies suggest that SGN-35 may have a potential clinical efficacy in ATL [101].

1.11 Therapeutic Recommendations for ATL (Fig. 1)

(a) *Chronic and smoldering ATL*: As indicated above, patients with indolent forms of ATL (smoldering or chronic) have a better prognosis than those with acute and lymphoma subtypes and are accordingly managed by a watchful waiting policy. A recent Japanese study showed a poor long-term prognosis in these patients who were treated by watch and wait policy until disease progression [56]. Furthermore, this study suggested that chemotherapy alone might be disadvantageous in these subtypes [56]. Clear prognostic factors that can predict the transformation to an aggressive form are lacking. Indeed, most patients with indolent ATL subtypes must be treated. The international meta-analysis reported an excellent survival (100% overall survival beyond 5 years) in patients with chronic and smoldering ATL who received first-line AZT/IFN antiviral therapy [76].

Based on these remarkable results, AZT/IFN is the standard first-line therapy for patients with indolent forms, outside the context of clinical trials (Fig. 1). However, continuous treatment is required to prevent relapse that occurs upon treatment discontinuation [102–104]. The recommended starting dosage for IFN is $5–6 \times 10^6$ IU/m^2/day and for AZT 600–900 mg/day (in three divided doses). These dosages can be reduced 1 month later to 600 mg/day in two divided doses

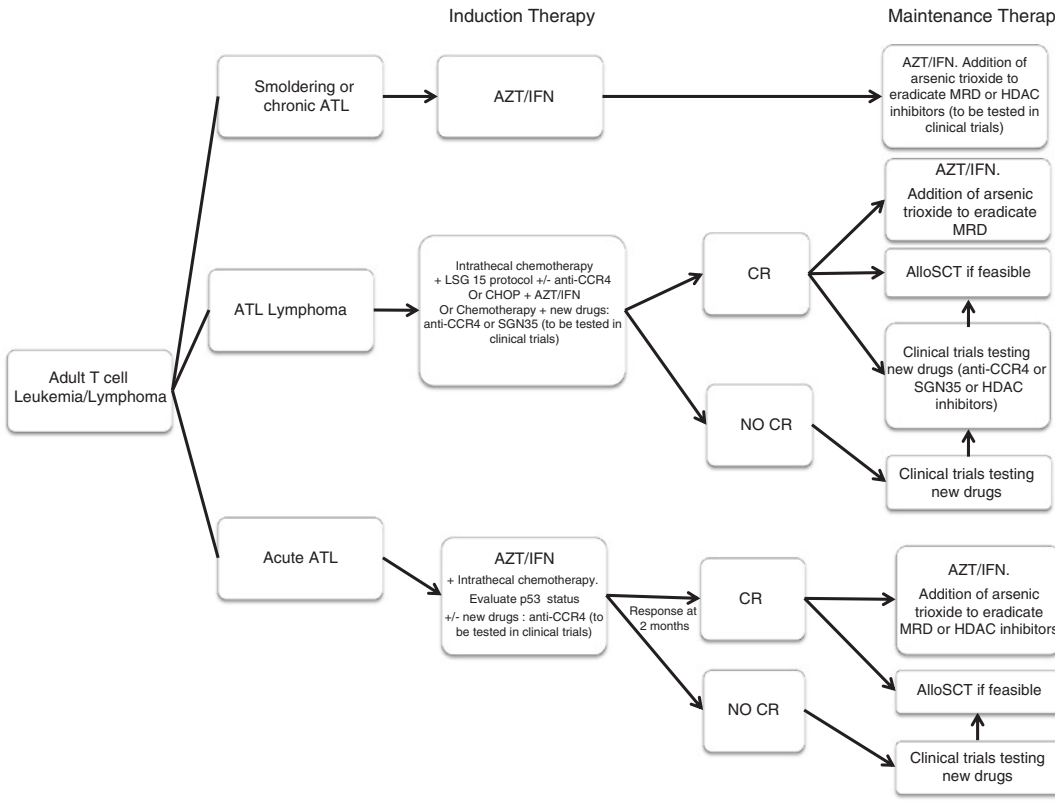

Fig. 1 Adult T cell leukemia/lymphoma therapy guidelines. *CR* complete remission

for AZT, and to 3×10^6 IU/m^2/day of IFN, which can also be replaced by a weekly injection of pegylated IFN alpha at a dose of 1.5 μg/kg. Based on the previously reported preclinical studies, clinical trials are currently testing the efficacy of adding arsenic trioxide to AZT/IFN combination as a consolidation therapy, with the ultimate goal of discontinuing treatment and achieving cure through potential LIC targeting [32, 79, 81–83].

(b) *ATL Lymphoma*: Based on the meta-analysis, initial chemotherapy is more effective than first-line antiviral therapy (AZT and IFN) alone in lymphoma ATL [76]. Therefore, patients with a lymphoma subtype should be preferably treated with first-line chemotherapy (Fig. 1). However, a recent British study showed that, in patients with lymphoma ATL, the combination of antiviral treatment with CHOP is superior to CHOP alone [77]. Based on several Japanese trials, the standard of care for ATL lymphoma is the LSG15 protocol. When treated with this chemotherapy protocol, CR rates were higher in lymphoma ATL (66.7%) than in acute ATL (19.6%) or chronic ATL (40%). However, due to rapid relapses, the overall

survival remains poor [60]. Consequently, a consolidation treatment is required. A high percentage of relapses after chemotherapy occurs in the central nervous system and accordingly, an intrathecal prophylaxis should be considered even in the absence of clinical symptoms. AlloSCT should be considered, when possible [64].

Based on promising preclinical data, clinical trials are currently evaluating the efficacy of two consolidation cycles of arsenic and IFN-α in patients who achieved CR, with encouraging preliminary results (Suarez, Hermine et al., unpublished data). Finally, the combination of chemotherapy with AZT/IFN antiviral therapy, or other new treatments, such as HDAC inhibitors, may improve the remission rate and patients' survival [33, 103, 104].

(c) *The acute form of ATL*: The results of several Japanese clinical trials clearly reported that chemotherapy protocols have only modest effects in acute ATL. Although the most intensive multi-agent chemotherapy protocol (LSG-15) has increased the response rate, median survival and overall survival remain poor [60, 61]. On the other hand, the worldwide meta-analysis showed that AZT/IFN combination significantly prolongs the survival of patients with acute ATL, especially in those who achieved CR [76]. Hence, outside the context of clinical trials, the recommended treatment for acute ATL is the combination of AZT and IFN (Fig. 1) [33, 103, 104]. However, in patients presenting with large tumor or severe bisphosphonates-resistant hypercalcaemia, initial chemotherapy may be needed.

The recommended starting dosage for IFN is $5–6 \times 10^6$ IU/m^2/day and for AZT 600–900 mg/day (in three divided doses). These dosages can be reduced 1 month later to 600 mg/day in two divided doses for AZT, and to $3–5 \times 10^6$ IU/m^2/day of IFN, which can also be replaced by a weekly injection of pegylated IFN alpha at a dose of 1.5 μg/kg.

Since a high percentage of relapses after chemotherapy occurs in the central nervous system, an intrathecal prophylaxis should be considered even in the absence of clinical symptoms. Preliminary results indicate that AZT/IFN combination is mostly effective in patients with functional p53 [78]. Therefore, evaluating p53 status is recommended in all patients with acute ATL before the initiation of anti-viral therapy [105]. Finally, as for chronic and smoldering ATL, long-term disease control requires continuous treatment to prevent relapse.

AlloSCT should also be considered for young acute ATL patients with acute ATL, if a suitable donor is available (Fig. 1). Similarly to other ATL subtypes and based on preclinical

data, the efficacy of arsenic and IFN as consolidation treatment after achieving complete remission is currently being tested in ongoing clinical trials.

1.12 Management of Hypercalcemia and Anti-infective Prophylaxis

Hypercalcemia associated with aggressive subtypes of ATL should be managed by hydration, bisphosphonates, and rapid initiation of the specific treatment of the disease. For the prophylaxis of Pneumocystis carinii pneumonia, viral infections and fungal infections, trimethoprim-sulfamethoxazole, valacyclovir, and anti-fungal agents are respectively recommended. Finally, to prevent a systemic strongyloidiasis in patients with an exposure history to the parasite responsible for the disease, prophylaxis with ivermectin and albendazole should be considered.

2 Conclusion

The clinical presentation of ATL plays a dominant role in defining treatment paradigms for this disease. The combination of AZT and IFN is effective in the leukemic subtypes of ATL and should be considered the recommended first-line therapy in this context [102–104]. This antiviral treatment clearly changed the natural history of ATL by significantly improving the long-term outcome of patients with chronic and smoldering ATL and a subset of patients with acute ATL expressing wild-type p53. Prior exposure to chemotherapy increases the rate of complications and disease resistance. We therefore recommend using AZT/IFN as first-line therapy in the leukemic forms, and intiating treatment with high doses of both AZT and IFN because lower doses are often ineffective. On the other hand, patients with lymphoma subtype benefit from combining chemotherapy with AZT/IFN, either concomitantly or sequentially. AlloSCT should always be considered in appropriate patients, if a suitable donor is available.

To prevent resistance and relapse of patients in CR, it is imperative to conduct clinical trials to evaluate novel targeted therapies such as the combination of arsenic and IFN, HDAC inhibitors, or monoclonal antibodies. Currently, due to the poor prognosis and unfavorable outcome of patients with aggressive ATL (acute and lymphoma forms), phase II studies are needed in the near future. In the indolent subtypes, randomized phase III study should be conducted to evaluate the efficacy of adding novel drugs to AZT/IFN, in order to achieve not only long-term disease control but also treatment discontinuation and cure of ATL. Finally, novel therapeutic strategies must also test the role of immune checkpoint inhibitors and/or of vaccines against viral proteins expressed in tumor cells or in accessory cells [49].

References

1. Takatsuki K, Uchiyama T, Sagawa K, Yodoi J (1977) Adult T cell leukaemia in Japan. In: Seno S, Takaku F, Irino S (eds) Topics in haematology. Excerpta Medica, Amsterdam, pp 73–77
2. Poiesz BJ, Ruscetti F, Gazdar A, Bunn P, Minna J, Gallo R (1980) Detection and isolation of type C retrovirus particles from fresh and cultured lymphocytes of a patient with cutaneous T-cell lymphoma. Proc Natl Acad Sci U S A 77:7415–7419
3. Hinuma Y, Komoda H, Chosa T, Kondo T, Kohakura M, Takenaka T, Kikuchi M, Ichimaru M, Yunoki K, Sato I, Matsuo R, Takiuchi Y, Uchino H, Hanaoka M (1982) Antibodies to adult T-cell leukemia-virus-associated antigen (ATLA) in sera from patients with ATL and controls in Japan: a nation-wide sero-epidemiologic study. Int J Cancer 29:631–635
4. Wattel E, Vartanian JP, Pannetier C, Wain-Hobson S (1995) Clonal expansion of human T-cell leukemia virus type I-infected cells in asymptomatic and symptomatic carriers without malignancy. J Virol 69(5):2863–2868
5. Mortreux F, Kazanji M, Gabet AS, de Thoisy B, Wattel E (2001) Two-step nature of human T-cell leukemia virus type 1 replication in experimentally infected squirrel monkeys (*Saimiri sciureus*). J Virol 75(2):1083–1089
6. Gessain A, Barin F, Vernant JC, Gout O, Maurs L, Calender A, De-Thé G (1985) Antibodies to human T-lymphotropic virus type-I in patients with tropical spastic paraparesis. Lancet 2:407–410
7. Vernant JC, Buisson G, Sobesky G, Arfi S, Gervaise G, Roman G (1987) Can HTLV-I lead to immunological disease. Lancet 2:404
8. Kaplan JE, Khabbaz RF (1993) The epidemiology of human T-lymphotropic virus types I and II. Med Virol 3:137–148
9. Paun L, Ispas O, Del Mistro A, Chieco-Bianchi L (1994) HTLV-I in Romania. Eur J Haematol 52(2):117–118
10. Gessain A (1996) Epidemiology of HTLV-1 and associated disease. In: Hollsberg P, Hafler DA (eds) Human T-cell lymphotropic virus type 1. Wiley, Chichester, pp 33–64
11. Abbaszadegan MR, Gholamin M, Tabatabaee A, Farid R, Houshmand M, Abbaszadegan M (2003) Prevalence of human T-lymphotropic virus type 1among blood donors from Mashhad, Iran. J Clin Microbiol 41(6):2593–2595
12. Okochi K, Sato H, Hinuma Y (1984) A retrospective study on transmission of adult T-cell leukemia virus by blood transfusion : seroconversion in recipients. Vox Sang 46:245–253
13. Hino S, Sugiyama H, Doi H, Ishimaru T, Yamabe T, Tsuji Y, Miyamoto T (1987) Breaking the cycle of HTLV-I transmission via carrier mother's milk. Lancet 2:158–159
14. Murphy E, Hanchard B, Figueroa J, Gibbs W, Lofters W, Campbell M, Goedert J, Blattner W (1989) Modelling the risk of adult T-cell leukemia/lymphoma in persons infected with human T-lymphotropic virus type I. Int J Cancer 43:250–253
15. Franchini G (1995) Molecular mechanisms of human T-cell leukemia/lymphotropic virus type I infection. Blood 86(10):3619–3639
16. Waldmann TA, Longo DL, Leonard WJ et al (1985) Interleukin 2 receptor (Tac antigen) expression in HTLV-I-associated adult T-cell leukemia. Cancer Res 45:4559s–4562s
17. Azimi N, Jacobson S, Leist T, Waldmann TA (1999) Involvement of IL-15 in the pathogenesis of human T lymphotropic virus type I-associated myelopathy/tropical spastic paraparesis: implications for therapy with a monoclonal antibody directed to the IL-2/15R beta receptor. J Immunol 163(7):4064–4072
18. Yoshida M (2001) Multiple viral strategies of HTLV-1 for dysregulation of cell growth control. Annu Rev Immunol 19:475–496
19. Kfoury Y, Nasr R, Hermine O, de The H, Bazarbachi A (2005) Proapoptotic regimes for HTLV-I–transformed cells: targeting Tax and the NF-kappaB pathway. Cell Death Differ 12:871–877
20. Grassmann R, Aboud M, Jeang KT (2005) Molecular mechanisms of cellular transformation by HTLV-1 Tax. Oncogene 24(39):5976–5985
21. Tabakin-Fix Y, Azran I, Schavinky-Khrapunsky Y, Levy O, Aboud M (2006) Functional inactivation of p53 by human T-cell leukemia virus type 1 Tax protein: mechanisms and clinical implications. Carcinogenesis 27(4):673–681
22. Taylor JM, Nicot C (2008) HTLV-1 and apoptosis: role in cellular transformation and recent advances in therapeutic approaches. Apoptosis 13(6):733–747
23. Jin DY, Spencer F, Jeang KT (1998) Human T cell leukemia virus type 1 oncoprotein Tax targets the human mitotic checkpoint protein MAD1. Cell 93(1):81–91
24. Boxus M, Twizere JC, Legros S, Dewulf JF, Kettmann R, Willems L (2008) The HTLV-1 Tax interactome. Retrovirology 5:76

25. Fraedrich K, Muller B, Grassmann R (2005) The HTLV-1 Tax protein binding domain of cyclin-dependent kinase 4 (CDK4) includes the regulatory PSTAIRE helix. Retrovirology 2:54
26. Matsuoka M, Jeang KT (2007) Human T-cell leukaemia virus type 1 (HTLV-1) infectivity and cellular transformation. Nat Rev Cancer 7(4):270–280
27. Nasr R, Chiari E, El-Sabban M et al (2006) Tax ubiquitylation and sumoylation control critical cytoplasmic and nuclear steps of NF-kappaB activation. Blood 107(10): 4021–4029
28. Lamsoul I, Lodewick J, Lebrun S et al (2005) Exclusive ubiquitination and sumoylation on overlapping lysine residues mediate NF-kappaB activation by the human T-cell leukemia virus tax oncoprotein. Mol Cell Biol 25(23):10391–10406
29. Kfoury Y, Nasr R, Favre-Bonvin A et al (2008) Ubiquitylated tax targets and binds the IKK signalosome at the centrosome. Oncogene 27(12):1665–1676
30. Kfoury Y, Setterblad N, El-Sabban M et al (2011) Tax ubiquitylation and SUMOylation control the dynamic shuttling of Tax and NEMO between Ubc9 nuclear bodies and the centrosome. Blood 117(1):190–199
31. Shirinian M, Kambris Z, Hamadeh L, Grabbe C, Journo C, Mahieux R, Bazarbachi A (2015) A transgenic *Drosophila melanogaster* model to study human T-lymphotropic virus oncoprotein tax-1-driven transformation in vivo. J Virol 89(15):8092–8095
32. El-Sabban ME, Merhi RA, Haidar HA et al (2002) Human T-cell lymphotropic virus type 1-transformed cells induce angiogenesis and establish functional gap junctions with endothelial cells. Blood 99(9):3383–3389
33. Bazarbachi A, Abou Merhi R, Gessain A et al (2004) Human T-cell lymphotropic virus type I-infected cells extravasate through the endothelial barrier by a local angiogenesis-like mechanism. Cancer Res 64(6):2039–2046
34. Arnulf B, Villemain A, Nicot C et al (2002) Human T-cell lymphotropic virus oncoprotein Tax represses TGF-beta 1 signaling in human T cells via c-Jun activation: a potential mechanism of HTLV-I leukemogenesis. Blood 100(12):4129–4138
35. Asquith B, Hanon E, Taylor GP, Bangham CR (2000) Is human T-cell lymphotropic virus type I really silent? Philos Trans R Soc Lond B Biol Sci 355(1400):1013–1019
36. Franchini G, Wong-Staal F, Gallo RC (1984) Human T-cell leukemia virus (HTLV-I) transcripts in fresh and cultured cells of patients with adult T-cell leukemia. Proc Natl Acad Sci U S A 81(19):6207–6211
37. Tendler CL, Greenberg SJ, Blattner WA et al (1990) Transactivation of interleukin 2 and its receptor induces immune activation in human T-cell lymphotropic virus type I-associated myelopathy: pathogenic implications and a rationale for immunotherapy. Proc Natl Acad Sci U S A 87(13):5218–5222
38. Gessain A, Louie A, Gout O, Gallo RC, Franchini G (1991) Human T-cell leukemia-lymphoma virus type I(HTLV-I) expression in fresh peripheral blood mononuclear cells from patients with tropical spastic paraparesis/HTLV-I-associated myelopathy. J Virol 65(3):1628–1633
39. Bangham CR (2003) The immune control and cell-to-cell spread of human T-lymphotropic virus type 1. J Gen Virol 84:3177–3189
40. Nasr R, El Hajj H, Kfoury Y, de Thé H, Hermine O, Bazarbachi A (2011) Controversies in targeted therapy of adult T cell leukemia/lymphoma: ON target or OFF target effects? Viruses 3:750–769
41. Sakashita A, Hattori T, Miller CW et al (1992) Mutations of the p53 gene in adult T-cell leukemia. Blood 79(2):477–480
42. Gabet AS, Mortreux F, Charneau P et al (2003) Inactivation of hTERT transcription by Tax. Oncogene 22(24):3734–3741
43. Kataoka K, Nagata Y, Kitanaka A, Shiraishi Y, Shimamura T, Yasunaga J et al (2015) Integrated molecular analysis of adult T cell leukemia/lymphoma. Nat Genet 47(11):1304–1315
44. Hasegawa H, Sawa H, Lewis MJ et al (2006) Thymus derived leukemia-lymphoma in mice transgenic for the Tax gene of human T-lymphotropic virus type I. Nat Med 12(4):466–472
45. Portis T, Harding JC, Ratner L (2001) The contribution of NF-kappa B activity to spontaneous proliferation and resistance to apoptosis in human T-cell leukemia virus type 1 Tax-induced tumors. Blood 98(4):1200–1208
46. Banerjee P, Rochford R, Antel J et al (2007) Proinflammatory cytokine gene induction by human T-cell leukemia virus type 1 (HTLV-1) and HTLV-2 Tax in primary human glial cells. J Virol 81(4):1690–1700
47. Arnulf B, Thorel M, Poirot Y et al (2004) Loss of the ex vivo but not the reinducible CD8-T-cell response to Tax in human T-cell leukemia virus type 1–infected patients with adult T-cell leukemia/lymphoma. Leukemia 18(1):126–132

48. Dassouki Z, Sahin U, El Hajj H, Jollivet F, Kfoury Y, Lallemand-Breitenbach V, Hermine O, de Thé H, Bazarbachi A (2015) ATL response to arsenic/interferon therapy is triggered by SUMO/PML/RNF4-dependent Tax degradation. Blood 125(3):474–482
49. Suehiro Y, Hasegawa A, Iino T, Sasada A, Watanabe N, Matsuoka M, Takamori A, Tanosaki R, Utsunomiya A, Choi I, Fukuda T, Miura O, Takaishi S, Teshima T, Akashi K, Kannagi M, Uike N, Okamura J (2015) Clinical outcomes of a novel therapeutic vaccine with Tax peptide-pulsed dendritic cells for adult T cell leukaemia/lymphoma in a pilot study. Br J Haematol 169(3):356–367
50. Mesnard JM, Barbeau B, Devaux C (2006) HBZ, a new important player in the mystery of adult T-cell leukemia. Blood 108(13): 3979–3982
51. Matsuoka M, Green PL (2009) The HBZ gene, a key player in HTLV-1 pathogenesis. Retrovirology 6:71
52. Yasuma K, Yasunaga J, Takemoto K, Sugata K, Mitobe Y, Takenouchi N, Nakagawa M, Suzuki Y, Matsuoka M (2016) HTLV-1 bZIP factor impairs anti-viral immunity by inducing co-inhibitory molecule, T cell immunoglobulin and ITIM domain (TIGIT). PLoS Pathog 12(1):e1005372
53. Shimoyama M (1991) Diagnostic criteria and classification of clinical subtypes of adult T-cell leukaemia-lymphoma. A report from the Lymphoma Study Group (1984–87). Br J Haematol 79:428–437
54. Tsukasaki K et al (2009) Definition, prognostic factors, treatment, and response criteria of adult T-cell leukemia-lymphoma: a proposal from an international consensus meeting. J Clin Oncol 27:453–459
55. Marçais A, Suarez F, Sibon D, Bazarbachi A, Hermine O (2012) Clinical trials of adult T-cell leukaemia/lymphoma treatment. Leuk Res Treat 2012:932175
56. Takasaki Y et al (2010) Long-term study of indolent adult T-cell leukemia lymphoma. Blood 115:433
57. Shimoyama M, Ota K, Kikuchi M et al (1988) Chemotherapeutic results and prognostic factors of patients with advanced non-Hodgkin's lymphoma treated with VEPA or VEPA-M. J Clin Oncol 6:128–141
58. Tobinai M, Shimoyama K, Minato. et al. (1994) Japan clinical oncology group phase II trial of second-generation LSG4 protocol in aggressive T- and B-lymphoma: a new predictive model for T- and B-lymphoma. Proc Am Soc Clin Oncol 13: 378.
59. Tsukasaki K et al (2003) Deoxycoformycin-containing combination chemotherapy for adult T-cell leukemia-lymphoma: Japan Clinical Oncology Group Study (JCOG9109). Int J Hematol 77:164–170
60. Yamada Yet al. (2001) A new G-CSF-supported combination chemotherapy, LSG15, for adult T-cell leukaemia-lymphoma: Japan Clinical Oncology Group Study 9303. Br J Haematol 113:375–382.
61. Tsukasaki K et al (2007) VCAP-AMP-VECP compared with biweekly CHOP for adult T-cell leukemia-lymphoma: Japan Clinical Oncology Group Study JCOG9801. J Clin Oncol 25:5458–5464
62. Tsukasaki K, Maeda T, Arimura K et al (1999) Poor outcome of autologous stem cell transplantation for adult T cell leukemia/lymphoma: a case report and review of the literature. Bone Marrow Transplant 23:87–89
63. Phillips AA, Willim RD, Savage DG et al (2009) A multi-institutional experience of autologous stem cell transplantation in North American patients with human T-cell lymphotropic virus type-1 adult T-cell leukemia/lymphoma suggests ineffective salvage of relapsed patients. Leuk Lymphoma 50:1039–1042
64. Hishizawa M et al (2010) Transplantation of allogeneic hematopoietic stem cells for adult T-cell leukemia: a nationwide retrospective study. Blood 116:1369
65. Uike N, Tanosaki R, Utsunomiya A, Choi I, Okamura J (2011) Can allo-SCTwith RIC cure ATLL? long-term survivors with excellent PS and with heterogenous HTLV-1 proviral load level. Retrovirology 8:A33
66. Bazarbachi A, Cwynarski K, Boumendil A, Finel H, Fields P, Raj K, Nagler A, Mohty M, Sureda A, Dreger P, Hermine O (2014) Outcome of patients with HTLV-1-associated adult T-cell leukemia/lymphoma after SCT: a retrospective study by the EBMT LWP. Bone Marrow Transplant 49(10):1266–1268
67. Itonaga H et al (2013) Treatment of relapsed adult T-cell leukemia/lymphoma after allogeneic hematopoietic stem cell transplantation: the Nagasaki Transplant Group experience. Blood 121:219–225
68. Gill PS et al (1995) Treatment of adult T-cell leukemia-lymphoma with a combination of interferon alfa and zidovudine. N Engl J Med 332:1744–1748
69. Hermine O et al (1995) Brief report: treatment of adult T-cell leukemialymphoma with zidovudine and interferon alfa. N Engl J Med 332:1749–1751

70. Bazarbachi A, Hermine O (1996) Treatment with a combination of zidovudine and alpha-interferon in naive and pretreated adult T-cell leukemia/lymphoma patients. J Acquir Immune Defic Syndr Hum Retrovirol 13(Suppl 1):S186–S190
71. Hermine O et al (2002) A prospective phase II clinical trial with the use of zidovudine and interferon-alpha in the acute and lymphoma forms of adult T-cell leukemia/lymphoma. Hematol J 3:276–282
72. White JD et al (2001) The combination of zidovudine and interferon alpha-2B in the treatment of adult T-cell leukemia/lymphoma. Leuk Lymphoma 40:287–294
73. Matutes E, Taylor GP, Cavenagh J et al (2001) Interferon alpha and zidovudine therapy in adult T-cell leukaemia lymphoma: response and outcome in 15 patients. Br J Haematol 113:779–784
74. Ratner L, Harrington W, Feng X et al (2009) Human T cell leukemia virus reactivation with progression of adult T-cell leukemia-lymphoma. PLoS One 4:e4420
75. Besson C, Panelatti G, Delaunay C et al (2002) Treatment of adult T-cell leukemia-lymphoma by CHOP followed by therapy with antinucleosides, alpha interferon and oral etoposide. Leuk Lymphoma 43:2275–2279
76. Bazarbachi A et al (2010) Meta-analysis on the use of zidovudine and interferon-alfa in adult T-cell leukemia/lymphoma showing improved survival in the leukemic subtypes. J Clin Oncol 28:4177–4183
77. Hodson A et al (2010) Addition of anti-viral therapy to chemotherapy improves overall survival in acute and lymphomatous adult T-cell leukaemia/lymphoma (ATLL). Blood 116(21):Abstr 3961
78. Datta A et al (2006) Persistent inhibition of telomerase reprograms adult Tcell leukemia to p53-dependent senescence. Blood 108:1021–1029
79. Bazarbachi A et al (1999) Arsenic trioxide and interferon-alpha synergize to induce cell cycle arrest and apoptosis in human T-cell lymphotropic virus type I-transformed cells. Blood 93:278–283
80. El-Sabban ME et al (2000) Arsenic-interferon-alpha-triggered apoptosis in HTLV-I transformed cells is associated with tax down-regulation and reversal of NF-kappa B activation. Blood 96:2849–2855
81. Nasr R et al (2003) Arsenic/interferon specifically reverses 2 distinct gene networks critical for the survival of HTLV-1-infected leukemic cells. Blood 101:4576–4582
82. El Hajj H et al (2010) Therapy-induced selective loss of leukemia-initiating activity in murine adult Tcell leukemia. J Exp Med 207:2785–2792
83. Kchour G et al (2009) Phase 2 study of the efficacy and safety of the combination of arsenic trioxide, interferon alpha, and zidovudine in newly diagnosed chronic adult T-cell leukemia/lymphoma (ATL). Blood 113:6528–6532
84. Kchour G, Rezaee R, Farid R et al (2013) The combination of arsenic, interferon alpha, and zidovudine restores an "immunocompetent-like" cytokine expression profile in patients with adult T-cell leukemia lymphoma. Retrovirology 10:91
85. Suarez F et al (2011) Arsenic trioxyde in the treatment of HTLV1 associated ATLL. Retrovirology 8:A59
86. Waldmann TA et al (1993) The interleukin-2 receptor: a target for monoclonal antibody treatment of human T-cell lymphotrophic virus I induced adult T-cell leukemia. Blood 82:1701–1712
87. Waldmann TA et al (1995) Radioimmunotherapy of interleukin-2R alpha expressing adult T-cell leukemia with yttrium-90-labeled anti-Tac. Blood 86:4063–4075
88. Moura I et al (2011) A neutralizing monoclonal antibody (mAb A24) directed against the transferrin receptor induces apoptosis of tumor T lymphocytes from ATL patients. Retrovirology 8:A60
89. Utsunomiya A et al (2011) Promising results of an anti-CCR4 antibody, KW-0761, for relapsed adult T-cell leukemia-lymphoma (ATL). Retrovirology 8:A40
90. Ishida T et al (2012) Defucosylated anti-CCR4 monoclonal antibody (KW-0761) for relapsed adult T-cell leukemia-lymphoma: a multicenter phase II study. J Clin Oncol 30:837–842
91. Ishida T, Jo T, Takemoto S, Suzushima H, Uozumi K, Yamamoto K, Uike N, Saburi Y, Nosaka K, Utsunomiya A, Tobinai K, Fujiwara H, Ishitsuka K, Yoshida S, Taira N, Moriuchi Y, Imada K, Miyamoto T, Akinaga S, Tomonaga M, Ueda R (2015) Dose-intensified chemotherapy alone or in combination with mogamulizumab in newly diagnosed aggressive adult T-cell leukaemia-lymphoma: a randomized phase II study. Br J Haematol 169(5):672–682
92. Olsen EA et al (2007) Phase IIB multicenter trial of vorinostat in patients with persistent, progressive, or treatment refractory cutaneous T-cell lymphoma. J Clin Oncol 25: 3109–3115

93. Whittaker SJ et al (2010) Final results from a multicenter, international, pivotal study of romidepsin in refractory cutaneous T-cell lymphoma. J Clin Oncol 28:4485–4491
94. Piekarz RL et al (2011) Phase 2 trial of romidepsin in patients with peripheral T-cell lymphoma. Blood 117:5827
95. Coiffier B et al (2012) Results from a pivotal, open-label, phase II study of romidepsin in relapsed or refractory peripheral T-cell lymphoma after prior systemic therapy. J Clin Oncol 30:631–636
96. Ramos J et al (2011) Targeting HTLV-I latency in adult T-cell leukemia/lymphoma. Retrovirology 8:A48
97. Afonso PV et al (2010) Highly active antiretroviral treatment against STLV-1 infection combining reverse transcriptase and HDAC inhibitors. Blood 116:3802–3808
98. Dearden CE et al (2001) High remission rate in T-cell prolymphocytic leukemia with CAMPATH-1H. Blood 98:1721–1726
99. Mone A et al (2005) Durable hematologic complete response and suppression of HTLV-1 viral load following alemtuzumab in zidovudine/IFN-a-refractory adult T-cell leukemia. Blood 106:3380–3382
100. Ravandi F et al (2009) Phase II study of alemtuzumab in combination with pentostatin in patients with T-cell neoplasms. J Clin Oncol 27:5425–5430
101. Maeda N, Muta H, Oflazoglu E, Yoshikai Y (2010) Susceptibility of human T cell leukemia virus type I-infected cells to humanized anti-CD30 monoclonal antibodies in vitro and in vivo. Cancer Sci 101:224–230
102. Bazarbachi A, Ghez D, Lepelletier Y et al (2004) New therapeutic approaches for adult T-cell leukaemia. Lancet Oncol 5:664–672
103. Hermine O, Wattel E, Gessain A, Bazarbachi A (1998) Adult T cell leukaemia: a review of established and new treatments. BioDrugs 10:447–462
104. Bazarbachi A, Suarez F, Fields P, Hermine O (2011) How I treat adult T-cell leukemia/lymphoma. Blood 118:1736–1745
105. Flaman JM et al (1995) A simple p53 functional assay for screening cell lines, blood, and tumors. Proc Natl Acad Sci U S A 92:3963–3967

INDEX

Claudio Casoli (ed.), *Human T-Lymphotropic Viruses: Methods and Protocols*, Methods in Molecular Biology, vol. 1582,
DOI 10.1007/978-1-4939-6872-5, © Springer Science+Business Media LLC 2017

D

E

F

G

H

I

K

L

M

N

O

P

R

S

T

V

W